NYO 9715
MITNE-10

THE EFFECT OF FUEL AND POISON MANAGEMENT ON NUCLEAR POWER SYSTEMS

by

N. B. McLeod, M. Benedict,

K. Uematsu, H. L. Witting, and K. S. Ram

June 1959-September, 1961

THE EFFECT OF FUEL AND POISON MANAGEMENT ON NUCLEAR POWER SYSTEMS

by

N. B. McLeod, M. Benedict,

K. Uematsu, H. L. Witting, and K. S. Ram

Distribution   No. of Copies

Division of Sponsored Research, MIT	1
Industrial Liason Office, MIT	5
MIT Library	2
MIT Computation Center	1
MIT Files	30
N. B. McLeod	20
AEC TIS	3
AEC Reports and Statistics Branch	1
D. Richtman	1
Donald H. Stewart	1
Harmon Potter	1
Saul Strauch	1
E. A. Eschbach	1
W. B. Lewis	1
D. P. Herron	1
S. Siegel	1
Harvey W. Graves	1
J. W. Weil	1
Dale F. Babcock	1

TABLE OF CONTENTS

LIST OF TABLES

LIST OF FIGURES

I. ABSTRACT

THE EFFECT OF FUEL AND POISON MANAGEMENT
ON NUCLEAR POWER SYSTEMS

by

N. B. McLeod, M. Benedict

K. Uematsu, H. L. Witting, and K. S. Ram

The FUELMOVE Code, which is described in this work, is a two-dimensional, two-group fuel depletion code developed for the purpose of studying the effect of fuel and control poison management on nuclear power systems which are fueled with U-235, U-238, and their irradiation products. The code source language is FORTRAN for use on IBM 704, 709, 7090 or Philco TRANSAC computers which have 32K of fast memory.

One of the principal advantages of the code is that it is capable of evaluating the important gross characteristics of reactor performance and their history throughout fuel lifetime with a minimum of computer time expenditure. A typical fuel history can be obtained in approximately one minute on the IBM 7090 computer. Its comparative accuracy is such that it is able to eliminate from further consideration all but the most promising fuel management techniques being considered under a given set of conditions.

FUELMOVE is actually written as two separate codes, the FUEL Code and the MOVE Code. In the FUEL Code, the homogenized reactor unit cell properties are evaluated as a function of flux-time. The properties at specified flux-times are then put out on punched cards and/or magnetic tape for subsequent use by the MOVE Code. The MOVE Code represents fuel by its flux-time, and fuel transfer by flux-time transfer. It evaluates flux and power density distributions, control poison requirements, the criticality factor and average core properties throughout fuel lifetime, and when fuel is discharged, it obtains the nuclide concentrations, fuel burnup, fuel cycle cost, and total energy cost.

The important fuel management techniques available in the MOVE Code are 1) Batch irradiation in which the entire core is replaced at one time, 2) Discontinuous Outin irradiation in which the

1

reactor is divided into equal-volume radial zones. Fuel is discharged from the central zone, fuel in the other zones is moved one zone inward and fresh fuel is charged to the outer zone. 3) Bidirectional irradiation in which fuel moves axially inside pressure tubes from one end of the reactor to the other end, with fuel moving in opposite directions in adjacent channels. Also available are continuous outin and continuous graded irradiations.

The important poison management techniques available in the MOVE Code are 1) Uniform removal of an arbitrary poison distribution, 2) Radial zone removal of an initially arbitrary poison distribution, 3) Axial bank removal of an initially arbitrary poison distribution, and 4) Poison removal to maintain a specified constant power density.

The MOVE Code treats cylindrical reactors with azimuthal symmetry, whose reflector can be represented by a reflector savings, and whose behavior can be represented by 150 regions, 10 axial by 15 radial. Up to five radial zones of arbitrary dimensions can be used, and up to five different fuel types can be specified at any one time, one per radial zone.

The neutron behavior model used in the FUEL Code has been checked by making a comparison of its predictions with experimental data on the irradiation of natural uranium metal in the NRX Reactor. The uranium and plutonium nuclide concentration predictions agree very well with the experimental values. In the comparison of reactivities, there is a constant discrepancy of about 0.6% in reactivity, which may be due to uncertainties in fission product yield data. If this discrepancy is removed, there is excellent agreement between the FUEL Code predictions and experiment.

The FUELMOVE Code was used to study the effect of various fuel and poison management techniques on the CANDU reactor, which is a D_2O moderated and cooled, 200 Mwe power reactor designed to use natural uranium fuel and the bidirectional fueling technique. This study showed the important relationship between neutron economy, fuel burnup, and control requirements. With bidirectional fueling, the fuel cost and control requirement are minimum, and fuel burnup and neutron economy maximum. With batch irradiation, the exact opposite is true. The discontinuous outin irradiation results in performance which is intermediate between the two extremes presented by the batch and bidirectional techniques. The use of bidirectional fuel management permits a fuel cost of about 1.1 mills/kwh at between 1.0 and 1.3% enrichment, based on A.E.C. prices and $60/kg fabrication cost. Batch irradiation fuel costs are over 2.0 mills/kwh while the discontinuous outin fuel costs are intermediate between these.

CHAPTER II

INTRODUCTION

The main objective of this work has been to develop a general systematic method for evaluating the effect of various fuel and poison management techniques on large thermal nuclear power systems in various stages of design or operation, and to illustrate the capability of this method by application to a specific reactor design. The method has been incorporated into the new nuclear reactor depletion code, FUELMOVE.

The approach taken to this problem by the FUELMOVE Code is best illustrated by contrast with other reactor depletion codes. Probably the best known are the CUREBO system of General Electric (A21), and the TURBO system of Westinghouse (C21). These systems, which are for the IBM 704 Computer, have been extended and rewritten for the Philco TRANSAC computer as the KARE system (A22) and TNT-1 (C22) respectively. They are similar in the following respects. First, their mesh spacings are usually substantially less than a neutron migration length. Secondly, fuel burnup is calculated on a point-by-point basis. These systems are therefore capable of burnup calculations with very detailed flux shapes. In certain burnup studies, however, this detail is neither necessary nor desirable. In particular, surveys of parameters such as enrichment do not require detailed flux shapes, provided the gross flux shape is accurate enough to yield the correct average leakage and power distribution.

The FUELMOVE Code, in contrast to the CUREBO and TURBO systems, uses mesh spacings which are generally the same order of size as the migration length. Also, fuel burnup is calculated on a flux-time basis rather than by point-by-point depletion. The result of this is that the FUELMOVE Code can perform burnup calculations in 1/10

3

to 1/20 of the computer time required by the more elaborate systems. The FUELMOVE Code does not attempt to obtain the flux fine-structure that is necessary for detailed studies of hot spots or the effect of individual control rods. Its major merit is that it is capable of evaluating the fuel burnup and gross power shapes of a large number of potential fuel and poison management techniques, and to do this with a minimum of computer time expenditure. Its comparative accuracy is such that it is able to eliminate from further study all but one or two of the most promising from a group of potential fuel and poison management techniques being studied under a given set of conditions.

The starting point in the development of FUELMOVE has been the nuclear reactor burnup code FUELCYC which was developed by R. T. Shanstrom (S41) in a previous phase of the Fuel Cycle Study Project at MIT. In the current phase of the study, emphasis has been placed on the fuel cycle as a part of the overall power system, rather than as a separate entity. This has led to consideration of the type of compromises that are necessary between fuel costs and fixed (capital) costs in the design of an optimum nuclear power system.

The neutron behavior model of FUELMOVE is similar to that of FUELCYC. The principal changes are in the treatment of fission products, the addition of (optional) burnable poison, more flexibility with regard to both thermal and resonance disadvantage factors, and simpler preparation of input data. The condensed Crout reduction technique developed by Shanstrom for the solution of the spatial flux equations in FUELCYC has been retained in FUELMOVE. Because it is both convenient and conservative of computer time, the FUEL-MOVE Code has been divided into two separate codes, the FUEL Code and the MOVE Code. In the FUEL Code, the flux-time dependence of nuclide concentrations and fuel properties is computed for a specified type and enrichment of fuel. This information plus geometrical data for the given reactor is subsequently used by the MOVE Code which computes spatial flux shapes and power densities during fuel burnup, obtains the discharged fuel properties and burnup and computes fuel cycle and total energy cost for a specified combination of the fuel and

4

poison management techniques which are written into the MOVE Code.

The common bases for comparison of the results of various fuel and poison management studies will now be developed, since this has been of some influence in the writing of FUELMOVE.

Generally, fuel and poison management studies on a particular reactor type will be based on a specific unit cell design. This will presumably have been evolved through the normal design compromises between safety, structural design, heat removal, reactivity and cost considerations. The assumption implied here is that a specified unit cell design is an adequate common starting point in a fuel and poison management survey.

A given unit cell design generally has a maximum permissible power density associated with it. This may be imposed by one or a combination of factors such as a central fuel temperature limit, a corrosion or film boiling limited cladding surface temperature, a maximum permissible heat flux, or a limit imposed by the rate of fission product release into the coolant. For example, in design of the CANDU reactor (L61), thermal output has been limited to a local linear power density of 537 watts/cm of fuel rod length. In any case, this type of limit will be a common factor in the study. Another parameter which may impose a limitation is the enthalpy rise of the coolant between inlet and outlet of the coolant channel, but this also depends upon coolant flow rate, and is therefore not the type of limit that might be generally applied in an analysis of fuel and poison management techniques. Therefore, only the limits imposed by a maximum permissible power density will be considered in this work.

Because comparisons will generally be made on the basis of energy cost, the unit cost data must be the same for each case, and should be as representative as possible of the cost situation that will prevail during operation of the reactor.

Additional common bases for comparison of fuel and poison management techniques will depend on the purpose of the study. If its purpose is part of the design study for a new reactor, then all comparisons should be based on peak-power-density-limited output from systems

operating at equal net power. If it involves changes to be made in a currently operating system, at current net output, comparisons will be based on fuel cost, and the effect of fueling down-time on total cost, since all other factors will be nearly constant. If a currently operating system is to be operated at increased output, by improving the power density distribution, comparisons will be based on peak-power-density-limited situations at constant core volume.

The above serves to introduce the following classifications of fuel and poison management studies, into one of which most studies will fall, depending upon its basic purpose.

(1) Fixed core volume, fixed output. Into this group fall burnup and fuel cycle cost surveys which generally are not limited by peak power density considerations. This study type is a convenient starting point for the other two study types.

(2) Fixed core volume, variable output. Into this group will fall those fuel and poison management studies aimed at increasing the output of a given reactor core. The output will be determined by the peak-to-average power density ratio, since the peak power density is specified. This study is best accomplished by normalizing the applicable results of the previous study classification (1) to the specified peak power density.

(3) Fixed output, variable core volume. Into this group will fall all initial design studies which have a specified output and a specified peak power density limitation. The core volume will be adjusted to yield the specified output and will be governed by the peak-to-average power density ratio, since the peak value is specified. This study is also best started using results from the first study classification.

In the writing of the FUELMOVE Code, an attempt has been made to keep relative degrees of approximation and/or model sophistication at a consistent level in each part of the code so as to produce accurate results in a minimum of computer time. Because of uncertainties in basic nuclear data, a high degree of model sophistication and compu-

6

tational accuracy is unjustified for a survey code such as FUELMOVE.

Certain factors not treated by the FUELMOVE Code may influence reactor design and fuel cycle optimization. For example, the coolant temperature and flow rate may affect the local maximum permissible power density. Also, local variations in power density due to control rods or lattice heterogenerities may be important. The effects of different fuel rod diameters and lattice spacings can be studied by treating these variations individually as different types of fuel.

To lend coherence and consistency to the studies performed in this work, a particular reactor design is studied. The 200 mwe CANDU reactor which uses D_2O moderator and coolant was chosen. This reactor is capable of essentially continuous fueling at full power and is therefore capable of being operated using virtually any practical fueling technique.

The CANDU reactor is the third of a sequence of reactors having progressively better neutron economy which have been studied by the MIT Fuel Cycle Project at the request of the AEC. The other two reactors are (1) the pressurized water reactor (Yankee) and the organic moderated reactor. The basic characteristics of the three reactors are listed in Table 2.1. Table 2.2 lists the theses which have been done at MIT on the Fuel Cycle Study Project.

The principal results of these theses have been summarized in two papers in Nuclear Science and Engineering (S22, B21).

Table 2.1 Characteristics of Reference Reactors

Reactor	Pressurized Water	Organic Moderated	Heavy Water
Megawatts			
Thermal	480	560	715
Net electric	134	150	200
Moderator			
Material	H_2O	Santowax R, 30% polymer, $CH_{1.35}$	D_2O
Pressure psia	2000	low	near atmosphere
Mean temp $^\circ$C	269°	316°	80°
Coolant	Moderator	Moderator	D_2O at 275°C. avg, 1475 psia
Cladding			
Material	Stainless steel	Finned aluminum	Zircaloy-2
Thickness, in.	0.020	---	0.015
Fuel			
Material	UO_2	96 w/o U, 3.5 Mo, 0.5 Si	UO_2
Density	10.07	18.40	10.2
w/o U-235	3.4	1.97	0.71
Form	Rods	Plates	Rods
Dimension, in.	0.29 dia.	---	0.55 dia.

Table 2.1   cont'd

Reactor	Pressurized Water		Organic Moderated		Heavy Water
Arrangement	0.42 in. ctr to ctr, square pitch, 305 or 306 rods per element, 76 elements		0.7 in. spacing, 18 plates per element, 257 elements		19 rod cluster in Zircaloy pressure tubes, 304 channels on 9.25 in. square pitch
Core Inventories, kg					
U in fuel	20,560		57,162		38,210
Cladding	6,133		14,329		4,070
Moderator & refl.					138,100
Coolant	2,668		10,612		2,787
Other	Zr	1,293	St. Steel	3,672	Zr	11,250 Pressure tubes
			Steel	1,082	Zr	4,586 Calandria tubes
			Mo	2,084		
			Si	298		
			Ni	243		
Thermal flux, rel. to					
Cladding	} 1.141		1.1		1.003
Coolant					1.1
Moderator					1.823
Other					1.265 Pressure tubes
					1.357 Calandria tubes
Core Dimensions, cm					
Equivalent radius	96.11		153.37		230.2
Active length	234.33		304.8		500.
Reflector Savings, cm					
Radial	7.5		15.52		58.45
Axial	7.5		15.60		2.1

Table 2.1   cont'd

Reactor	Pressurized Water	Organic Moderated	Heavy Water
D, diff. coeff., cm	0.2755	0.604	1.002
γ, Fermi age, cm^2	51.5	81.5	143.5
ϵ, Fast fission factor	1.0584	1.053	1.0173
p_8, U-238 res. escape prob.	0.738	0.729	0.8925
B^2, Geometric buckling m^{-2}	6.93	2.903	1.08
Avg. Power Density kw/l	70.6	24.86	8.60
Avg. Specific Power kw/kg U	23.3	9.8	18.7
p_{MOD}, resonance escape probability for structural materials	0.942	1.000	1.000

Table 2.2 Previous Fuel Cycle Theses at M.I.T.

Author	R. T. Shanstrom	P. Steranka	S. L. Amberg	C. T. McDaniel	M. Waucquez	K. Uematsu	J. M. Neill
Reference	NYO 2131 S41	M. S. Thesis S21	M. S. Thesis A23	M. S. Thesis M21	M. S. Thesis W21	M. S. Thesis U21	M. S. Thesis N21
Reactor	Pressurized Water (Yankee)	Pressurized Water (Yankee)	Organic Moderated	Pressurized Water (Yankee)	Organic Moderated	Graphite Moderated Gas-cooled	Th-fueled (Indian Point)
Fuel	UO_2	UO_2	96 w/o U 3.5 w/o Mo 0.5 w/o Si	UO_2	96 w/o U 3.5 w/o Mo 0.5 w/o Si	UC	$ThO_2 +$ $U^{235}O_2$
Fuel Management Techniques	Batch, Continuous: Outin, In-out, Graded	Batch with Radial zone poisoning, Bidirectional	Batch Graded	Discontinuous Outin	Discontinuous and Continuous Outin	Batch, Bidirectional	Batch
Code	FUELCYC	Extended FUELCYC	FUELCYC	Modified FUELCYC	Modified FUELCYC	Extended FUELCYC	WATTHO

CHAPTER III

SUMMARY

A. FUELMOVE CODE DESCRIPTION

1. Introduction

The FUELMOVE Code is a two-dimensional, two-group fuel
depletion code written for the purpose of studying the effect of fuel and
control poison management on nuclear power systems. The code
source language is FORTRAN, for use on IBM 704, 709, 7090 or
Philco TRANSAC computers which have 32K fast memories.

The approach to the problem of fuel and poison management
is as follows. The homogenized reactor unit cell properties are evalu-
ated as a function of flux-time. Then, representing fuel by its flux-
time and fuel transfer by flux-time transfer, the reactivity and power
histories of nuclear fuel can be obtained for various fuel and poison
management techniques. This data is then used to evaluate fuel cycle,
and total energy costs. Because the above computation falls naturally
into two separate parts, the FUELMOVE Code is written in two sections:

1. The FUEL Code calculates the unit cell properties as a
   function of flux-time and transfers the results to magnetic
   tape and/or punched cards.
2. The MOVE Code, using the output of the FUEL Code,
   calculates macroscopic core properties such as flux and
   power density during operation, moves fuel in various
   specified ways, adjusts control poison for criticality, and
   when spent fuel is discharged, computes burnup and also
   energy cost.

The objective of the FUELMOVE Code is to provide the means
of evaluating the fuel burnup and gross power shape histories of a large

12

number of potential fuel and poison management techniques, and to do this with a minimum of computer time expenditure. In order to minimize computer time, an attempt is made to maintain a comparable level of accuracy between numerical methods and the neutron behavior model, so that the magnitude of error from these sources will be less than that due to the uncertainties in basic nuclear data. As typical examples of computer time expenditure using an IBM 7090, the FUEL Code will obtain complete flux-time histories of different reactor unit cells at the rate of one to two per minute and the MOVE Code will use about one minute of time in computing the reactor core properties during irradiation and final energy costs for batch irradiation, using a 7×7 mesh size.

An outline of the basic features and calculational techniques of each part of the FUELMOVE Code will now be given, followed by a summary of code capabilities and limitations.

2. The FUEL Code

The basic steps in the FUEL Code computation of fuel properties as a function of flux-time are outlined below.

1) The necessary input and control data are read in.
2) From the specified material concentrations and the energy dependence of cross sections which is written into the code, the neutron energy spectrum below 0.45 ev is obtained by solving the Wilkins equation.
3) Using this thermal spectrum, plus the energy dependence of neutron cross sections, thermal-spectrum-averaged cross sections are obtained.
4) Resonance escape probabilities are computed from resonance integrals, nuclide concentrations and resonance disadvantage factors.
5) Using thermal plus resonance reaction rates, the changes in nuclide concentrations in a specified flux-time interval are obtained from a fourth-order difference solution of the material balance equations.

13

6) The thermal spectrum, average cross sections and resonance escape probabilities are re-evaluated, and the required properties at this flux-time step are computed.

7) Steps 5 and 6 are repeated a specified number of times, so that all properties in the desired flux-time range are evaluated.

8) The fuel properties at specified flux-times are put onto punched cards and/or magnetic tape for subsequent use by the MOVE Code.

3. The MOVE Code

The MOVE Code uses the flux-time properties from the FUEL Code plus input data specifying core geometry to obtain the fuel, flux, and power density behavior during fuel burnup for a specified fuel and poison management technique.

The MOVE Code uses two-dimensional diffusion theory in an axially symmetric cylinder, with two groups of neutron leakage, fast and thermal.

The fuel management techniques written into the MOVE Code are:

1) Batch Irradiation of fuel which is fixed in place in the core. Criticality is maintained by the use of control poison.

2) Discontinuous Outin Irradiation in which the reactor core is divided into a number of equal-volume radial zones. When the reactor which is operated batchwise ceases to be critical with all the control poison removed, the fuel in the central zone of the reactor is discharged and the fuel in the other zones is moved one zone inward, with new fuel being charged to the now vacant outermost zone.

3) Discontinuous Bidirectional Irradiation in which the fuel in a given axial channel is divided into a number of equal lengths. When the reactor, which is operated batchwise, ceases to be critical with all of the control poison removed, fuel is pushed axially, and in opposite directions in adjacent channels, until

14

one of the lengths of fuel is discharged. This discharged fuel may be recharged to the adjacent channel, or new fuel can be charged.

4) Continuous Bidirectional Irradiation in which fuel moves at a constant axial velocity along a channel from one end of the reactor where it was charged to the opposite end where it is discharged. Fuel moves in opposite directions in adjacent channels, and the charging rate is adjusted so as to maintain criticality without the use of control poison.

5) Continuous Outin Irradiation in which fuel rods are charged to the outside of the reactor core, are moved radially inward and are discharged from the central axis of the reactor. The fuel charge rate is adjusted so that the reactor is just critical without the use of control poison.

6) Continuous Graded Irradiation in which fuel rods are irradiated while fixed in place in the reactor. They are replaced individually so that every region of the reactor contains fuel elements distributed uniformly in exposure between the fresh and discharge burnup condition. The fuel charge rate is adjusted to maintain criticality without the use of control poison.

The poison management techniques written into the MOVE Code are:

1) Uniform removal of control poison with an arbitrary spatial distribution. The magnitude is varied for reactivity control.

2) Radial zone poison removal of an arbitrary initial shape. The magnitude is computed for initial criticality. Poison is removed starting at the bottom of the outermost zone and progressing axially upward. When poison has been removed from one zone, removal starts on the next zone toward the center.

3) Axial bank poison removal of an arbitrary initial shape. The magnitude is computed for initial criticality. Poison is then removed, starting at the bottom of the core, and is removed axially, the height of the control rods being uniform radially.

15

4) Poison removal for constant power density. The spatial distribution of the poison is determined by a desired input power density shape. Burnup proceeds until the approach of a zero or negative poison condition causes a change to a specified alternate poison removal technique.

5) A constant fixed poison, arbitrary shape. This poison can be used in conjunction with those mentioned above, except that it is not removable. Its purpose is solely that of power density shaping.

6) Uniform removal of a poison with specified relative spatial distribution whose magnitude is varied for reactivity control. When the poison has been completely removed, removal is started on additional control poison whose specified shape and magnitude has been held constant up to this point. Removal of this latter poison can take place uniformly, by radial zone or axial bank removal, as outlined above.

The MOVE Code obtains the thermal flux shape in the following manner. The neutron balance in any region of the reactor is expressed in finite difference form in terms of the flux in that region and the four adjacent regions. Some of the parameters in the balance equation are dependent upon the properties and hence the flux-time of the fuel in that region, while other parameters depend upon the geometry of the region. A system of linear equations, one for each region, is hereby obtained, and these can be solved by an iterative Crout Reduction technique, to obtain the flux in each region. In order that this flux be the correct flux, however, the neutron balance on the whole reactor must be such that the reactor is just critical. In the batch-type irradiations, this means that the correct control poison must be used, and in the continuous irradiations, the fuel charging rate must be adjusted so as to just maintain criticality.

Actually, before the above procedure can be applied, it is necessary to know the flux-time in each region of the reactor so that the properties and hence the flux coefficients in the system of equations can be obtained. There are two general methods of doing this. In batch-

type irradiations, the flux-times everywhere will be zero at the start-of-life. Hence, the fluxes can be obtained by solving the system of equations using the properties at zero flux-time. If these fluxes are assumed to remain constant for a specified time, the flux-times at this new time are obtained directly. Batch irradiation proceeds step-by-step, with the new flux-time in each region being obtained by adding the new flux-time increment to the old flux-time. When the reactor ceases to be critical without control poison, part, or all of the fuel is discharged, and the flux-times at discharge are used to obtain the nuclide concentrations and burnup of the spent fuel, and fuel costs can then be obtained.

In the continuous irradiations, a somewhat different approach is taken when evaluating flux-times in each region. If a characteristic flux-time of fuel discharged is specified, all flux-times in the reactor can be related to this number in a manner which depends upon the particular fueling technique, and which requires knowledge of the spatial flux shape. Hence, a double-iterative process is required, in which an assumed flux shape is used with an initial characteristic flux-time estimate. The inner iteration is performed to obtain the correct flux shape corresponding to the given characteristic flux-time estimate. The outer iteration is performed to obtain the characteristic flux-time which corresponds to a just-critical reactor. As before, the discharge flux times are used to obtain fuel burnup and fuel cost.

4. The Limitations of FUELMOVE

There are two basic reasons for the limitations to the FUEL-MOVE Code. The first of these is the fact that because of the large mesh spacing, it is impossible to follow local flux and power density variations which may be due to lattice heterogeneities and control rods. Hence, the detailed effects of various control rod removal programs cannot be adequately treated, although their gross effects can.

The second basic limitation is imposed by the range of validity of the assumption that fuel behavior during irradiation can be adequately represented as a function of the single variable, thermal flux-time. This is a valid assumption provided that resonance reaction rates are

either small compared to thermal, or can be adequately predicted. The major cause of potential difficulty with resonance reaction rates is the behavior of P_1, the fast non-leakage probability. This quantity is assumed to be a constant in the computation of fuel properties during irradiation, and in large power reactors this is a valid assumption.

The FUELMOVE Code will therefore be limited in applicability to large reactors in which the majority of fissions occur at thermal energies, whose spatial characteristics are adequately represented by up to 150 regions, 10 radial by 15 axial, and whose reactor unit cell may be treated as an equivalent homogenized unit cell.

B. THE EVALUATION OF THE NEUTRON BEHAVIOR MODEL

The neutron behavior model of the FUEL Code was evaluated by comparing its predictions of the irradiation behavior of natural uranium metal NRX fuel rods, with actual measurements of nuclide concentrations and reactivity changes which were obtained as the result of the cooperative efforts of scientists at Chalk River, Canada, and Harwell, England.

Good agreement between experimental nuclide concentrations data and concentrations predicted by the FUEL Code was found for U^{235}, Pu^{239} and Pu^{240}. Experimental concentrations of Pu^{241} and Pu^{242}, however, increased somewhat more rapidly with flux-time than predicted by the MOVE Code, without adjusting any cross-sections. For these nuclides, better agreement between experimental data and the FUEL Code was obtained by modifying the treatment of resonance absorption of Pu^{240}, which is handled in the FUEL Code by the Crowther-Weil technique (C42). When the cross-section for resonance neutrons in uranium metal fuel was changed from the true value of 1152 bifa (barns per initial fissile atom) to an adjusted value of 230 bifa, good agreement between experiment and the FUEL Code was obtained for all nuclides, as shown in Figure 3.1. Table 5.4, p. 176, shows, however, that even with the true cross-section of 1152 bifa, agreement between experiment and prediction is still satisfactory.

Shown in Figure 3.2, is the comparison of reactivity change in bifa between the experimental data and FUEL Code predictions, using the original value of fuel scattering cross-section (1152 bifa) and the changed value (230 bifa). Both predicted values are lower than the observed values by about 8 bifa. The discrepancy which is apparent here has also been noted by the Canadian group at Chalk River (W41), using a neutron behavior model which is different from that of the FUEL Code. There is a presumption, therefore, that the models may not be wholly responsible for the discrepancy.

Because of the correspondence in shape after the initial discrepancy, there is a possibility that a short term effect is to blame, possibly inaccuracies in the yields of the Sm group fission products. A one-year time lapse between end of irradiation and reactivity measurement may also have some bearing on the discrepancy.

When the initial discrepancy is removed, as shown in Figure 3.3, there is excellent agreement in reactivity shape. Also shown on this
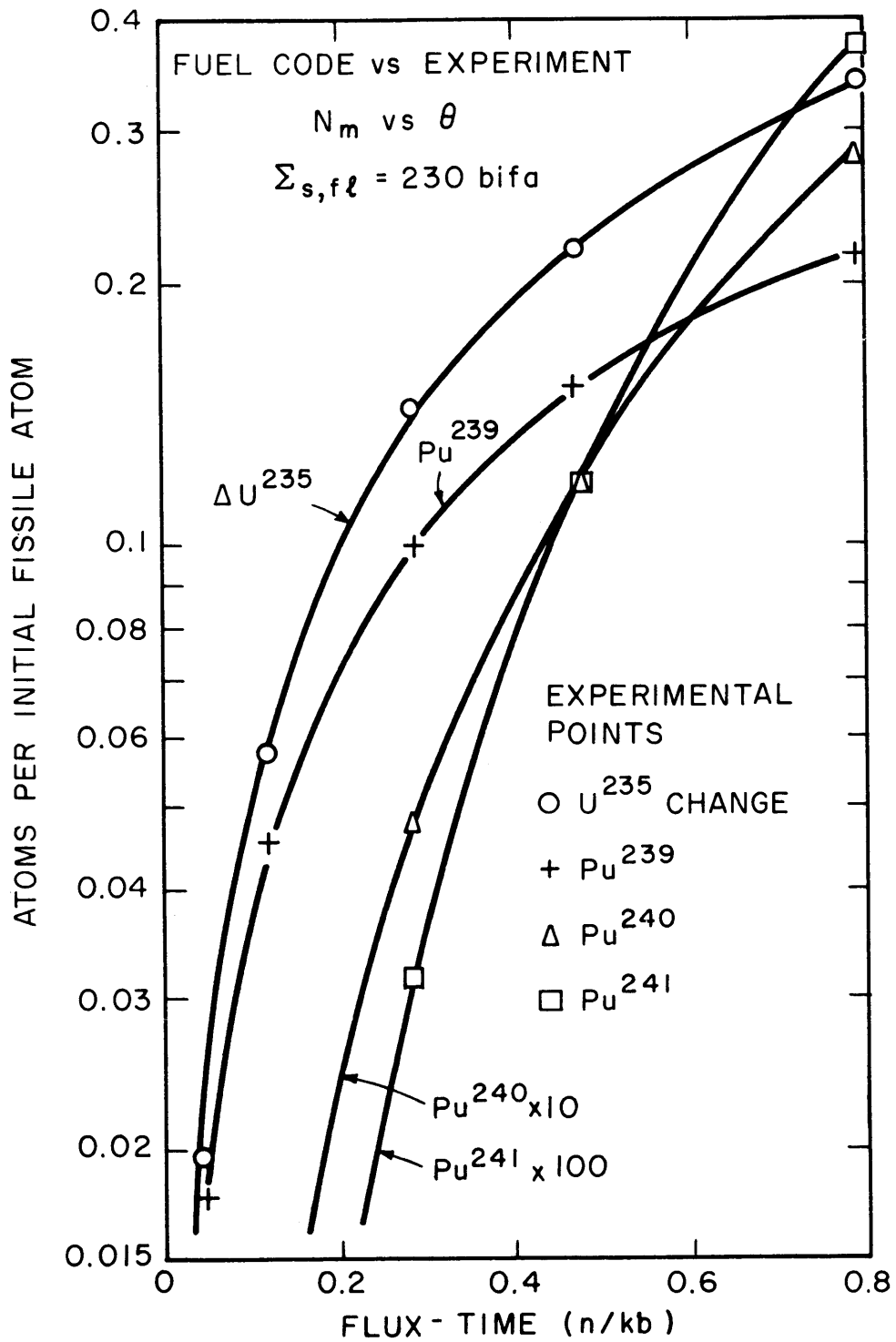
FIG. 3.1 FUEL CODE NUCLIDE
CONCENTRATIONS COMPARED
WITH EXPERIMENTAL ANALYSIS
OF IRRADIATED NRX RODS

20
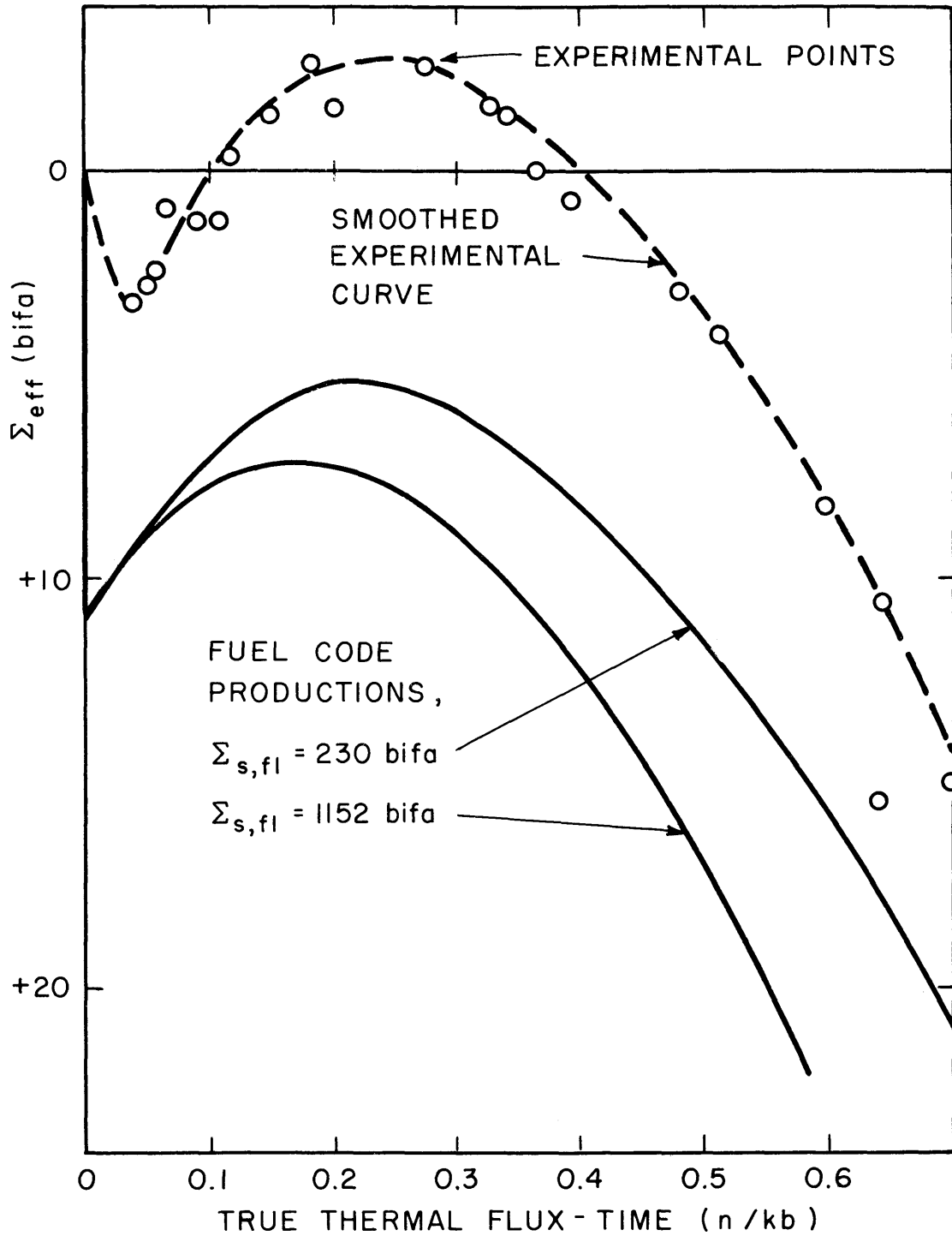
FIG. 3.2 REACTIVITY CHANGE: EXPERIMENT vs
FUEL CODE PREDICTION

21
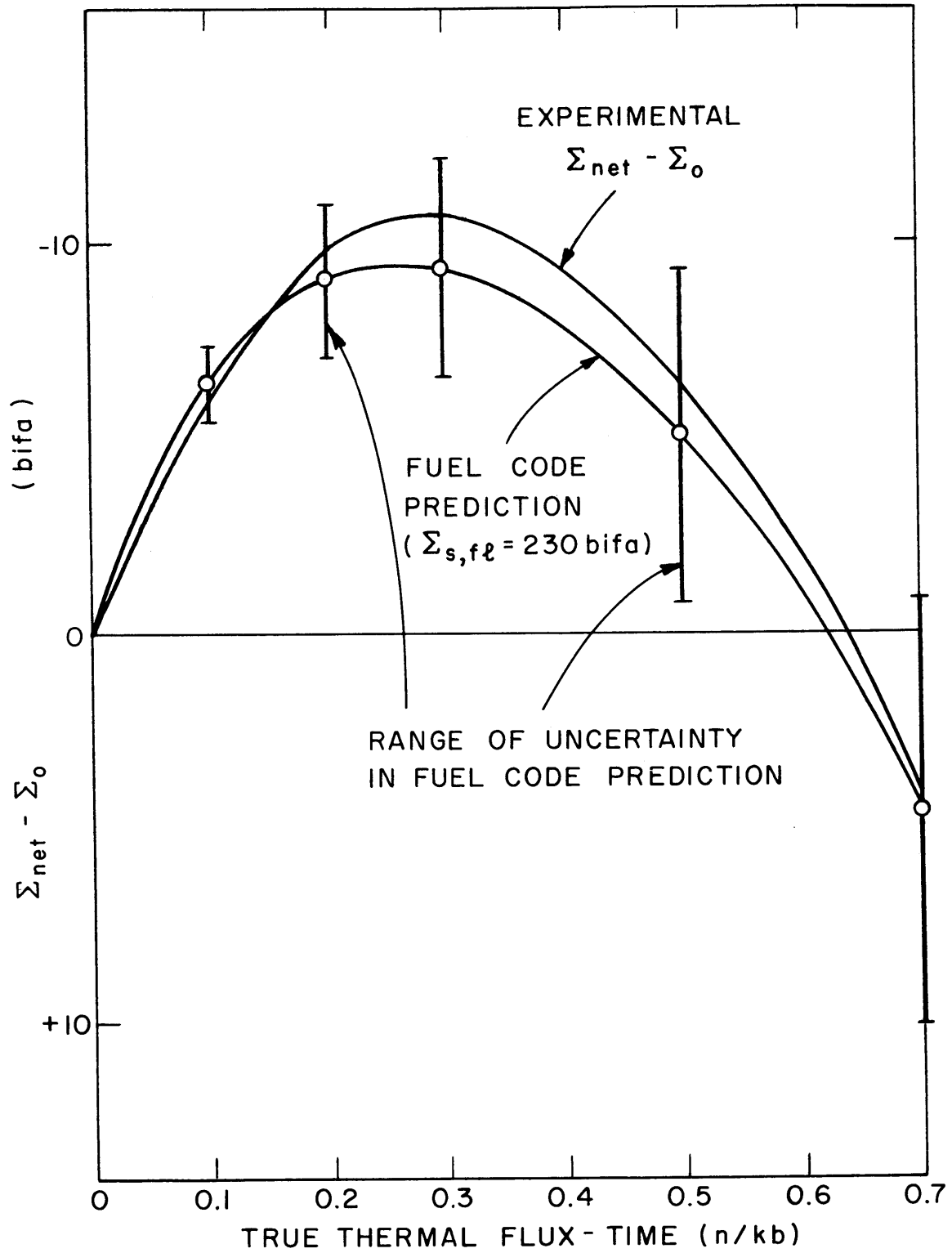
FIG. 3.3 THE EFFECT OF UNCERTAINTIES IN BASIC NUCLEAR DATA

graph is the range of uncertainty in the FUEL Code prediction due to uncertainties in basic nuclear data used in the Code. This large range of uncertainty indicates that if the FUEL Code is given adequate data on initial conversion ratio and the Pu^{240} disadvantage factor, that uncertainties in basic nuclear data will be more dominant than neutron behavior model errors.

C. THE RESULTS FROM THE STUDY OF FUEL AND POISON MANAGEMENT TECHNIQUES

1. Introduction

The FUELMOVE Code has been used in a study of possible fuel and poison management techniques in the CANDU reactor, which is the 200 mwe, D_2O moderated and cooled, pressure tube power reactor presently under construction at Douglas Point, Ontario. This reactor is being designed specifically to use natural uranium oxide fuel and the bidirectional fueling technique.

2. FUEL Code Results

The FUEL Code was used to obtain the various properties required by the MOVE Code in its calculation. These properties were obtained at certain discrete enrichments from natural to 2.5 a/o. One of the significant ways of summarizing these results is given in Figure 3.4, which shows k_∞ as a function of flux-time for various enrichments. The k_∞ is defined here as the production rate of thermal neutrons divided by the absorption rate of thermal neutrons. In addition to this, a study of the potential usefulness of burnable poison was performed, using Li^6 (σ_0 = 945b) as the burnable poison. Initial Li concentration was adjusted to obtain initial k_∞'s of 1.1 and 1.2 for various discrete enrichments from 1.3 to 2.0 a/o. The resulting flux-time behavior at 1.5 a/o is shown in Figure 3.5.

3. The MOVE Code Results

The common bases for comparison of various fuel and poison management techniques will depend upon the objective of the study. If a new reactor system is being designed, the comparison of techniques should be on the basis of equal power output from reactor cores operating at some specified limit, such as a maximum permissible power density limit. The comparisons in this work have been made on this basis.

The important fuel management techniques studied in this work are bidirectional, batch and discontinuous outin irradiation, and the summary given below will be in that order.

$$K_\infty = \frac{\epsilon \nu \Sigma_f \, p}{(1 - \epsilon \langle \eta (1-p) \rangle)(\Sigma - \Sigma_{xe} + C_5 \Sigma_{xe,max})}$$

C_5 - Xe Fraction BURNED

ENRICHMENT	C_5
NAT	0.90
1.0 %	0.885
1.5 %	0.87
2.5 %	0.84
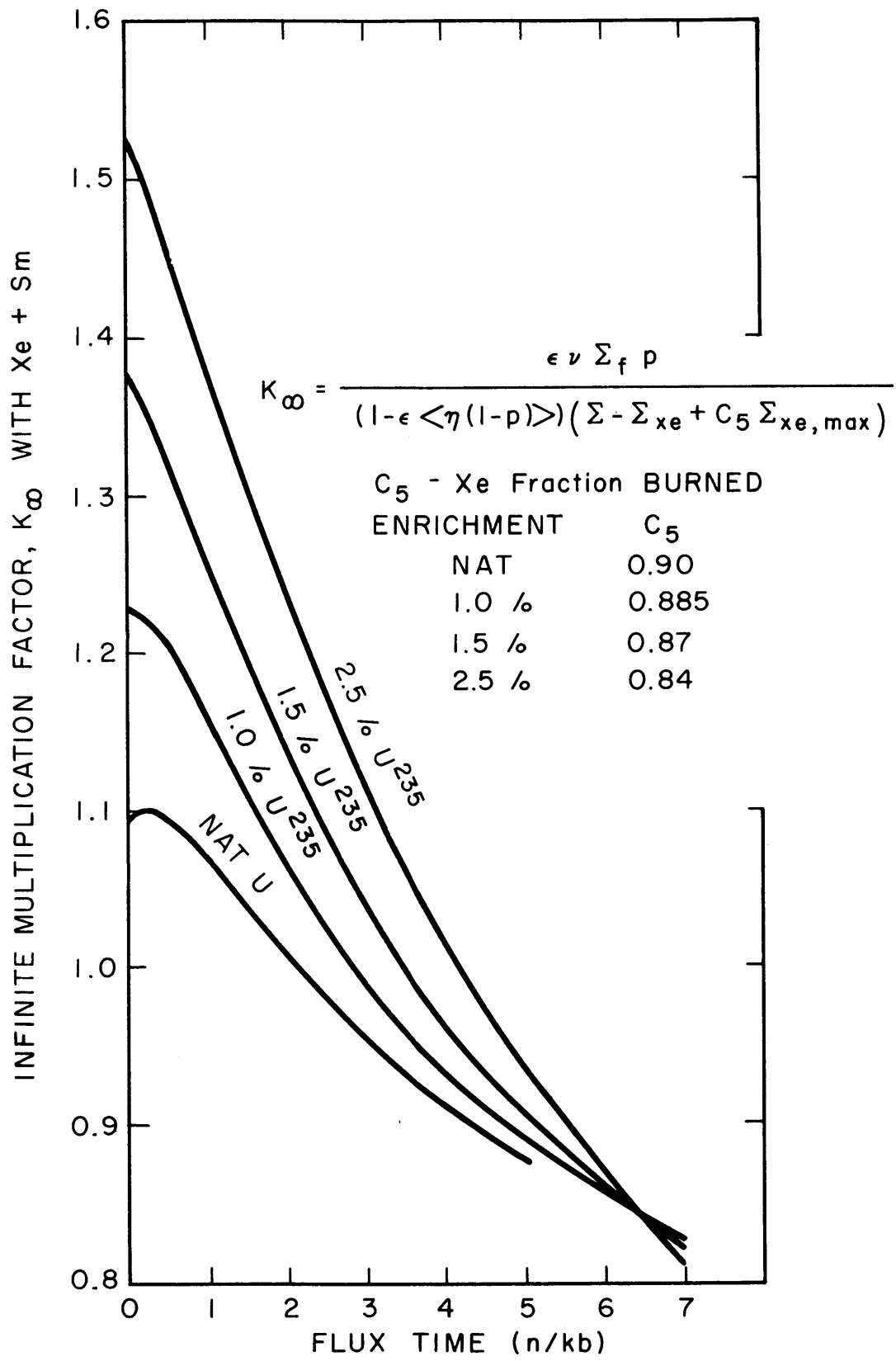
FIG. 3.4   VARIATION OF K_∞ DURING
BURNUP, CANDU REACTOR UNIT
CELL AT VARIUS ENRICHMENTS

25
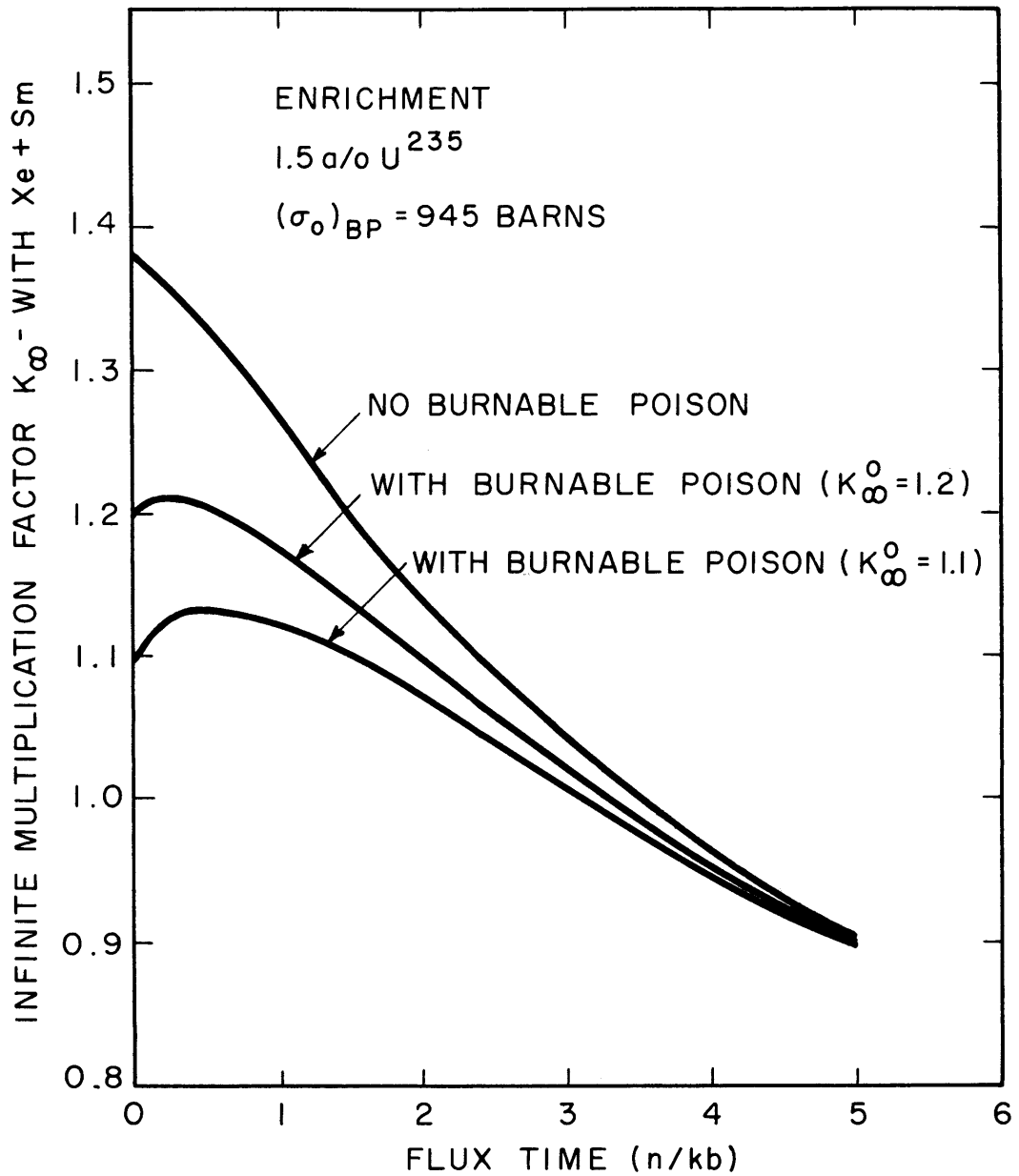
FIG. 3.5 THE FLUX-TIME BEHAVIOR OF K_∞
WITH VARIOUS AMOUNTS OF BURNABLE
POISON AT 1.5 a/o U^{235}

The actual CANDU reactor will use bidirectional fuel management with the reactor divided into two radial zones. In order to flatten the power distribution, the fuel in the inner zone is irradiated to about 1.35 times the burnup of the outer zone. An average burnup of 8850 MWD/T is predicted (H_{42}) when operating at a maximum power density of 17.0 kw/l. The MOVE Code predictions of 9,080 MWD/T and 17.5 kw/l are 2.5% and 3% higher than the reference design values. Figure 3.6 shows a contour plot of the relative power density in the reference design, as predicted by the MOVE Code.

An enrichment survey for the continuous bidirectional fueling technique in CANDU was performed, with the radial variation of discharge burnup specified in one of three ways: uniform discharge burnup, uniform axial velocity of the fuel, or with the radial variation adjusted to obtain minimum peak power density. The results of this survey are summarized in Figures 3.7, 3.8, and 3.9. Figure 3.7 shows the variation of the peak-to-average power density ratio. In general, the vertical differences among the three curves are due to differences in the radial flatness in the three methods of fueling, whereas the variation with enrichment is due to the inherent axial flatness which is characteristic of the enrichment.

Figure 3.8 shows the average burnup as a function of enrichment. The important points to notice here are the burnup penalties associated with the increased flatness obtained with V_z uniform or θ_d for minimum power density, and the fact that the percentage burnup penalty decreases with increasing burnup. Shown in Figure 3.9 are the fuel cycle costs which have a broad minimum in the range between 1.0 a/o and 1.5 a/o enrichment. The sensitivity of these costs to the method of specifying discharge burnup should be noted at each enrichment. The fuel costs for natural uranium are very dependent upon leakage, which increases when the power distribution is flattened. Costs will also be most sensitive at natural enrichment to changes in the amount of absorption in structural materials such as pressure tubes and fuel cladding.

The fuel and power distribution behavior was investigated for the period following the onset of bidirectional fueling. Due to the flatness of the power distribution at the end of batch irradiation, the problem of maintaining the peak-to-average power density ratio at a value less than
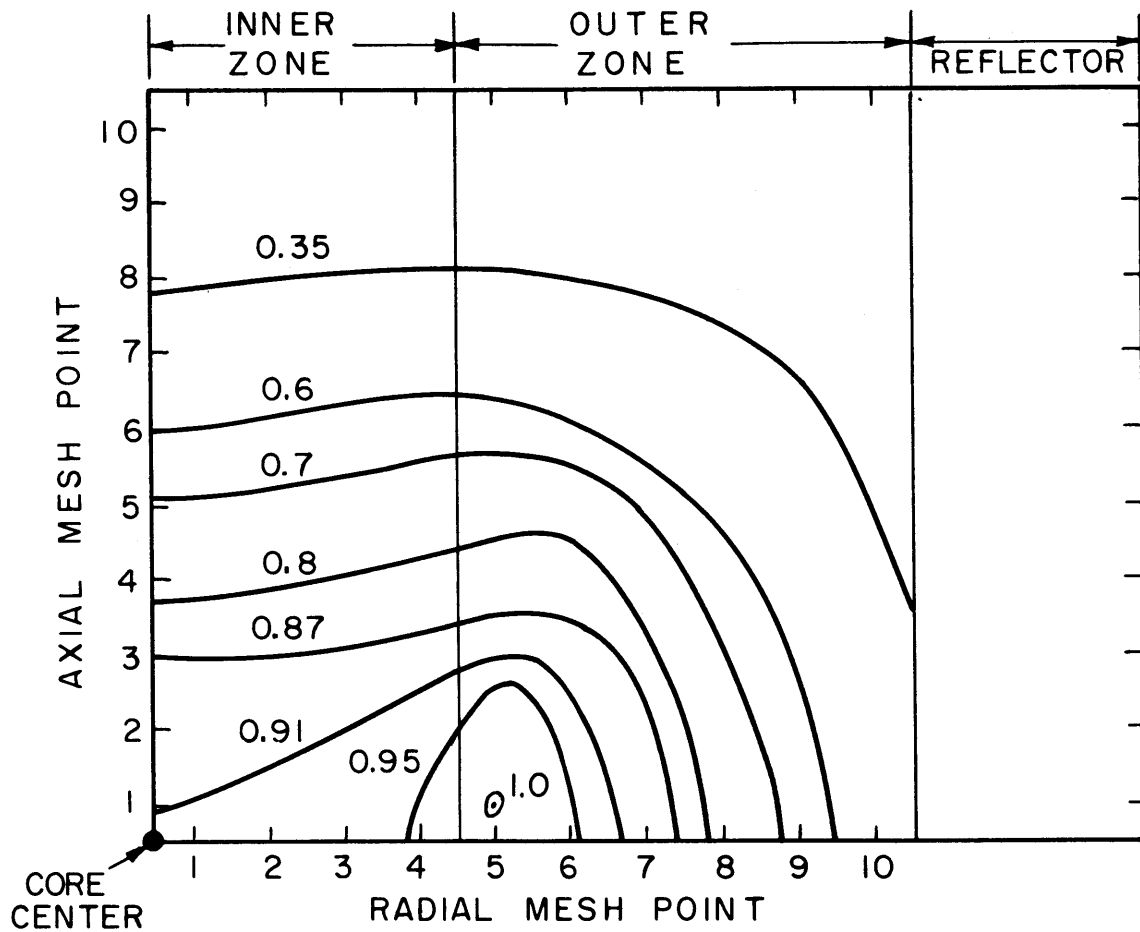
FIG. 3.6 CONTOUR PLOT OF THE RELATIVE POWER DENSITY, CANDU REFERENCE DESIGN
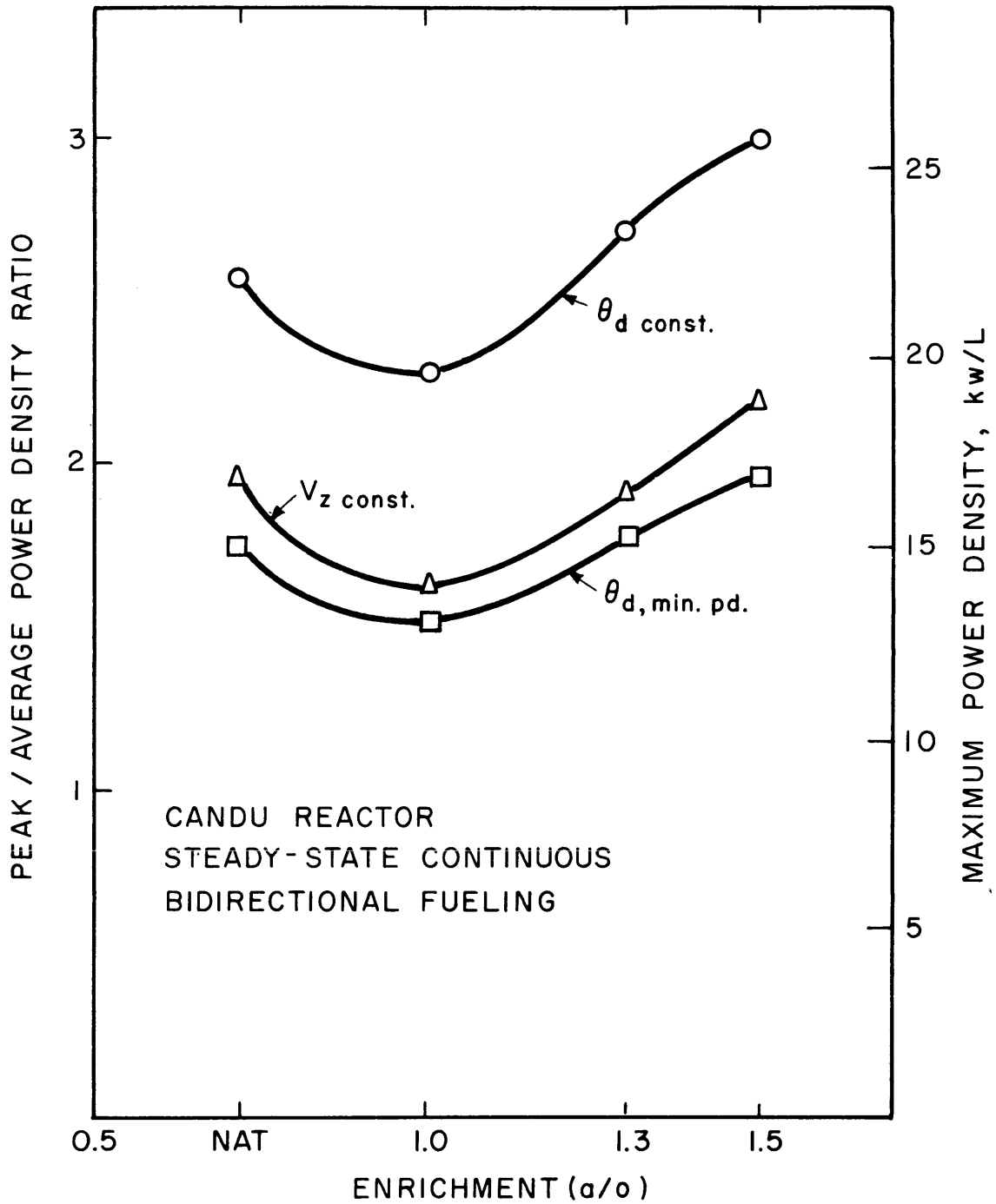
FIG. 3.7 THE PEAK-TO-AVERAGE POWER DENSITY
RATIO IN THE CANDU REACTOR AT
VARIOUS ENRICHMENTS AND RADIAL
SPECIFICATIONS OF DISCHARGE FLUX-TIME
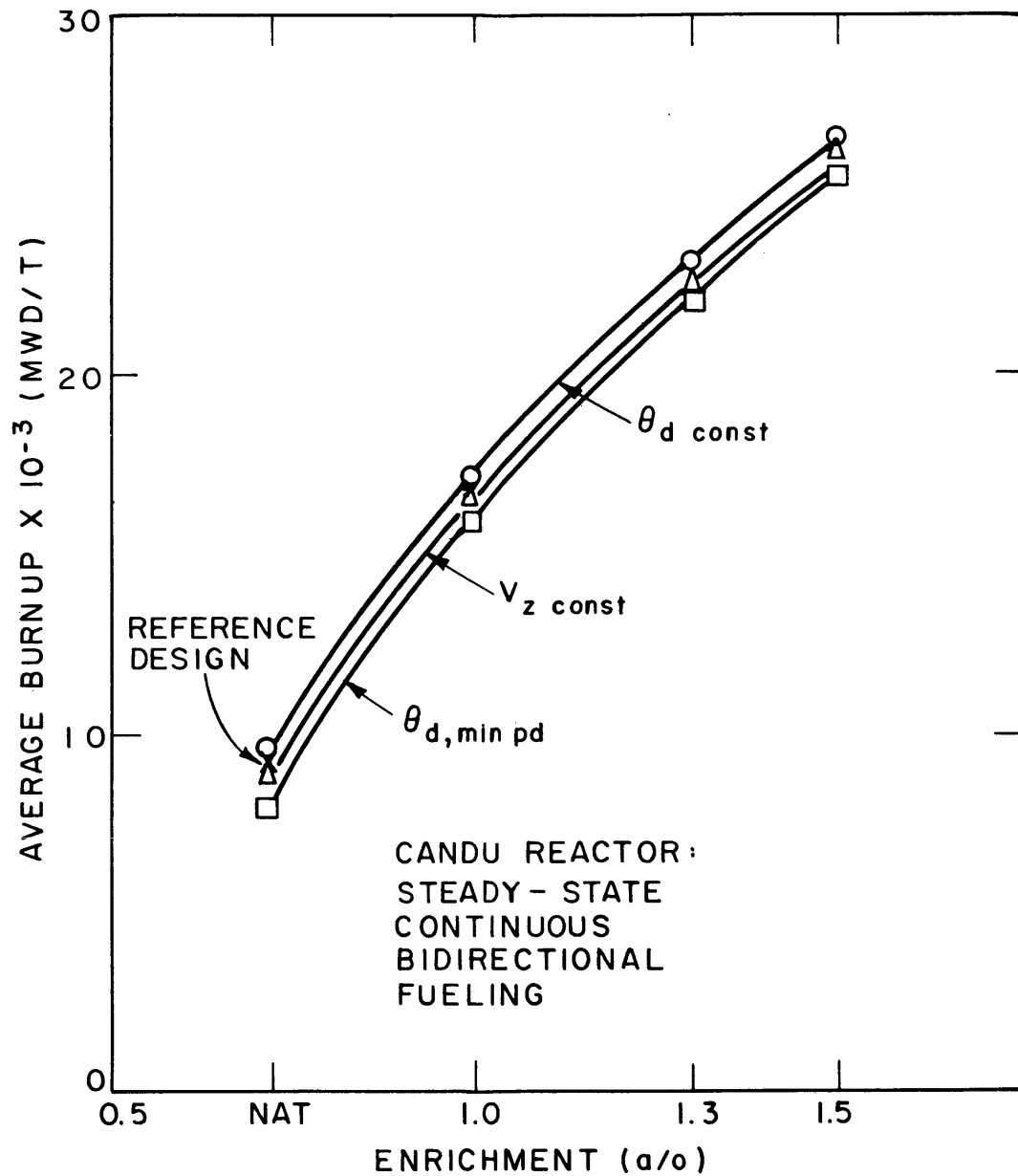
FIG. 3.8 AVERAGE BURNUP IN THE CANDU REACTOR AS
A FUNCTION OF ENRICHMENT FOR VARIOUS WAYS
OF SPECIFYING THE RADIAL SHAPE OF DISCHARGE
FLUX - TIME
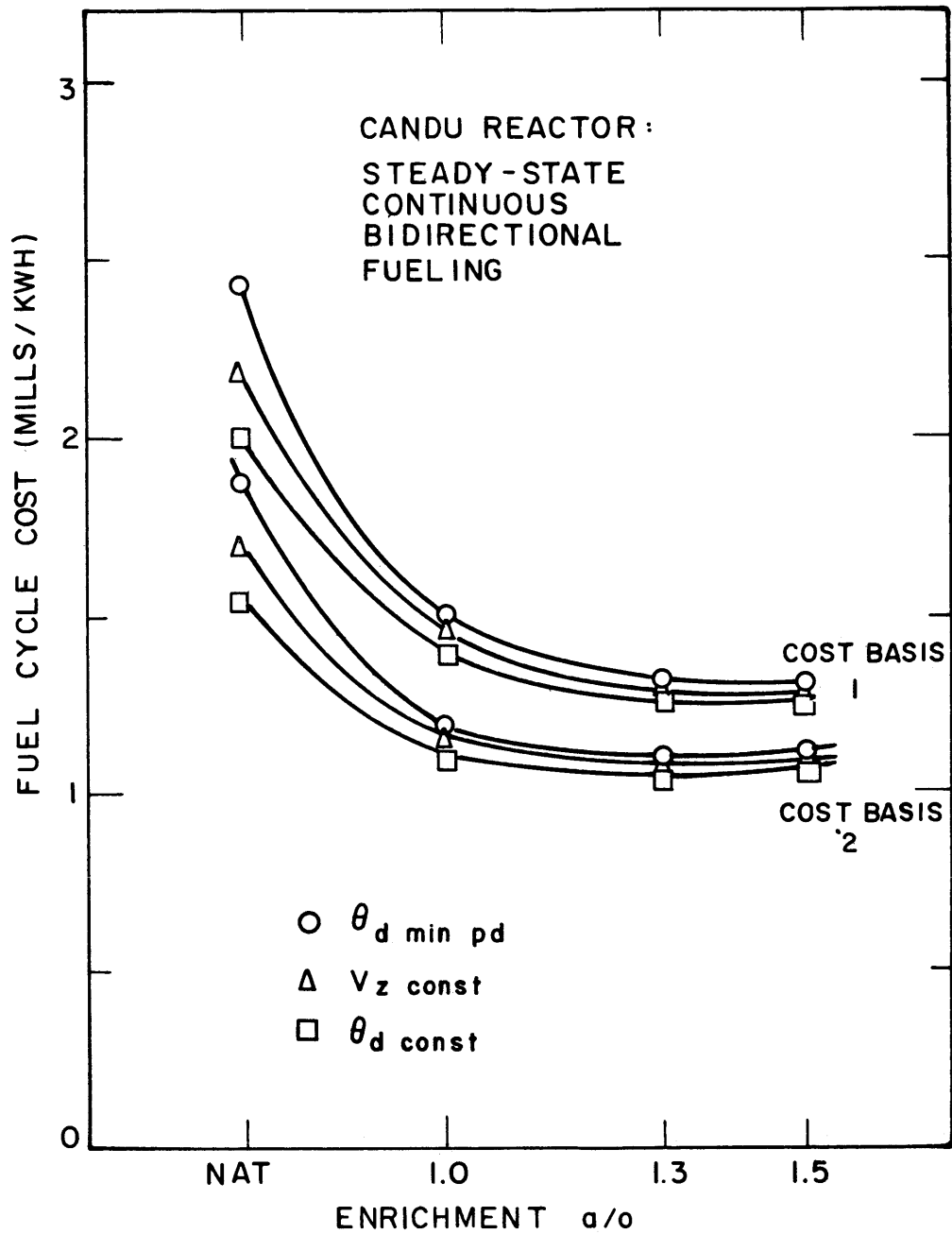
FIG. 3.9 NET FUEL CYCLE COST IN THE CANDU
REACTOR AT VARIOUS ENRICHMENTS AND
RADIAL SPECIFICATIONS OF DISCHARGE
FLUX - TIME

the steady-state ratio is not important until about half the fuel in the initial batch loading is discharged. Even then, the peaking is not severe, although it exceeds the steady-state value by about 10% for a short period.

The important variables considered in batch irradiation, in addition to enrichment, are the spatial distribution and removal of control poison, the use of zones of different enrichment and the use of burnable poison. It became quickly evident for the relatively high enrichments required in batch irradiation, that the best poison removal technique would have to be similar to uniform poison removal, since in axial bank and radial zone poison removal, excessive peaking occurs in the regions from which control poison has been removed. A fair degree of flattening can be obtained and maintained if the outer radial regions have less control poison. The use of zones of different enrichment is not justified on a fuel cost basis, since a single optimum enrichment will yield cheaper fuel costs. The fuel cycle cost is shown in Figure 3.10 for batch irradiation. The enrichment for minimum fuel cycle cost is apparently somewhat higher than 1.75 a/o, although it is doubtful that this high an enrichment would be practical due to the large excess reactivity.

The use of burnable poison is not justified as a means to reduce the total cost of control rods, since burnup losses cost more than any potential savings in control costs. However, the use of burnable poison is definitely justified for reactors which cannot use an optimum enrichment because of control limitations. This can be seen in Figure 3.11 in which fuel cycle cost is plotted against control poison requirement. It is apparent that use of burnable poison would effect substantial fuel cost savings in reactors in which fuel enrichment is limited by a maximum control requirement to a value substantially below an optimum enrichment, in this case 1.75 a/o.

The important problems to be considered with Discontinuous Outin Irradiation are the choice of enrichment, the choice of the number of radial zones, whether to use axial inversion of the fuel, how to control reactivity, and finally, how best to start up the reactor. The choice of the number of zones will be based on the degree to which better fuel

CANDU REACTOR
BATCH IRRADIATION

UNIFORM POISON

COST BASIS 1
COST BASIS 2
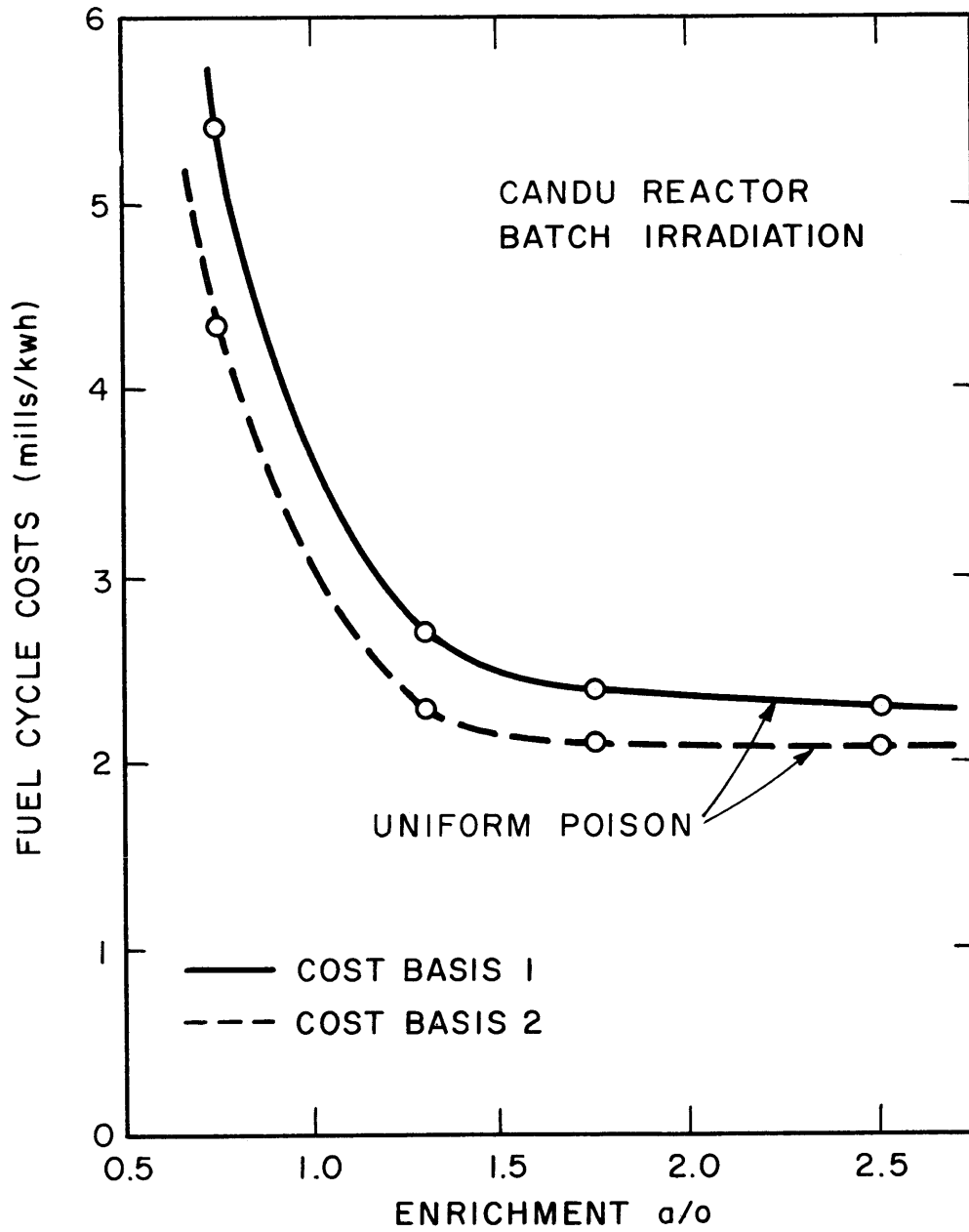
FIG. 3.10   NET FUEL CYCLE COST AS A
FUNCTION OF ENRICHMENT
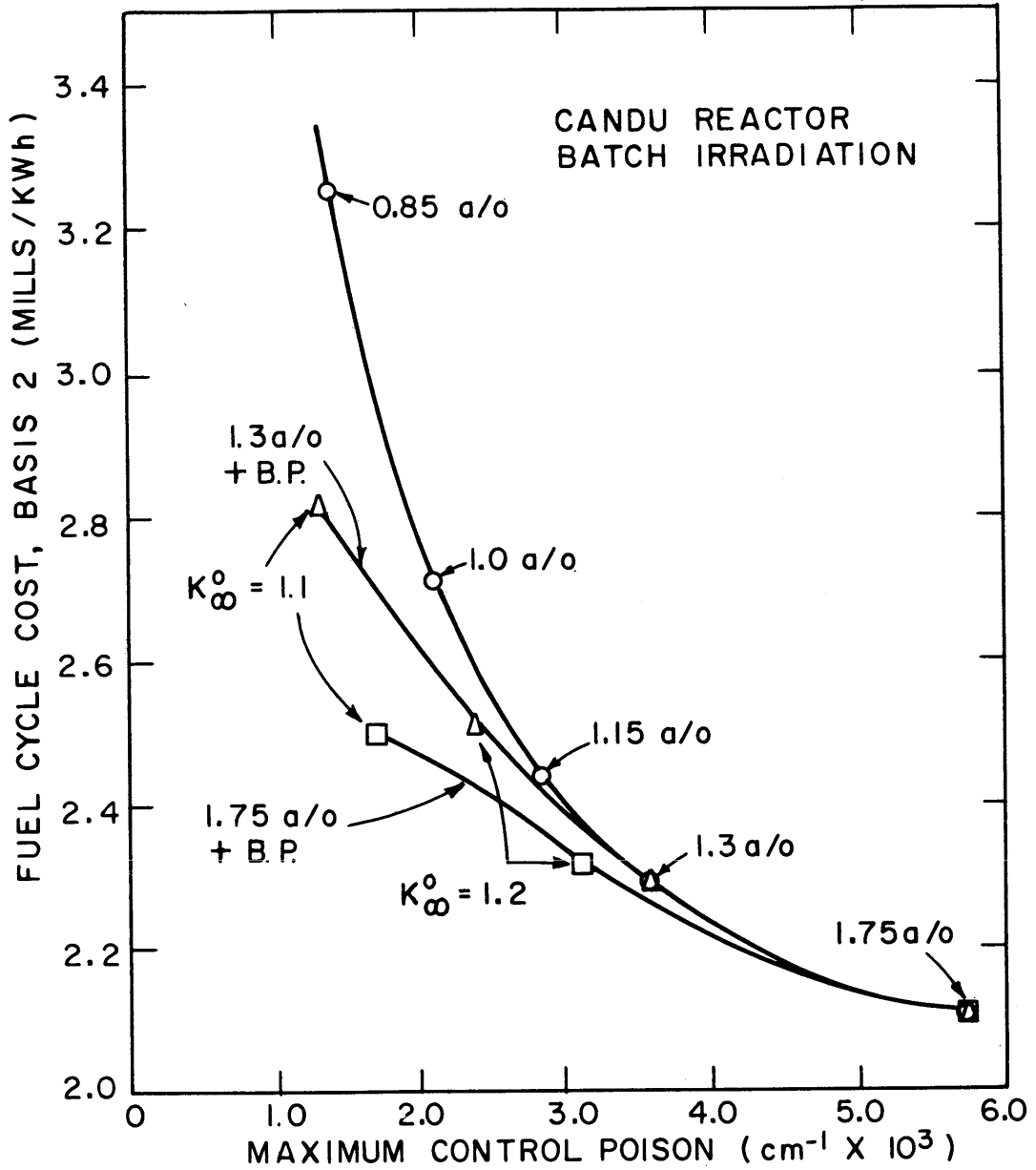
FIG. 3.11 GRAPH ILLUSTRATING THE USE OF BURNABLE
POISON IN CONTROL LIMITED REACTORS

34

burnup and declining control requirement is offset by increased fueling down-time and the increased amount of spent fuel handling as the number of zones is increased. Generally, two or three zones will result in the best over-all performance. The use of axial inversion with two radial zones is completely unjustified due to excessive flux peaking. However, axial inversion with three zones has definite promise since increased burnup is obtained, although there is more flux peaking than if no axial inversion were used. In steady-state operation, the fuel in the central zones, being partially depleted, requires less control. Hence, the spatial distribution of control poison should be such that the majority of the control rods will be in the outer zones. Here again, a poison removal technique which is similar to uniform poison removal will give the least peaking difficulty.

The problem of starting up the discontinuous outin fueling technique will be resolved by resorting to the least costly of two alternative methods. In the first, the steady-state control system is used, and the central regions are charged with fuel of an enrichment which is equivalent in reactivity to the fuel which will be moved into those zones in the steady-state. In the second, the reactor is loaded uniformly with fuel and extra control is provided in addition to the steady-state control requirement. In the second case, the extra control will be used only once, on startup, and fuel costs will be smaller than in the first case. In the first case, however, the steady-state is reached more quickly, without the expense of the extra control. Under the assumptions of this study, it is probably cheaper to use the first alternative, since burnup losses were smaller than the probable cost of additional control.

With regard to fuel enrichment, Figure 3.1 2 shows the total energy cost as a function of enrichment for reactors optimized for steady-state operation. The minimum total energy cost is seen to occur between 1.3 and 1.5 a/o. The flattest power distributions are found at these enrichments, which permits use of the smallest core volumes. The minimum _fuel_ cost occurs near 1.75 a/o enrichment.

The continuous graded and outin methods of fueling were also studied for the CANDU reactor, although no emphasis is put on these techniques as practical operating procedures.

COST BASIS 2

CANDU REACTOR
2-ZONE DISCONTINUOUS
OUTIN IRRADIATION
POWER : 200 MWE
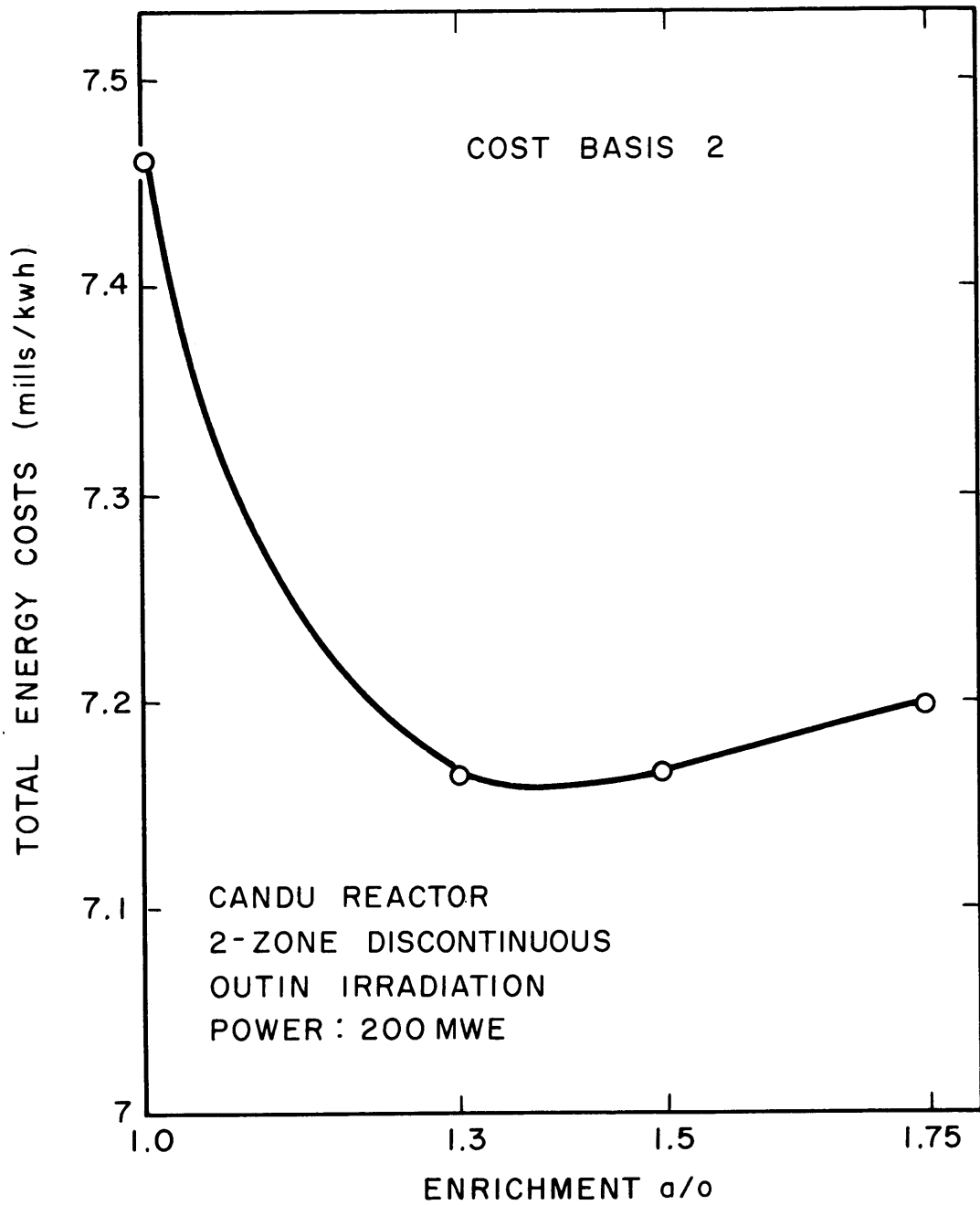
FIG. 3.12   THE VARIATION OF TOTAL ENERGY COST
WITH ENRICHMENT FOR REACTORS AT
CONSTANT OUTPUT AND FIXED PEAK
POWER DENSITY IN STEADY
STATE OPERATION

36

A comparison of the three important fuel and poison management techniques that are emphasized in this study is given in Figures 3.13 and 3.14. Figure 3.13 shows that the total energy cost decreases with improving neutron economy going from batch, to discontinuous outin to continuous bidirectional fueling. The enrichment at minimum cost also is lower, the better the neutron economy. A basic assumption in this graph is that the end-of-life is determined by criticality criteria only. Figure 3.14 shows the same basic data except that here, the end-of-life is governed by a maximum permissible fuel burnup, with the enrichment picked so that the criticality end-of-life will coincide with the maximum burnup end-of-life. The advantages of the better neutron economy fuel management techniques are still evident at any specified maximum burnup.
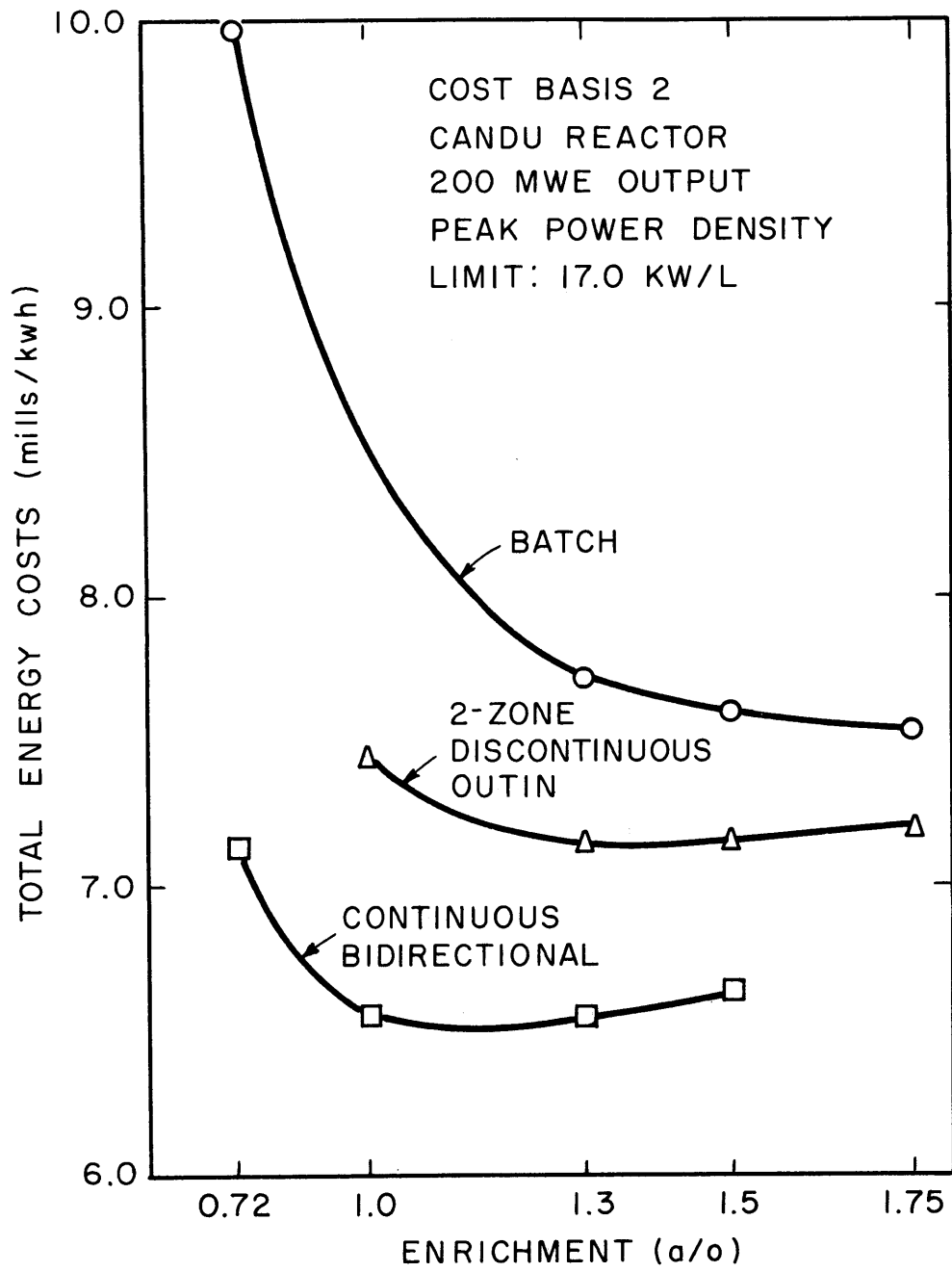
FIG. 3.13   THE TOTAL ENERGY COST AS A
FUNCTION OF ENRICHMENT FOR
VARIOUS FUEL AND POISON
MANAGEMENT TECHNIQUES
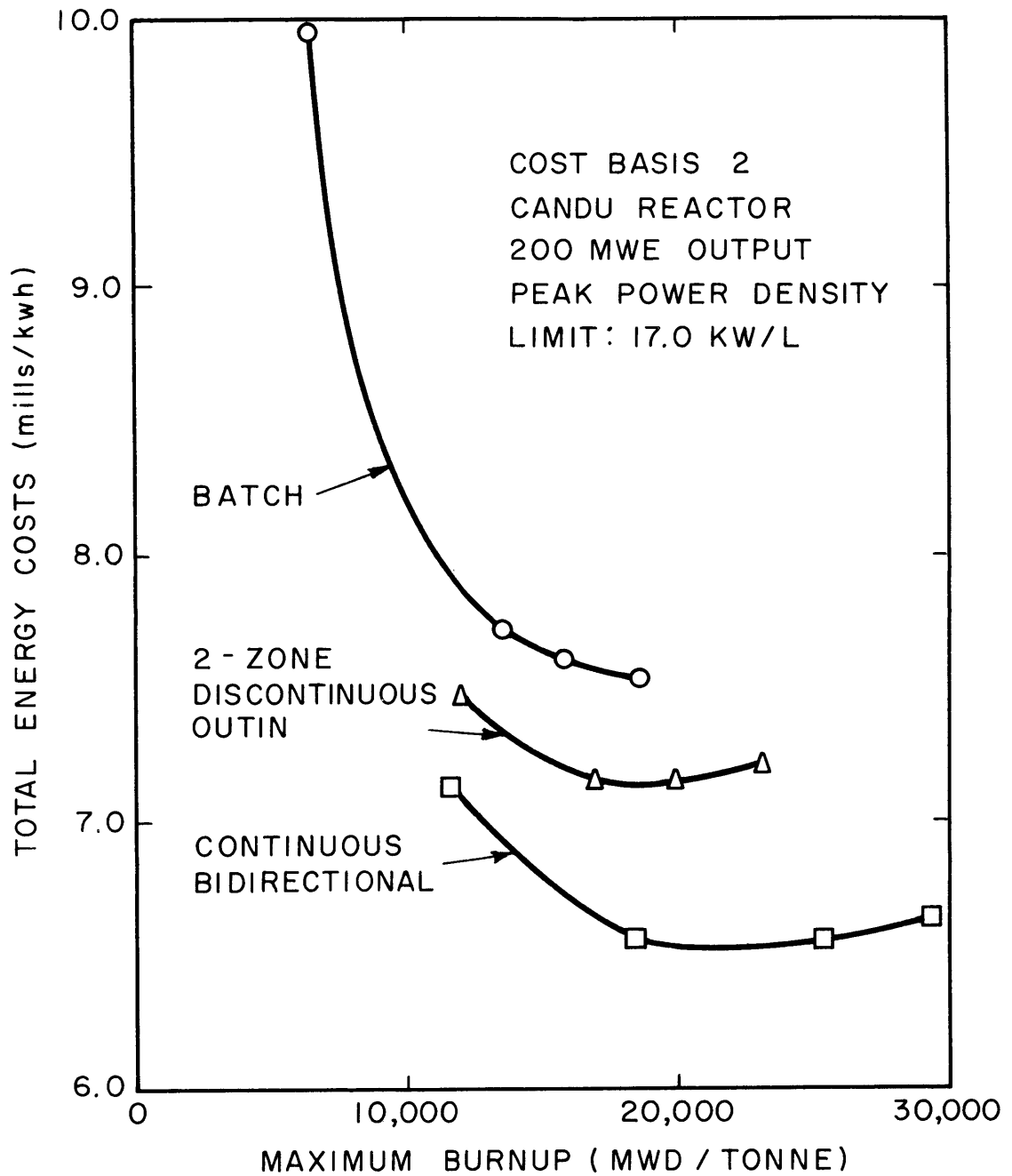
FIG. 3.14   TOTAL ENERGY COST AS A FUNCTION
OF MAXIMUM BURNUP FOR VARIOUS
FUEL AND POISON MANAGEMENT
TECHNIQUES

39

CHAPTER IV

FUELMOVE CODE DESCRIPTION AND CALCULATIONAL TECHNIQUES

A. INTRODUCTION

The FUELMOVE Code approaches the problems of fuel and poison management in the following way. The homogenized reactor unit cell properties are evaluated as a function of flux time. Then, representing fuel by its flux-time, and fuel transfer by flux-time transfer, the reactivity and power histories of various fuel movements can be obtained and used to evaluate energy costs.

The above calculation falls naturally into two separate parts. Because of this, it is both convenient and conservative of computer time to divide the FUELMOVE Code into two sections:

1. The FUEL Code calculates the unit cell properties as a function of flux-time and transfers the results to magnetic tape and/or punched cards.

2. The MOVE Code, using the output of the FUEL Code, calculates macroscopic core properties such as flux and power during operation, moves fuel in various ways and adjusts control poison for criticality, and when spent fuel is discharged, computes burnup and energy cost.

A description of the basic features and calculational techniques of each part of the FUELMOVE Code follows.

B. THE FUEL CODE

1. Introduction

This part of FUELMOVE calculates nuclide concentrations and various criticality properties of the reactor unit cell as a function of flux-time.

As input data, it is given initial fuel nuclide concentrations, flux disadvantage factors, fuel volume fraction, and the absorption and slowing down properties of the moderator (non-fuel) region, along with certain other parameters which are necessary to give the initial neutron balance within a unit cell. Hence, if experimental reactivity data is available, it is possible to match the initial code-calculated reactivity with experimentally determined values.

Using the input data, along with basic nuclear data which have been written into the code, the thermal neutron spectrum is evaluated, from which effective cross sections are obtained. Using nuclide concentrations and these effective cross-sections, reaction rates are obtained, and these are used to evaluate new nuclide concentrations and properties, a specified flux-time step away.

This process is repeated in step-wise fashion, evaluating nuclide concentrations and criticality properties at each step until a specified number of steps have been made. The results can be obtained in printed form, on punched cards and/or on magnetic tape all under input control option. These results will be used as input data for the MOVE Code.

Two basic assumptions have been made in the technique outlined above. The first is that the reactor unit cell can be effectively represented by a volume-flux weighted homogenized equivalent. This appears to be justified in view of the reasonable agreement between experimental concentrations and reactivities and those predicted using the homogenized unit cell model. The success of this

41

relatively crude model suggests that the errors due to a neutron behaviour model may be less than those due to uncertainties in basic nuclear data, such as cross sections and fission neutron yields.

The second assumption is that the nuclide concentrations and unit cell properties are a function of flux-time, but are independent of flux magnitude and past flux history. Flux magnitude dependence occurs when the decay rate of some important nuclide is of the same order as its burnup rate, which is proportional to flux. Xenon 135 has this characteristic, but fortunately its decay and absorption products do not differ enough in effect to cause any difficulty and Xe absorptions can be obtained as a flux-dependent fraction of the flux-independent maximum. In the U^{238}-Pu conversion chain, Np^{239} has a decay half-life which is too short relative to its absorption cross section to cause any appreciable dependence on flux magnitude. Therefore, it has been assumed that U^{238} is converted directly to Pu^{239}. Pu^{241} has a decay half-life which is long relative to its cross section, but at low fluxes a small fraction of Pu^{241} decays, thereby being removed from the Pu chain. This small effect is allowed for by computing the ratio of decay of Pu^{241} to burnout for an assumed average flux, which effectively removes flux dependence from the U^{238}-Pu chain.

A source of dependence on fast flux history is the dependence of resonance reaction rates on the fast non-leakage probability. This does not create serious difficulty provided the reactor has a small resonance reaction rate compared to thermal, or if an accurate estimate of the fast non-leakage probability is available and remains relatively constant during fuel burnup. Since FUEL-MOVE has been written to study large thermal power reactors in which fast leakage is small, the fast flux history dependence should give no difficulty. Smaller reactors are not so amenable to treatment by the FUELMOVE Code since they tend to be more epithermal,

and also because they are usually highly reflected, so that the reflector savings treatment used in FUELMOVE is inaccurate.

In the sections below, further detail is given on various aspects of the neutron behavior model, which is a modification and extension of that used by Shanstrom in FUELCYC (S41). First the energy behavior is described, with details on both the thermal and resonance regions. The nuclide concentration equations are then developed and the properties dependent on flux-time are obtained.

2. The Neutron Cycle

Figure 4.1 shows the energy model of the neutron cycle. In it, fission neutrons are produced in thermal and resonance absorption and are multiplied by fast fission in U^{238}. The slowing down process starts and it is assumed that all fast leakage takes place before slowing down into the resonance region. In the resonance region, concurrent absorptions occur in the U^{235}, U^{238}, Pu^{239}, Pu^{241} and fission product resonances, with neutron production in the U^{235}, Pu^{239} and Pu^{241} resonances. Following this, successive resonance absorptions occur in U^{236}, Pu^{242}, Pu^{240} and burnable poison, if any. Resonance absorptions in non-fuel materials, such as cladding, are not treated as part of the resonance reactions, but have been included as a part of the moderator region thermal reactions.

Following the resonance region, neutrons enter the thermal region where they undergo absorption or leakage. The MOVE Code does not require any estimate of thermal leakage or control poison absorption, but it is implicit in closing the neutron cycle in Figure 4.1 and in equating slowing down density to thermal absorption plus leakage, that the unit cell has an effective multiplication factor of unity, which will be the situation in all studies made by the MOVE Code.

The FUEL Code does require an estimate of P_1, the fast

PRODUCTION   ABSORPTION   LEAKAGE

$$\frac{q}{\epsilon}\left(\frac{\epsilon\eta_8-1}{\eta_8-1}\right)$$

$$\frac{q}{\epsilon}\frac{(\epsilon-1)\eta_8}{(\eta_8-1)}$$

FAST EFFECT IN U-238

$$\frac{q}{\epsilon}\left(\frac{\epsilon-1}{\eta_8-1}\right)$$

$$q=\frac{\epsilon\nu\Sigma_f\phi}{1-\epsilon P_1<(1-p)\eta>}$$

q/ϵ

Ⓐ   FAST LEAKAGE

$q(1-P_1)$
$$=-D_1\nabla^2\phi_1$$

$$q_1=qP_1=\Sigma_1\phi_1$$

Ⓒ

RESONANCE ABSORPTION IN U238, U235, Pu239, Pu241, AND FISSION PRODUCTS

$qP_1<(1-p)\eta>$

$qP_1(1-p_5p_8p_9p_{11}p_7)$

$$q_2=q_1p_5p_8p_9p_{11}p_7$$

RESONANCE ABSORPTION IN U-236

$q_2(1-p_6)$

$$q_3=q_2p_6$$

RESONANCE ABSORPTION IN Pu 242

$q_3(1-p_{12})$

$$q_4=q_3p_{12}$$

RESONANCE ABSORPTION IN Pu 240

$q_4(1-p_{10})$

$$q_5=q_4p_{10}$$

RESONANCE ABSORPTION IN BURNABLE POISON

$q_5(1-p_{13})$

$$q_6=q_5p_{13}=qP_1p=p\Sigma_1\phi_1$$

$\nu\Sigma_f\phi$

Ⓑ   THERMAL ABSORPTION AND LEAKAGE

$-D\nabla^2\phi$

$(\Sigma+\Sigma_w)\phi$

FIG. 4.1 THE NEUTRON CYCLE

44

non-leakage probability, in order to evaluate the proper resonance reaction rate. This estimate can be obtained in any reasonable way, such as Fermi Age Theory or, if available, a number obtained from a MOVE Code test case could be employed.

The nuclide notation and subscripting appearing in Figure 4.1 is that used throughout the FUELMOVE Code. In it, 5, 6 and 8 represent U^{235}, U^{236} and U^{238}, respectively; 7 or FP refers to fission products; 9, 10, 11 and 12 refer to Pu^{239}, Pu^{240}, Pu^{241} and Pu^{242}; and 13 is burnable poison. The subscripts 1, 2, 3 and 4 are used to represent the fission properties of U^{238} fast fission, U^{235}, Pu^{239} and Pu^{241}, respectively.

3. The Thermal Region

In order to obtain reaction rates in the thermal region, effective cross sections must be obtained. This is done by calculating a hardened neutron spectrum and averaging the cross sections over this spectrum.

3.1 The Neutron Spectrum

The thermal neutron flux spectrum for the homogenized unit cell is calculated from the Wilkins equation:

$$x^2 \frac{d^2Y}{dx^2} + (2x^3 - 3x)\frac{dY}{dx} + (2x^2 - 4x^2 A(x) + 3)Y = 0 \qquad (4B1)$$

where x, the normalized velocity at energy E is given by

$$x = (E/kT_{mod})^{1/2} \qquad (4B2)$$

kT_{mod} is neutron energy at moderator temperature T_{mod}

Y, the flux per unit velocity,

is $\frac{d\phi}{dx}$

45

A(x), the hardening parameter at normalized velocity, x,

$$\text{is } \Sigma_a(x) \Big/ \xi \Sigma_s$$

$\Sigma_a(x)$ is the total homogenized macroscopic absorption cross section, evaluated at normalized velocity, x.

$\xi \Sigma_s$ is the slowing down power of the unit cell.

The Wilkins spectrum reduces to a $1/E$ flux per unit energy at large x, (high energy) for essentially $1/v$ absorbers, and reduces to the Maxwell Boltzman spectrum at low energies in the case of zero absorption. The numerical method of solution involves a series solution of the equation at low energy to provide startup values for a fifth order Milne solution of the flux at subsequent points. This is fully described in S41.

In order to evaluate the hardening parameter, A(x), it is necessary to know the microscopic cross section at each x for all nuclides in the unit cell.

3.2 The Energy Dependence of Thermal Cross Sections

A convenient method for the evaluation of certain important cross sections as a function of velocity or energy has been provided by Westcott (W41) who has tabulated the parameters a, b, c and e for use in the Breit-Wigner equation

$$\sigma(E) = \frac{1}{\sqrt{E}} \left\{ a + \sum_{i=1}^{7} \frac{c_i}{b_i + (E-e_i)^2} \right\} \text{ barns} \qquad (4B3)$$

This equation is used for U^{235}, Pu^{239} and Pu^{241} fission and absorption, and Pu^{240} and Pu^{242} absorption. In the thermal region, U^{236}, U^{238}, the fission products, burnable poison, and moderator cross sections are treated as $1/v$ absorbers.

3.3 Effective Thermal Cross Sections

Having obtained the microscopic cross sections at each x, the hardening parameter A(x) in the Wilkins equation is obtained and the flux spectrum can now be generated. The effective thermal cross sections are then calculated by means of simple spectrum weighting over the range from zero to the upper energy limit, E_c, which is specified as input to the code.

$$\bar{\sigma} = \frac{\int_0^{E_c} \frac{d\phi}{dE} \sigma(E) dE}{\int_0^{E_c} \frac{d\phi}{dE} dE} \text{ barns} \tag{4B4}$$

The $1/v$ cross sections of materials such as burnable poison, initial fission product and the moderator cross sections are obtained from

$$\bar{\sigma} = \sigma_0 \left(\frac{v_0}{\bar{v}}\right) \text{ barns} \tag{4B5}$$

where σ_0 is the 2200 m/s value, obtained as input data.

$v_0/\bar{v}$ is evaluated from the effective U^{238} cross section.

$v_0/\bar{v} = \bar{\sigma}_8/2.72$.

v_0 = 2200 m/s.

$\bar{v}$ = average neutron velocity.

As a matter of interest, the neutron temperature, t_{neut}, is also calculated from

$$v_0/\bar{v} = \frac{\pi}{4} \sqrt{\frac{T_0}{t_{neut} + 273.2}} \tag{4B6}$$

or $t_{neut} = \frac{\pi}{4} \times 293.7 \, (\bar{v}/v_0)^2 - 273.2^{\circ}C.$ (4B7)

3.4 Other Nuclear Data Used in the FUEL Code

Table 4.1 gives the normalization of the cross sections used, plus the other basic nuclear data written into the FUEL Code. These values are World Weighted Average values as tabulated in W41.

3.5 Definition of Flux and Flux-time

In the FUELMOVE Code the flux, ϕ, is defined as the average thermal flux in the fuel, and flux-time is the time integral of this average thermal flux.

An alternative system is used at Chalk River and Harwell. Here flux, ϕ_0, is defined as thermal plus epithermal neutron density times v_0, 2200 m/sec. Flux-time is the time integral of this 2200 m/s flux.

The relationship between these two conventions is of interest when comparing results obtained in each system, and is also used in the FUEL Code when calculating fission product cross sections as a function of flux-time.

The relationship between ϕ and ϕ_0 is given by

$$\phi = \phi_0 \frac{n_{th}}{n_{th} + n_{epi}} \left(\frac{\bar{v}}{v_0}\right)$$ (4B8)

where n_{th} is the density of thermal neutrons,

n_{epi} is the density of epithermal neutrons,

and $\bar{v}/v_0$ was obtained in the previous section.

The flux-times are related in the same manner.

The epithermal neutron density is obtained, assuming a 1/E

48

TABLE 4.1 NUCLEAR DATA

Nuclide	σ_{2200}, barns	Inf. Dilution Res. Integral RI^{∞}, barns	α	ν	Fission Yields	
					y_{Xe}	y_{Sm}
U^{235}(abs)	683.04	370	0.365 (res)	2.45	0.064	0.01649
U^{235}(fiss)	581.95	271				
U^{236}(abs)	7.00	257				
U^{238}(abs)	2.72	282				
U^{238}(fast f)			0.0687 (fast)	2.60	0.06	0.03154
Pu^{239}(abs)	1029.1	478.5				
Pu^{239}(fiss)	742.15	319	0.5 (res)	2.885	0.053	0.03315
Pu^{240}(abs)	277.87	8350				
Pu^{241}(abs)	$1.3765\sigma_{f,11}$	781				
Pu^{241}(fiss)	1015.2	567.5	0.3765 (res)	3.06	0.061	0.035
Pu^{242}(abs)	30.09	1015				

$T_{1/2}$, Xe = 9.13 hr.

$T_{1/2}$, Pu^{241} = 13.2 yr.

epithermal flux, and a slowing down density qP_1 from

$$\frac{n_{epi}}{n_{th}} = 2\sqrt{\frac{E_0}{E_c}}\ (\frac{\bar{v}}{v_0})\ \frac{qP_1}{\xi\Sigma_s\phi} \tag{4B9}$$

where E_c is the thermal cutoff energy, (0.45 ev) and

E_0 = 0.0253 ev.

3.6 The Treatment of Fission Products

Fission products are classed as belonging to one of three groups. Xenon is in a group by itself, since its effective cross section depends on flux. The remaining fission products with cross sections greater than 10,000 barns are in a group called the Samarium group. The members of this group have decay half lives which are long enough relative to their cross sections so that their effective cross sections are equal to the actual values.

These first two groups are said to saturate, since their macroscopic cross sections reach an equilibrium in which production rates equal destruction rates of the high cross section fission products.

The third group contains all fission products whose cross sections are less than 10,000 barns. These fission products do not saturate, but accumulate during burnup, their accumulation being one of the main effects which impose reactivity limits on fuel burnup. The macroscopic absorption cross section of this group is given by

$$\Sigma_{FP} = N_{FP} \cdot \sigma_{FP}$$

$$(N_{FP} \equiv N_7)$$

where N_{FP} is the fission-product-pair concentration and σ_{FP} is the average cross section per fission product pair. This average

50

cross section, since it is an average over many fission product nu-
clides, will be made up of some large and some small cross section
materials. The largest cross section material has the largest prob-
ability of absorbing a neutron; and, when it does, the resulting nu-
clide tends to have a lower cross section, this being a consequence
of pairing the unpaired nuclear neutron which is often the cause of
the large cross section. Hence, the average cross section of a
fission product pair tends to drop during irradiation.

A convenient technique for representing this decreasing cross
section has been proposed by Hurst (H43). If a <u>batch</u> of fission
products is irradiated, the effective 2200 m/s cross section is given
as a function of the 2200 m/s flux-time, θ_0 , by

$$\hat{\sigma}_{FP}(\theta_0) = y_1 \sigma_1 e^{-\sigma_1 \theta_0} + y_2 \sigma_2 e^{-\sigma_2 \theta_0} + y_3 \sigma_3 e^{-\sigma_3 \theta_0} \tag{4B10}$$

The quantities y_i and σ_i are the yields and cross sections
of three pseudo fission products. These are chosen to give the best
fit to data obtained in a detailed study of the various neutron absorp-
tion chains of the fission products from the different fissile nuclides.

The above pseudo-yield and -cross section data can be used
to obtain the cross sections when the fission products are not irradi-
ated batchwise, but build up in any given manner. This is done from
the equation

$$\sigma(\theta_0) = \int_0^{\theta_0} \hat{\sigma}(\theta_0 - \theta_0') \frac{1}{N_{FP}} \frac{dN'_{FP}}{d\theta_0'} d\theta_0' \tag{4B11}$$

For fission products from U^{235}

$$\frac{1}{N_{FP}} \frac{dN'_{FP}}{d\theta_0'} d\theta_0' = \hat{\sigma}_5 \frac{e^{-\hat{\sigma}_5 \theta_0'} d\theta_0'}{1 - e^{-\hat{\sigma}_5 \theta_0}} \tag{4B12}$$

51

where $\hat{\sigma}_5$ is effective 2200 m/sec. absorption cross section.

Solving (4B11) for U^{235} fission products

$$\sigma(\theta_0) = \sum_{i=1}^{3} y_i \sigma_i e^{-\sigma_i \theta_0} \frac{\hat{\sigma}_5}{\hat{\sigma}_5 - \sigma_i} \frac{1 - e^{-(\hat{\sigma}_5 - \sigma_i)\theta_0}}{1 - e^{-\hat{\sigma}_5 \theta_0}} \qquad (4B13)$$

Note that Eq. (4B13) also applies to fission products from exponential burnout of initial Pu^{239}.

For fission products from Pu^{239} for the case where there is no initial Pu in the fuel,

$$\frac{1}{N_{FP}} \frac{dN'_{FP}}{d\theta'_0} d\theta'_0 = \frac{\hat{\sigma}_9 (1 - e^{-\hat{\sigma}_9 \theta'_0}) d\theta'_0}{(\hat{\sigma}_9 \theta_0 - (1 - e^{-\hat{\sigma}_9 \theta_0}))} \qquad (4B14)$$

Solving (4B11) for Pu^{239} fission products,

$$\sigma(\theta_0) = \sum_{i=1}^{3} y_i \sigma_i \left\{ \frac{\frac{\hat{\sigma}_9}{\sigma_i}(1 - e^{-\sigma_i \theta_0}) - \frac{\hat{\sigma}_9}{\sigma_9 - \sigma_i}(e^{-\sigma_i \theta_0} - e^{-\hat{\sigma}_9 \theta_0})}{\hat{\sigma}_9 \theta_0 - (1 - e^{-\hat{\sigma}_9 \theta_0})} \right\} \qquad (4B15)$$

The following data for the pseudo yields and cross sections of fission products from U^{235} and Pu^{239} is taken from C41. These are the values for batch irradiation (Eq. 4B10).

	σ_1	$y_1 \sigma_1$	σ_2	$y_2 \sigma_2$	σ_3	$y_3 \sigma_3$
U^{235}	25	21.30	300	34.11	600	-7.74
Pu^{239}	25	30.50	300	57.81	600	-27.36

In order to use these data in the practical situations

represented by Eq. (4B13) and (4B15), a fit was made at 3 points, $\theta_0 = 0$, 3n/kb and 7n/kb in the form

$$\sigma_{FP}(\theta_0) = A_1 e^{-25\theta_0} + A_2 e^{-300\theta_0} + A_3 e^{-600\theta_0} \qquad (4B16)$$

The parameters obtained for A are given below

	A_1	A_2	A_3
$U_{FP}^{235}(\hat{\sigma}_5 = 683)$	23.75	45.08	-21.16
$Pu_{FP}^{239}(\hat{\sigma}_9 = 1402)$	31.63	68.53	-39.22 ($N_9(0) \neq 0$)
$Pu_{FP}^{239}(\hat{\sigma}_9 = 1402)$	52.81	23.69	-15.55 ($N_9(0) = 0$)

The FUEL Code is capable of treating any combination of the following types of fission products.

Fission products from (1) exponential burnout of initial U^{235}

(2) exponential burnout of initial Pu^{239}

(3) exponential buildup of Pu^{239}

(4) batch irradiation of initial U^{235}
and Pu^{239} fission products.

The last group is evaluated by assuming equal amounts of U^{235} and Pu^{239} fission products whose characteristics are those of a mixture irradiated to 2n/kb.

Once the effective 2200 m/s fission product cross section has been obtained, the average value is computed from

$$\bar{\sigma}_{FP} = \sigma_{FP} \frac{v_0}{\bar{v}}$$

In the actual computation, it is assumed that all fission products which are not from U^{235} have the characteristics of Pu^{239}.

The Pu^{239} group then includes fast fission in U^{238} and Pu^{241} fission products.

Resonance integrals for fission products from U^{235} and Pu^{239} can be supplied as input data. These initial values are assumed to change during irradiation in the same manner as the thermal cross sections and are obtained from the formula

$$\frac{RI_{FPi}(\theta)}{RI_{FPi}(0)} = \frac{\sigma_{FPi}(\theta)}{\sigma_{FPi}(0)} \qquad i = 5, 9$$

The fission product resonance integrals that have been used in this study were obtained from B42. These are 181 barns and 264 barns for the fission products from U^{235} and Pu^{239} respectively.

4. The Resonance Region

Referring to Figure 4.1, the fast leakage is assumed to occur prior to the resonance region. Within the resonance region, concurrent absorptions occur in the U^{235}, U^{238}, Pu^{239}, Pu^{241} and fission product resonances, with neutron production in the U^{235}, Pu^{239} and Pu^{241} resonances. Following this consecutive absorptions occur in U^{236}, Pu^{242}, Pu^{240} and burnable poison. Resonance absorptions in the non-fuel part of the cell are included as part of the moderator absorption cross section.

Resonance escape probability of the nuclide m is calculated from

$$p_m = e^{-\frac{C_1 N_m (RI)_m^{\infty}}{\psi_{1,m}}} \qquad (4B17)$$

where

$$C_1 = \frac{V_{fl}}{\int \Sigma_s (1 - V_{fl})} \qquad (4B18)$$

$\int \Sigma_s$ = slowing down power of the moderator region.

V_{fl} = volume fraction of fuel in the unit cell.

N_m = concentration in the fuel, of nuclide m.

$(RI)_m^{\infty}$ = infinite dilution resonance integral of m.

$\psi_{1,m}$ = resonance disadvantage factor of m.

The resonance disadvantage factor can be treated in several ways by the FUEL Code. The disadvantage factor for U^{238} is held constant at its initial (input) value. The disadvantage factor for the remaining nuclides can be held constant, treated by means of the Crowther-Weil technique (C42) or by a constant times the Crowther-Weil value. All work described in this report uses the Crowther-Weil calculation of disadvantage factors for all nuclides except U^{238}, namely

$$\psi_{1,m} = 1 + \frac{N_m (RI)_m}{\Sigma_{s,fl}} \qquad (4B19)$$
$$m \neq 8$$

where $\Sigma_{s,fl}$ is the macroscopic scattering cross section of the fuel (input data).

The disadvantage factor for U^{238}, $\psi_{1,8}$, is input data to the FUEL Code. It is best chosen so that the corresponding value of p_8 will yield an initial conversion ratio which matches experimentally determined numbers or calculated values. This avoids the difficulty of determining the exact definition which has been used to yield a value of p_8.

For a reactor in which the change in U^{235} concentration varies with flux-time as

$$\Delta N_5 = a_5 \theta + b_5 \theta^2 \qquad (4B20)$$

and the plutonium concentration varies as

$$N_9 = a_9 \theta + b_9 \theta^2 \tag{4B21}$$

the initial conversion ratio can be computed from the plutonium concentration at flux times θ_1 and θ_2, $N_{9,1}$ and $N_{9,2}$, and the change in U^{235} concentrations at the same flux times, $\Delta N_{5,1}$, and $\Delta N_{5,2}$ by:

$$ICR = -\frac{(\frac{\theta_2}{\theta_1})^2 N_{9,1} - N_{9,2}}{(\frac{\theta_2}{\theta_1})^2 \Delta N_{5,1} - \Delta N_{5,2}} \tag{4B22}$$

The resonance reaction rate for nuclide m is given by $<1 - p_m>$, and this quantity is defined differently for different nuclides

$$<1 - p_m> = \frac{\ln p_m}{\ln p_5 p_7 p_8 p_9 p_{11}} (1 - p_5 p_7 p_8 p_9 p_{11}) \tag{4B23}$$

$$m = 5, 7, 8, 9, 11$$

$$<1 - p_6> = p_5 p_7 p_8 p_9 p_{11} (1 - p_6) \tag{4B24}$$

$$<1 - p_{12}> = p_5 p_7 p_8 p_9 p_{11} p_6 (1 - p_{12}) \tag{4B25}$$

$$<1 - p_{10}> = p_5 p_7 p_8 p_9 p_{11} p_6 p_{12} (1 - p_{10}) \tag{4B26}$$

$$<1 - p_{13}> = p_5 p_7 p_8 p_9 p_{11} p_6 p_{12} p_{10} (1 - p_{13}) \tag{4B27}$$

The resonance reaction rate for non-fuel materials is proportional to $(1 - p_{mod})$, which is input data. This can be obtained from

$$(1 - p_{mod}) \approx \sum_{all\ mod} \frac{V_i N_i (RI)_i}{\xi \Sigma_s (1 - V_{fl})} \qquad (4B28)$$

where V_i is the volume fraction of material i.

For a $1/v$ absorber with 2200 m/s cross section of σ_0, the infinite dilution resonance integral is given by

$$RI = \int_{E_c}^{\infty} \sigma(E) \frac{dE}{E} = 2\sigma_0 \sqrt{\frac{E_0}{E_c}} \qquad (4B29)$$

where $E_0 = 0.0253$ ev.

When the cutoff energy E_c is 0.45 ev

$$RI^{\infty} = 0.474\ \sigma_0$$

5. The Flux-Time Properties and the Nuclide Concentration Equations

To predict neutron balances and power production at each point in a reactor, it is necessary to know seven homogenized unit cell properties, which are obtained from nuclide concentrations, cross sections, nuclear constants, and unit cell parameters. These seven properties are given below

1)
$$\Sigma_f = \left\{ \sum_{m=5,9,11} N_m \sigma_{f,m} \right\} V_{fl} \qquad (4B30)$$

57

2) $\quad \nu \Sigma_f = \left\{ \displaystyle\sum_{m=5,\,9,\,11}' \nu_m N_m \sigma_{f,m} \right\} V_{fl}$ $\qquad$ (4B31)

3) $\quad \dfrac{1-p}{1+\alpha} = \displaystyle\sum_{m=5,\,9,\,11} \dfrac{<1 - p_m>}{1 + \alpha_m}$ $\qquad$ (4B32)

4) $\quad <\eta\,(1-p)> = \displaystyle\sum_{m=5,\,9,\,11} \dfrac{\nu_m}{1+\alpha_m} <1 - p_m>$ $\qquad$ (4B33)

5) $\quad p = p_5 p_7 p_8 p_9 p_{11} p_6 p_{12} p_{10} p_{13}$ $\qquad$ (4B34)

6) $\quad \Sigma_{xe,\,max} = \Sigma'_{xe,\,max} \cdot V_{fl}$ $\qquad$ (4B35)

where $\Sigma'_{xe,\,max}$ is the unhomogenized maximum Xe cross section which will be evaluated below.

7) $\quad \Sigma_{TOT} - \Sigma_{xe} = \left\{ \displaystyle\sum_{m=5}^{13} N_m \sigma_m + \Sigma'_{sm} \right\} \cdot V_{fl} + \Sigma_{mod}$ $\qquad$ (4B36)

where Σ_{mod}, the homogenized moderator cross section is

$$\Sigma_{mod} = \Sigma_{0,\,mod}(\frac{v0}{v})(1 - V_{fl})\,(1 + A_\psi \cdot \theta)\,\psi + \frac{q}{\phi}\,p\,P_1(1 - p_{mod})$$

$\qquad$ (4B37)

where $(1 + A_\psi \cdot \theta)$ is the thermal flux disadvantage factor,

58

which as input data can be supplied as a linear function of flux time if desired.

$\Sigma_{0,\,mod}$ is the 2200 m/s moderator region cross section, unhomogenized, and is input data.

$(1 - p_{mod})$ is the resonance capture probability of the moderator region and is also input data.

q/ϕ, the slowing down density per unit flux is obtained from

$$q/\phi = \frac{\epsilon \nu \Sigma_f}{1 - \epsilon P_1 \langle \eta(1 - p)\rangle} \tag{4B38}$$

Σ'_{sm} is the unhomogenized Sm group cross section which will be evaluated below.

The evaluation of nuclide concentrations during burnup is accomplished by numerical integration of the equations given below. These are identical to those used by Shanstrom in FUELCYC, except that a burnable poison equation has been added. They are reproduced here as a matter of convenience. The notation and symbols used have been defined previously. The differential equations representing nuclide concentration changes are:

$$U^{235}: \quad \frac{dN_5}{d\theta} = -N_5\sigma_5 - (\frac{q}{\phi})P_1\langle 1 - p_5\rangle \tag{4B39}$$

$$U^{236}: \quad \frac{dN_6}{d\theta} = N_5(\sigma_5 - \sigma_{f,5}) - N_6\sigma_6 \tag{4B40}$$

$$+ (\frac{q}{\phi})P_1\left\{ \frac{\alpha_5}{1 + \alpha_5}\langle 1 - p_5\rangle - \langle 1 - p_6\rangle \right\}$$

$$U^{238}: \quad \frac{dN_8}{d\theta} = -N_8\sigma_8 - (\frac{q}{\phi})\left\{ P_1\langle 1 - p_8\rangle + \frac{\epsilon - 1}{\epsilon(\eta_8 - 1)} \right\} \tag{4B41}$$

59

Pu^{239}: $\dfrac{dN_9}{d\theta} = N_8 \sigma_8 - N_9 \sigma_9$ (4B42)

$$+ \frac{q}{\phi} \left\{ P_1 (<1 - p_8> - <1 - p_9>) + \frac{a_8 (\epsilon - 1)}{(1 + a_8)\epsilon(\eta_8 - 1)} \right\}$$

Pu^{240}: $\dfrac{dN_{10}}{d\theta} = N_9 (\sigma_9 - \sigma_{f,9}) - N_{10} \sigma_{10}$ (4B43)

$$+ \frac{q}{\phi} P_1 \left\{ \frac{a_9}{1 + a_9} <1 - p_9> - <1 - p_{10}> \right\}$$

Pu^{241}: $\dfrac{dN_{11}}{d\theta} = N_{10} \sigma_{10} - N_{11} \left(\sigma_{11} + \frac{\lambda_{11}}{\phi} \right)$ (4B44)

$$+ \frac{q}{\phi} P_1 \left\{ <1 - p_{10}> - <1 - p_{11}> \right\}$$

Pu^{242}: $\dfrac{dN_{12}}{d\theta} = N_{11} (\sigma_{11} - \sigma_{f,11}) - N_{12} \sigma_{12}$ (4B45)

$$+ \frac{q}{\phi} P_1 \left\{ \frac{a_{11}}{1 + a_{11}} <1 - p_{11}> - <1 - p_{12}> \right\}$$

Burnable Poison: $\dfrac{dN_{13}}{d\theta} = - N_{13} \sigma_{13} - \frac{q}{\phi} P_1 <1 - p_{13}>$ (4B46)

Fission Product Pairs

$$\frac{dN_7}{d\theta} = \sum_{m=5,9,11} N_m \sigma_{f,m}$$ (4B47)

$$+ \frac{q}{\phi} \left\{ \frac{\epsilon - 1}{(1 + a_8)\epsilon(\eta_8 - 1)} + P_1 \sum_{m=5,9,11} \frac{<1 - p_m>}{1 + a_m} \right\}$$

60

The Maximum Xenon Cross Section, Unhomogenized

$$\Sigma'_{xe,max} = \sum_{m=5,9,11} y_{xe,m} N_m \sigma_{f,m} \tag{4B48}$$

$$+ \frac{q}{\phi} \left\{ \frac{y_{xe,8}(\epsilon - 1)}{(a_8 + 1)\epsilon(\eta_8 - 1)} + P_1 \sum_{m=5,9,11} \frac{y_{xe,m}<1 - p_m>}{1 + a_m} \right\}$$

The Samarium Group Cross Section, Unhomogenized

$$\Sigma'_{sm} = \sum_{m=5,9,11} y_{sm,m} N_m \sigma_{f,m} \tag{4B49}$$

$$+ \frac{q}{\phi} \left\{ \frac{y_{sm,8}(\epsilon - 1)}{(1 + a_8)\epsilon(\eta_8 - 1)} + P_1 \sum_{m=5,9,11} \frac{y_{sm,m}<1 - p_m>}{1 + a_m} \right\}$$

The nine equations (4B30) to (4B38) are numerically solved using a fourth order Runge-Kutta-Gill method (G42). The nuclide concentrations are then available at a specified number of points separated by a specified interval, and the seven properties can be evaluated at each of the points.

While the FUEL Code can calculate the above nuclide concentrations and properties at up to 60 points equally spaced in flux-time, it can transfer only a maximum of 15 points, also equally spaced, to tape or punched card for use by the MOVE Code. The MOVE Code, which represents fuel by its flux-time, obtains the fuel properties by interpolating between the known values which have been computed and transferred to it by the FUEL Code.

6. The Definition of k_∞

It is instructive to consider the value of infinite multiplication factor which this neutron behavior model would yield. There are actually two different numbers which can be obtained, depending upon the definition of k_∞ used. While these numbers are different except for k_∞ equal to unity, it does not matter which is used, provided it is used consistently and provided comparisons are made only with numbers obtained using the same definition.

The two definitions are:

1) k_∞ = $\dfrac{\text{thermal neutron production rate}}{\text{thermal neutron consumption rate}}$

$$= \frac{\epsilon \, \nu \Sigma_f p}{\Sigma_{TOT}(1 - \epsilon <\eta(1 - p)>)} \tag{4B50}$$

2) k_∞ = $\dfrac{\text{epi-resonance neutron production rate}}{\text{thermal plus resonance consumption rate}}$

$$= \frac{\epsilon \, \nu \Sigma_f p}{\Sigma_{TOT}} + \epsilon \, \langle \eta(1 - p) \rangle \tag{4B51}$$

where Σ_{TOT} is the total homogenized unit cell thermal absorption cross section.

These are equivalent only at k_∞ = 1.

The FUEL Code performs the calculation of k_∞ as given by the first definition.

C. MOVE CODE

1. Introduction

It is in the MOVE Code that the effect of fuel and poison management on nuclear power systems is actually evaluated. The fuel and its properties, which have been obtained by the FUEL Code, are characterized by a flux-time. The reactivity properties at this flux-time, plus neutron-diffusion theory, and a method of control poison management are all that is required to evaluate the flux and power shape at a point in time. At a later time, these flux-times, augmented by their flux-time changes and moved in various ways corresponding to fuel movements, are used to re-evaluate the flux and power shapes. In this way, a complete flux and power shape history is obtained for all the fuel in the reactor and final properties, such as burnup, can be obtained from discharge flux-times.

1.1 Geometrical Specifications

The code is written for two-dimensional (R-Z) analysis of a finite cylindrical reactor core, with or without axial symmetry and with specification of fuel properties in a maximum of 150 regions, 10 radial by 15 axial. Fluxes and leakages are evaluated using two-group diffusion theory and reflectors are treated by means of the reflector savings technique.

Up to five different radial zones, each with different fuel properties, can be used, with an arbitrary number of radial mesh points per zone and, within certain limits, an arbitrary radial mesh spacing.

1.2 Methods of Poisoning for Reactivity Control and Flux Shaping

Poison control of reactivity is achieved by means of absorbers with an equivalent cell-homogenized absorption cross-section. It is necessary to assume that the control absorber does not alter

the neutron spectrum which has been computed by the FUEL Code. In addition to the techniques outlined below, it is possible to use a $1/v$ burnable poison in the fuel. This cannot be done directly by the MOVE Code but must be specified as input data to the FUEL Code, since burnable poison can be treated only as a part of the flux-time-dependent fuel absorption cross section which must be calculated by the FUEL Code. The methods of poison control of reactivity used in the MOVE Code are outlined below:

1) Uniform poison removal, in which the spatial distribution of poison has a specified relative shape. Its magnitude is varied for reactivity control.

2) Radial zone poison removal with arbitrary initial shape. Poison is removed starting at the bottom and progressing axially upward, in the outermost zone. When poison is totally removed from one radial zone, the removal proceeds on the next zone toward the center.

3) Axial bank poison removal from an initial condition in which the relative distribution of poison is specified and the absolute level of poison to make the reactor critical initially is computed. Poison is then removed, starting at the bottom of the core, and is removed axially, the height of the control rods being uniform radially.

4) Poison removal for constant power density. The spatial distribution of the poison is determined by a desired input power density shape. Burnup proceeds until the approach of a zero or negative poison condition causes a change to a specified alternate poison removal technique.

5) A constant fixed poison, arbitrary shape. This poison can be used in conjunction with those mentioned above, except that it is not removable. Its purpose is solely that of power density shaping.

6) Uniform removal of a poison with specified relative spatial distribution whose magnitude is varied for reactivity control. When the poison has been completely removed, removal is started on additional control poison whose specified shape and magnitude has been held constant up to this point. Removal of this latter poison can take place uniformly, by radial zone or axial bank removal, as outlined above.

1.3 Fuel Management Capability

The types of fuel management which can be treated by the MOVE Code fall naturally into one of three types, batch irradiation, steady-state irradiation, or transient irradiation. Each type is described in more detail below.

1) <u>Batch irradiation.</u> A reactor core is loaded and then irradiated with reactivity controlled during irradiation by means of one of the poison management techniques mentioned above. When the reactor is just critical with all of the control poison removed, all of the fuel is discharged. Batch irradiation can be considered either as a complete fuel cycle or as the first phase of another fuel cycle.

2) <u>Steady-state irradiation.</u> In this type of irradiation, the reactor has reached an equilibrium condition in which core properties are either constant or periodic in time. When core properties are constant in time, spent fuel is continuously replaced by fresh fuel in various ways at such a rate that the reactor is always just critical without the use of control poison. When core properties are periodic in time, the most burnt out fraction of the fuel is replaced discontinuously by fresh fuel, the remainder of the fuel being moved in various ways; and the reactor is then run batchwise using control poison to maintain criticality. By the time this periodic condition has been reached, charging, discharging and movement will have been repeated often enough that the discharge burnups will be equal,

and flux and power shapes will have identical histories during each cycle.

In the MOVE Code, the following particular steady-state fuel movements can be treated.

(a) Continuous

    (i) Bidirectional: Short fuel elements are charged continuously at one end of a fuel channel, moved steadily along the channel and are discharged at the opposite end. The fuel moves in opposite directions in adjacent channels. The fuel charge rate is adjusted so that the reactor is just critical without the use of control poison.

    (ii) Outin: Fuel rods are charged to the outside of the reactor core, moved radially inward, and are discharged from the axis of the reactor. The fuel charge rate is adjusted so that the reactor is just critical without the use of control poison.

    (iii) Graded: Fuel rods, fixed in place in the reactor, are irradiated batchwise and replaced individually on such a schedule that every region of the reactor contains fuel elements distributed uniformly in exposure between the fresh and discharge burnup condition. The fuel charge rate is adjusted so that the reactor is just critical without the use of control poison.

    (iv) Graded-Outin: This is a combination of graded and outin in which some radial regions are run as graded, with others being run as outin.

(b) Discontinuous

    (i) Outin: The reactor core is divided into a number of radial zones of equal volume. At the end of a

cycle, fuel is discharged from the center zone; all other fuel zones are moved one zone inward and fresh fuel is loaded into the outer zone. This operation can be performed with or without axial inversion, in which fuel is divided in the middle and each half turned end for end and returned to the reactor.

(ii) Bidirectional: Each channel is divided axially into a number of equal parts. At the end of a cycle, the most burnt out end part of each channel is discharged, and new fuel is charged at the opposite end, pushing the other fuel toward the discharge end. These operations are set up so that adjacent channels move in opposite directions.

3) Transient fuel irradiation. Into this classification fall those fuel management cases which are concerned with the non-equilibrium reactor startup period, between batch irradiation and the final steady-state irradiation. The MOVE Code is capable of analyzing the startup features of

(i) Continuous Bidirectional

(ii) Discontinuous Bidirectional

(iii) Discontinuous Outin

2. Spatial Behavior

2.1 Introduction

The treatment of neutron spatial behavior is generally similar to that used by Shanstrom in FUELCYC (S41). The principal differences are that the ∇^4 term in the composite two-group equation is no longer neglected and that variable radial mesh spacing can be used. Iteration convergence has also been improved, and a control poison iteration option added.

67

2.2 The Composite Two-Group Diffusion Equation

Referring to Fig. 4.1 for the neutron energy cycle, neutron balances on the two groups of neutrons give the following steady-state equations, with the fast group properties characterized by subscript 1 and thermal group properties by the absence of a subscript. The balance equation for fast neutrons entering and leaving the fast leakage group Ⓐ is

$$q = \Sigma_1 \phi_1 - D_1 \nabla^2 \phi_1 \tag{4C1}$$

The balance equation for thermal neutrons entering and leaving the thermal group Ⓑ is

$$p\Sigma_1 \phi_1 = (\Sigma + \Sigma_w)\phi - D\nabla^2 \phi \tag{4C2}$$

where D_1 and D are diffusion coefficients.

Σ_1 and Σ are removal cross sections.

Σ_w is the poison thermal absorption cross section necessary to maintain criticality.

q is the slowing down density.

p is the total resonance escape probability $(p_5 p_6 p_7 p_8 p_9 p_{10} p_{11} p_{12} p_{13})$.

In order to facilitate solution of the two-group equations, it is convenient to put them into a form which involves only thermal group constants, plus the Fermi Age, $\tau = D_1/\Sigma_1$. This is accomplished as follows:

Referring again to Fig. 4.1 and taking a neutron balance at point Ⓒ :

$$\frac{q}{\epsilon} = \nu \Sigma_f \phi + (q + D_1 \nabla^2 \phi_1) < \eta(1 - p)> \tag{4C3}$$

or rewriting

$$q = \frac{\epsilon}{1 - \epsilon < \eta(1 - p)>} [\mathcal{V} \Sigma_f \phi + <\eta(1 - p)> D_1 \nabla^2 \phi_1] \qquad (4C4)$$

With this value of q, Eq. (4C1) can be rewritten as:

$$- D_1 \nabla^2 \phi_1 [\frac{1}{1 - \epsilon < \eta(1 - p)>}] + \Sigma_1 \phi_1 = \frac{\epsilon \, \mathcal{V} \Sigma_f \phi}{1 - \epsilon < \eta(1 - p)>} \qquad (4C5)$$

Rearranging Eq. (4C2)

$$\phi_1 = \frac{1}{p\Sigma_1} [(\Sigma + \Sigma_w)\phi - D\nabla^2 \phi] \qquad (4C6)$$

When Σ_1 is independent of position,

$$D_1 \nabla^2 \phi_1 = \mathcal{T} \nabla^2 [\frac{(\Sigma + \Sigma_w)\phi - D\nabla^2 \phi}{p}] \qquad (4C7)$$

where $\mathcal{T}$, the Fermi Age, is equal to D_1/Σ_1 .

Rearranging Eq. (4C5)

$$\Sigma_1 \phi_1 = \frac{\epsilon \mathcal{V} \Sigma_f \phi + D_1 \nabla^2 \phi_1}{1 - \epsilon < \eta(1 - p)>} \qquad (4C8)$$

Eliminate $\Sigma_1 \phi_1$ from Eq. (4C2), using Eq. (4C8), and $D_1 \nabla^2 \phi_1$ from the resulting equation, using Eq. (4C7). The following equation results, this being the form used in computation:

$$- D\nabla^2 \phi + (\Sigma + \Sigma_w)\phi = \frac{p}{1 - \epsilon < \eta(1 - p)>} \left\{ \epsilon \mathcal{V} \Sigma_f \phi + \mathcal{T} \nabla^2 [\frac{(\Sigma + \Sigma_w)\phi - D\nabla^2 \phi}{p}] \right\}$$

$$(4C9)$$

It is also convenient to evaluate the fast leakage as a fast non-leakage probability, P_1, which by definition is given by:

$$P_1 = \frac{q + D_1 \nabla^2 \phi_1}{q} \qquad (4C10)$$

Substituting (4C4) into (4C10) gives the computational form,

$$P_1 = \frac{\epsilon \nu \Sigma_f \phi + D_1 \nabla^2 \phi_1}{\epsilon [\nu \Sigma_f \phi + <\eta(1-p)> D_1 \nabla^2 \phi_1]} \qquad (4C11)$$

where $D_1 \nabla^2 \phi_1$ is evaluated in Eq. (4C7).

Substituting (4C10) in (4C3) gives Eq. (4B38), here repeated,

$$\frac{q}{\phi} = \frac{\epsilon \nu \Sigma_f}{1 - \epsilon P_1 <\eta(1 - p)>} \qquad (4C12)$$

which has been used in computing nuclide concentration changes.

2.3 The Difference Form of the Diffusion Equation

A general analytic solution of equation (4C9) would be impossible, although certain special cases could be solved. To obtain a general solution then, it is necessary to use finite difference techniques. Thus, the reactor core will be represented by a matrix of discrete mesh points. Each point, being at the center of the region it represents, is considered to have the average properties of its region. The composite two-group equation, when in difference form, relates the flux at each mesh point to the flux at adjacent points, with each mesh point requiring one equation. Therefore, when evaluating the fluxes in an n x m array, it is necessary to solve n x m simultaneous equations in flux.

Fig. 4.2 shows the mesh representation of a core quadrant
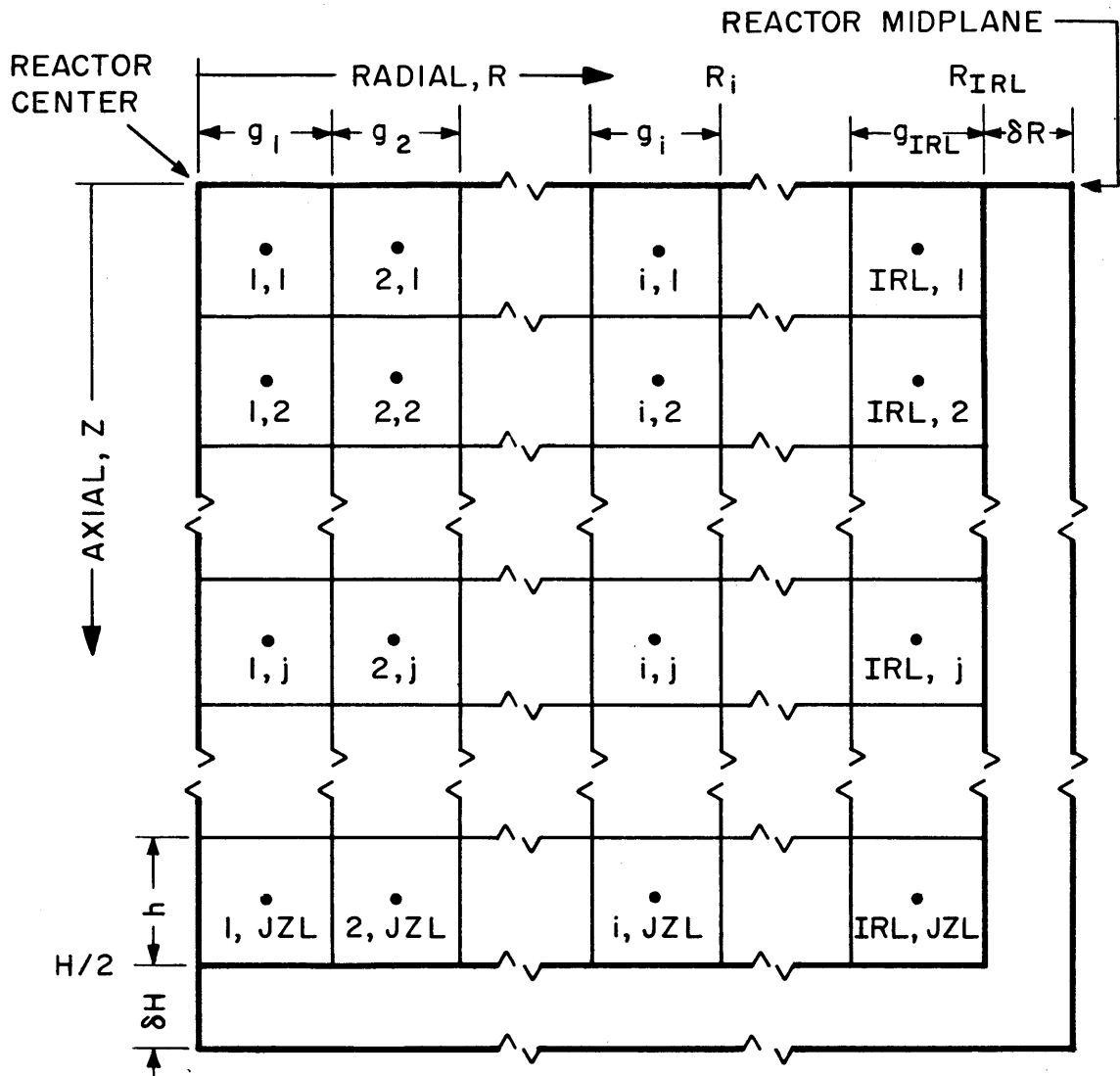
NOTE: IF THERE IS NO AXIAL SYMMETRY, THERE WILL BE AN
AXIAL REFLECTOR SAVINGS AT THE TOP OF THE MESH
AS WELL AS AT THE BOTTOM, AND AT THE REACTOR
CENTER WILL NOT BE NEAR POINT (1,1)

FIG. 4.2 MESH REPRESENTATION OF A CORE QUADRANT
SHOWING AXIAL AND RADIAL REFLECTOR SAVINGS

with the radial and axial indexing convention used, subscript i being used for radial points and j being used for axial.

The ∇^2 operator in cylindrical co-ordinates is given by,

$$\nabla^2 = \frac{d^2}{dr^2} + \frac{1}{r}\frac{d}{dr} + \frac{d^2}{dz^2} \qquad (4C13)$$

In Eq. (4C9), there is also a ∇^4 term. Because the solution is achieved by an iterative process and because the ∇^4 term is small compared to the ∇^2 terms, the direct calculation of ∇^4 can be avoided by substituting for the $D\nabla^2\phi$ term on the right side of Eq. (4C9) its value from the previous iteration, adding the poison cross section, dividing by the resonance escape probability and performing the ∇^2 operation on the resulting quantity.

The five point difference equation for $\nabla^2\phi_{i,j}$, with variable mesh spacing, g_i , and constant axial mesh spacing, h , is given by:

$$\nabla^2\phi_{i,j} = \frac{2}{g_i}\left\{\frac{\phi_{i+1,j}}{g_i + g_{i+1}} + \frac{\phi_{i-1,j}}{g_i + g_{i-1}} - \phi_{i,j}\left[\frac{1}{g_i + g_{i+1}} + \frac{1}{g_i + g_{i-1}}\right]\right\}$$

$$+ \frac{1}{R_i - g_i/2}\left\{\frac{\phi_{i+1,j}}{g_i + g_{i+1}} - \frac{\phi_{i-1,j}}{g_i + g_{i-1}} + \frac{\phi_{i,j}}{g_i}\left[\frac{g_{i+1}}{g_i + g_{i+1}} - \frac{g_{i-1}}{g_i + g_{i-1}}\right]\right\}$$

$$+ \frac{1}{h^2}\left\{\phi_{i,j+1} + \phi_{i,j-1} - 2\phi_{i,j}\right\} \qquad (4C14)$$

where R_i is the radius of the outer edge of the ith mesh.

The composite two-group equation can now be written in five point difference form, using the notation of Shanstrom,

$$\sum_{u=1}^{5} d_{i,j,u} \cdot \phi_u = e_{i,j}\phi_{i,j} \qquad (4C15)$$

where u is understood to imply the following indices

u	radial, axial indices
1	i, j
2	i-1, j
3	i+1, j
4	i, j-1
5	i, j+1

and $d_{i,j,u}$ and $e_{i,j}$ have the following values

$$e_{i,j} = \epsilon \left(\frac{\nu \Sigma_f p}{1 - \epsilon <\eta(1-p)>} - (\Sigma + \Sigma_w) \right)_{i,j} \tag{4C16}$$

$$d_{i,j,u} = -C_{3i,j,u} \cdot C_{4i,j,u} \tag{4C17}$$

where $C_{4i,j,u} = D + \left(\frac{\tau p}{1 - \epsilon <\eta(1-p)>} \right)_{i,j} \left[\frac{\Sigma + \Sigma_w - D \frac{\nabla^2 \phi}{\phi}}{p} \right]_u$

$$\tag{4C18}$$

Note that $-D\nabla^2\phi/\phi$ is the leakage term obtained from the previous iteration. This iteration process and the evaluation of the mesh point properties will be described later.

$$C_{3i,j,u} = \frac{1}{h^2} \qquad u=4, 5 \tag{4C19}$$

$$= 0 \qquad u=4, \ j=1, \ \text{and} \ u=5, \ j=JZL$$

$$C_{3i,j,3} = \frac{1}{(g_i + g_{i+1})} \left(\frac{2}{g_i} + \frac{1}{R_i - g_{i/2}} \right) \quad i<IRL \tag{4C20}$$

$$= 0 \qquad i=IRL$$

73

$$C_{3i,j,2} = \frac{1}{(g_i + g_{i-1})} \left(\frac{2}{g_i} - \frac{1}{R_i - g_{i/2}} \right) \qquad i \neq 1 \qquad (4C21)$$

$$= 0 \qquad\qquad i = 1$$

$$C_{3i,j,1} = \frac{1}{g_i} \left(C_{7,i} - \left(\frac{2}{g_i + g_{i+1}} + \frac{2}{g_i + g_{i-1}} - \frac{1}{R_i - g_{i/2}} \right) \right.$$

$$\left. \left(\frac{g_{i+1}}{g_i + g_{i+1}} - \frac{g_{i-1}}{g_i + g_i - 1} \right) \right) + \frac{1}{h^2} (C_{8,j} - 2) \qquad (4C22)$$

except that when $i = IRL$, $g_{i+1} = g_{IRL}$

and when $i = 1$, $g_{i-1} = g_1$

$C_{7,i}$ and $C_{8,j}$ take into account the boundary conditions and are zero at interior points. The radial boundary conditions are those of zero current at the center and zero flux at a distance δR beyond the core. The axial boundary conditions with axial symmetry are those of zero current at the mid plane and zero flux at a distance δH beyond the core. Without axial symmetry, the zero extrapolated flux applies at both ends of the core. These conditions are expressed as follows:

$$C_{7,i} = 0 \qquad\qquad i \neq IRL \qquad (4C23)$$

$$= \left(\frac{\delta R - g_{i/2}}{\delta R + g_{i/2}} \right) \left(\frac{1}{g_i} + \frac{1}{2R_i - g_i} \right) \qquad i = IRL$$

$$C_{8,j} = 0 \qquad\qquad 2 \leq j \leq JZL - 1 \qquad (4C24)$$

$$= \frac{\delta H - \frac{h}{2}}{\delta H + \frac{h}{2}} \, , \begin{cases} j = JZL \\[6pt] J = 1, \ ZSYM \neq 0 \end{cases}$$

$$= 1 \qquad\qquad j = 1, \ ZSYM = 0$$

2.4 The Evaluation of Mesh Properties

The d and e terms in equations (4C16) and (4C17) contain certain fuel properties whose dependence on flux-time has been computed in the FUEL Code and whose values at certain discrete flux-times have been transferred to the MOVE Code. When the flux-time at a mesh point is given, the property $P(\theta)$ is determined in the following way by the Lagrangian interpolation procedure (H44) from the properties $P(\theta_1)$, $P(\theta_2)$ ... $P(\theta_L)$ at θ_1, θ_2 ... θ_L, respectively.

$$P(\theta) = \sum_{i=1}^{L} ALAG(i, \theta) \cdot P(\theta_i) \qquad (4C25)$$

where the Lagrangian coefficients, $ALAG(i, \theta)$, are given by:

$$ALAG(i, \theta) = \frac{(\theta_1 - \theta)(\theta_2 - \theta) \ldots (\theta_{i-1} - \theta) \cdot (\theta_{i+1} - \theta) \ldots (\theta_L - \theta)}{(\theta_1 - \theta_i)(\theta_2 - \theta_i) \ldots (\theta_{i-1} - \theta_i) \cdot (\theta_{i+1} - \theta_i) \ldots (\theta_L - \theta_i)}$$

$$(4C26)$$

It is characteristic of the ALAG coefficients that their sum is unity. It is also characteristic that their individual magnitudes are the order of unity provided they are evaluated somewhere between or at the outermost fit points. When evaluated outside of this range, their magnitudes can become considerably greater than unity; and, when they are summed up on the computer, round-off errors become important and their sum may be different from unity. This fact is used in the MOVE Code to prevent the unjustified use of properties obtained for a point well outside of the range of the fit points. The program is stopped if the sum of the coefficients is not within .5% of unity.

The flux-time dependent reactivity properties which are required for the d and e matrix calculation are:

1) The total homogenized thermal absorption cross section,

not including the variable control poison, Σ_w ,

$$\Sigma = (\Sigma_{TOT} - \Sigma_{xe}) + \frac{\phi}{\phi + \frac{\lambda_{xe}}{\sigma_{xe}}} \Sigma_{xe,\,max} + \Sigma_{wa} \qquad (4C27)$$

where $\Sigma_{TOT} - \Sigma_{xe}$ = non xenon, homogenized unit cell absorption cross section.

$\Sigma_{xe,\,max}$ = maximum xenon, homogenized unit cell absorption cross section (at very high flux).

$\dfrac{\phi}{\phi + \dfrac{\lambda_{xe}}{\sigma_{xe}}}$ = fraction of xe which is burnt out.

$\lambda_{xe},\,\sigma_{xe}$ = are the xenon decay constant and absorption cross section, respectively.

Σ_{wa} = a fixed, non-varying absorption cross section, specified as input data. It is normally used only for flux shaping studies.

2) The production of fission neutrons from thermal absorption, $\nu\Sigma_f$.

3) The production of fission neutrons from resonance absorption, $< \eta(1 - p)>$.

4) The resonance escape probability, p.

The flux-time dependent properties needed for the evaluation of power densities are:

1) The thermal fission cross section, Σ_f .

2) The resonance fission probability $(\frac{1-p}{1+a})$.

In addition to the above, the nuclide concentrations are required as functions of flux-time for the evaluation of energy cost and burnup.

2.5 Solving the Set of Simultaneous Difference Equations

The set of difference equations (4C15) written in matrix form is

$$d\phi = e\phi \qquad\qquad (4C28)$$

The matrix elements d and e are functions of the flux-time to which fuel at each lattice point has been exposed and of the control poison cross section Σ_w (if any), and also have some dependence on flux due to the flux-dependent effective Xe cross section.

Dependence on flux is effectively eliminated by evaluating the effective Xe cross section with the aid of the flux at each point obtained in earlier iterations.

The flux-time to which fuel has been exposed will have been determined by the effect of the fuel management procedure being studied on the prior irradiation history of fuel at each point in the reactor.

We then have, in effect, a system of n x m equations in n x m flux vectors, with the matrix elements d and e functions of Σ_w. The greatest value of Σ_w for which these homogeneous equations have a consistent solution is the amount of control poison which makes the reactor just critical.

In the solution procedure used in the MOVE Code, an approximate solution of the system of equation (4C28) for the relative fluxes is obtained with an initial value of Σ_w without first determining whether Σ_w is the value corresponding exactly to a critical reactor. This is possible because of the particular way in which the terms of the difference equation have been distributed between the left and right sides of (4C28), with terms arising from the second difference operator

on the left and the remaining terms on the right. Experience has shown that values for the relative fluxes obtained by the iterative procedure now to be described are not greatly affected by the value of Σ_w used, provided it is reasonably close to the value corresponding to a criticality of unity, at which the matrix [d - e] is singular.

An initial set of values of the relative fluxes at each point $\phi_n^{(1)}$ are selected, with the relative fluxes normalized so that their average is unity. These assumed relative fluxes are substituted in the right side of (4C28):

$$d\phi = e\phi^{(1)} \tag{4C29}$$

This resulting system of inhomogeneous equations is solved for a second set of relative fluxes, which after normalization so that their average is unity, are called $\phi^{(2)}$. The modified Crout reduction procedure described by Shanstrom (S41) is used for this purpose. The procedure is repeated until none of the normalized relative fluxes changes by more than a specified amount from one iteration to the next.

It is characteristic of this type of iterative solution that successive flux estimates differ from the true value by an error term whose magnitude tends to decrease exponentially. This fact is utilized to accelerate the flux convergence. The Aiken δ^2 extrapolation technique[†] is used to make this exponential extrapolation, if the flux has not converged within 5 iterations. If the fluxes on three successive iterations are ϕ_k, ϕ_{k-1} and ϕ_{k-2}, the extrapolated flux, ϕ_k', is given by

$$\phi_k' = \phi_k - \frac{(\phi_k - \phi_{k-1})^2}{\phi_k - 2\phi_{k-1} + \phi_{k-2}} \tag{4C32}$$

This extrapolation technique is used only in every other

†   See Reference H44.

iteration loop, since three successive flux estimates of the same unextrapolated sequence are not available for use in every loop.

Once the flux has converged, a check of core criticality is made using a flux-volume weighted neutron balance on the whole reactor. This criticality, C', is given by

$$
C' = \frac{\sum_{}^{all\ i,j} \left\{ \frac{q}{\phi} P_1 pV\phi \right\}_{i,j}}{\sum_{all\ i,j}^{} \left\{ [\Sigma + \Sigma_w - \frac{D\nabla^2\phi}{\phi}] V \cdot \phi \right\}_{i,j}} \tag{4C30}
$$

If this criticality is different from unity by more than a specified amount, the procedure used to adjust the reactor to criticality will depend on the method of fuel management being employed.

In batch irradiation or discontinuous methods of fueling, fuel remains fixed in place in the reactor and criticality is maintained by choice of the correct control poison cross section, Σ_w.

In continuous methods of fueling, Σ_w is zero, and criticality is maintained by a proper choice of fuel feed composition and rate of fuel movement through the reactor.

The following paragraphs describe the calculation procedure used in batch or discontinuous fueling to determine Σ_w when criticality is maintained by adjusting Σ_w. The calculation procedure used in continuous fueling methods to find the combinations of fuel feed composition and rate of movement needed to maintain criticality is described later in Section IV. 3. 3.

Control of reactivity by adjustment of Σ_w may be accomplished either by means of a uniform change of poison magnitude, while keeping the relative spatial distribution of poison constant, or by keeping Σ_w constant at some points and removing poison

79

completely from others. In either case, a good initial estimate of Σ_w can be obtained from an initial guess for the relative flux distribution or from the result of a previous iteration. For example, in uniform poison removal, the relative poison magnitude, Σ_{wn}, is specified. It is necessary to evaluate the normalization constant, Σ_{wl}, so that the absolute magnitude, Σ_w, can be obtained. This is accomplished by a simple flux-volume weighted neutron balance on the whole reactor in the form

$$\Sigma'_{wl} = \frac{\displaystyle\sum_{\text{all } i,j} \left\{ [\frac{q}{\phi}P_1 p - \Sigma + \frac{D\nabla^2\phi}{\phi}] V \cdot \phi \right\}_{i,j}}{\displaystyle\sum_{\text{all } i,j} \left\{ \Sigma_{wn} \cdot V \cdot \phi \right\}_{i,j}} \qquad (4C31)$$

where $(\Sigma_{wn})_{ij} = (\Sigma_w)_{ij}/\Sigma_{wl}$

The matrix elements d and e in Eq. (4C28) are evaluated using this initial estimate of the poison cross section Σ_w. The relative flux distribution, ϕ, is computed by the iteration procedure described above, involving the Crout reduction technique. The poisoned criticality, C', is evaluated using Eq. (4C30); and, if C' differs from unity by more than a specified amount, a new estimate of Σ_w is obtained. In order to damp out oscillations in this outer iteration loop on Σ_w, a damping factor, f_d, is employed, using the previous value of Σ_{wl} and the latest value, Σ'_{wl}, obtained from Eq. (4C31).

$$(\Sigma_{wl})_{new} = f_d(\Sigma_{wl})_{old} + (1 - f_d)\Sigma'_{wl} \qquad (4C32)$$

80

The value of f_d used in the present code is 0.5, which gives adequate $\sum_w$ convergence. The maximum number of $\sum_w$ iteration loops is a specified input control parameter.

2.6 The Evaluation of Overall Core Properties

When the flux shape has been determined, it is possible to evaluate the flux magnitudes necessary to maintain a given average power density, PDENAV kw/litre of core, as well as the power density shape. In addition, the production, absorption, and leakage rates can be evaluated.

The total fission cross section is evaluated at each point in the reactor from the flux-time at the point

$$\sum_f^{TOT}(i,j) = \sum_f(i,j) + \frac{q}{\phi}(i,j) \left\{ P_1 \frac{(1-p)}{1+a} + \frac{\epsilon - 1}{\epsilon(1 + a_8)(\eta_8 - 1)} \right\} \quad (4C33)$$

The central flux needed to maintain an average power density, PDENAV kw/litre, with relative fluxes $\phi(i,j)/\phi(1,1)$, and at 196 Mev per fission or 3.14×10^{-11} watt sec. per fission is given by

$$\phi(1,1) = \frac{PDENAV \displaystyle\sum_{i=1}^{IRL} \sum_{j=1}^{JZL} V_{i,j}}{3.14 \times 10^{-11} \displaystyle\sum_{i=1}^{IRL} \sum_{j=1}^{JZL} \left(\sum_f^{TOT} \cdot \frac{\phi}{\phi_{11}} \cdot V\right)_{i,j}} \quad (4C34)$$

In the MOVE Code, the fuel discharge occurs when the unpoisoned criticality of the reactor reaches CRIT, an input number usually specified to be unity. As a measure of how close to this condition a given situation is, an unpoisoned core criticality is obtained. This quantity has no physical significance except that

81

given by its definition,

$$C = \frac{\text{total thermal production rate}}{\text{total thermal absorption rate, less removable control poison absorption + total thermal leakage}}$$

$$= \frac{\displaystyle\sum_{i=1}^{IRL} \sum_{j=1}^{JZL} (qP_1pV)_{i,j}}{\displaystyle\sum_{i=1}^{IRL} \sum_{j=1}^{JZL} (\Sigma\phi - D\nabla^2\phi)_{ij} V_{ij}} \qquad (4C35)$$

Note that the fixed, non-varying control poison, Σ_{wa}, is included as part of the thermal absorption in the above definition.

When the core reaches an unpoisoned criticality of unity, spent fuel must be discharged, or in the case of certain fuel movements, spent fuel must be replaced at such a rate as to maintain criticality. When fuel is discharged, a cost analysis is performed to evaluate the fuel cycle cost of energy from it.

The cost analysis requires initial and average discharge nuclide concentrations, fuel burnup and time in the reactor. The nuclide concentrations are obtained from the flux-time initially and at discharge. The burnup, B, is obtained from the final volume average fission product pair concentration, $\overline{N}_{fp}$, the initial fuel nuclide concentrations, N_m^0 , by

$$B = 0.917 \times 10^6 \frac{\overline{N}_{FP}}{12 \displaystyle\sum_{\substack{m=5 \\ m \neq 7}} N_m^0} \frac{MWD}{\text{Tonne of fuel fed}} \qquad (4C36)$$

This is based on a heat of fission of 196 Mev and an initial fuel molecular weight of 238.

The full power time in the reactor can be evaluated in one of two ways, which are equivalent. In batch fuel irradiation, the flux-time definition is used.

$$t_R = 3.17 \times 10^{16} \times \sum_{0}^{\text{DISCHG}} \frac{\Delta\theta_{1,1}}{\phi_{1,1}} \text{ years} \qquad \dagger \qquad (4C37)$$

where the summation takes place from zero flux-time in neutrons/barn, to discharge.

The alternative procedure uses an energy balance on a known average burnup and the specified average power density, PDENAV kw/l , turned into fuel power density by dividing by V_{fl} , the volume fraction of fuel.

$$t_R = 0.993 \times 10^6 \frac{\overline{N}_{FP} V_{fl}}{\text{PDENAV}} \text{ years} \qquad \ddagger \qquad (4C38)$$

where $\overline{N}_{FP}$ has the units $\dfrac{\text{fission product pair}}{\text{barn cm of fuel}}$.

3. Fuel Management Procedures

This section gives calculational details of the fuel management procedures which are written into the MOVE Code and which have been outlined in the introduction to this section, IV-C.

$\dagger \qquad 3.17 \times 10^{16} = \dfrac{10^{24} \text{ b/cm}^2}{365 \times 86,400 \text{ sec/yr}}$

$\ddagger \qquad 0.993 \times 10^6 = \dfrac{10^{24} \text{b/cm}^2 \times 10^3 \text{cm}^3/1 \times 3.14 \times 10^{-14} \frac{\text{kwsec}}{\text{fission}}}{3.154 \times 10^7 \text{ sec/year}}$

3.1 Batch Irradiation and Poison Management

In batch irradiation, the fuel remains in a fixed location in the core and is irradiated until all control poison has been removed. This is the irradiation mode used for startup of new reactor cores and for the discontinuous fuel movements in which fuel is irradiated batchwise between fuel changes. Control poison is needed to hold down excess reactivity during all batch irradiations.

The irradiation procedure is as follows. The flux-times, which are zero for new fuel, are used to evaluate the properties in each region, and the fluxes and power densities are obtained. The fluxes are assumed to remain constant for a time, which is specified as a central flux-time step.

The flux-times in each region are augmented in the following manner

$$\theta'_{i,j} = \theta_{i,j} + ZET2 \cdot \frac{\phi_{i,j}}{\phi_{1,1}} \qquad (4C39)$$

where $\theta'_{i,j}$ is the new flux-time.

$\theta_{i,j}$ is the current flux-time.

ZET2 is the central flux-time step.

This stepwise procedure is repeated with uniform central flux-time increments until the reactor approaches an unpoisoned criticality of unity, at which time the step size is changed so as to give a final criticality of unity. In this way, a flux and power history of the fuel is obtained, and this is then used to evaluate the effectiveness of the particular fuel distribution and poison management technique being studied.

Because control poison is generally used only during batch-type irradiation, it is convenient to outline here the various control

84

poison options that are available in the MOVE Code. It should be re-called that no matter how much control poison is present, it is assumed that the neutron flux spectrum is the same as has been cal-culated in the FUEL Code for the absence of control poison. This is a necessary assumption when the fuel properties are to be a function of flux-time only. In addition to the control poison techniques men-tioned below, it is also possible to use a $1/V$ burnable poison which is an integral part of the fuel and, as such, must be calculated as a unique fuel type by the FUEL Code.

1) <u>Uniform poison removal.</u> The spatial shape of the poison is either uniform or zero, or else it can have a relative shape speci-fied as input data. The magnitude of the poison necessary for a just-critical core is calculated from a thermal neutron balance on all regions of the core.

Uniform poison removal with constant spatial shape corres-ponds to the "chemical shim" technique, in which a soluble poison is used in the moderator, its concentration being adjusted to maintain criticality. Uniform poison removal could also be accomplished in reactors with a large number of control rods. The same fraction of control rods would be removed from all regions, the fraction being adjusted for criticality.

2) <u>Radial zone poison removal.</u> Initially, the spatial shape of the poison is either uniform or zero, or else its relative shape is specified as input data. Its magnitude is determined initially so as to maintain criticality with no Xe or Sm poisons and is held constant. Criticality is maintained during subsequent burnup by removing poison from the outermost poisoned radial zone, starting at the bottom of the zone and moving upward until all poison is removed. Poison removal then commences at the bottom of the next inner radial zone, the process being repeated until no removable control poison remains in the core.

3) <u>Axial bank poison removal.</u>   This is identical to radial
zone poison removal except that poison is removed from all radial
zones simultaneously, starting at the bottom and working axially up-
ward until no removable control poison remains in the core.

4) <u>Poison removal for constant power density distribution.</u>
An input power density distribution, plus flux-times at each point
enable the calculation of the flux at each point.   First, the flux-times
are used to evaluate the total fission cross section at each point:

$$\Sigma_{f,\,TOT} = \Sigma_f + \frac{q}{\phi}\,(P_1(\frac{1-p}{1+a}) + \frac{\epsilon-1}{\epsilon(\eta_8-1)(\alpha_8+1)})$$ (4C40)

P_1 , the fast non-leakage probability, is the only term in the
above expression which cannot be obtained from flux-time, since it
depends upon the fast flux distribution.   However, since the reso-
nance term, containing P_1 , is generally smaller than the thermal,
a previous value for P_1 can be used, to be followed by an optional
recomputation of $\Sigma_{f,\,TOT}$ and ϕ if the new flux shapes yield
markedly different values for P_1 .

The flux is obtained from the specified power density,
Pd kw/litre, by means of the relation

$$\phi_{i,\,j} = 3.18 \times 10^{10}\,(\frac{Pd}{\Sigma_{f,\,TOT}})_{i,\,j}$$ (4C41)

where 3.18×10^{10} is the number of fissions per watt-sec.   at 196 Mev.
per fission.

The leakage terms, $- D\,\frac{\nabla^2\phi}{\phi}$ and P_1 are obtained in the
normal way from the fluxes.   At this point, the computation of
$\Sigma_{f,\,TOT}$ and ϕ can be repeated with the new value of P_1 .

Having obtained the leakage terms, it is possible to evaluate

86

the Σ_W at each point from a simple neutron balance.

$$(\Sigma_W)_{i,j} = \left\{ \frac{q}{\phi} P_1 p - \Sigma + D \frac{\nabla^2 \phi}{\phi} \right\}_{i,j} \tag{4C42}$$

Burnout proceeds at this constant power density distribution until a zero or negative poison condition approaches at any point in the core. Poison removal is subsequently accomplished by one of the techniques mentioned above, which means that the required power density shape can no longer be maintained.

Physically, this situation may be difficult to duplicate. This technique is academically interesting, however, since it represents an optimum situation. It is also useful in the study of burnup-flux shape relationships.

5) <u>Constant fixed poison.</u> This poison technique does not permit variation during burnup and is, therefore, not used for reactivity control. Its main purpose is that of flux flattening. Its value at each point is given as input data or else it is set equal to zero everywhere in the core.

Physically, this technique is fairly easy to duplicate, as the poison is constant in time and fixed in position.

6) <u>Uniform poison removal plus absolute poison removal.</u> This technique is a combination of several of the above techniques. There are initially two types of control poison in one of which, the spatial shape and absolute magnitude are specified. The other is a poison whose relative spatial shape is specified, but whose magnitude is varied for reactivity control. As the fuel is burned, the variable poison is decreased uniformly until none remains. At this point, removal of the absolute poison commences. This removal may be accomplished in one of three ways which have been described above: uniform poison removal, radial zone poison removal, or axial bank

poison removal.

Physically, this technique can represent the combined use of chemical shim and control rods in reactivity management. The chemical shim is completely removed first and is followed by removal of the control rods in a specified manner.

3.2 Discontinuous Outin Irradiation

In the discontinuous outin fuel movement, the reactor core is divided into a number of equal-volume radial zones. When fuel is to be moved, the central zone is discharged; fuel in all other zones is moved one zone closer to the center; and fresh fuel of specified composition is charged to the vacant outermost zone. The reactor is then run batchwise until it is just critical with no poison, at which time the outin movement is repeated. There are several possibilities in specifying the actual manner of fuel transfer from one zone to the next zone closer to the center. If the fuel elements can be divided in two, they may be inverted axially during transfer so that the fuel at the top and bottom of the core during the preceding period will be at the center during the coming irradiation. Also, the relative fuel position, with respect to the radial zone boundaries, can be maintained, or else the fuel can be mixed during transfer. These two possibilities involve a flux-time gradient transfer or an average flux-time transfer, respectively. Any or all of the above optional features may be changed at any time or kept the same for all transfers.

Poison control of reactivity and the calculation of flux-time changes during burnup are identical to those described for batch irradiation. The method used in the option of representing fuel transfer by means of flux-time gradient transfer is described below.

The flux-time within each zone is fitted by means of the Lagrangian polynomials, with respect to the parameter, f, which is the volume fraction of the zone which lies between the radial point, i, and the inner boundary of the zone.

$$f_i = \frac{R_i^2 - R_{IN}^2}{R_0^2 - R_{IN}^2} \qquad (4C43)$$

where $\quad R_i \quad$ = radial location.

$\qquad R_{IN} \quad$ = inner radius of zone.

$\qquad R_{OUT} \quad$ = outer radius of zone.

The flux time at any point, f, is then obtained from the flux times at f_1, f_2 ... f_n (which are θ_1, θ_2 ... θ_n) by means of

$$\theta(f) = \sum_{i=1}^{n} ALAG(i) \cdot \theta_i \qquad (4C44)$$

where $\quad ALAG(i) = \dfrac{(f - f_1) \ldots (f - f_{i-1})(f - f_{i+1}) \ldots (f - f_n)}{(f_i - f_1) \ldots (f_i - f_{i-1})(f_i - f_{i+1}) \ldots (f_i - f_n)}$

$$(4C45)$$

Since the coefficients $ALAG(i)$ are functions only of the quantities f, which are fixed geometrical parameters, they need be calculated only once.

3.3 Continuous Bidirectional Irradiation

In the continuous bidirectional fuel irradiation, fuel is moved continuously in the axial direction and in opposite directions in adjacent channels. The velocity of the fuel is adjusted so as just to maintain criticality without the use of control poison, although the constant fixed poison technique can be used for flux shaping. It is also possible to control the flux shape by means of radial variation of fuel burnup. The fuel in the central channels undergoes greater

burnup than the remainder of the fuel, and this tends to flatten the power distribution. The radial variation of burnup is specified by relating either discharge flux-times or axial velocities to those at the center of the core.

In the MOVE Code, the bidirectional fuel movement is written in two parts, one for the transient period following the initial batch irradiation and the other for studying the steady state. The basic features of each are outlined below.

Transient Bidirectional Fuel Movement

The transient bidirectional fuel movement accepts the flux-times at the end of batch irradiation. The bidirectional charging operation is then started, and the velocity necessary to maintain criticality is found by iteration. The relative push-velocity as a function of radius is specified, as is the amount of fuel movement between velocity iterations. It is possible to recharge the fuel that was just discharged from the adjacent channel, or to charge new fuel. It is also possible to change from recharging of discharged fuel to new fuel charge when the discharged fuel exceeds a specified flux-time. These optional features can be changed at any time or kept the same throughout reactor life.

The computational method for obtaining later flux-times after a time step has been taken, given the earlier flux-times and fluxes before the time step was taken, is outlined below. The basic assumption is that fuel motion is continuous along the channels, but the fluxes and fuel properties need to be reevaluated only at discrete intervals of time, during which the fuel moves a fraction of a mesh point, f. The later flux-time $\theta'(j)$ at a point j, is then expressed in terms of earlier flux-times, θ, and fluxes by,

$$\theta'(j) = \theta(j \pm f) + \frac{1}{V_z} \int_{Z_{j\pm f}}^{Z_j} \phi dz \qquad (4C46)$$

90

where V_z is the axial velocity, which is the quantity to be evaluated by iteration. The positive and negative signs refer to fuel moving toward and away from the mid-plane of the reactor, respectively.

The above equation can be written in finite difference form as follows: The later flux-time $\theta_1'(j)$ of fuel which has arrived at the jth mesh point while traveling away from the midplane of the reactor is related to the earlier flux-time at adjacent points $\theta_1(j)$ and $\theta_1(j-1)$ by

$$\theta_1'(j) = (1 - f) \cdot \theta_1(j) + f \cdot \theta_1(j - 1)$$

$$+ \frac{h}{2V_z} \left\{ \phi'(j) + (1 - f) \cdot \phi(j) + f \cdot \phi(j - 1) \right\} \quad j \neq 1 \qquad (4C47)$$

Similarly, the later flux-time $\theta'(j)$ of fuel traveling away from the midplane of the reactor is

$$\theta'(j) = (1 - f) \cdot \theta(j) + f \cdot \theta(j + 1)$$

$$+ \frac{h}{2V_z} \left\{ \phi'(j) + (1 - f)\phi(j) + f \cdot \phi(j - 1) \right\} \quad j \neq JZL \qquad (4C48)$$

Here h is the axial mesh spacing,

$\phi'(j)$ is the later flux-time at j, and

$\phi(j)$ is the earlier flux-time at j.

The above two equations can be used at $j = 1$ and $j = JZL$ if the following substitutions are made to account for boundary conditions on flux and flux-time:

In Eq. (4C47):

$$\left. \begin{array}{l} \phi(j - 1) = \phi(1) \\[2mm] \theta(j - 1) = \theta(1) \end{array} \right\} \quad \text{for } j = 1$$

91

In Eq. (4C48):

$$\left.\begin{array}{l} \phi(j+1) = \phi(JZL)\ \dfrac{\delta H - \dfrac{h}{2}}{\delta H + \dfrac{h}{2}} \\[6em] \theta(j+1) = \theta_1(JZL) \qquad ILOAD \neq 0 \\[1em] \qquad\quad\ = 0 \qquad\qquad\ ILOAD = 0 \end{array}\right\} \quad \text{for } j = JZL$$

where δH is the axial reflector savings and ILOAD is the recharge control parameter which is zero for new fuel charging and unity for recharge of the adjacent channel discharge.

An initial estimate of the axial velocity needed to maintain criticality after completion of batch irradiation may be obtained by assuming that fuel in the central channel will have received at discharge 50% greater flux-time than it had at the end of batch irradiation while at the midplane of the reactor. If V_z is the required velocity,

$$\theta_1(1, JZL) = \theta_1(1,1) + \frac{h}{V_z} \sum_{j=1}^{JZL} \phi(1, j) \qquad (4C49)$$

$$= 1.5\ \theta_1(1,1)$$

Therefore, an initial estimate of the velocity may be obtained from

$$V_z = \frac{2h \displaystyle\sum_{j=1}^{JZL} \phi(1, j)}{\theta_1(1, 1)} \qquad (4C50)$$

Once the flux-times in adjacent channels are obtained, the fuel properties are calculated. The average properties of fuel in the

adjacent channels are then obtained, using flux-weighting for the thermal properties and slowing down density weighting for the non-thermal properties. Since it is assumed that the thermal fluxes in the adjacent channels are equal, the thermal properties in each channel are given equal weights.

Having obtained the average properties at each point, corresponding to the particular axial velocity estimate used, the fluxes and criticality are evaluated by the methods described in Section C2.5 of this chapter, with the control poison cross section, Σ_w, set equal to zero. The criticality obtained is characteristic of the given axial velocity estimate.

If the criticality is different from unity by more than a specified amount, a new axial velocity estimate is made. The second velocity estimate, $V_{z,2}$, depends upon the criticality, C, and the first estimate $V_{z,1}$ in the following manner

$$V_{z,2} = V_{z,1}/1.2 \qquad\qquad C>1$$

$$\text{or} \qquad V_{z,2} = (1.2)V_{z,1} \qquad\qquad C<1$$

For axial velocity iterations past the second, the estimate for the kth iteration is given in terms of the estimates and resultant criticalities at $k-1$ and $k-2$ by

$$\frac{1}{V_{z,k}} = \frac{1}{V_{z,k-1}} + \left\{ \frac{1}{V_{z,k-2}} - \frac{1}{V_{z,k-1}} \right\} \left\{ \frac{1-C_{k-1}}{C_{k-2}-C_{k-1}} \right\} \qquad (4C51)$$

The above velocity iteration proceeds until the velocity necessary to yield unit criticality is obtained at which time a cost calculation is performed on the discharged fuel, if any, and the next step is started.

Steady Bidirectional Fuel Movement

The steady state bidirectional fuel movement iterates on the discharge flux-time necessary to maintain criticality. The discharge flux-times at all radii must be specified relative to the characteristic discharge flux-time either as flux-time relative to the characteristic or as axial velocity relative to the central channel velocity, which is then assumed to have a discharge flux-time equal to the characteristic.

Since the iterative procedures used to find the characteristic discharge flux-time, which just maintains criticality, are similar for all continuous steady-state fueling methods, the procedure for bi-directional irradiation will be described in general terms, applicable to all fueling methods.

Two estimates of the characteristic discharge flux-time, to which all discharge flux-times are related, are given as input data. The flux-times and, hence, fuel properties at all points in the core are obtained using the first input estimate plus the current flux shape in a manner which depends upon the particular fuel movement being studied.

Using the properties obtained from these flux-times, the flux is calculated using the methods described in Section C2.5 of this chapter, with the control poison cross section, $\sum_w$, set equal to zero. Still using the first input characteristic discharge flux-time, the flux-times at each point are re-evaluated. To avoid possible oscillations, however, a specified damping factor, f_d, is used between successive flux-time estimates at each point, in the following manner

$$\theta_k = \theta_{new} \cdot f_d + \theta_{k-1}(1 - f_d) \qquad (4C52)$$

where θ_k is the flux-time estimate to be used for the kth iteration, θ_{new} is the flux-time calculated using the latest flux, and θ_{k-1} is the flux-time used for the previous iteration.

94

This iteration cycle is repeated until the criticality converges to a number which is characteristic of the first input flux-time estimate. If this criticality is different from unity by more than a specified amount, the iteration cycle is repeated, this time using the second input flux-time estimate, until a converged criticality factor characteristic of the second input estimate is obtained.

If the second criticality factor is not unity, a third discharge flux-time estimate is made, assuming a linear extrapolation of the previous results to a criticality of unity. If the two input estimates, θ_1 and θ_2 yield characteristic criticalities, C_1 and C_2, then the new discharge flux-time estimate, θ_3, is given by

$$\theta_3 = \theta_2 + (\theta_2 - \theta_1) \frac{(C_2 - 1)}{(C_1 - C_2)} \tag{4C53}$$

In order to avoid extrapolations in the wrong direction due to too loose convergence criteria, all extrapolations past the third are based on a least-squares linear fit of the past three flux-times and their characteristic criticalities. The change in the flux-time for the $k + 1$ st iteration from the value assumed for the first iteration $\theta_{k+1} - \theta_1$, is then given by the following equation in $\theta_k - \theta_1$, $\theta_{k-1} - \theta_1$ and $\theta_{k-2} - \theta_1$:

$$\theta_{k+1} - \theta_1 = \frac{\sum (\theta_i - \theta_1)^2 \cdot \sum (C_i - 1) - \sum (\theta_i - \theta_1) \cdot \sum [(\theta_i - \theta_1) \cdot (C_i - 1)]}{\sum (\theta_i - \theta_1) \cdot \sum (C_i - 1) - 3 \cdot \sum [(\theta_i - \theta_1)(C_i - 1)]} \tag{4C54}$$

where the summation is taken from $i = k - 2$ to $i = k$.

An assumption generally made in bidirectional fuel cycle calculations in that the fuel attains one-half of its discharge flux-time

when it is one-half of the way through the reactor at its midplane.
This implies that fluxes are identical in adjacent channels in spite of
the fact that adjacent channels contain fuel of different properties
(except at the midplane), because they move in opposite directions
and have different flux-times everywhere except at the midplane.
While the MOVE Code does not attempt to evaluate the actual flux-
time at the midplane, it is possible to specify this quantity relative
to the discharge flux-time, and to obtain a consistent solution in which
the adjacent channel fluxes are different by an amount necessary to
yield the correct flux-time at the midplane. This is done by making
the assumption that the flux difference between adjacent channels is
proportional to the flux-time difference between the two channels
times the average flux. This assumption is the best compromise
between the actual physical situation and simplicity of calculation,
since the flux and flux-time differences are readily available; and
errors due to the assumption will be very small, since the overall
effect is not very great. The mathematical representation of the
steady-state bidirectional fuel movement will now be given.

First, the discharge flux-time must be specified as a func-
tion of radius. This is done by relating the discharge flux-times at
each radial point to the current characteristic discharge flux-time,
or by relating the axial velocities at each radial point to central
channel velocity. In the latter the central channel discharge flux-
time is set equal to the current characteristic discharge flux-time.
The factor $f(r)$ is input data, which is interpreted as either the
relative discharge flux-time or relative fuel velocity and is specified
at up to 10 radial points.

In order to specify discharge flux-time, $\theta_d(r)$ as a function
of radius, in terms of θ_k , the initial or current discharge flux-time
parameter, the following form is used:

$$\theta_d(r) = \theta_k \cdot f(r) \tag{4C55}$$

If the velocities relative to the central channel are specified, $\theta_d(r)$ is given from the definition of flux-time,

$$\theta_d(r) = \int \phi(r, z)dt \tag{4C56}$$

$$\text{or} \qquad \theta_d(r) = \frac{1}{V_z \cdot f(r)} \int_0^H \phi(r, z)dz \tag{4C57}$$

where V_z is the axial velocity, to which the axial velocities at all radii are related, and H is the reactor height.

This is put in useful form by noting the definition of θ_k,

$$\theta_k = \theta_d(1) = \frac{1}{V_z \cdot f(1)} \int_0^H \phi(1, z)dz \tag{4C58}$$

$f(1)$ is the value of the factor in the central channel.

Eliminating V_z, the desired form is obtained:

$$\theta_d(r) = \theta_k \cdot \frac{f(1)}{f(r)} \frac{\displaystyle\int_0^{H/2} \phi(r, z)dz}{\displaystyle\int_0^{H/2} \phi(1, z)dz} \tag{4C59}$$

The limits of integration have been changed due to axial symmetry.

In the following, the flux-times in adjacent channels are evaluated in terms of flux and the discharge flux-time. In the treatment given in this section, it is assumed that the flux-time at the midplane of the reactor is equal to one-half of the flux-time at

97

discharge. A consequence of this assumption is that the fluxes are equal in two channels which are adjacent but with fuel moving in opposite directions.

A refinement of the above in which the flux-time at the mid-plane of the reactor differs from one-half the discharge flux-time by a specified fraction, F, is treated in Appendix B. The treatment outlined below is actually a special case, with F = 0.

The discharge flux-times at all radii have been related to the current characteristic discharge flux-time. The flux-times at all points are then obtained using these discharge flux-times plus the fluxes. Subscript 1 refers to the channel with fuel moving toward the midplane of the reactor, and subscript 2 refers to the adjacent channel, with fuel moving away from the midplane.

$$\text{If} \qquad A(r, z) = \frac{\displaystyle\int_0^z \phi(r, z)\,dz}{\displaystyle\int_0^{H/2} \phi(r, z)\,dz} \qquad\qquad (4C60)$$

where $z = 0$ is the midplane of the core.

Then, θ_1 and θ_2 are given by

$$\theta_1(r, z) = \theta_d(r)\left\{\frac{1}{2} - A(r, z)\right\} \qquad\qquad (4C61)$$

$$\theta_2(r, z) = \theta_d(r)\left\{\frac{1}{2} + A(r, z)\right\} \qquad\qquad (4C62)$$

In order to obtain the average of properties in adjacent channels, the thermal properties are weighted with their fluxes (here assumed equal) and the non-thermal properties are weighted with their slowing down densities.

An additional problem in bidirectional fuel management should be mentioned. The unaveraged maximum power density may occur at a position different from the position of the computed maximum power density averaged over the two adjacent channels. It is, therefore, necessary to compute the single-channel maximum power density separately. The ratio of unaveraged to averaged maximum power densities is a factor which multiplies the computed peak to average power density ratio to give the effective peak to average ratio. This factor becomes larger as the averaged maximum power density gets further from the midplane of the channels.

3.4 Discontinuous Bidirectional Irradiation

In this method of irradiation, the most burnt out end fraction of each channel is discharged, with fuel being charged to the opposite end, pushing the remaining fuel axially toward or into the vacant end of the channel. Fuel is pushed in opposite directions in adjacent channels. Several options are possible when the fuel is being manipulated. The fuel being charged can be new fuel, or it can be discharged fuel which can be reinserted with or without axial inversion. It is not necessary to move fuel in all channels, nor is it necessary to move the same number of fuel elements in each channel. By specifying a recharge flux-time criterion, it is possible to prevent the recharging of fuel with too great a burnup. In the MOVE Code, it is possible to change the above mentioned options at any time or to keep them the same throughout the reactor lifetime.

Poison control of reactivity and the calculation of flux-time changes during burnup are identical to those described for batch irradiation.

3.5 Continuous Outin and Graded Irradiation

These two methods of fuel irradiation are of interest mainly as limiting cases of discontinuous fuel irradiation and are treated in the MOVE Code only in their steady-state condition. In outin, fuel

spends equal time per unit volume and progresses from the periphery of the core to the center, after which it is discharged. The time per unit volume is adjusted to maintain criticality with no control poison.

In continuous graded irradiation, fuel elements extending the full length of the core remain fixed in place for their entire life. A fixed fraction of the fuel elements in each annular zone of the reactor is removed per unit time, so that each zone contains fuel elements distributed in flux-time between zero and the maximum appropriate to that zone. The rate of replacement of fuel in each zone is so adjusted that the reactor is and remains just critical without control poison. The rate of replacement in every zone may be set so that the maximum burnup experienced by fuel in each zone is the same, or the relative maximum burnup may be given a specified dependence on radius.

In the MOVE Code, it is possible to have a multi-region reactor, part of which uses outin irradiation and the remainder using graded fuel irradiation. It is also possible by specifying center discharge burnup as a function of radius to achieve flux flattening in the graded fuel movement.

In graded fuel irradiation, the discharge flux-time is specified as a function of radius using θ_k, the input or current characteristic discharge flux-time, and f(r), which is supplied at up to 10 radial positions,

$$\theta_d(r) = \theta_k \cdot f(r) \tag{4C63}$$

The flux-times at all other points in the reactor are related to $\theta_d(r)$ in the following manner

$$\theta(r, z) = \theta_d(r) \frac{\phi(r, z)}{\phi(r, 1)} \tag{4C64}$$

It will be recalled, however, that this flux-time is only the

maximum of a uniform distribution of flux-times from zero to this maximum. The properties characteristic of this maximum flux-time are, therefore, not the properties at the maximum, but an average of properties from zero to the maximum. The average property $\bar{P}(\theta)$, characterized by the maximum flux-time, θ, is given by

$$\bar{P}(\theta) = \frac{\displaystyle\int_0^\theta W(\theta')P(\theta')d\theta'}{\displaystyle\int_0^\theta (\theta')d\theta'} \qquad (4C65)$$

where $P(\theta')$ is the property as a function of flux-time.

$\quad$ $W(\theta')$ is an importance weighting function which is assumed
$\qquad$ to be unity in this work.

$\quad$ Since $P(\theta')$ is given by

$$P(\theta') = \sum_{i=1}^{N} ALAG(i,\theta') \cdot P(\theta_i) \qquad (4C66)$$

where $P(\theta_i)$ is the property at a discrete point, θ_i, and

$$ALAG(i,\theta') = \frac{(\theta' - \theta_1) \cdots (\theta' - \theta_{i-1})(\theta' - \theta_{i+1}) \cdots (\theta' - \theta_N)}{(\theta_i - \theta_1) \cdots (\theta_i - \theta_{i-1})(\theta_i - \theta_{i+1}) \cdots (\theta_i - \theta_N)}$$

$$(4C67)$$

Eq. (4C65) can now be written as

$$\bar{P}(\theta) = \sum_{i=1}^{N} \frac{I(i,\theta)}{(\theta_i - \theta_1) \cdots (\theta_i - \theta_N)} P(\theta_i) \qquad (4C68)$$

where $I(i, \theta) = \dfrac{1}{\theta} \displaystyle\int_0^\theta (\theta' - \theta_1) \dots (\theta' - \theta_{i-1})(\theta' - \theta_{i+1}) \dots (\theta' - \theta_N) d\theta'$

$$(4C69)$$

In general,

$$I(i, \theta) = \frac{\theta^{N-1}}{N} + C_1 \frac{\theta^{N-2}}{N-1} + \dots + C_{N-2} \frac{\theta}{2} + C_{N-1} \qquad (4C70)$$

where the coefficients, C, are obtained from the flux-time points, θ_1, θ_2, $\dots$ θ_N by expanding the integrand of Eq. (4C69).

In outin fuel irradiation, the axial flux-time distribution along the central fuel element at discharge from the central axis of the core, is related to θ_k, the input or current characteristic discharge flux-time by

$$\theta_d(z) = \theta_k \frac{\displaystyle\int_0^R \phi(r, z)r \, dr}{\displaystyle\int_0^R \phi(r, 1)r \, dr} \qquad (4C71)$$

The flux-times at all points in the reactor are related to $\theta_d(z)$ by

$$\theta(r, z) = \theta_d(z) \frac{\displaystyle\int_r^R \phi(r, z)r \, dr}{\displaystyle\int_0^R \phi(r, z)r \, dr} \qquad (4C72)$$

3. 6 The Manipulation of Absolute Poison for Power Distribution Control in the Steady State Fuel Movements

The use of a poison with specified magnitude and spatial distribution in conjunction with the steady-state fuel movements is

justified only if the power distribution in the core is thereby improved, since its presence is usually detrimental to fuel burnup. The improved power distribution can be used in one of two ways to offset the cost penalty associated with loss of fuel burnup. A peak-power-density-limited core operating at the limit can be reduced in size while maintaining the same power output if the power density distribution is improved. Alternatively, the same core operating at its limit can operate at a higher total power level with an improved power distribution.

There are two major factors associated with the use of an absolute poison in power distribution control. The first is related to the degree of power flattening desired and is generally associated with poison magnitude. The second and less important factor is concerned with obtaining the best burnup possible for a given degree of flattening. The peak-to-average power density ratio is the indication of this flattening. There are generally many ways of obtaining a given peak-to-average ratio, but only one of these will yield minimum neutron leakage and hence largest fuel burnup. This second factor is, therefore, generally associated with poison distribution.

The approach taken in the MOVE Code to the problem of power distribution control is to obtain the best degree of power flattening. No specific attempt is made to make fine adjustments in the power distribution to optimize burnup, and hence the results are not necessarily optimum with respect to burnup, but should be reasonably close since this is generally only of secondary importance.

After obtaining the power distribution and other characteristics of one of the steady-state continuous fuel movements in which a specified magnitude and distribution of absolute poison has been used for power distribution control, it is possible to adjust the poison on the basis of its current power distribution in order to improve that distribution. This is done with the following empirical formula at

103

each mesh point

$$\Sigma'_{wa} = \Sigma_{wa} + \frac{\Sigma_{wa,\,max}}{2} \left\{ \frac{POWD}{PDENAV} - 1 : 1 \right\} \qquad (4C73)$$

where Σ'_{wa} is the new poison estimate to be used.

Σ_{wa} is the current poison magnitude.

$\Sigma_{wa,\,max}$ is the maximum poison in the core.

POWD is the current power density at the point.

PDENAV is the core average power density.

When the above adjustment has been made at all points in the core, the new poison values are all renormalized so that their maximum value is equal to the previous maximum.

4. The Cost Analysis

4.1 Introduction

The main objective of this work is the evaluation of various fuel and poison management techniques that might be used in large nuclear power plants. The basis for evaluation is the effect that these techniques have on the total energy cost. In this section the method of cost analysis is outlined and the unit costs used are given.

4.2 Components of the Total Energy Cost

The cost of producing energy in a nuclear power system is made up of

    1) Fuel cycle costs, consisting of

        (a) Costs of fuel materials and the processes used to prepare fuel for use in the reactor and to reclaim fuel after use, and

        (b) Charges for rental of fuel materials and interest on

working capital tied up in fuel.

2) Charges for capital investment in the reactor and power station.

3) Operating costs.

In the cost calculation model used in this work, there are 10 items in the material and process part of the fuel cycle cost, 4 in the fuel rental and interest part of the fuel cycle cost, 2 in the capital cost and 2 in the operating cost part of the total energy cost. Table 4.2 names each of these items, lists the input data required by the code for each item and gives numerical values for the input data used in the present work for the two different cost analysis bases.

4.3 Cost Bases

Cost Basis 1 makes use of unit costs and other parameters, the majority of which have been recommended by the USAEC. Cost Basis 2 has been obtained from published (G41) estimates of capital costs, interest rates, and fabrication costs in Canada. This basis is of particular interest because the CANDU Reactor is of Canadian design, and will be built under Canadian financing terms, which are more favorable to capital investment than U.S. terms. While the Canadians do not plan to recover the plutonium from the spent fuel immediately, this analysis will assume that reprocessing does take place, since it appears that this will lower fuel costs somewhat. Both cost bases use the new U^{235} price schedule established by the USAEC on May 30, 1961 (U41).

Also, the results from the Canadian cost basis will be used as the cost criterion in the design study, since this reactor concept shows to best advantage under financing conditions such as exist in Canada. The detailed procedure for calculating energy costs from the input data will now be described.

4.4 Calculation of Material and Process Items in the Fuel Cycle Cost

Figure 4.3 shows the fuel process flow sheet assumed in

105

TABLE 4.2 INPUT DATA FOR COST CALCULATIONS

i	DESCRIPTION	MAT'L ADJ. FACTOR	COST BASIS 1	COST BASIS 2	UNITS	REFERENCE
	1a. Material and Process Costs	f_i	UNIT COST, C_i			
1	Natural U or UO_2	1.015	28.70	28.70	\$/kg U	L41
2	UF_6 from AEC	1.018	Eq. (4C75)		\$/kg U	U41
3	Conversion: $UF_6 \rightarrow$ U or UO_2	1.018	12.50*	12.50*	\$/kg U	L41
4	Fuel Fabrication	1.015	85.30	60.60	\$/kg U	R41
5	Shipping	1.00	15.45	15.45	\$/kg fuel	S 42
6	Reprocessing: Solvent Extr.	0.99	Eq. (4C80)		\$/kg fuel	U42
7	Conversion: $UO_2(NO_3)_2 \rightarrow UF_6$	0.987	Eq. (4C81 or 82)		\$/kg U	U42, U43
8	Credit: UF_6 to AEC	0.987	Eq. (4C75)		\$/kg U	U41
9	Conversion: $Pu(NO_3)_4 \rightarrow Pu$	0.98	1500	1500	\$/kg Pu	U42
10	Credit: Pu to AEC	0.98	9500	9500	\$/kg Pu	U44

*   Cost of converting UF_6 to U has been assumed the same as the cost of converting UF_6 to UO_2.

TABLE 4.2 (CONTINUED)

i	DESCRIPTION	COST BASIS 1	COST BASIS 2	UNITS	REFERENCE
	1b. Fuel Lease and Interest Charges	ANNUAL CHARGE			
11	UF_6 Lease: outside reactor, F_U	0.0475	0.045	per year	U44, G41
12	Fuel Working Cap: outside reactor, F_W	0.06	0.045	per year	S42, G41
13	UF_6 Lease: inside reactor, F_U	0.0475	0.045	per year	U44, G41
14	Fuel Working Cap: inside reactor, F_W	0.06	0.045	per year	S42, G41
	II. Capital Costs	UNIT COST, C_i			
15	Reactor part of plant	224	224	$/kwe	G41
16	Remainder of plant	183	183	$/kwe	G41
	Annual Charges on Capital	ANNUAL CHARGE			
15	Reactor part FCAPR	0.14	0.0813	per year	G41
16	Remainder FCAPNR	0.14	0.0731	per year	G41
	III. Operating Costs	UNIT COST, C_i			
17	Reactor part	4.37	4.37	$/kwe yr	G41
18	Remainder	2.78	2.78	$/kwe yr	G41
	U^{235} weight fraction for blend XOPT	0.	0.0142		Step 2

TABLE 4.2 (CONTINUED)

OTHER PARAMETERS	SYMBOL	VALUE	UNITS	REFERENCE
Daily charge for reprocessing plant	D_6	17,100	\$/day	H41
Unit conversion cost: $UO_2(NO_3)_2$ to				
$\quad UF_6 < 5\%$	$D_{7;1}$	5.60	\$/kg U	U42
$\quad\quad > 5\%$	$D_{7;2}$	32.00	\$/kg U	U42
Weight fraction U^{235} in UF_6 of zero value	x_0	0.00277	--	--
Unit cost of separative work	C_E	37.286	\$/kg U	U41
Batch size of fuel for reprocessing	WTF	38,210	kg	--
Pre-reactor time for UF_6 lease	TUPR	0.60	yr	--
Pre-reactor time for working capital	TWPR	0.50	yr	--
Post-reactor time for UF_6 lease	TPOST	2.33	yr	--
Load factor, non fuel movement	L_0	0.8	--	S42
Net efficiency	γ	0.2795	--	G41
Average specific power	SPPDAV	18.725	kw/kg	--
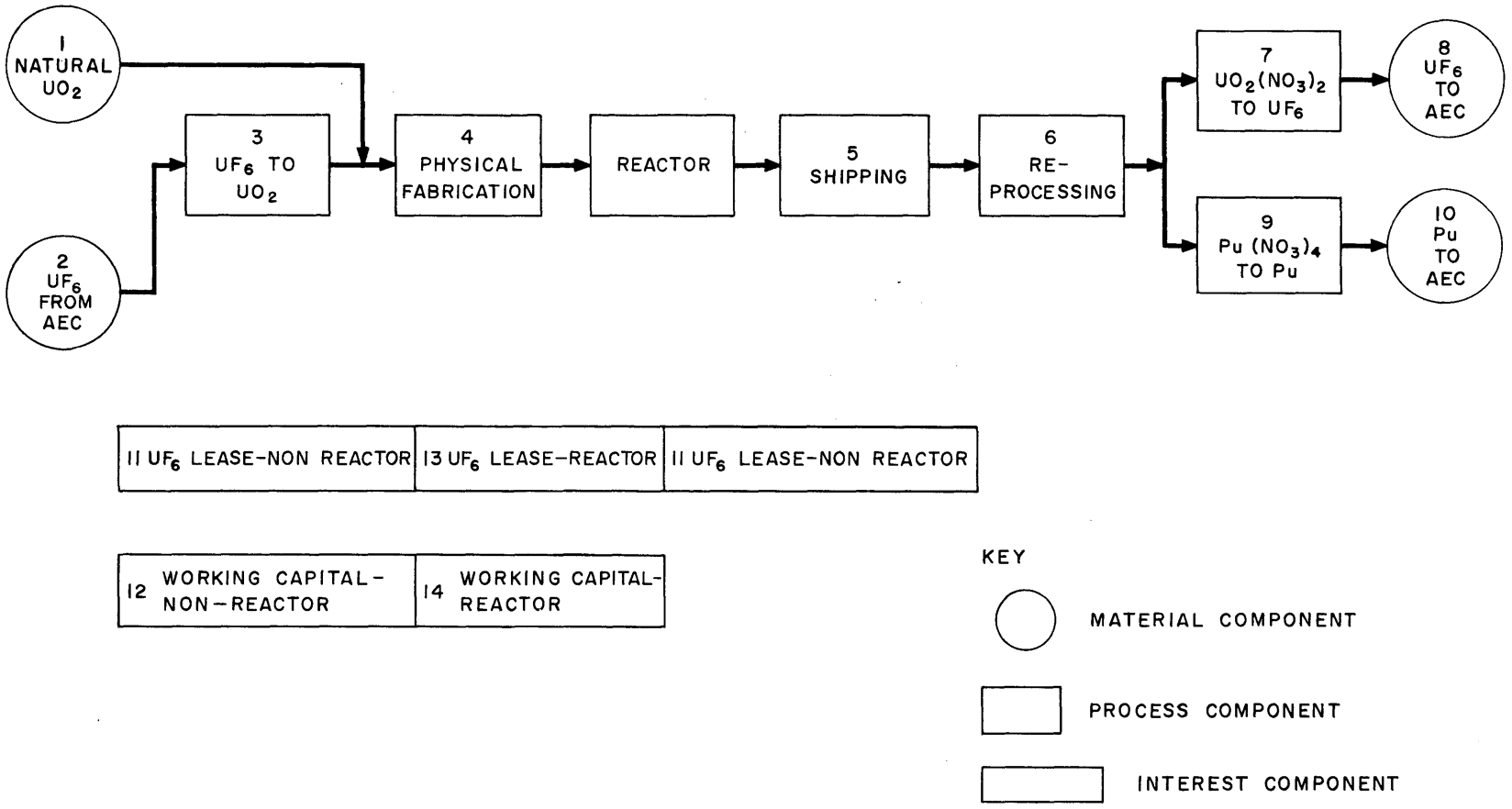
FIG. 4.3 PROCESS FLOW SHEET FOR FUEL CYCLE COST ANALYSIS

evaluating the fuel cycle cost. Each of the numbered circles represents a material whose value is charged or credited to the fuel cycle cost. Each of the numbered rectangles represents a process whose cost contributes to the fuel cycle cost. The contribution of each item of Figure 4.3 to the net fuel cycle cost $\overline{C}_i$ is evaluated by an equation of the form

$$\overline{C}_i = C_i \cdot f_i \cdot W_i \left(\frac{1000}{24 \cdot B \cdot \gamma}\right) \frac{\text{mills}}{\text{kwh}} \quad 1 \leq i \leq 10 \qquad (4C74)$$

where

C_i = unit cost of the ith material or process step, evaluated as described below and expressed in $ per kg. of the "material i."

W_i = ratio of the mass of "material i" on which cost C_i is based, to the mass of fuel material fed to the reactor, with no allowance for process losses. W_i is computed by the code from the concentrations, N_m, of nuclides in the fuel entering or leaving the reactor, by the equations to be given below.

f_i is the "material adjustment factor", given in Table 4.2 which takes processing losses into account. For a process step ahead of the reactor, f_i is the ratio of "material i" entering the process step to "material i" entering the reactor. For a process step following the reactor, f_i is the ratio of "material i" leaving the process step to "material i" leaving the reactor.

B = average burnup in Mwd per tonne of fuel fed to the reactor.

γ = net thermal efficiency.

The quantities W_i depend on the concentrations of uranium

and plutonium isotopes in fuel fed to and discharged from the reactor. Nuclide concentrations N_m^o in fuel fed to the reactor are given as input data for each case studied. Nuclide concentrations N_m in fuel discharged from the reactor are computed by the code from the flux-time to which each unit of fuel has been exposed, and are appropriately averaged over the part of the core being discharged at a particular time. The burnup, B, is proportional to the concentration of fission products in discharged fuel.

1) **The Cost of UO_2.** In this cost code, the cost C_1 of natural uranium in the form of UO_2 is input data which has been assigned the value $28.70/kg U for ceramic grade. This cost is based on a price of $5.50/lb. U_3O_8 for uranium ore concentrates in the form of yellow cake, combined with a cost of $5.75/lb UO_2 for converting yellow cake to ceramic grade UO_2, an estimate provided by Mr. H. Lambertus (L41) of the Spencer Chemical Co.

To obtain UO_2 containing more than the natural abundance of U^{235}, it is necessary to use enriched UF_6 from the U.S. Atomic Energy Commission. The AEC's schedule (U41) for the price C_p in $/kg of uranium of enrichment x weight fraction U^{235}, in the form of UF_6, may be represented with good accuracy by the equation

$$C_p(x) = C_E \left[(2x - 1) \ln \frac{x(1 - x_0)}{x_0(1 - x)} + \frac{(x - x_0)(1 - 2x_0)}{x_0(1 - x_0)} \right] \qquad (4C75)$$

Where

$\qquad C_E \quad = \quad$ unit cost of separative work, $ 37.286/kg.

and $\qquad x_0 \quad = \quad$ the enrichment at which uranium in the form of UF_6 would have zero value, 0.00277.

When

$\qquad x \quad = \quad$ 0.007115, the weight fraction of U-235 in natural uranium,

$$C_p = \$\ 23.49/kg.$$

Under cost basis 1, applicable to U.S. economic conditions, UO_2 of an enrichment other than natural is assigned a cost computed from the cost of uranium of that enrichment in the form of UF_6 plus the cost of converting UF_6 to UO_2. Although there is a range of enrichments below around 0.015 in which it would be theoretically possible to produce UO_2 more economically by blending natural UO_2 purchased at \$ 28.70/kgU with UO_2 made from UF_6 enriched to around 0.015 weight fraction in U-235, restrictions in the U.S. AEC's agreement for leasing enriched UF_6 make such blending uneconomic. In the U.S. enriched UF_6 may only be leased from the AEC, and not purchased.

In Canada, however, enriched UF_6 may be purchased outright from the USAEC. Under these conditions, there is a range of U-235 weight fractions between natural uranium x_1 and an optimum weight fraction for blending, x_{opt}, in which production of UO_2 by blending is economically justified. The relationship between the x_{opt}, x_1, the unit cost of natural UO_2, C_1, the unit cost of enriched uranium given by Eq. (4C75) and the unit cost of converting UF_6 to UO_2, C_3 \$/kg U^{235}, may be derived as follows:

The unit cost $C(x)$ of UO_2 containing x weight fractions U^{235} made by blending natural uranium and UF_6 containing x_2 weight fraction U^{235} is

$$C(x) = \frac{x_2 - x}{x_2 - x_1} C_1 + \frac{x - x_1}{x_2 - x_1} \left\{ C_3 x_2 + C_E \left[(2x_2 - 1) \ln \frac{x_2(1 - x_0)}{x_0(1 - x_2)} \right. \right.$$

$$\left. \left. + \frac{(x_2 - x_0)(1 - 2x_0)}{x_0(1 - x_0)} \right] \right\} \tag{4C76}$$

To find x_{opt} at which $C(x)$ is a minimum, $\dfrac{\partial C(x)}{\partial x_2}$ is evaluated and

set equal to zero. This value of x_{opt} is used as input data for Canadian cost basis 2.

In cost basis 1, x_{opt} is assigned the value zero. As the cost code is written, this has the effect of excluding blending and providing all uranium of enrichment different from natural in the form of UF_6.

2) <u>Evaluation of mass ratios and unit costs.</u> We are now in position to describe the procedure used by the cost code to evaluate the mass ratios W_i and unit costs C_i of the fuel cycle steps 1 through 10. This procedure starts with the initial concentrations N_m^o of nuclides in reactor fuel and the final concentrations N_m in fuel discharged from the reactor. Initial concentrations are given as input data. Final concentrations will have been computed from the discharge flux-time of the fuel movement being analyzed. Concentrations are expressed in units of atoms per barn cm.

<u>Steps 1 and 2.   Cost of Uranium Feed</u>

The weight fraction of U^{235} in reactor feed, x^o, is evaluated from the atomic concentrations in reactor feed, N_m^o,

$$x^o = \frac{235 N_5^o}{W_d} \tag{4C77}$$

where

$$W_d = 235 N_5^o + 236 N_6^o + 238 N_8^o \tag{4C78}$$

x^o is compared with the weight fraction of U^{235} in natural uranium, 0.007115. If the two are within $\pm$ .5% of each other, all of the feed is taken in the form of natural uranium, with

$$W_1 = 1$$

$$W_2 = 0$$

and, on cost bases 1 and 2

$$C_1 = 28.70$$

When x^o deviates significantly from 0.007115, the quantity

$$FNAT \equiv \frac{x_{opt} - x^o}{x_{opt} - 0.007115} \qquad (4C79)$$

is computed. If FNAT is greater than unity or less than zero, all of the feed is provided in the form of UF_6 of enrichment x^o, with

$$W_1 = 0$$

$$W_2 = 1$$

and

$$C_2 = C_p(x^o)$$

with C_p given by Eq. (4C75).

In cost basis 1, assignment of the value zero to x_{opt} gives FNAT > 1 for x > 0.007115, and ensures that enriched uranium feed will be all in the form of UF_6, as is required for this cost basis. In cost basis 2, when $x^o > x_{opt}$, FNAT = 0, and all feed is in the form of UF_6.

When 0 < FNAT < 1, feed is produced by blending FNAT kg of natural UO_2 with 1 - FNAT kg of UO_2 from UF_6 of optimum enrichment. In this case,

$$W_1 = FNAT$$

$$W_2 = 1 - FNAT$$

and

$$C_2 = C_p(x_{opt})$$

114

This possibility arises in cost basis 2 when

$$0.007115 < x^o < x_{opt}$$

Step 3.   Conversion of UF_6 to UO_2

Approximate data for the conversion of UF_6 to ceramic grade UO_2 obtained from Mr. H. Lambertus (L41) of the Spencer Chemical Co. lead to a conversion cost of $5.00 per pound UO_2, or $12.50/kg U, with a maximum loss of 0.3% in the conversion, and holdup of 4 weeks between shipment of UF_6 from the AEC to receipt of UO_2 by the fuel fabricator.   The unit conversion cost C_3 is supplied as input data, which for the present work is taken to be

$$C_3 = \$12.50/kg\ U.$$

Also $W_3 = W_2$

Step 4.   Physical Fabrication of Fuel

This step comprises forming ceramic grade UO_2 into pellets (0.55 inches in diameter in the CANDU reactor), charging these pellets into cladding tubes (made of Zircaloy-2 15 mils thick in the CANDU reactor), sealing the tubes and assembling them into elements. The unit cost of fabrication C_4, in $/kg fuel, is input data, and $W_4 = 1.0$,

For Zircaloy-clad fuel fabricated in the United States, Rickert (R41) has estimated the unit cost of fabrication to be $58 per kg U plus $12 per foot of fuel.   Since UO_2 fuel of density 10.2 g/cm^3, 0.55 inches in diameter, contains 0.421 kg of U per foot, the unit fabrication cost for elements for the CANDU reactor, on cost basis 1, is

$$58 + 12/0.421 = \$86.57/kg\ U$$

The uranium loss in fabrication is estimated (R41) to be 1.5%.   The unit cost of fuel fabrication per kg UO_2 entering this step is then

$$C_4 = 86.57/1.015 = \$85.30$$

For Zircaloy-clad fuel fabricated in Canada, Smith (S43) has estimated that the cost of finished fuel elements made up of natural UO_2 will be \$80/kg UO_2 or \$90.70/kg U; this cost includes the cost of UO_2. Since we are assuming that the cost of natural UO_2 in Canada on cost basis 2 is the same as in the U.S., \$28.70/kg U, the fabrication cost on cost basis 2 will be

$$C_4 = \frac{90.70}{1.015} - 28.70 = \$60.60$$

per kg U entering Step 4.

Step 5. Storage and Shipping of Spent Fuel

Unit cost C_5 in \$/kg fuel is input data, which for cost bases 1 and 2 has been taken to be \$15.45/kg (S42).

$$W_5 = 1.0$$

In cases where spent fuel is not to be reprocessed, C_5 may be taken as the cost of storage and/or ultimate disposal.

Step 6. Reprocessing of Spent Fuel

Reprocessing costs and losses are based on the U.S. AEC's charges for these services (U42), which have been evaluated for a hypothetical multipurpose reprocessing plant. In computing this cost, it is assumed that the reprocessing plant is rented on a per diem basis, D_6 \$/day, for actual running time, plus start-up and clean-up time. The running time depends on the batch size, WFL kg, and the reprocessing rate, R kg/day. R is a function of enrichment, being 1000 kg/day for less than 4 w/o and $40/x_p$ for greater than 4 w/o, where x_p is the weight fraction U^{235} in discharged fuel. The start-up and clean-up time, t, is given by

$$t = 2 \qquad\qquad WFL/R \leq 2$$

$$t = WFL/R \qquad\qquad 2 \leq WFL/R \leq 8$$

$$t = 8 \qquad\qquad WFL/R \geq 8$$

and, hence, the unit cost, C_6 , in \$/kg fuel is

$$C_6 = \frac{D_6(t + WFL/R)}{WFL} \tag{4C80}$$

$$W_6 = 1$$

There is an optimum batch size, WFL, at which the sum of the start-up clean-up charge plus the interest charges on the working capital during batch accumulation are a minimum. In this work, the batch size is chosen equal to the reactor charge, since this can be shown to be close to the optimum situation. The current value of D_6 is \$17,100/day (H41). Reprocessing losses are 1% (U42).

Step 7.   Conversion of $UO_2(NO_3)_2$ to UF_6

Cost C_7 in \$/kg U, is dependent on the discharge enrichment x_p, and is given by

$$C_7 = D_{7,1} \qquad\qquad x_p \leq .05 \tag{4C81}$$

$$= D_{7,2} \qquad\qquad x_p > .05 \tag{4C82}$$

where

$$x_p = \frac{235N_5}{235N_5 + 236N_6 + 238N_8} \tag{4C83}$$

$D_{7,1}$ and $D_{7,2}$ are input data, which for this work are taken as \$5.60 and \$32.00/kg U (U42). Losses are 0.3% (U43).

W_7 in kg U/kg fuel is calculated from

$$W_7 = \frac{235N_5 + 236N_6 + 238N_8}{W_d} \; ; \quad x_p > x_0 \qquad (4C84)$$

$$= 0 \; ; \quad x_p < x_0$$

$$W_7 = W_2 \text{ if } W_7 > W_2$$

This last constraint is based on the assumption that UF_6 credit can be extended only to that fraction of the fuel which came initially from UF_6, with no credit being given for burnt out natural uranium.

Step 8. Return of UF_6 to AEC

Cost C_8 in \$/kg U, is obtained from the discharge enrichment, x_p, and equation (4C75)

$$C_8 = C_p(x_p) \qquad x_p > x_0$$

$$C_8 = 0 \qquad x_p \le x_0$$

W_8 in kg U/kg fuel from

$$W_8 = - W_7 \text{ (this is a credit term)}$$

Step 9. Conversion of $Pu(NO_3)_4$ to Pu

Cost C_9 in \$/kg Pu is input data, here taken as \$1,500/kg Pu (U42)

W_9 in kg Pu/kg fuel from

$$W_9 = \frac{239N_9 + 240N_{10} + 241N_{11} + 242N_{12}}{W_d} \qquad (4C85)$$

Losses are 1% (U43).

Step 10.   Sale of Pu to AEC

Cost C_{10} in \$/kg Pu is input data.

The credit which the U. S. AEC will give for plutonium at the time when this reactor will be discharging spent fuel has not been definitely established.   When the new price scale for UF_6 was set (U44), it was noted that a fuel value of about \$9,500/kg PU would be consistent with the price given for highly enriched UF_6.   This value has been used for C_{10} in the present work.

W_{10} in kg Pu/kg fuel from

$$W_{10} = - W_9 \text{ (this is a credit term)}$$

The various non-interest fuel cycle cost components may now be obtained in \$/kg fuel charged from

$$\overline{C_i'} = f_i \cdot W_i C_i \quad \text{\$/kg fuel} \quad 1 \leq i \leq 10 \tag{4C86}$$

These are converted to mills/kwh by

$$\overline{C}_i = \overline{C}_i' \left(\frac{1000}{24 \cdot B \cdot \gamma} \right) \frac{\text{mills}}{\text{kwh}} \quad 1 \leq i \leq 10 \tag{4C87}$$

At this point in the computation, a check is made on several of the unit costs to see if the process which they represent is justified.   If the credit for UF_6 is less than the cost of conversion of $UO_2(NO_3)_2$ to UF_6, then the code sets

$$\overline{C}_7 = \overline{C}_8 = 0$$

Similarly, if the Pu value is less than the cost of converting $Pu(NO_3)_4$ to Pu, the code sets

$$\overline{C}_9 = \overline{C}_{10} = 0$$

119

Finally, if the solvent extraction will cost more than the credits obtained therefrom, the code sets

$$\overline{C}_6 = \overline{C}_7 = \overline{C}_8 = \overline{C}_9 = \overline{C}_{10} = 0$$

A zero cost for any of these processes implies either that they are not to be used, or are economically unjustified.

Having obtained the non-interest fuel cycle cost components, it is possible to evaluate the interest charges.

4.5 Calculation of Interest Items of the Fuel Cycle Cost

The model used in the evaluation of the UF_6 lease and working capital charges is shown in Figure 4.4. The working capital includes the costs of natural uranium, conversion of UF_6 to U or UO_2 and fuel fabrication.

The pre- and post-reactor UF_6 lease charges are based on the initial and final UF_6 values, respectively, while the charge during the time the fuel is in the reactor is based upon the mean of initial and final UF_6 values. This makes the assumption (S42) that payments will be made to the AEC out of operating income during burnup in step with UF_6 depletion.

It is also assumed that operating income reduces the working capital to zero at the time fuel is discharged. Actually, working capital is tied up in the difference between final plutonium value and the reprocessing-conversion costs. However, it is assumed that these will approximately cancel, leaving a final working capital of zero.

The fuel cycle interest charges are computed as follows.

Step 11. Non-reactor UF_6 Lease

$$\overline{C}_{11} = [\overline{C}_2 \cdot \text{TUPR} - \overline{C}_8 \cdot \text{TPOST}] \, F_U \qquad (4C88)$$

120

UF$_6$ INVENTORY LEASE
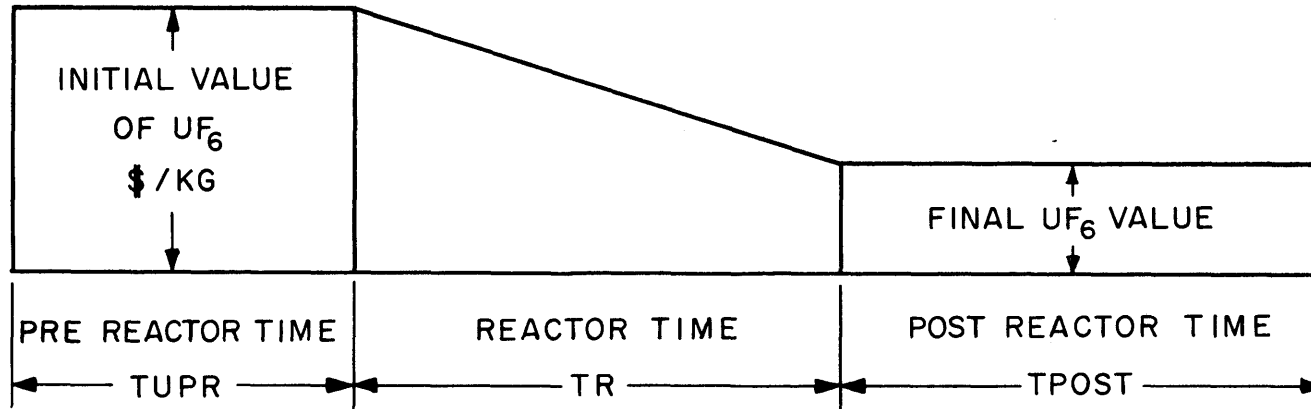
WORKING CAPITAL
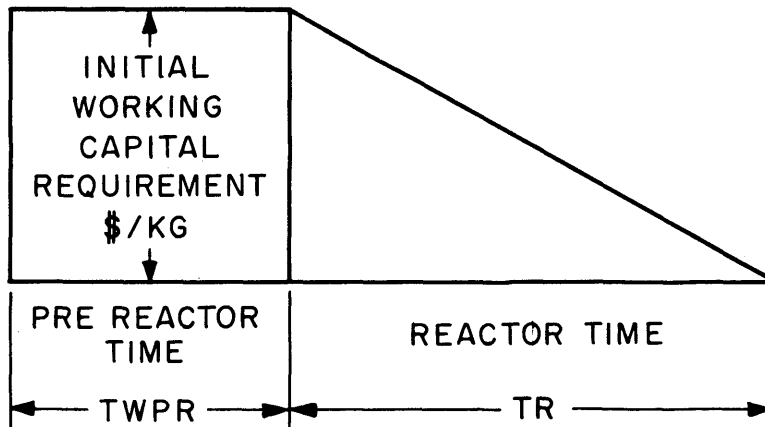
FIG. 4.4 MODEL USED FOR FUEL CYCLE INTEREST CHARGES

where TUPR is the pre-reactor time in years needed to prepare

UF_6 for use in the reactor and will be equal to about

1/2 of the lead time, if fuel elements are supplied

continuously while a full reactor charge is being

accumulated.

TPOST   is the post-reactor time in : years.

F_U is the UF_6 lease rate expressed as a fraction/yr.

The above three quantities are input data. The minus is used with

$\overline{C}_8$, because $\overline{C}_8$, a credit term, is negative.

Step 12. Non-reactor Working Capital Costs

$$\overline{C}_{12} = [C_1 + C_3 + C_4] \cdot TWPR \cdot F_W \qquad (4C89)$$

where TWPR is the pre-reactor time in years, and again will be

equal to about 1/2 of the working capital lead time.

F_W is the working capital interest rate in fraction/yr.   These

two quantities are input data.

Step 13. Reactor-time UF_6 lease

$$\overline{C}_{13} = [\overline{C}_2 - \overline{C}_8] \ \frac{TR \cdot F_U}{2 \cdot L_o} \qquad (4C90)$$

where TR, the reactor time, is obtained internally by the code.

L_O, the load factor is input data.

Step 14. Reactor Time Working Capital Costs

$$\overline{C}_{14} = [\overline{C}_1 + \overline{C}_3 + \overline{C}_4] \ \frac{TR \cdot F_W}{2L_o} \qquad (4C91)$$

The Process Times Associated with the Fuel Cycle.

The following times have been proposed (H41) for the

evaluation of pre-reactor and post-reactor use charges on fuel material and working capital.

Pre-reactor

Transit to Conversion Site	20 days
Conversion	30 days
Fabrication	90 days
Transit to Reactor	20 days
Pre-reactor Inventory	60 days
Total	220 days

Post-reactor

Decay Storage	120 days
Batch Accumulation	--------
Transit to Reprocessing Site	20 days
Reprocessing Time	--------
Conversion	21 days
Transit to AEC	20 days

The evaluation of TWPR and TUPR, the pre-reactor times for working capital and UF_6 lease, respectively, will depend upon whether use charges are included in the unit charges for conversion and fabrication. The evaluation of TPOST will involve a combination of decay storage and batch accumulation, since these two will overlap in some cases, plus transit and reprocessing times.

For this work, the pre-reactor UF_6 lease time will be taken as 220 days or 0.6 years. The working capital pre-reactor time will be taken as about 35 days less than the above, or 0.5 years.

For the CANDU reactor with bidirectional fuel scheduling, the post reactor time, TPOST, will be of significance only in the non-natural uranium fuel studies, since it is needed only for UF_6 lease charge evaluation. Since the batch size has been chosen equal to one core fuel mass, the batch accumulation time will equal the average reactor residence time which is the order of two years at 1% enrichment. TPOST has, therefore, been assigned the value of 2.33 years, this being the time required to accumulate one batch plus allowing for

decay storage of the most recently discharged fuel.

4.6 Plant Capital and Operating Costs

It is not the intention of this work to study in detailed fashion the capital and operating costs of the reactor and power plant. However, provision has been made to include them in the cost analysis so as to emphasize the compromises that are necessary among the optimum fuel cycle cost conditions, in order that minimum total energy cost be achieved.

Because of the particular types of analyses that will be made, the plant capital and operating cost components of the total energy cost are classified as being associated either with the reactor or the non-reactor part of the power plant. This broad classification can be used to suit the purposes of the individual analysis. For example, if the results obtained from fuel management studies of a reactor system with fixed core volume and electrical generating capacity are to be used in evaluating the effect on energy cost of raising the electrical output to a limit set by a peak permissible power density, all costs associated with the direct generation of electricity, such as steam generators, turbines, electrical generators and transformers, should be included in the non-reactor component. On a unit energy cost basis, these are relatively insensitive to total power output variations. The remainder of the costs, the reactor costs, will be inversely proportional to the total power output. It would, therefore, be relatively easy to scale the results from the constant volume, fixed output studies to yield fairly accurate costs for the constant volume, peak power density limited case.

Step 15. Reactor Capital Costs

$$\overline{C}_{15} = \frac{C_{15} \cdot FCAPR}{8.766 \ L} \qquad \text{mills/kwh} \qquad (4C92)$$

Step 16. Non-reactor Capital Costs

$$\overline{C}_{16} = \frac{C_{16} \cdot FCAPNR}{8.766\ L}\ \text{mills/kwh} \qquad (4C93)$$

Step 17. Reactor Operating Costs

$$\overline{C}_{17} = \frac{C_{17}}{8.766\ L}\ \text{mills/kwh} \qquad (4C94)$$

Step 18. Non-reactor Operating Costs

$$\overline{C}_{18} = \frac{C_{18}}{8.766\ L}\ \text{mills/kwh} \qquad (4C95)$$

where L = the overall load factor, calculated as outlined below.

C_{15} = reactor unit capital costs in $/kwe.

C_{16} = non-reactor unit capital costs in $/yr/kwe.

C_{17} = reactor unit operating costs in $/yr/kwe.

C_{18} = non-reactor unit operating costs in $/yr/kwe.

FCAPR = annual fractional interest rate on installed "reactor" capital cost.

FCAPNR = interest rate on "non-reactor" capital cost.

The above unit costs C_{15} to C_{18}, as well as FCAPR and FCAPNR, were input data for the cost calculation. These terms generally make up the most important components of the total energy costs, and the choices made for their values can markedly influence

125

the optimum operating range of a particular system. Their effect on the minimum cost would not be as great, due to the nature of the optimizing process.

Typical procedure for evaluation of these unit costs can be found in (S42).

The overall load factor, L, is given by

$$L = L' \cdot L_o$$

L_o is the plant load factor, assuming only normal maintenance down-time and variation in consumer demand, with no refuelling down-time. A recommended (S42) value for L_o is 0.8 (input data).

L', the refuelling load factor due to the refuelling down-time, is given by

$$L' = \frac{TR/L_o}{TR/L_o + DELTD} \qquad (4C96)$$

where DELTD is the down-time in years for one refuelling operation (input data), and TR is the "full power" reactor time obtained from the fuel cycle calculations.

4.7 Alternative Cost Breakdown

The above costs can alternatively be broken down as follows, with the fuel cycle costs grouped according to the Edison Electric system, E41 .

Net fuel material cost $\overline{C}_{mt}$ is

$$\overline{C}_{mt} = \overline{C}_1 + \overline{C}_2 + \overline{C}_4 + \overline{C}_8 + \overline{C}_{10} \qquad (4C97)$$

The fabrication cost $\overline{C}_{fb}$ is

$$\overline{C}_{fb} = \overline{C}_3 + \overline{C}_4 \qquad (4C98)$$

The reprocessing cost $\overline{C}_{rp}$ is

$$\overline{C}_{rp} = \overline{C}_5 + \overline{C}_6 + \overline{C}_7 + \overline{C}_9 \qquad (4C99)$$

The UF_6 lease charge $\overline{C}_1$ is

$$\overline{C}_1 = \overline{C}_{11} + \overline{C}_{13} \qquad (4C100)$$

The working capital charge $\overline{C}_{wc}$ is

$$\overline{C}_{wc} = \overline{C}_{12} + \overline{C}_{14} \qquad (4C101)$$

In addition, the following non-fuel-cycle components of the total energy cost are included in this particular cost breakdown.

The non-fuel plant capital investment charge $\overline{C}_{cap}$ is

$$\overline{C}_{cap} = \overline{C}_{15} + \overline{C}_{16} \qquad (4C102)$$

The total plant operating cost charge $\overline{C}_{op}$ is

$$\overline{C}_{op} = \overline{C}_{17} + \overline{C}_{18} \qquad (4C103)$$

4.8   The Evaluation of Energy Costs During the Startup and Transient Periods

The method of cost analysis which has been described in the

127

previous sections is actually a steady-state energy cost analysis and, as such, is a specific case of a general method of cost analysis. In order to evaluate energy costs in the pre-steady-state transient condition, it is necessary to develop and use this general cost analysis technique. This method could be called the "instantaneous energy cost" technique, since it is capable of giving energy costs at any time during the lifetime of the system. The remainder of this section is devoted to the description of the method used in the MOVE Code to evaluate transient energy costs.

The various components of unit energy cost can be classed as time-dependent, fuel-burnup-dependent, or both time- and burnup-dependent. The allocation of the time-dependent components poses no problems, and in some special cases, the burnup-dependent costs cause no difficulty. Whenever a spent fraction of a reactor core is replaced, however, it is always a problem to properly allocate its contribution to the total power output and the burnup component of the unit energy cost at all times during the fuel's residence in the core. A correct allocation can be made only for the case of constant or periodic (in time) power density, unless one undertakes the formidable (and often impossible) task of measuring and recording the contribution of each bit of fuel to power production at all times. The specific details of the general difficulty mentioned above will become more evident as the calculational procedure, which follows, is outlined.

Our cost analysis assumes that a nuclear power system is operating at a thermal power, P, with a net efficiency, γ. During the time interval from t to t + Δt, it produces electrical energy valued on a unit cost basis at C(t) (mills per kwh, say). C(t) might be called the "instantaneous" unit energy cost. Then it can be said that the total cost of the net electrical energy produced in Δt is equal to the total expenditures incurred by the system in the interval Δt. These total expenditures include the decrease in the value of the fuel

128

in Δt, plus the interest charges on the fuel, plus the interest charges on the total plant investment, and also the operating costs. This may be expressed as:

$$\gamma \cdot P \cdot \Delta t \cdot C(t) = \sum_{\text{all } i} [(V_i(t) - V_i(t + \Delta t) + \frac{R_i \cdot \Delta t}{L}] F_i M$$

$$+ (I \cdot i_c + O) \frac{\Delta t}{L} \qquad (4C104)$$

where V_i is the value per unit mass of the ith element.

F_i is the fraction in the ith element, of the total fuel mass.

M is the total core mass.

R_i is the composite rate of interest payments on fuel inventory and fuel fabrication working capital for the ith element.

I is the total capital (non-fuel) investment of the plant.

O is the expenditure rate of operating costs.

L is the load factor.

i_c is the composite interest rate on capital investment, including interest, depreciation, insurance and taxes, where applicable.

The problem arises of how to evaluate the fuel value decrease term, which includes material value changes (U^{235} depletion, plus debits or credits for Pu value changes), charges for fuel processing, fuel fabrication, and pre-reactor interest charges. While it is possible to obtain the change in material value, as well as the energy output in Δt, knowing only the flux-time and the change in flux-time of the fuel, it is not possible to rigorously evaluate the other charges without knowing, as well, the final (discharge) burnup

of the fuel. Hence, it is evident that if one requires the unit energy cost at time t, one must wait until all the fuel that was in the core at time t has been discharged, unless, of course, the system is in steady-state, where, by definition, the discharge burnup is a known (constant) value.

Even then the problem is not in tractable form, as it is still necessary to keep track of flux-times and rates of change of flux-time at each point in the reactor at all times. Two simplifying assumptions are justified to reduce computational time and computer storage requirements, at very slight loss to absolute accuracy and negligible loss to comparative accuracy. Part of the need for flux-time records can be eliminated by assuming an average fuel value decrease term in which one takes a certain fraction of the initial minus the discharge value of the fuel. Since these charges are burnup dependent, the fraction used is the fraction of the discharge burnup incurred in the time Δt. The equation (4C104) can then be rewritten

$$
C(t) = \sum_{\text{all } i} [(V_i(0) - V_i(\text{final})) \frac{\Delta B_i}{B_i} \frac{1}{\Delta t} + \frac{R_i}{L}] \frac{F_i M}{\gamma \cdot P} + \frac{(I \cdot i_c + O)}{\gamma \cdot P \cdot L}
$$

(4C105)

where B_i is the discharge burnup of the ith element.

ΔB_i is the change in burnup in Δt of the ith element.

Similarly (4C105) can be rewritten as

$$
C(t) = \sum_{\text{all } i} \left\{ \frac{(V_i(0) - V_i(\text{final}))}{\gamma B_i} \left[\frac{M \cdot F_i}{P} \cdot \frac{\Delta B_i}{\Delta t} \right] \right.
$$
$$
\left. + \frac{R_i \cdot t_i}{L \cdot B_i} \left[\frac{M \cdot F_i}{\gamma P} \frac{B_i}{t_i} \right] \right\} + \frac{(I \cdot i_c + O)}{\gamma \cdot P \cdot L}
$$

(4C106)

130

where t_i is the time the ith element spends in the reactor.

The particular arrangement of the latter equation is justified by being in convenient calculational form, as will become more evident later. Of the above terms, the only one not readily available is $\Delta B_i/\Delta t$, which, of course, is the specific power of the ith element (in watts/gram, say) at the time t. The second assumption needed to eliminate the necessity of space-time records, has to do with the evaluation of this $\Delta B_i/\Delta t$ term. It should be assumed to be equal to a related quantity readily available. Inspection of the equation shows that there are two such terms, P/M, which is the core average specific power, and B_i/t_i, which is the time average specific power of the ith element.

We will assume that

$$\frac{\Delta B_i}{\Delta t} = \frac{B_i}{t_i} \tag{4C107}$$

as this is exact in certain steady state fueling methods and is always nearly correct.

The core average specific power in watts per gram is given by

$$\frac{P}{M} = \sum_{\text{all } i} \frac{F_i \Delta B_i}{\Delta t} \tag{4C108}$$

which, with assumption (4C107), becomes

$$\frac{P}{M} = \sum_{\text{all } i} \frac{F_i B_i}{t_i} \tag{4C109}$$

With the substitutions (4C107) and (4C108), the equation used to

131

compute the instantaneous power cost becomes

$$C(t) = \sum_{\text{all } i} \left\{ \left(\frac{V_i(0) - V_i(\text{fin})}{\gamma \cdot B_i} + \frac{R_i \cdot t_i}{L \cdot \gamma \cdot B_i} \right) \cdot W_i \right\} + \left(\frac{I \cdot i_c + O}{\gamma \cdot P \cdot L} \right)$$

(4C110)

where

$$W_i = \frac{F_i \cdot B_i}{t_i} \bigg/ \sum_{\text{all } i} \frac{F_i B_i}{t_i}$$

(4C111)

In the above form, the term in the innermost bracket represents the unit fuel cycle cost of the energy from the ith element. The term W_i is simply a specific power-mass weighting which gives proper credit to the contribution of the ith element toward the total "instantaneous" energy cost.

For a reactor designed for a fixed power output, the core average specific power is a constant, given as input data

$$\frac{P}{M} = \text{SPPDAV} \quad \text{w/gm}$$

(4C112)

An indication of the magnitude of the error introduced by assumption (4C107) is afforded by seeing whether

$$\sum_{\text{all } i} \frac{F_i B_i}{t_i \cdot \text{SPPDAV}} = 1$$

(4C113)

As a consistency check, the value of this last summation for each time interval is obtained and printed out with the cost analysis.

In a typical cost analysis, then, the fuel cycle cost is calculated and printed out as each block of fuel is discharged. This data

132

is appropriately weighted and stored; and, when all of the fuel that was present at a time t has been discharged, the total unit energy cost at time t is obtained and printed out.

At the end of the cost analysis, three useful quantities are printed out. The mass fraction of the core represented in the cost analysis is given, and this should be unity since all the fuel in the core at a particular time should be represented. The refueling load factor which was defined previously is also given.

Finally, the consistency check, the actual value of the summation in equation (4C113) is printed out. There are three reasons why this quantity may be different from unity, since it represents not only a check on the assumption of constant specific power

$(\dfrac{\Delta B_i}{\Delta t} = \dfrac{B_i}{t_i})$ but is also a check on two different ways of calculating

reactor time, t_i, and two different ways of evaluating burnup, B_i , of the "i^{th} element" of fuel.

Reactor time is evaluated (Section C2. 6 of this chapter)

either directly, in the form $t_i = \displaystyle\int_0^\theta \dfrac{d\theta_i}{\phi_i}$, or else indirectly, in

the form t_i = Burnup/Average power output; and these are not necessarily exactly equal since the integral form is actually evaluated as a summation over many flux-time intervals in which the flux is assumed constant over each interval.

Similarly, burnup of fuel can be obtained either from its fission product concentration (i. e. , flux-time) or from its known power history in the reactor. The fission product concentration method uses the assumption of a constant P_1, fast non-leakage probability, whereas a known power history would likely have a slightly different and varying value for P_1. Hence, the epithermal

contributions to fission and burnup could be different in the two cases.

However, a 5% deviation of the consistency check from unity does not imply a 5% error in the cost calculation, since the error in the cost calculation is at least partly removed through normalization as can be seen in equation (4C111). This means that the sum of the weighting factors, W_i, will always be unity, and the errors will then become dependent upon the accuracy of these weights relative to each other. However, since the costs that will be weighted will generally be quite similar and, in some cases, equal, the effect of errors in the relative weights is further diminished to the point where they will be small relative to the more fundamental errors due to uncertainties in basic nuclear data.

D. MACHINE AND TIME REQUIREMENTS

FUELMOVE is written in FORTRAN for compilation and use on an IBM 704, 709 or 7090, or Philco TRANSAC, or other equivalent machine with 32 K of fast memory. The current version uses magnetic tape input, with the tape made up prior to running from a card-to-tape reader. The current version uses logical tape 4 for input, with the number of the output tape specified as input control data. Also under control option is the FUEL Code output for use by the MOVE Code. This output can be put on magnetic tape for direct use by MOVE, or it can be put on tape for subsequent punching on cards, the cards then being used by MOVE.

The fast storage requirement of the actual FUEL Code in octal units is $(31166)_8$ with the MIT input-output system, functions, loader, and post mortem routine requiring an additional $(16027)_8$. The common storage extends from $(77461)_8$ down to $(76415)_8$.

Estimated time in minutes for calculation of one problem by the FUEL Code on an IBM 704 or 709 is

$$t = r + .15 + m(.01 + IL(.001 \, \delta_P + .0008)) \text{ minutes}$$

134

where   r = read-in and sign-off time.

   m = number of flux-time steps taken (=NUMPOZ).

   IL = number of velocity points used in obtaining the flux spectrum and effective cross section.

   δ_P is the flux spectrum print option and = 0 if not desired.

Estimation of time required for a fuel movement calculation by the MOVE Code on an IBM 704 or 709 is more complicated and involves some idea of the number of steps or iterations necessary to obtain unit criticality. As a rule, however, one fuel management case solved with a 7 x 7 mesh takes from 3 to 4 minutes. Times taken on the IBM 7090 will be about one-fifth of 704 or 709 times.

The fast storage requirement of the MOVE Code is such that virtually all of the memory capacity, $(77777)_8$, is required, using the standard Fortran II FMS loader and input-output routines. The common storage extends from $(77461)_8$ down to $(56002)_8$ and the lower storage extends up to about $(55200)_8$. It is always possible to reduce this storage requirement by use of correction cards to remove the transfer vector of unwanted subroutines.

E.   THE MAIN PROGRAM FLOW CHARTS

The manner in which the theory described above has been applied in writing the two codes, FUEL and MOVE, is illustrated by reference to the following computer logic flow diagrams. Only the MAIN programs of each code are presented here, with the subroutines being given in Appendix D.

The symbols used are similar to those recommended by the American Institute of Chemical Engineers (A41) and are given in Fig. 4. 5. The numbering of the subroutines corresponds to the numbering used in Appendix D.

135
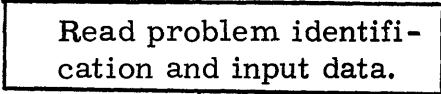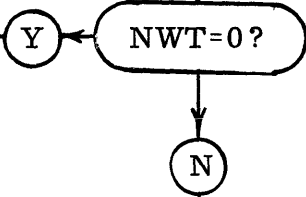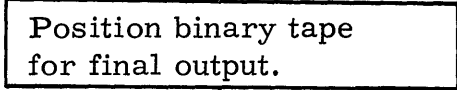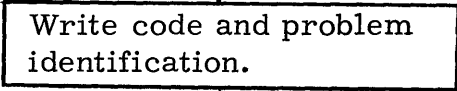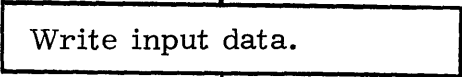
Symbol	Meaning
	Input, output, and calculations.
	Decisions and branches.
3 HALT(N)	Program error stop number N (Transfers to subroutine HALT which writes N).
Y	Decision identifier: Y means yes; N means no; 1, branch 1, etc.
N SUB	Transfer to and return from subprogram SUB which is described in number N of Appendix D.
N	Connection for sections of logic: transfer is from or to step N.
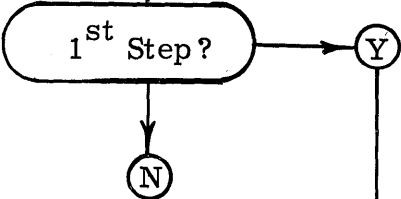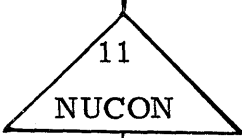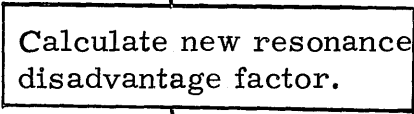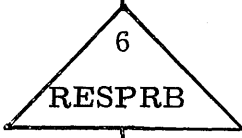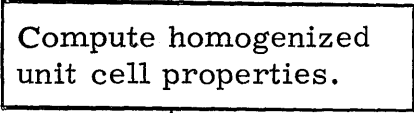
Figure 4. 5. Symbols Used for Computer Logic Flow Charts.

The Main Program of the FUEL Code

Step	Flow Chart	Comments	Fortran Statement Number

1. START

2. /40\   Entry for subsequent problem.   27

3. Read problem identification and input data.   27

4. Y ← NWT=0?   Input control parameter.
    N

5. Position binary tape for final output.   FUEL Code Binary output may be used as MOVE Code Input.   32-38

6. Write code and problem identification.   40-45

7. CLOCK   Writes date and time.

8. Write input data.   60-70

137

Step	Flow Chart	Comments	Fortran Statement Number
9.	**4** PTCS	Calculate micro-scopic cross section vs. velocity.	100
10.	**5** CONST	Tabulate constant nuclear data.	
11.	N ← IPSI > 0 ?	Input control parameter	112
	Y		
12.	Read in resonance disadvantage factor.		115
13.	Calculate resonance disadvantage factor.		120
14.	Set INIT=1.	INIT is a logic control parameter.	125
15.	**6** RESPRB	Calculate resonance escape probabilities.	

Step	Flow Chart	Comments	Fortran Statement Number

128

16.

△ 7
AVGCS2

Calculate spectrum
averaged thermal
cross sections.

128

17.

(INIT ?) → (2)

(1)

18.

Calculate Xe and
Sm poisoning.

150-260

19.

Set INIT=2.

20.

△ 2
TIMECK(1)

Write the time.

139
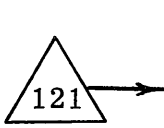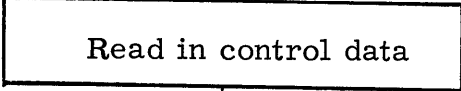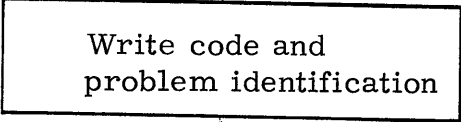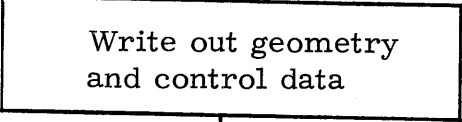
Step	Flow Chart	Comments	Fortran Statement Number
21.	△ 30	Re-entry point for next flux-time stop.	300
22.	1ˢᵗ Step? → Ⓨ Ⓝ		
23.	△ 11 NUCON	Calculate nuclide concentrations at new flux-time	320
24.	Calculate new resonance disadvantage factor.		340-344
25.	△ 6 RESPRB	Compute new resonance escape probabilities.	
26.	Compute homogenized unit cell properties.		345-353

Step	Flow Chart	Comments	Fortran Statement Number

27. Write all unit cell properties at current flux-time. — 355

28. Calculate fission product cross section and resonance integral. — 360-367

29. △ 7 AVGCS2 — Compute new spectrum-average thermal cross sections — 370

30. Have NUMPOZ steps been taken? → Ⓝ — 375

Ⓨ

△ 21

31. △ 3 TIMECK(2) — Write time.

32. Calculate Lagrangian Coefficients, and select properties for transfer to MOVE Code — 385-400

Step	Flow Chart	Comments	Fortran Statement Number
33.	Y ← (NPT=0?) N	Input control parameter	500
34.	Write output on tape for off-line card punching	Optional punched card output.	510
35.	Y ← (NWT=0?) N	Input control parameter	590
36.	Write output data on binary tape.	Optional binary tape output.	599
37.	Y ← (IPRNT=0?) N	Input control parameter	600
38.	Write output data.		601
39.	2 TIMECK(3)	Write time.	607
40.	2	Start new problem.	

142

The Main Program of the MOVE Code
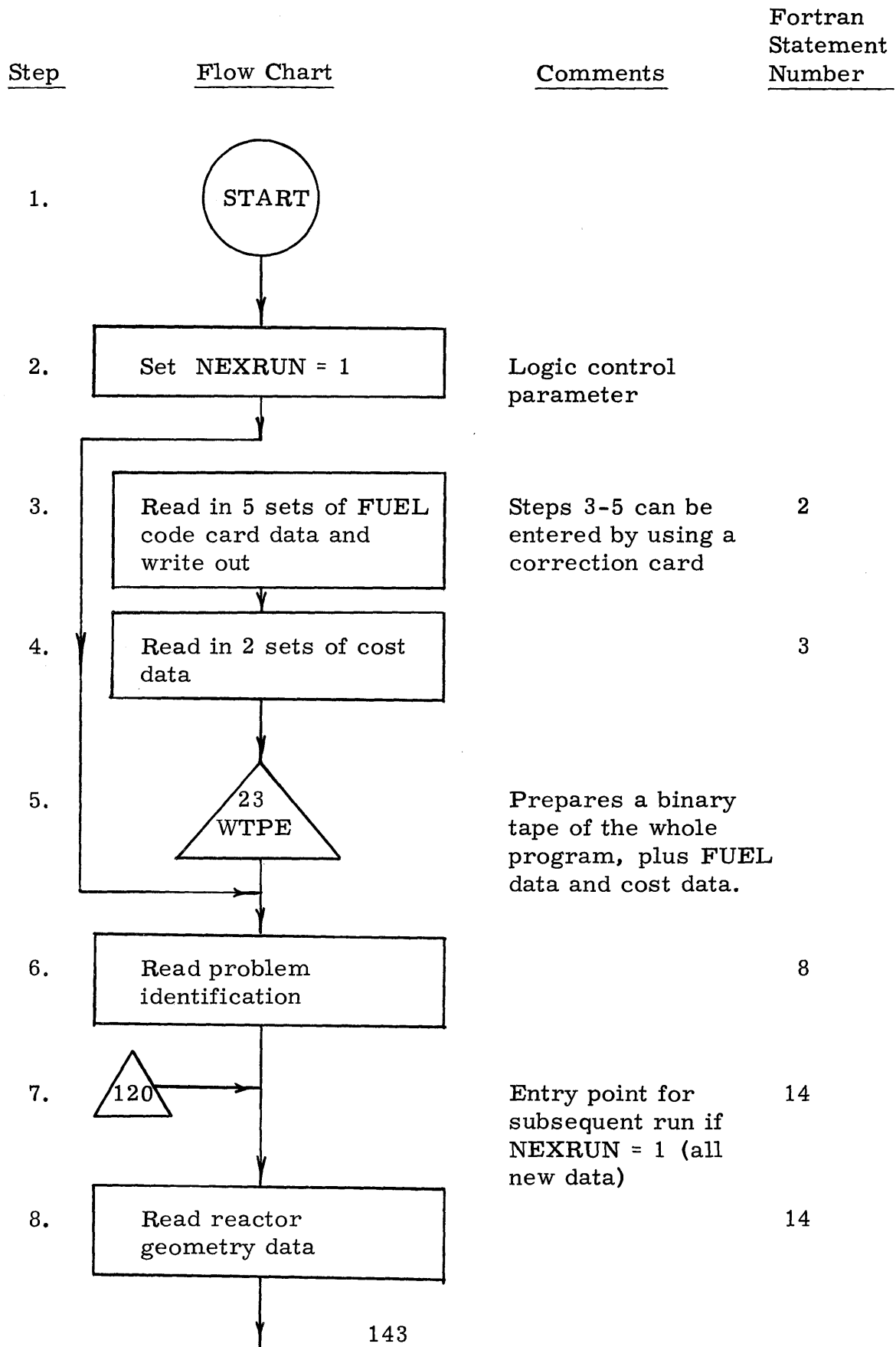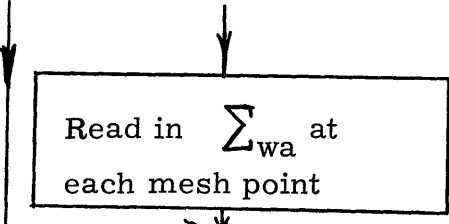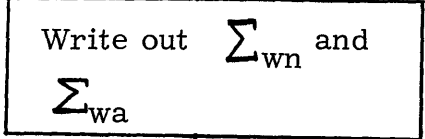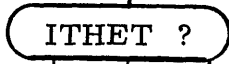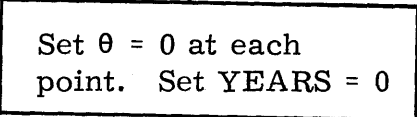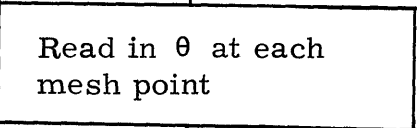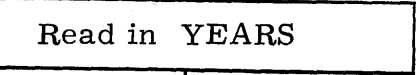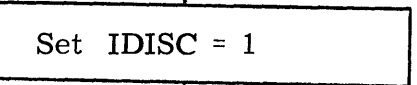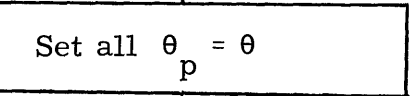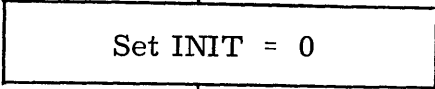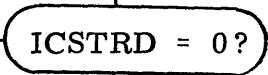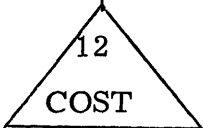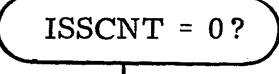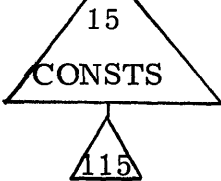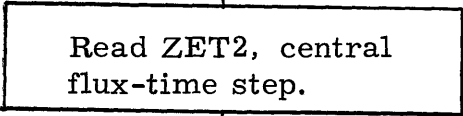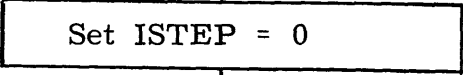
Step	Flow Chart	Comments	Fortran Statement Number
1.	START		
2.	Set NEXRUN = 1	Logic control parameter	
3.	Read in 5 sets of FUEL code card data and write out	Steps 3-5 can be entered by using a correction card	2
4.	Read in 2 sets of cost data		3
5.	23 WTPE	Prepares a binary tape of the whole program, plus FUEL data and cost data.	
6.	Read problem identification		8
7.	120	Entry point for subsequent run if NEXRUN = 1 (all new data)	14
8.	Read reactor geometry data		14

143

Step	Flow Chart	Comments	Fortran Statement Number
9.	△ 121 →	Entry point for subsequent run if NEXRUN = 2 (new control data)	16
10.	Read in control data		16
11.	△ 123 →	Entry point for subsequent run if NEXRUN = 3	22
12.	Write code and problem identification		22
13.	CLOCK	Writes date and time	
14.	Write out geometry and control data		

144

Step	Flow Chart	Comments	Fortran Statement Number

15. NEXRUN ? — Logic control parameter

① ② ③ → △22

16. NRT > 0? — 29

Ⓝ Ⓨ

17. NLOAD > 0? — 30

Ⓨ Ⓝ

18. Read NLOAD groups of FUEL code binary tape records, logical tape NRT — Binary tape input of FUEL Code data — 31-39

19. NLOAD > 0? Ⓝ — 40

Ⓨ

20. Read NLOAD groups of FUEL code cards — Card input of FUEL Code data — 41

145

Step	Flow Chart	Comments	Fortran Statement Number

21. Write FUEL code data — 53

22. △15 —

23. Initialize radial zone properties from zone input data — 80-85

24. △4 SPACON — Calculates space constants

25. (IPRT2 = 0 ?) — Input print control parameter

Y   N

26. Write out "Space constants" — Normally bypassed — 86

27. Set up initial flux shapes — 89-90

28. Make initial leakage estimates —

Step	Flow Chart	Comments	Fortran Statement Number

29. (I POWD = 0?)   Input read control parameter for power density — 91

Y   N

30. Read in power density at all mesh points — 92

31. (I NORMP ?)   Input control parameter for normalized poison — 93

<0   0   >0

32. Set $\sum_{wn} = 1$ — 95-99

33. Read in $\sum_{wn}$ at each mesh point — 100

34. (IABSP ?)   Input control parameter for absolute poison — 108

<0   0   >0

35. Set $\sum_{wa} = 0.$ — 110-112

Step	Flow Chart	Comments	Fortran Statement Number

36. Read in $\sum_{wa}$ at each mesh point — 115

37. Write out $\sum_{wn}$ and $\sum_{wa}$ — 116-122

38. ITHET ? — Input control parameter for flux-time — 124

<0 0 >0

39. Set $\theta = 0$ at each point. Set YEARS = 0 — 125-127

40. Read in θ at each mesh point — 130-131

41. Read in YEARS

42. Set IDISC = 1 — Control parameter for discontinuous fuel movements — 132

43. Set all $\theta_p = \theta$ — θ_p is used in some discontinuous fuel movements — 133

148

Step	Flow Chart	Comments	Fortran Statement Number

44. Set INIT = 0 — Logic control parameter — 135

45. ICSTRD = 0 ? — Input cost data control parameter

Y   N

46. 12 COST — Enter COST to read cost data — 136

47. ISSCNT = 0 ? — Input logic control parameter

Y   N

48. 15 CONSTS — Entry for the continuous steady state fuel movements: graded, outin, bidirectional — 140

115 — Transfer to end of program

50. Read ZET2, central flux-time step. — 150

51. Set ISTEP = 0 — Loop control parameter

Step	Flow Chart	Comments	Fortran Statement Number

52. IBATCH = 0 ? — Input control parameter to bypass Batch calculation.

Y   N

53. △84 — Write ZET2 and IPOIS — Entry point after fuel shuffle. — 155

54. △99 114 →

55. Set LPCNT = 1 ISM = 0 ICTEST = 1 ICONPD = IPOWD — Logical control parameters. ISM controls the Xe and Sm fission product poison — 170

56. △72, 83 → — Re-entry point for next flux-time step calculation — 172

57. IDISC = 1 ? — — 172

Y   N

58. Compute average properties of mixed fuel at each point — Used in discontinuous bidirectional fueling — 173-183

△5 PTPROP

Step	Flow Chart	Comments	Fortran Statement Number

59.
Compute properties of fuel at each point

△ 5 PTPROP

Normal computation of properties   184-185

60. (LPCNT = 1?)

Y   N

61.
Compute new time in years

62.
Write out the central flux-time, and the time in years

63. △ TIMECK (2)

64.
Store the current criticality value

May be needed for flux-time extrapolation

Step	Flow Chart	Comments	Fortran Statement Number

65. ICONPD = 0 ?   —   Input control parameter for constant power density.

66. Y   N

14 CONPWD   —   Calculate flux shape and core properties for constant power density.   195

67. 6 SPACE 2   —   Calculate flux shape and core properties.   200

68. ICTEST ?   —   Logic control parameter (see Step 54)   235

1   2   3

76

73

69. Set ISM = 1 / ICTEST = 2   —   Logic control parameters. Start of initial loop, no Xe and (if flux-time = 0) no Sm poison

Step	Flow Chart	Comments	Fortran Statement Number

70.   Is C > CRIT?   Criticality check

      Y   N

71.   3 / HALT(5)   Stop for too low initial hot, clean criticality   243

72.   56   Exit to start of hot, poisoned flux-time steps

73.   68   Entry from step 68:   250

74.   Will next step result in criticality C < CRIT?

      N   Y

75.   Set ICTEST = 3

Step	Flow Chart	Comments	Fortran Statement Number

76.

68. →

77. Does C = CRIT ± DELCRT ?

CRIT and DELCRT are input parameters: CRIT normally equals unity — 260

N   Y

78. 84

Exit to calculate end-of-batch conditions

79. Make new estimate of central θ step — 262

80. Increase value of flux time at each point, also value of θ_p.

θ_p is used in some discontinuous fuel movements

81. LPCNT = LPCNT + 1

82. Is the central flux time step $> 10^{-6}$ n/kb?

Y   N

83. 56   3

HALT(5)

Stop to prevent erroneous looping

Step	Flow Chart	Comments	Fortran Statement Number

84. △ 53, 78 — Entry point for calculation of end-of-batch conditions — 268

85. Write out final flux-times. — 269-275

86. IMUV = ? — Input parameter: controls entry to various fuel management procedures

(1) (2) (3) (4) (5) → △108 — Discontinuous Bidirectional

→ △105 — Transient Bidirectional

→ △100 — Discont. outin: Steady-State

→ △91 — Discont. outin: Transient

87. △ 11 NCGTHV — Compute average N_m, Burnup, Reactor time for each zone — End-of-batch conditions.

88. Write out results of above computation

155

Step	Flow Chart	Comments	Fortran Statement Number

89. △ 12 COST — Compute fuel cycle cost for each zone, and total energy cost — 350

90. △ 115 — —

91. △ 86 — Entry for outin: discontinuous, transient — 400

92. IEXIT = 1 / ISTEP = ISTEP + 1 — Control parameters

93. △ 104 — — 405

94. (NSTEP > ISTEP ?) — NSTEP is an input control parameter — 405

N   Y

95. Set IEXIT = 0 — —

96. △ 104 — — 420

97. △ 20 SHUFFL — — 420

Step	Flow Chart	Comments	Fortran Statement Number
98.	IEXIT = 0 ?	Check for end of calculation	430
99.	Y 115 N 54	Start new run or continue current run	
100.	86	Entry for outin: discontinuous, steady-state	500
101.	IEXIT = 1 ISTEP = ISTEP + 1	Control parameters	
102.	Are all flux-times within 1% of the previous end-of-batch values ?	Convergence check	510-520
103.	Y IEXIT=0 N		
104.	96 93		

Step	Flow Chart	Comments	Fortran Statement Number

105.

△ 86

Entry for start of transient continuous bidirectional.

600

106.

△ 21 TRNSNT

107.

△ 115

108.

△ 86

Entry for discontinuous bidirectional

650

109.

IEXIT = 1

ISTEP = ISTEP + 1

Control parameters

110.

NSTEP > ISTEP ?

NSTEP is an input control parameter

N   Y

111.

Set IEXIT=0

660

Step	Flow Chart	Comments	Fortran Statement Number

Step		Comments	Fortran Statement Number
112.	22 / DISCNT		670
113.	IEXIT = 0 ?		
114.	Y N / 54		
115.	49 / 90, 99 / 107	Entry point for start of new run.	700
116.	Set INCOST=0		700
117.	2 / TIMECK(4)		
118.	Read in identification, and NEXRUN		

159

Step	Flow Chart	Comments	Fortran Statement Number

119.	NEXRUN = ?	Designator for new input data	
120.	7 (via circle 1)	All new data	
121.	9 (via circle 2)	New control data	
122.	Read in certain new control data	Partially new control data: New enrichment, new fuel and poison methods.	750
123.	11		

160

CHAPTER V

EVALUATION OF THE NEUTRON BEHAVIOR MODEL

A. INTRODUCTION

The conclusive test of the validity of any model which represents a physical situation is how successfully its predictions agree with any experimental data that can be made available.

In particular, a neutron behavior model developed for the prediction of fuel behavior during burnup in a nuclear power reactor, should be capable of the accurate prediction of nuclide concentrations and reactivities at all times during fuel burnup.

The most complete available experimental data on concurrent concentrations and reactivity changes during burnup comes from the cooperative efforts of scientists at Chalk River, Canada, and Harwell, England. Natural uranium r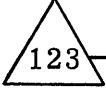ods were irradiated in the NRX reactor, with nuclide concentrations being measured at Chalk River and reactivities determined in the pile oscillator of the GLEEP reactor at Harwell. The essential details of this series of experiments and the interpretation of the results are given below. This work is described in references W51, H51, W52, and C51.

161

B. THE EXPERIMENT AND EXPERIMENTAL DATA

1. The Samples

Twenty-one uranium samples, 6 in. long and 1.36 in. in diameter, were cut from standard NRX metal rods and canned in aluminum, with provision made for flux-time measurement by means of cobalt wires. Each piece of uranium weighed 2710 gms. Eighteen of the samples completed irradiation, one was destroyed, and two were kept as unirradiated standards.

2. The Irradiation

The reactivities of the samples were measured at Harwell prior to irradiation, using the GLEEP pile oscillator. They were then irradiated to various levels in NRX, near the center of the lattice. A year after completion of the irradiation, the samples were remeasured in GLEEP. Five of the irradiated samples were subsequently analysed at Chalk River for uranium and plutonium isotope concentration.

3. The Pile Oscillator

The GLEEP pile oscillator has been described by Littler (L51). In the measurement of the NRX rods, the sample is oscillated in a square wave motion, being in the reactor for 20 sec. and out of the reactor for 20 sec. A balance technique is used, in which an absorber with characteristics similar to the sample is exchanged with the sample, being in the "in" position when the sample is in the "out" position of the oscillator and vice versa. This enables the GLEEP pile oscillator to measure a change in effective cross section with a standard error of 0.34 mm^2, equivalent to 0.13 barns per initial fissile atom (W51).

4. The Interpretation of Pile Oscillator Measurements.

Experimental measurements from a pile oscillator can be

162

interpreted by defining an apparent absorption cross section as:

$$\Sigma_{app} = \frac{\% \text{ pile modulation of sample}}{\% \text{ modulation of standard boron}} \cdot \Sigma_B \qquad (5B1)$$

where Σ_B is a boron standard absorber with known cross section.

This apparent absorption cross section will be equal to the true absorption cross section only in two cases of limited interest; namely (1) the unknown is equal in geometry and cross section to the standard, or (2) both the unknown and the standard can be classed as "infinitely dilute absorbers" in the sense that there is no depression in the flux due to their presence in the reactor and no neutrons are produced as a result of absorptions.

The above statement serves to introduce the two major effects which are to be taken into account in the interpretation of experimental results. The first is the effect of thermal flux depression in the sample, and the second involves the treatment of fission in a sample, and the relative importance of thermal and fission neutrons. The evaluation of these effects involves the measurement of flux depression as a function of absorption cross section and the measurement of the relative importance of fission neutrons. This is, in effect, a calibration of the pile oscillator with respect to absorbing and fissioning nuclides.

In order to compare experimental data on apparent cross sections, or apparent cross section changes with theoretical values, two different approaches can be taken. In one, the theoretical cross section and nuclide concentration data is reduced to the experimental form using the experimental functions of flux depression and fission neutron importance. The other, and opposite approach, is to reduce the experimental data to a form directly comparable to theoretical values. This would involve a separation of the thermal absorption

term from the fission production term which could be accomplished best by having two calibrated pile oscillators with substantially different characteristics with regard to thermal and fission neutrons.

The first method requires only one pile oscillator, but requires that the thermal flux disadvantage factors be accurately known as a function of sample absorption and production, and that the relative importance of fission neutrons be accurately determined. The second method, requiring two calibrated pile oscillators, would yield its best results when the two calibration characteristics were substantially different.

The Chalk River-Harwell program uses the first approach, and their experiments and calculations are given in detail in references W51 and W52. Gunst et al, (G51) have described work at Bettis, using a technique similar to the second method above, except that a control rod worth technique was used to obtain reactivities in two different locations in the same reactor. In this experiment, the samples were measured immediately on discharge from the reactor, and the Xe transient was followed until it died out, the asymptotic reactivities then being obtained. In the Chalk River-Harwell experiments, there was a year lapse between the end of irradiation and the measurements. On the other hand, pile oscillator measurements are inherently more accurate than control rod worth techniques, and separation of absorption and fission effects adds to uncertainties.

The GLEEP pile oscillator measurements have an uncertainty of 0.13 barns per initial fissile atom, equivalent in natural uranium to about 0.00011 in reactivity, whereas the final Bettis results expressed as $\pm$ 1% in η/η_o are equivalent to about 0.01 in reactivity uncertainty. However, the direct reactivity measurements which are used in the results from Bettis have substantially less uncertainty than the final results. The difference is due to the form chosen for presentation of the final results, and involves added uncertainties

because of the separation of the absorption and fission effects. While this separation may be advisable in certain situations, it is not a necessary condition for the evaluation of a neutron behavior model.

Comparison of the reactivity change observed in the GLEEP reactor with that predicted by the FUEL Code is made in terms of Σ_{eff}. The "observed" Σ_{eff} is obtained from observed cross sections, Σ_{app} through Eq. (5B2)

$$\Sigma_{eff} = \frac{F_o}{F} [\Sigma_{app}(\text{irradiated}) - \Sigma_{app}(\text{unirradiated})] \qquad (5B2)$$

where F_o is the average flux in the boron standard and F is the average flux in the unirradiated sample. F_o/F equals 2.13 in the experiments described.

The "calculated" Σ_{eff} is actually both calculated and experimental. Calculated changes in nuclide concentrations are used to obtain changes in the absorption cross section Σ_a and in the fission cross section Σ_f. While the relative change in flux at the sample can be obtained either theoretically or experimentally, a theoretical approach was used in this work. The experimental part of the "calculated" Σ_{eff} involves the evaluation of W, the worth of fast neutrons relative to thermal neutrons. The "calculated" Σ_{eff} is related to the above factors by

$$\Sigma_{eff} = (1 + \frac{\Delta F}{F})(\Sigma_a - \epsilon W \nu \Sigma_f)_{irrad} - (\Sigma_a - \epsilon W \nu \Sigma_f)_{unirrad}$$

$$= (1 + \frac{\Delta F}{F})(\Sigma'_a - \epsilon W \nu \Sigma'_f) + \frac{\Delta F}{F}(\Sigma_a - \epsilon W \nu \Sigma_f)_{unirrad}$$

$$\qquad (5B3)$$

165

where $F + \Delta F$ is the average flux in the irradiated sample

Σ_a is the absorption cross section

Σ_a' is the change in absorption cross section

$\nu\Sigma_f$ is the fission neutron production

$\nu\Sigma_f'$ is the change in fission neutron production

ϵ is the fast fission factor

W   is the importance of fast neutrons relative to thermal neutrons

Calibration of the GLEEP pile oscillator with samples of different U^{235} enrichment showed that the term ϵW had the value 0.886. Using standard properties of natural uranium, and ϵW, the value of 154.1 was obtained for the group $(\Sigma_a - \epsilon W \nu\Sigma_f)_{unirrad}$. Hence for purposes of calculating Σ_{eff} from predicted changes in Σ_a and $\nu\Sigma_f$, Eq. (5B3) becomes

$$\Sigma_{eff} = (1 + \frac{\Delta F}{F})(\Sigma_a' - 0.886 \nu\Sigma_f') - 154.1 \frac{\Delta F}{F} \text{ bifa} \qquad (5B4)$$

In order to use this equation, it is necessary to know how $\Delta F/F$ is affected by changes in fuel composition. The expression obtained on theoretical grounds (W52) is

$$1034.3 \frac{\Delta F}{F} = -0.61 \Sigma_a' + 0.09 \nu\Sigma_f' + 0.04 \Sigma_9 + 0.17 \Sigma_{10} \text{ bifa} \qquad (5B5)$$

This was obtained assuming a neutron current into the rod comprising a Maxwellian thermal component with a $1/E$ epithermal component. The Pu^{239} and Pu^{240} terms in the expression are present due to resonance effects in these nuclides. The quantity 1034. 3 bifa is the initial uranium (2200 m/s) cross section.

While the experiment does not actually measure the reactivity change of NRX rods, it yields a number which is approximately proportional to reactivity change, and which is representative of changes in the neutron behavior during burnup. The method is therefore equivalent to reactivity measurement, and comparisons of theory and experiment are equally valid.

When Σ_{eff} is expressed in 2200 m/s barns change per initial fissile atom, reactivity change for natural uranium is given approximately by

$$\delta\rho \approx \frac{\Sigma_{eff}}{\epsilon p \nu_5 \sigma_{f,5}} \approx \frac{\Sigma_{eff}}{1200}$$

The results of the experimental "reactivity" change will be presented in Section C, below, along with the results predicted by the FUEL Code, for purposes of comparison.

5. The Evaluation of Nuclide Concentrations

In addition to "reactivity" measurements in the pile oscillator, five of the eighteen samples which completed irradiation were analysed chemically to evaluate the plutonium concentration relative to uranium, followed by mass spectrometer analysis of both the uranium and plutonium samples to obtain their isotopic composition (H51).

Then, making the valid assumption that the very small changes in U^{238} concentration can be obtained from a theoretical calculation, the relative isotope concentrations of U and Pu are obtained. It is convenient to express these relative concentrations in atoms per initial fissile atom.

The results of the chemical-mass spectrometer analysis of the five irradiated NRX rods will be presented concurrently with the presentation of the FUEL Code predictions.

C. THE FUEL CODE PREDICTIONS

1. Introduction

In this section, a short description of the NRX reactor will be given, and the preparation of the FUEL Code input data will be outlined. The predictions of the FUEL Code will be compared with experimental nuclide concentrations and "reactivities", and the overall uncertainties in the results due to experimental errors and uncertainties in basic nuclear data will be evaluated.

2. The NRX Reactor

The NRX Reactor is a heavy water moderated, graphite reflected, natural uranium research reactor, located at Chalk River, Canada. It operates at 40 MWt and is cooled by light water. The moderator is maintained at an average of 38°C, and atmospheric pressure. The reactor physics data necessary for the calculations are tabulated in Table 5.1.

3. Preparation of NRX Input Data for the FUEL Code

The actual values of input data used are tabulated in Table 5.2. Those quantities which do not appear specifically are to be set equal to zero.

The normalization is expressed in terms of the initial fissile atom concentration. The nuclide concentration units are atoms per initial fissile atom (aifa) and certain of the cross sections are in barns per initial fissile atom (bifa). This convention is used in this case because experimental results are expressed in barns change per initial fissile atom.

Since only the fuel properties are to be compared, the moderator absorptions need not be considered, but the slowing down properties must be retained, since these are used in both the thermal spectrum computation and the calculation of resonance escape

169

Table 5.1 Reactor Physics Data for NRX

Item	Value	Reference
Fuel Material	Natural uranium metal (ρ = 18.9 gm/cc)	
Slowing down power, $\xi \Sigma_s$ (D$_2$O, H$_2$O mixture)	0.195 cm^{-1}	K$_{51}$, pg. 18
Volume ratio of moderator to fuel V_{mod}/V_{fl}	27	C$_{41}$, pg. 18
Moderator Temperature	38°C	C$_{41}$, pg. 30
Initial Conversion Ratio	0.77	C$_{41}$, pg. 30
Fast Fission Factor, ϵ	1.036	C$_{41}$, pg. 30
Fast Leakage, $B^2 \tau$	0.05	L$_{52}$, pg. 6

Table 5.2 FUEL Code Input Data for the NRX Reactor

Item	Value	Units
N_5^o	1.0	Aifa
N_8^o	137.785	Aifa
EVCUT	0.45	ev
SDP	15,400	Bifa
TMOD	38	^{o}C
PSI1(8)	23.73	-
C1	6.49 E-5	$Bifa^{-1}$
EPSI	1.036	-
P1IN	0.9542	-
SGOXEG	2.868 E+6	Barns
VFL (PSEUDO VALUE)	0.5	-
POWERD	1.742 E+5	kw/litre/ifa
ZETA	0.0001	Neutrons/Barn Cm
SGMSFL	1152 and 230	Bifa
SGOIN7	47.67	Barns
RIUFP	181	Barns
RIPFP	264	Barns
FPFCTR	1.0	-

171

probability.

The general description of the input data preparation is given in Appendix A. Only those quantities which require special treatment due to the special normalization of units will be mentioned. Any quantity not mentioned below is to be obtained in the normal manner as outlined in Appendix A.

The slowing down power, SDP, is computed from

$$SDP(Bifa) = \frac{V_{mod}/V_{fl} \times \int \Sigma_s (cm^{-1}) \times 238 \times 10^{24}(\frac{barns}{cm^2})}{.007115 \times 6.025 \times 10^{23} \times 18.9(gm/cc)} \qquad (5C1)$$

$C_1 = 1/SDP$, since V_{fl} must be set at 0.5

in order to be equal to $(1 - V_{fl})$, due to the fact that the volume weighting is included directly in SDP.

Two other quantities are best obtained by a trial and error process involving a test run of the code. PSI1 (8) is adjusted to yield an initial conversion ratio of 0.77. POWERD is adjusted to yield a 2200 m/s flux of 2×10^{13}. The latter is needed only to compute the effective Xenon cross section which in turn is used only as part of the spectrum hardening parameter.

The scattering cross section of the fuel, SGMSFL, should be based on 8.3 barns per U atom or 1152 bifa. It will be recalled that SGMSFL appears only in the computation of resonance disadvantage factor, as described in Section IVB4. The resonance disadvantage factor ψ_1, m for nuclide m is given by Eq. (4B19) here repeated.

$$\psi_1, m = 1 + \frac{N_m(RI^\infty)_m}{SGMSFL} \qquad (4B19)$$

$m \neq 8$

172

In a well thermalized reactor, such as NRX, the only important nuclide which is directly affected to any degree by its resonance reaction rate is Pu^{240}, whose infinite dilution resonance integral, RI^{∞} is 8350 barns. Because they are formed from Pu^{240}, the nuclides Pu^{241} and Pu^{242} are indirectly affected by the Pu^{240} resonance behavior.

The use of the true value of 1152 bifa for SGMSFL in the NRX apparently underestimates the resonance disadvantage factor for Pu^{240}. A value of 230 bifa yields better agreement with the experimental results. Two sets of results will be given, one using 230 bifa, the other using 1152 bifa for SGMSFL.

4. FUEL Code Predictions and Experimental Data.

Table 5.3 gives the actual numerical results for the NRX unit cell as obtained by the FUEL Code. It will be recalled that the cross sections are spectrum-average thermal values, and that flux-times are the true thermal flux-times. The first four "homogenized properties" can be "dehomogenized" by multiplying by two, to give the average values in bifa.

Table 5.4 compares nuclide concentrations computed by the FUEL Code with those obtained from chemical and mass spectrometer analyses of five uranium rods irradiated to different flux-times. The results using SGMSFL = 230 bifa are also presented graphically in Fig. 5.1.

Tables 5.5 and 5.6 give the total cross section changes for use in the reactivity comparison for the two different values of SGMSFL. These values are the sum of the thermal cross section changes given in Tables 5.7 and 5.8 and the resonance cross sections. These cross sections are spectrum averages and are related to the effective 2200 m/s values by Eqs. (4B8) and (4B9), resulting in the form

173

Table 5.3 Unit Cell Properties During Burnout: NRX Reactor, Natural Enrichment

Thermal Cross Sections (barns)	Flux Time θ (n/kb)					
	0, Xe + Sm	0.10	0.20	0.30	0.50	0.70
$\sigma_{5,f}$	441.5	441.5	441.5	440.7	440.2	439.9
$\sigma_{9,f}$	710.7	710.7	711.3	711.8	712.6	713.2
$\sigma_{11,f}$	897.8	897.8	897.6	897.5	897.3	897.2
σ_5	519.9	519.9	519.5	519.0	518.4	518.1
σ_6	5.51	5.51	5.51	5.50	5.50	5.49
$\sigma_7 = \sigma_{FP}$	37.6	37.6	36.8	36.5	36.0	35.6
σ_8	2.142	2.142	2.140	2.139	2.136	2.135
σ_9	1041.3	1041.3	1042.5	1043.5	1045.1	1046.2
σ_{10}	232.2	232.2	232.0	231.9	231.8	231.7
σ_{11}	1235.8	1235.8	1235.6	1235.4	1235.1	1235.0
σ_{12}	24.0	24.0	24.0	24.0	23.9	23.9
AIFA						
N_5	1.000	0.949	0.900	0.853	0.768	0.691
N_6	0.	7.860 E-3	1.530 E-2	2.235 E-2	3.535 E-2	4.699 E-2
$N_7 = N_{FP}$	0.	4.768 E-2	9.584 E-2	0.144	0.242	0.340
N_8	137.8	137.7	137.7	137.7	137.6	137.5

Table 5.3 (Cont'd)

AIFA	Flux Time θ (n/Kb)					
	θ, Xe + Sm	0.10	0.20	0.30	0.50	0.70
N_9	0	3.859 E-2	7.344 E-2	0.105	0.159	0.203
N_{10}	0	6.530 E-4	2.463 E-3	5.238 E-3	1.311 E-2	2.342 E-2
N_{11}	0	1.627 E-5	1.199 E-4	3.641 E-4	1.325 E-3	2.836 E-3
N_{12}	0	1.551 E-7	2.190 E-6	1.018 E-5	6.534 E-5	2.067 E-4
Homogenized Properties						
$\Sigma_{XE\ MAX}$	15.43	15.19	15.16	15.11	14.95	14.73
$\Sigma - \Sigma_{XE}$	411.7	419.6	426.1	431.7	440.9	447.7
Σ_f	220.7	223.1	224.6	225.5	226.1	225.4
$\nu\Sigma_f$	540.8	552.5	561.6	568.9	579.0	584.3
$(1-p)/(1+\alpha)$	5.832 E-3	6.410 E-3	6.829 E-3	7.140 E-3	7.550 E-3	7.782 E-3
$(1-p)$	1.440 E-2	1.612 E-2	1.739 E-2	1.834 E-2	1.963 E-2	2.042 E-2
p	0.8916	0.8898	0.8880	0.8860	0.8825	0.8798
Σ_{MOD}	0	0	0	0	0	0
Other Properties						
$\theta_o = n v_o t$(n/Kb)	0	0.08038	0.1607	0.2410	0.4015	0.5620
T_{NEUT}, $^oC.$	98	98	99	99	100	101

Table 5.4 FUEL Code and Experimental NRX Nuclide Concentrations

Nuclide	True Thermal Flux-time	Nuclide Concentration (AIFA)		
		FUEL Code		Experimental
		$\Sigma_{s, fl} = 230$	$\Sigma_{s, fl} = 1152$	
U^{235} ΔN_5	0.0432	0.0226	0.0230	0.0196 + 0.0014
	0.1149	0.0590	0.0600	0.0576 + 0.0014
	0.2822	0.1388	0.1411	0.1439 + 0.0014
	0.4780	0.2236	0.2272	0.2197 + 0.0022
	0.7878	0.3412	0.3462	0.3451 + 0.0017
Pu^{239} N_9	0.0432	0.0171	0.0172	0.0175 + 0.0003
	0.1149	0.0440	0.0442	0.0451 + 0.0010
	0.2822	0.0995	0.0997	0.0999 + 0.0048
	0.4780	0.1534	0.1536	0.1535 + 0.0011
	0.7878	0.2189	0.2189	0.2168 + 0.0016
Pu^{240} $N_{10} \times 10^2$	0.0432	0.0126	0.0126	0.0128 + 0.0003
	0.1149	0.0855	0.0858	0.0838 + 0.0020
	0.2822	0.4688	0.4700	0.476 + 0.0200
	0.4780	1.2110	1.2050	1.192 + 0.010
	0.7878	2.8450	2.7650	2.800 + 0.027
Pu^{241} $N_{11} \times 10^2$	0.0432	0.00013	0.00014	0.0001 + 0.0001
	0.1149	0.0025	0.0025	0.0017 + 0.0004
	0.2822	0.0311	0.0322	0.0317 + 0.0017
	0.4780	0.1210	0.1340	0.118 + 0.002
	0.7878	0.3740	0.458	0.377 + 0.004
Pu^{242} $N_{12} \times 10^2$	0.0432	-	-	-
	0.1149	-	-	-
	0.2822	-	-	-
	0.4780	-	-	-
	0.7878	0.0311	0.0361	0.0294 + 0.0014
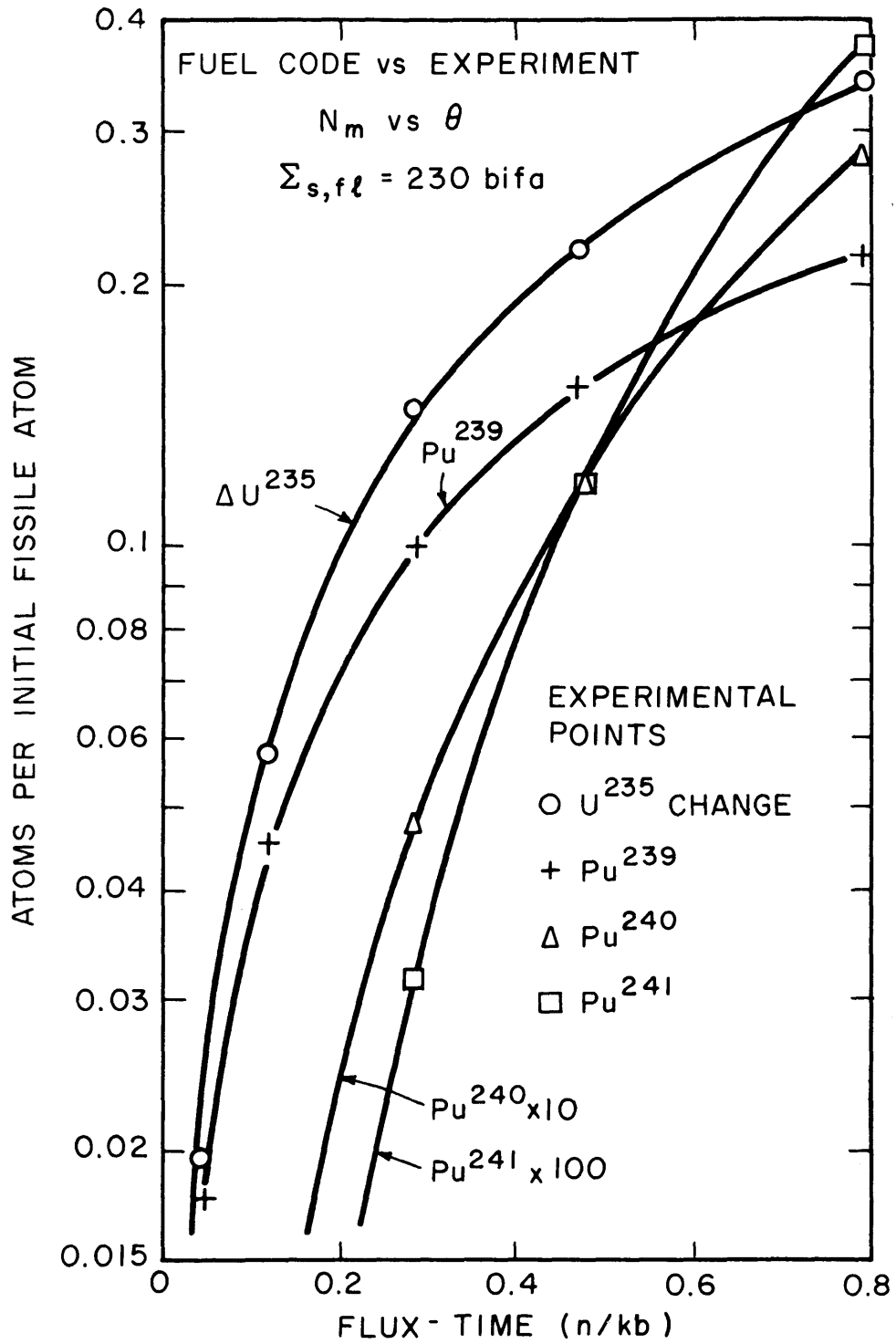
FIG. 5.1   FUEL CODE NUCLIDE
CONCENTRATIONS COMPARED
WITH EXPERIMENTAL ANALYSIS
OF IRRADIATED NRX RODS

177

Table 5.5 Total Cross Section Changes:

NRX Rods in GLEEP Spectrum, SGMSFL = 1152 BIFA

Cross Section Change	True Thermal Flux-time (n/Kb)				
	0.1	0.2	0.3	0.5	0.7
Σ_5'	-28.1	-55.2	-80.8	-127.9	-170.1
Σ_6	0.1	0.4	0.5	0.8	1.1
Σ_8'	-0.2	-0.7	-1.1	-1.9	-2.3
Σ_9	41.6	79.1	113.0	171.0	218.5
Σ_{10}	0.6	2.0	4.1	9.8	16.6
Σ_{11}	0.0	0.1	0.5	2.0	4.5
Σ_{FP}	2.5	4.8	7.1	12.0	16.8
Σ_{SM}	8.9	9.4	9.8	10.5	11.0
Σ_a'	25.4	39.9	53.1	76.3	96.1
$(\nu\Sigma_f)_5'$	-58.2	-114.5	-167.5	-265.2	-352.5
$(\nu\Sigma_f)_9$	81.8	155.6	222.3	336.7	429.4
$(\nu\Sigma_f')_{11}$	0.0	0.0	0.9	4.3	9.9
$\nu\Sigma_f'$	23.6	41.4	55.7	75.8	86.8

178

Table 5.6 Total Cross Section Changes:

NRX Rods in the GLEEP Spectrum, SGMSFL = 230 BIFA

Cross Section Change	True Thermal Flux-time (n/kb)				
	0.1	0.2	0.3	0.5	0.7
Σ_5'	-27.0	-53.2	-77.8	-123.2	-164.0
Σ_6	0.1	0.4	0.5	0.8	1.1
Σ_8'	-0.2	-0.7	-1.1	-1.9	-2.4
Σ_9	41.5	78.8	112.5	170.1	216.9
Σ_{10}	0.6	1.9	3.7	8.1	12.6
Σ_{11}	0.0	0.1	0.5	1.8	3.8
Σ_{FP}	2.5	4.7	7.0	11.5	15.9
Σ_{SM}	8.9	9.4	9.8	10.5	11.0
Σ'	26.4	41.4	55.1	77.7	94.9
$\Sigma_{5,f}\nu_5'$	-56.2	-110.4	-161.6	-256.0	-340.6
$\Sigma_{9,f}\nu_9$	81.6	155.0	221.2	334.4	426.2
$\Sigma_{11,f}\nu_{11}$	0.0	0.3	1.1	3.9	8.4
$\Sigma_f\nu'$	25.4	44.9	60.7	82.3	94.0

179

Table 5.7 Thermal Cross Section Changes:
NRX Rods in the GLEEP Spectrum, SGMSFL = 1152 BIFA

Cross Section Change	True Thermal Flux-time (n/kb)				
	0.1	0.2	0.3	0.5	0.7
$\Sigma_5^{th'}$	-27.3	-53.5	-78.3	-123.9	-164.7
Σ_6^{th}	0.0	0.1	0.1	0.2	0.3
$\Sigma_8^{th'}$	-0.1	-0.4	-0.8	-1.3	-1.6
Σ_9^{th}	40.2	76.6	109.5	165.9	211.9
Σ_{10}^{th}	0.2	0.6	1.2	3.0	5.3
Σ_{11}^{th}	0.0	0.1	0.5	1.9	4.3
Σ_{FP}^{th}	1.8	3.5	5.2	8.7	12.1
Σ_{SM}^{th}	8.9	9.4	9.8	10.5	11.0
$\Sigma_a^{th'}$	23.7	36.4	47.2	65.0	78.6
$(\nu\Sigma_f)_5^{th'}$	-56.7	-111.4	-163.1	-258.0	-342.8
$(\nu\Sigma_f)_9^{th}$	79.2	150.8	215.5	326.6	416.8
$(\nu\Sigma_f)_{11}^{th}$	0.0	0.3	0.9	4.1	9.5
$(\nu\Sigma_f)^{th'}$	22.5	39.7	53.3	72.7	83.5

Table 5.8 Thermal Cross Section Changes:

NRX Rods in the GLEEP Spectrum, SGMSFL = 230 BIFA

Cross Section Change	True Thermal Flux-time (n/kb)				
	0.1	0.2	0.3	0.5	0.7
$\Sigma_5^{th'}$	-26.8	-52.7	-77.1	-122.1	-162.4
Σ_6^{th}	0	0.1	0.1	0.2	0.3
$\Sigma_8^{th'}$	-0.1	-0.4	-0.8	-1.3	-1.7
Σ_9^{th}	40.2	76.6	109.5	165.9	211.9
Σ_{10}^{th}	0.2	0.6	1.2	3.0	5.4
Σ_{11}^{th}	0	0.1	0.5	1.7	3.6
Σ_{FP}^{th}	1.8	3.5	5.2	8.7	12.1
Σ_{SM}^{th}	8.9	9.4	9.8	10.5	11.0
$\Sigma^{th'}$	24.2	37.2	48.4	66.6	80.2
$\Sigma_{5,f}^{th}\nu_5'$	-55.8	-109.6	-160.4	-254.0	-337.8
$\Sigma_{9,f}^{th}\nu_9$	79.2	150.7	215.4	326.4	416.6
$\Sigma_{11,f}^{th}\nu_{11}$	0	0.3	1.0	3.7	8.0
$\Sigma_f^{th}\nu'$	23.4	41.4	56.0	76.1	86.8

181

$$\frac{\sigma}{\sigma_o} = \frac{(n_{th} + n_{epi})v_o}{n_{th} \bar{v}} = \frac{\theta_o}{\bar{\theta}} \qquad (5C2)$$

The total cross section is composed of the thermal and the resonance cross section and is obtained from the FUEL Code equation:

$$\sum_m^{TOT} = \sum_m^{TH} + \sum_m^{R} \qquad (5C3)$$

where

$$\sum_m^{TH} = N_m \sigma_m \qquad (5C4)$$

$$\sum_m^{R} = q/\phi \, P_1 <1 - p_m> \qquad (5C5)$$

It will be recalled that the results given above will be for the NRX neutron spectrum, whereas the comparison is to be made on the basis of the GLEEP spectrum. It has been assumed that the thermal 2200 m/s effective cross sections are identical in both reactors. The slowing down density per unit thermal flux, q/ϕ , is set equal to 1.1 times (W52) the initial value of q/ϕ in the NRX reactor, as is characteristic of the GLEEP reactor. The GLEEP spectrum resonance cross section can then be obtained from Eq. (5C5).

Eqs. (5B4) and (5B5) can be used with the spectrum average cross sections calculated in the FUEL Code, if the equations are rewritten as

$$\sum_{eff} = \frac{\theta}{\theta_o} (1 + \frac{\Delta F}{F})(\sum_a' - 0.886 \, \nu \sum_f') - 154.1 \frac{\Delta F}{F} \qquad (5C6)$$

182

and:

$$1034.3 \, \frac{\Delta F}{F} = \frac{\theta}{\theta_o} \left\{ - 0.61 \, \Sigma_a' + 0.09 \, \nu\Sigma_f' + 0.04 \, \Sigma_9 + 0.17 \, \Sigma_{10} \right\}$$

<div align="right">(5C7)</div>

where the cross sections are now understood to be spectrum average, instead of effective 2200 m/s. The ratio θ/θ_o is 1.244 for the series of results presented for the NRX reactor.

Table 5.9 gives the results of the calculation of the terms appearing in Eqs. (5C6) and (5C7), along with final values of Σ_{eff}, both theoretical and experimental.

These results are presented graphically in Fig. 5.2. Included for comparison, are the experimental results.

The discussion of the FUEL Code predictions of reactivity and nuclide concentrations will be given in Section D of this chapter, following the discussion below of the significance of experimental errors and uncertainties in basic nuclear data.

5. The Significance of Errors and Uncertainties

There are three types of errors which are of importance in this comparison of theory and experiment. First, there are direct experimental uncertainties in reactivity, and in flux-time measurements. The stated uncertainty in the GLEEP reactivity measurements is 0.13 bifa, and the cobalt flux-time monitors have an activity uncertainty of 2%, which will result in a flux-time uncertainty of a minimum of 2%, assuming that the cobalt monitors are operating on the nearly-linear part of their activity-flux-time characteristic, well below saturation. Because of the shape of the Σ_{eff} vs. flux-time curves (Fig. 5.2), the total experimental uncertainty in Σ_{eff} is made up almost completely of reactivity measurement uncertainty for irradiations below about 0.3 n/kb. The flux-time uncertainty

Table 5.9 Calculation of Σ_{EFF} and Comparison with Experiment: $\Sigma_{s,fl}$ = 1152 BIFA

θ	θ_o	$\Delta\Sigma_{TOT}$*	$\Delta\nu\Sigma_{f\,TOT}$*	$\dfrac{\Delta F}{F}$	$\dfrac{\theta}{\theta_o}(1 + \dfrac{\Delta F}{F})$	$\Sigma_{net} =$ $\Delta\Sigma_{TOT}$ $-0.886\Delta\nu\Sigma_f$	Σ'_{eff}* Fuel Code	Smoothed Experimental Σ_{eff}
0.1	0.0804	25.4 (26.4)	23.6 (25.4)	-0.0144	1.228	4.5 (3.9)	7.7 (7.0)	0.7
0.2	0.161	39.9 (41.4)	41.4 (44.9)	-0.0211	1.220	3.2 (1.6)	7.2 (5.2)	-2.2
0.3	0.241	53.1 (55.1)	55.7 (60.7)	-0.0276	1.212	3.7 (1.3)	8.8 (5.9)	-2.3
0.5	0.402	76.3 (77.7)	75.8 (82.3)	-0.0382	1.198	9.1 (4.8)	16.8 (11.6)	3.6
0.7	0.562	96.1 (94.9)	86.8 (94.0)	-0.0463	1.188	19.2 (11.6)	29.9 (20.9)	14.8

* Values in parentheses are for $\Sigma_{s,fl}$ = 230 BIFA

184
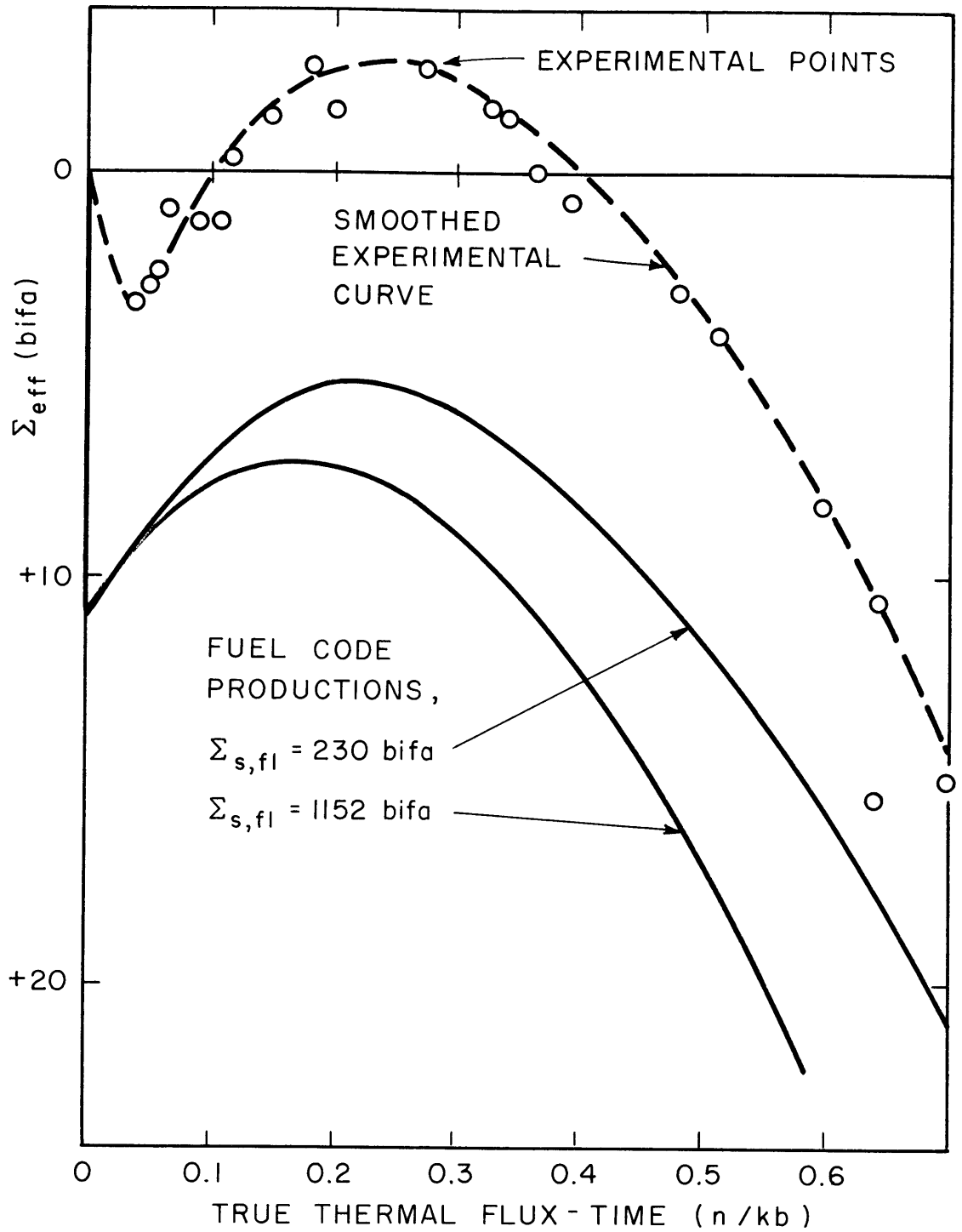
FIG. 5.2   REACTIVITY CHANGE: EXPERIMENT vs
FUEL CODE PREDICTION

185

then starts to become important, and above 0.6 n/kb the experi-mental uncertainty in Σ_{eff} is made up almost completely of flux-time uncertainty, and hence, to a good approximation the percentage uncertainty in Σ_{eff}, above 0.6 n/kb will equal the percentage un-certainty in flux-time which is a minimum of 2%.

The second type of error is that associated with uncertainties in the basic nuclear data used as fundamental constants in the code. In particular the values used for the fission and absorption cross sections, and neutron yields in fission of U^{235} and Pu^{239} are most important at lower burnups, with the higher Pu isotopes becoming more and more important as burnup increases. The fission product cross section uncertainty is also important.

The third type of error is due to inaccuracies in the neutron behavior model used.

In order to evaluate the FUEL Code neutron behavior model errors in the calculation of the NRX unit cell behavior during burn-up, it is necessary to obtain an estimate of the probable error due to uncertainties in basic nuclear data. This is done as follows:

The basic problem is to evaluate the uncertainty in the FUEL Code predicted value of Σ_{eff}. Actually, it is more convenient to deal with the quantity $\Sigma_{net}(W_{52})$ given by

$$\Sigma_{net} = \theta/\theta_o (\Sigma_a' - 0.886 \Sigma_f') = \frac{\Sigma_{eff} + 154 \, \Delta F/F}{1 + \frac{\Delta F}{F}} \qquad (5C8)$$

A conservative estimate of the uncertainty in Σ_{net} can be obtained by considering only the uncertainties in U^{235} and Pu^{239} absorption and fission parameters, plus the uncertainty in the fission product cross section. The effects of uncertainties in other terms can be shown to be smaller than the above factors over the irradiation range considered. Σ_{net} can then be rewritten, separating

186

it into the three important components above, plus the others.

$$\Sigma_{net} = \frac{\theta}{\theta_0} \ (\Sigma_a' - 0.886 \nu \Sigma_f')_5 + (\Sigma_a - 0.886 \nu \Sigma_f)_9$$

$$+ (\Sigma_a)_{FP} \qquad + \text{Other} \qquad\qquad (5C9)$$

Then, using the standard propagation of errors formula, the uncertainty in Σ_{net}, $\delta \Sigma_{net}$, is given by

$$(\delta \Sigma_{net})^2 = (\frac{\theta}{\theta_0})^2 \left\{ [\delta (\Sigma_a' - 0.886 \nu \Sigma_f')_5]^2 \right.$$

$$\left. + [\delta (\Sigma_a - 0.886 \nu \Sigma_f)_9]^2 + [\delta \Sigma_{FP}]^2 \right\}$$

$$= (\theta/\theta_0)^2 \left\{ \delta_5^{\ 2} + \delta_9^{\ 2} + \delta_{FP}^{\ 2} \right\} \qquad (5C10)$$

It is implicit in the above formula that all uncertainties be in independent variables. This will not cause any difficulty, with one exception. An initial microscopic cross section, σ^o, cannot be considered independent of the same cross section, σ, evaluated in a slightly different neutron spectrum at a later time. While there may be some slight uncertainty due to neutron spectrum change uncertainty, the ratio, σ^o/σ, can be treated as a constant, with zero uncertainty. The three components of $\delta \Sigma_{net}$ can now be evaluated.

U^{235}: Assuming $N_5 = N_5^o \ e^{-\sigma_5 \theta}$,

$$A = \Sigma_5' - 0.886 \nu \Sigma_{f,5}'$$

$$= N_5^O \sigma_5 \left\{ e^{-\sigma_5 \theta} - \left(\frac{\sigma_5 O}{\sigma_5}\right) - 0.886 \eta_5 \left[e^{-\sigma_5 \theta} - \left(\frac{\sigma_{f,5} O}{\sigma_{f,5}}\right) \right] \right\}$$

$$(5C11)$$

$$\delta_5^2 = \left(\frac{\delta A}{\delta \sigma_5}\right)^2 \delta \sigma_5^2 + \left(\frac{\delta A}{\delta \eta_5}\right)^2 \delta \eta_5^2$$

$$= \left[\Sigma_5' - \sigma_5 \theta \left(\Sigma_5 - 0.886 \nu_5 \Sigma_{f,5} \right) \right]^2 \left(\frac{\delta \sigma_5}{\sigma_5}\right)^2$$

$$+ \left[0.886 \nu_5 \Sigma_{f,5}' \right]^2 \left(\frac{\delta \eta_5}{\eta_5}\right)^2 \qquad (5C12)$$

Pu^{239}: Assuming $N_9 = \dfrac{N_8^O \sigma_8}{\sigma_9} \left[1 - e^{-\sigma_9 \theta} \right]$

$$B = \Sigma_9 - 0.886 \nu \Sigma_{f,9}$$

$$= N_8^O \sigma_8 \left[1 - e^{-\sigma_9 \theta} \right] \left[1 - 0.886 \eta_9 \right] \qquad (5C13)$$

$$\delta_9^2 = \left(\frac{\delta B}{\delta \sigma_8}\right)^2 \delta \sigma_8^2 + \left(\frac{\delta B}{\delta \sigma_9}\right)^2 \delta \sigma_9^2 + \left(\frac{\delta B}{\delta \eta_9}\right)^2 \delta \eta_9^2$$

$$= \left[\Sigma_9 - 0.886 \nu_9 \Sigma_{f,9} \right]^2 \left(\frac{\delta \sigma_8}{\sigma_8}\right)^2 + \left[0.886 \nu_9 \Sigma_{f,9} \right]^2 \left(\frac{\delta \eta_9}{\eta_9}\right)^2$$

$$+ \left[\theta \sigma_9 \left(\frac{\Sigma_8}{\Sigma_9} - 1\right)\left(\Sigma_9 - 0.886 \nu_9 \Sigma_{f,9} \right) \right]^2 \left(\frac{\delta \sigma_9}{\sigma_9}\right)^2 \qquad (5C14)$$

188

Fission products:

$$\delta_{FP}^2 = (\textstyle\sum_{FP})^2 (\frac{\delta\sigma_{FP}}{\sigma_{FP}})^2 \tag{5C15}$$

In the above development, the microscopic cross sections are understood to contain both thermal and effective resonance components. A conservative estimate of cross section uncertainties is obtained by assuming that the percentage uncertainty is identical to the percentage uncertainty in the 2200 m/s cross section values.

In Table 5.10, the magnitudes and uncertainties of the eight independent variables considered in this study are given. The values used are world consistent values, with two exceptions. ν_5 has been taken as 2.45 $\pm$ 0.02 instead of the world consistent value of 2.43 $\pm$ 0.02, and it was assumed that there was a 10% uncertainty in the low cross section fission products. In the same table, FUEL code thermal plus effective resonance microscopic cross sections are given.

Table 5.11 gives the actual FUEL Code values of the three terms needed to obtain the overall uncertainty in Σ_{net} as given by Eqs. (5C12), (5C14), and (5C15). Table 5.12 gives the actual calculation steps, broken down so as to illustrate the relative contribution of each uncertainty.

In order to compare reactivity shapes without the complication imposed by the initial discrepancy, the experimental and FUEL Code results may be presented as is done in Fig. 5.3 with both curves starting at the same zero point. The FUEL Code curve of $\Sigma_{net} - \Sigma_o$ has been obtained by subtracting the zero flux-time Sm group fission product cross section Σ_o = 8.9 bifa, from Σ_{net} as given in Table 5.8 for SGMSFL = 230 bifa and converting to effective 2200 m/s cross

189

Table 5.10 Uncertainties in Basic Nuclear Data

(World Weighted except for ν_5)

Parameter	Value	% Uncertainty
η_5	2.07 ± 0.01	0.48
ν_5	2.45 ± 0.02	0.82
η_9	2.08 ± 0.02	0.96
ν_9	2.89 ± 0.03	1.04
2200 m/s Values		
$(\sigma_o)_5$	683 ± 3	0.44
$(\sigma_o)_{f,5}$	582 ± 4	0.69
$(\sigma_o)_9$	1028 ± 8	0.78
$(\sigma_o)_{f,9}$	742 ± 4	0.54
$(\sigma_o)_8$	2.71 ± 0.02	0.74
$(\sigma_o)_{FP}$	-	10.0 (assumed)
FUEL Code Values		
σ_5	530.2	—
σ_9	1071	—

Table 5.11 FUEL Code Data for Uncertainty Determination

Parameter	Values in BIFA				
$\theta n/kb$	0.1	0.2	0.3	0.5	0.7
Σ_5	502.6	476.4	451.8	406.4	365.6
Σ_5'	-27.0	-53.2	-77.8	-123.2	-164.0
$\nu_5\Sigma_{f,5}$	1042.4	988.2	937.0	842.6	758.0
$\nu_5\Sigma_{f,5}'$	-56.2	-110.4	-161.6	-256.0	-340.6
$\sigma_5\theta$	0.053	0.106	0.159	0.265	0.372
Σ_9	41.5	78.8	112.5	170.1	216.9
$\nu_9\Sigma_{f,9}$	81.6	155.0	221.2	334.4	426.2
$\sigma_9\theta$	0.107	0.214	0.321	0.535	0.750
Σ_8	406.4	405.9	405.5	404.7	404.2
Σ_{FP}	2.5	4.7	7.0	11.5	15.9

191

Table 5.12 Computation of Uncertainties in BIFA

Term	Uncertainty				
Flux-time, θ	0.1	0.2	0.3	0.5	0.7
$L = - [\sum_5' - \sigma_5 \theta(\sum_5 - 0.886 \nu_5 \sum_{f5})](\frac{\delta\sigma_5}{\sigma_5})$	0.02	0.05	0.08	0.15	0.22
$M = 0.886 \nu_5 \sum_{f,5}' (\frac{\delta\eta_5}{\eta_5})$	0.24	0.47	0.69	1.09	1.45
$N = - [\sum_9 - 0.886 \nu_9 \sum_{f,9}](\frac{\delta\sigma_8}{\sigma_8})$	0.23	0.43	0.62	0.93	1.19
$O = 0.886 \nu_9 \sum_{f,9} (\frac{\delta\eta_9}{\eta_9})$	0.69	1.32	1.88	2.84	3.62
$P = \theta\sigma_9 (\frac{\sum_8}{\sum_9}) - 1)(\sum_9 - 0.886 \nu_9 \sum_{f,9})(\frac{\delta\sigma_9}{\sigma_9})$	0.22	0.41	0.54	0.72	0.81
$Q = \sum_{FP} (\frac{\delta\sigma_{FP}}{\sigma_{FP}})$	0.25	0.47	0.70	1.15	1.59
$\delta^2 = L^2 + M^2 + N^2 + O^2 + P^2 + Q^2$	0.698	2.540	5.183	11.982	19.856
$\delta\sum_{net} = \frac{\theta}{\theta_o} \delta$; $\frac{\theta}{\theta_o} = 1.244$	1.04	1.98	2.83	4.31	5.54
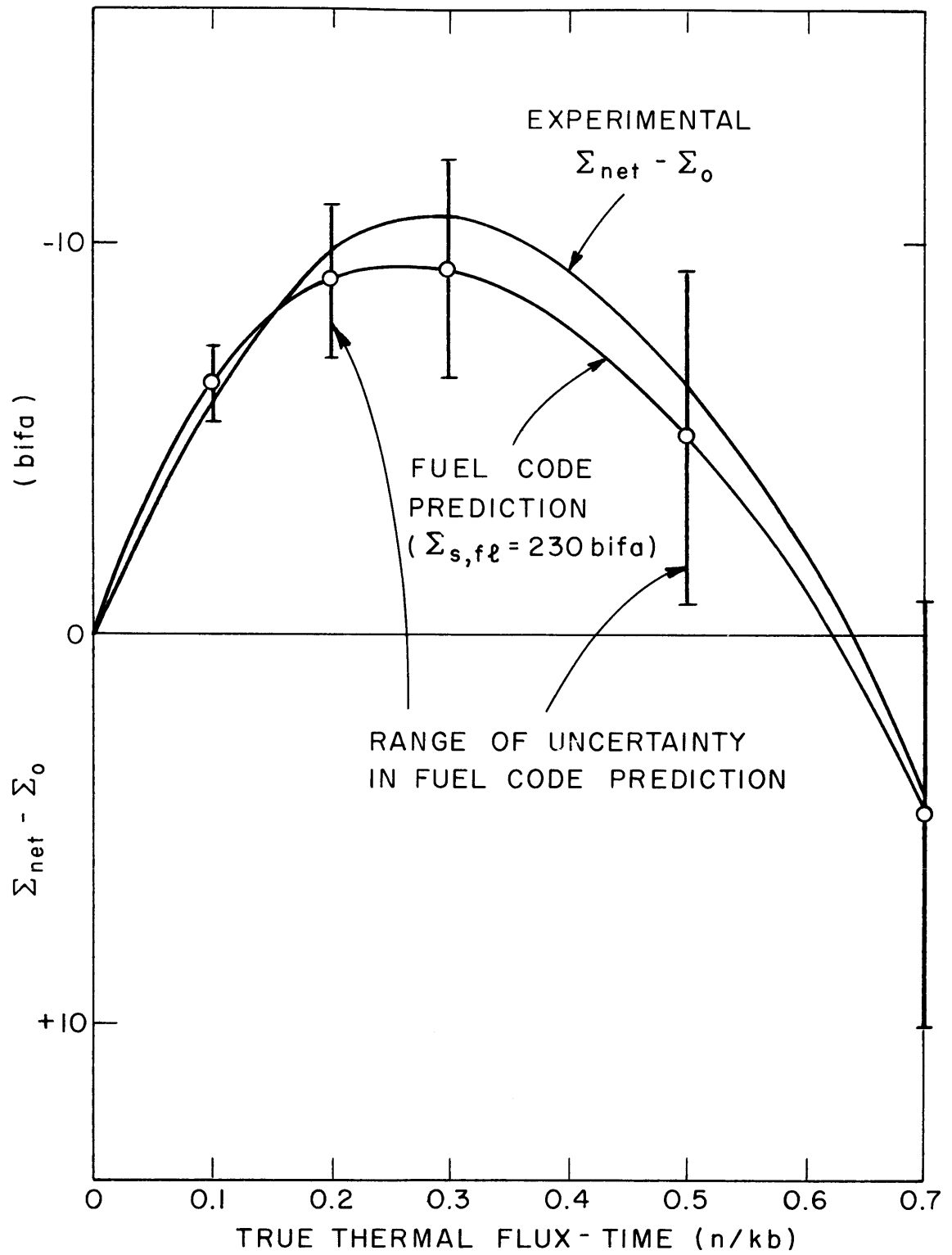
FIG. 5.3   THE EFFECT OF UNCERTAINTIES IN
BASIC NUCLEAR DATA

193

sections by multiplying by $\theta/\theta_o = 1.244$. The experimental curve of $\sum_{net} - \sum_o$ was obtained by subtracting $\sum_o = 4.2$ bifa from $\sum_{net}$ in Fig. 3b of W_{52}. In this case, $\sum_o$ was obtained by a linear extrapolation back to $\theta_o = 0$ of the part of the curve in which the Sm group had reached equilibrium. Both curves are then plotted starting at $\sum_{net} - \sum_o = 0$ at $\theta = 0$. Also, as part of the comparison, the uncertainty in the FUEL Code prediction due to basic nuclear data uncertainty is shown.

D. DISCUSSION OF RESULTS

1. Nuclide Concentrations

Referring to Table 5.4, it can be seen that there is good agreement between FUEL Code predictions and experimental values of nuclide concentrations for all nuclides, using the true value of SGMSFL, 1152 bifa. It is apparent, however, at higher flux-times, that a trend is starting toward too-large concentrations of Pu^{241} and Pu^{242}. This is probably due to underestimation of the Pu^{240} disadvantage factor, causing too fast a buildup of Pu^{241} and Pu^{242} at the higher flux-times. The use of the value of 230 bifa for SGMSFL can be seen to yield more nearly correct Pu^{241} and Pu^{242} concentrations at higher flux-times.

Using the adjusted value of 230 bifa for SGMSFL, the worst discrepancy between prediction and experiment is in ΔN_5 at the lowest irradiation. There is a fair possibility that the experimental value is in error, since it would yield an initial conversion ratio of about 0.9, which is substantially higher than the actual value of about 0.77.

The remainder of the experimental points are randomly situated on either side of the FUEL Code curves, as can be seen by referring to Fig. 5.1. It will be noted that the theoretical values are generally outside the range of the stated error given in Table 5.4. This error, however, is the statistical error of the combined mass spectrometer and chemical analyses, and does not include the 2% uncertainty in the flux time, which is the dominant uncertainty in the experimental values at flux-times greater than 0.2 n/kb. When both types of uncertainty are taken into consideration, there is excellent consistency between experiment and the FUEL Code predictions of nuclide concentrations.

195

2. Reactivity

Referring to Fig. 5.2, it is apparent that a major discrepancy exists between experiment and the predictions of the FUEL Code. This deviation is larger than can be attributed to uncertainties in basic nuclear data as shown in Fig. 5.3. The same effect is noted in the comparison of experiment and theory by the Canadian group at Chalk River (W_{41}) using a neutron behavior model which is different from that of the FUEL Code. Because the discrepancy is confirmed by two somewhat different neutron behavior models, there is a presumption that the models are not wholly responsible for the discrepancy.

Due to the correspondence in reactivity shapes after the initial discrepancy, it would appear that some short term effect is to blame, possibly the Sm group of large cross section fission product poisons, or an initial large cross section impurity in the samples prior to irradiation. If the Sm group of fission products are the cause of the discrepancy, their fission yields will be in error by substantially more than their stated uncertainties. This explanation is therefore improbable unless it is possible that the chemically determined Sm yield is somehow different from the high cross section nuclear yield. The alternative explanation, involving the possible presence of a high cross section impurity in the unirradiated samples has been considered and rejected (W_{41}), since this could account for at most, 20% of the observed error.

The one year lapse of time between the end of irradiation and the reactivity measurement may also be associated with the discrepancy, although the specific mechanism is open to conjecture.

If the initial uncertainties discussed above are removed, the relative shapes of the FUEL Code and experimental reactivities can be compared. It is apparent from Fig. 5.2 that the reactivity shape is somewhat sensitive to the resonance reaction rate which depends

on the value of SGMSFL. It was mentioned previously that the true value of SGMSFL, 1152 bifa, was causing a trend toward too-high Pu^{241} and Pu^{242} nuclide concentrations at the higher flux-times, indicating a resonance disadvantage factor which was too small. A value of 230 bifa for SGMSFL gives results which compare more satisfactorily with experiment. The experimental nuclide concentrations can be considered as the experimental data required to evaluate the resonance disadvantage factors. Fig. 5.3 has been drawn using the "experimental" value of SGMSFL, 230 bifa.

3. The Significance of Uncertainties in Basic Nuclear Data

It is informative to evaluate the relative uncertainty contributions of each individual parameter to the total reactivity uncertainty as obtained in the error analysis. This is done by examining Table 5.11.

Most prominent is the uncertainty in η_9, followed in importance by the uncertainties in σ_{FP}, η_5, σ_8, and σ_9. The most interesting conclusion is that the uncertainty contribution of σ_5 is unimportant over the range considered. It should also be noted that the total uncertainty is very nearly proportional to flux-time.

Referring to Fig. 5.3, it is apparent that if the initial discrepancy discussed above is eliminated, there is a very satisfactory correspondence between the experimental and the FUEL Code predicted reactivity behavior over the range considered. Specifically, the experimental curve lies well within the limits of probable error due to nuclear data uncertainties.

The implication of the above is as follows: Provided the discrepancy at low flux-times is not a direct neutron behavior model error, the errors due to the FUEL Code model are insignificant when compared with the probable errors due to uncertainty in the basic nuclear data. A consequence of this is that in view of the relatively

197

simple homogenized unit cell model used in the FUEL Code and the good agreement with experiment that was attained, further sophistication of the model is unjustified for well moderated reactor fuel burnup calculations, since the limiting error is not in the model, but in the basic nuclear data that must be used in all neutron behavior models irrespective of their degree of sophistication.

In view of the fact that uncertainties due to nuclear data were shown to be approximately proportional to flux-time the above conclusions can be extrapolated with a fair degree of confidence to higher burnups than were analysed in this work. The same conclusions can probably be made for more epithermal reactors, although with somewhat less confidence, due to the fact that predictions of resonance neutron behavior could not be fully checked by the NRX experiments in which thermal effects are predominant. In particular, the necessity to use an adjusted value of SGMSFL in order to achieve agreement with experiment points out the approximate nature of the Crowther-Weil treatment of resonance disadvantage factors, which is used in the FUEL Code.

In conclusion, it can be said that the FUEL Code, with its current library of cross sections and other basic nuclear data, is capable of accurate prediction of nuclide concentrations and reactivity during fuel burnout in well thermalized reactors, within the limits imposed by uncertainties in the basic nuclear data.

This conclusion has two reservations. First, the unresolved initial discrepancy and its possible implications should be recalled. Second, the FUEL Code must be given an adequate start by providing initial reactivity and conversion ratio data and, if available, data for the resonance disadvantage factor of Pu^{240}. In both the case of the unresolved initial discrepancy and the lack of data on the Pu^{240} resonance disadvantage factor, the FUEL Code will yield results which are on the conservative side with respect to reactivity prediction.

CHAPTER VI

FUEL AND POISON MANAGEMENT STUDIES:

THE CANDU REACTOR

A. INTRODUCTION

This chapter deals with the effect of fuel and poison management
on a particular nuclear power system, the 200 mwe CANDU reactor
which is to be built at Douglas Point on Lake Huron, near Kincardine,
Ontario.

The primary reason for the choice of the CANDU reactor as the
reference design in this study is that this reactor, being capable of
essentially continuous fueling at full power, is not limited to one of the
discontinuous batch-type irradiations, but can be operated using almost
any fuel management technique. In addition, a D_2O reactor will gener-
ally have lower fuel costs, but higher fixed (capital investment) costs,
as compared to an H_2O reactor of the same output. Hence, the com-
promises that can be made between fuel costs and fixed costs in a D_2O
reactor will be shown in greater contrast than in an H_2O reactor system,
in which these two costs are more nearly equal.

In this chapter, the reference design for the CANDU reactor will
be described. Some of this data will then be used in the preparation of
the input data for the FUEL Code which will be used to evaluate the
CANDU unit cell properties as a function of flux-time at various enrich-
ments. The FUEL Code output, plus additional data from the CANDU
reference design will then be used as input to the MOVE Code for the
actual study of the various fuel and poison management techniques.

B. THE CANDU REFERENCE DESIGN

The CANDU reactor is cooled, moderated and reflected by heavy water with the geometric layout of a horizontal cylinder. It is fueled with zircalloy-clad uranium oxide rods in clusters of 19 rods. These clusters, which are 12 inches long, are contained in horizontal zircalloy pressure tubes which are insulated from the calandria tubes and moderator, by a CO_2-filled gap. The actual design specifies bi-directional fueling with natural uranium, but this study will consider other fueling techniques and enrichments, as well.

Table 6.1 lists all the information required for calculation of the FUELMOVE input data. Because the final design of CANDU was not fixed at the time this study was made, it was necessary to select one of the most promising current designs. The reactor unit cell data has been taken from L61, p. 25, design NPD-4-C3. The gross reactor characteristics were taken from a more recent report, H42, design 2-79.

Table 6.1   CANDU Reference Design

Gross Characteristics: Reference

Net Electrical Power	200 mwe	H42
Power removed by coolant	672.6 mwt	H42
Fraction of power to coolant	0.94	H42
Power produced from fission	715.5 mwt	-
Net efficiency	0.2795	-

Geometry:

Core Length	500 cm	H42
Core Radius	230.2 cm	H42
Reflector thickness: Radial	69.8 cm	H42
Axial	0. cm	H42
Number of channels	304	-
Pitch of fuel clusters (square)	23.4 cm	-

Temperatures:

Coolant: outlet	$299^\circ C$	L61
inlet	$247^\circ C$	L61
Moderator	$80^\circ C$	A61

Unit Cell Characteristics:

Cross-Sectional Areas and Disadvantage Factors,

Fuel-UO_2	27.957 cm^2	1.000	L42
Cladding + Extras-Zr_2	4.079 cm^2	1.0028	L42
Coolant-D_2O	21.484 cm^2	1.1*	L42
Pressure Tube-Zr_2	11.275 cm^2	1.2647	L42
Gap	16.263 cm^2	-	L42
Calandria Tube-Zr_2	4.596 cm^2	1.3569	L42
Moderator	461.890 cm^2	1.8232	L42
Total	547.544 cm^2		

*Assumed value

Table 6.1   (con't)

Nuclear Parameters		Reference
Fermi Age, τ	143.5 cm^2	L42
Fast fission factor, ϵ	1.0173	L42
Buckling, B^2	1.0824 m^{-2}	L42
Initial Conversion Ratio	0.77	A61
Resonance escape probability in U-238, p_8 (ICR = 0.77)	0.8925	-

In-core Inventories (based on 304 channels 500 cm. long)

Material	Volume, m^3	Mass, tonnes
UO_2	4.25	43.35
U	-	38.21
Zr	3.03	19.70
D_2O: coolant	3.27	2.76
moderator	70.21	75.55
reflector	58.13	62.55
total	-	140.86

Characteristics of Core Materials

Material	Mol. wt	Density (gm/cc)	σ_o (b)	σ_s (b)	σ_{tr} (b)
UO_2	270.10	10.2	-	-	16
Zircalloy-2	91.2	6.5	0.212	0.0176	7.94
D_2O: coolant	20.03	0.845	0.00225	5.4	10.55
moderator	20.03	1.076	0.00225	5.4	10.55

C. THE FUEL CODE CALCULATIONS

1. The Preparation of FUEL Code Input Data

Table 6.2 gives the value of the various items of input data required by the FUEL Code. The actual computation of these numbers is shown in Appendix A: Operational Information, since it was desirable to give there an example of a specific calculation.

One point does merit special mention. It was shown in Chapter V that the resonance disadvantage factors were somewhat underestimated for uranium metal rods in the NRX reactor, if the true value of SGMSFL were used. Due to lack of specific data on the resonance disadvantage factors in uranium oxide, the true value of SGMSFL has been used. It will be recalled that if there is a discrepancy, this will yield results which are conservative with respect to reactivity and hence burnup. Also, the comparative accuracy of the results for the different cases studied will be unaffected.

2. The CANDU Fuel Properties During Burnup

The details of the FUEL Code calculations of CANDU fuel properties during burnup for various enrichments are given in Appendix E, Tables 1 to 9.

It is informative to examine certain aspects of the behavior of some of these properties. Figure 6.1 shows the CANDU flux spectrum for natural uranium, both at the start of irradiation and at an irradiation of 3.5 n/kb, corresponding to about 10,000 Mwd/tonne. Also shown is the upper end, and the position of the peak $(3/2 \, kT_{mod})$ of a Maxwell-Boltzmann spectrum at moderator temperature.

Table 6.2   FUEL Code Input Data for CANDU (Natural Uranium)

Item	Value	Units
N_5^o	1.64×10^{-4}	atoms/barn cm.
N_8^o	2.259×10^{-2}	atoms/barn cm.
EVCUT	0.45	ev
SDP	0.16135	cm^{-1}
TMOD	85.27	^{o}C
PSI1(8)	18.68	-
C1	0.3335	cm^{-1}
EPSI	1.0173	-
P1IN	0.9847	-
SIGOMD	3.19×10^{-4}	cm^{-1}
SGOXEG	3.03×10^{6}	barns
VFL	0.05106	-
PSI	1.7136	-
POWERD	8.5956	kw/litre
ZETA	0.00025	neuts/barn
SGMSFL	0.3595	cm^{-1}
ANBP	0.	atoms/barn cm.
SIGOBP	0.	barns
SGOIN7	47.67	barns
TAU	143.5	cm^{2}
D	1.002	cm
PDNLIM	17.01	kw/litre
RIUFP	181	barns
RIPFP	264	barns
FPFCTR	1.0	-
APSI	0.	barns/neut
RIBP	0.	barns
OMPMOD	6.34×10^{-3}	-

Control Parameters:		
IL	49	
NUMPOZ	31	
NUMSPA	3	
IPSI	0	

(The remaining control parameters are output options which it is unnecessary to list here.)

The positions of the initial and final peaks are almost identical, and are somewhat hardened with respect to the moderator temperature. Figure 6.1 shows that the type of hardening which occurs during burnup is due to an increase in the slowing down density per unit thermal flux which is a consequence of the increase in $\nu\Sigma_f$ due to Pu buildup. Practically none of the hardening is due to the temperature change of an equivalent Maxwell-Boltzmann thermal flux, which is the type of hardening assumed by the technique often used to estimate a change in an absorption cross section. This employs an equation of the form:

$$T_{neut} = T_{mod}\left\{1 + \alpha \frac{\Sigma}{\xi\Sigma_s}\right\} \qquad (6C1)$$

where

α is a proportionality constant

Σ is the homogenized absorption cross section evaluated at T_{mod}

$\xi\Sigma_s$ is the homogenized slowing-down power.

Figure 6.2 illustrates the effect of the spectrum change on several spectrum-averaged absorption cross sections. The increase in the dE/E component which is caused by the initial increase in $\nu\Sigma_f$ causes the nearly 1/v cross sections of U^{235}, U^{238} and Pu^{242} to decrease. However, Pu^{239} and Pu^{241} have large resonances at 0.3 ev just below the thermal cutoff region at 0.45 ev. The increase in the epithermal component is enough to cause an increase in the spectrum-averaged Pu^{239} cross section, but leaves the Pu^{241} value virtually unchanged.

The conclusion that must be made in view of the above results is that prediction of spectrum average cross section changes during burnup
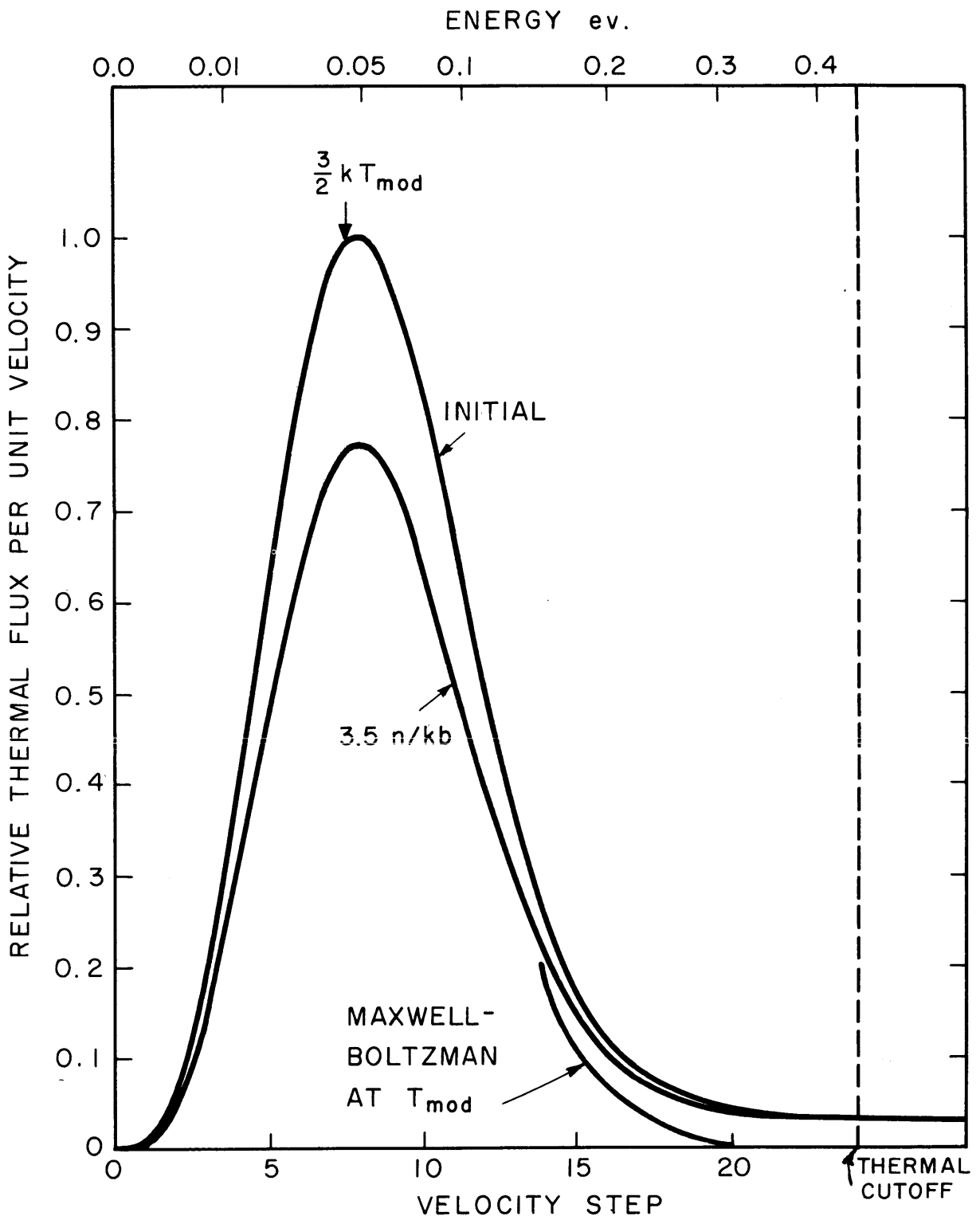
FIG. 6.1   CANDU FLUX SPECTRA NATURAL URANIUM
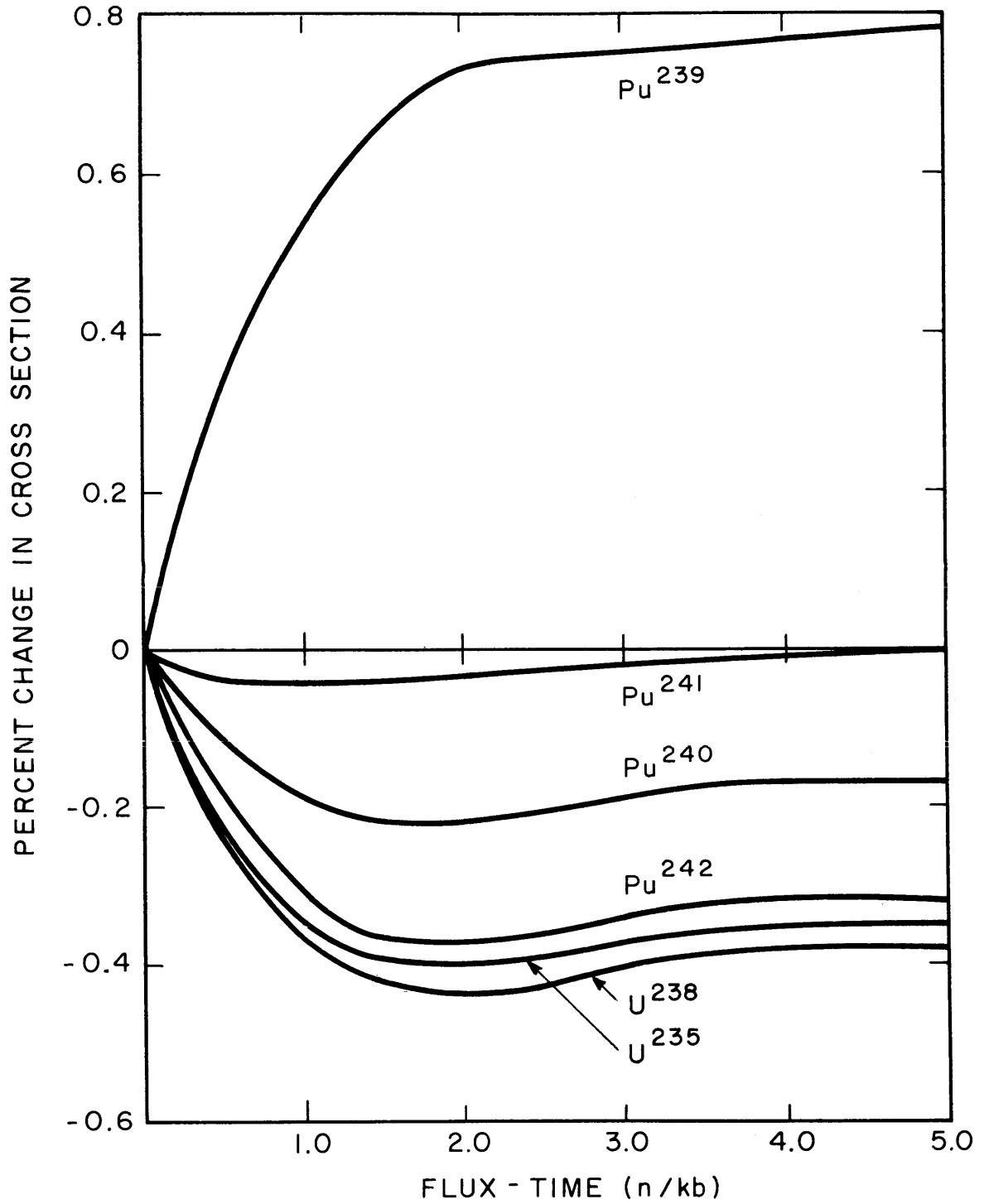
FIG. 6.2   PERCENT CHANGE IN CROSS SECTIONS
DURING BURNUP-NATURAL URANIUM,
CANDU REACTOR

by means of a neutron temperature change (Equation 6C1) is incorrect, inasmuch as the predominant spectrum change is associated with a change in the dE/E component at the high energy end of the thermal region.

At enrichments above 1%, the dE/E component does not increase, since the burnout of U^{235} always dominates over the buildup of Pu^{239}, and the $\nu\Sigma_f$ will always decrease. This results in an increase in the spectrum-averaged cross sections of the essentially $1/v$ cross section nuclides, and a decrease in Pu^{239} cross section, for reasons which are exactly opposite to those described above for an increasing dE/E component during burnup of natural uranium.

In Figure 6.3, the fuel composition change during burnup of natural uranium is given. Figure 6.4 shows the manner in which the seven homogenized unit cell properties vary during burnup. Five of these properties are neutron balance parameters. They are used to evaluate k_∞, given by equation (4B50)

$$k_\infty = \frac{\epsilon \, [\nu \, \Sigma_f] \, [p]}{(1 - \epsilon \, [<\eta \, (1-p)>]) \, ([\Sigma_{tot} - \Sigma_{Xe}] + C_5 [\Sigma_{Xe, \, max}])} \qquad (6C2)$$

where the five properties are in brackets and C_5 is the fraction of Xe which is burned. C_5 is evaluated from the flux level necessary to maintain a power density of 8.59 kw/litre, and is listed in Figure 6.5, in which k_∞ is given for various enrichments during burnup.

Finally, Figure 6.6 shows the relation between flux-time and burnup for various enrichments. This relationship is not quite linear because the fission cross section varies somewhat with flux-time, and the curves shown in Figure 6.6 are actually proportional to the flux-time integral of the fission cross section.
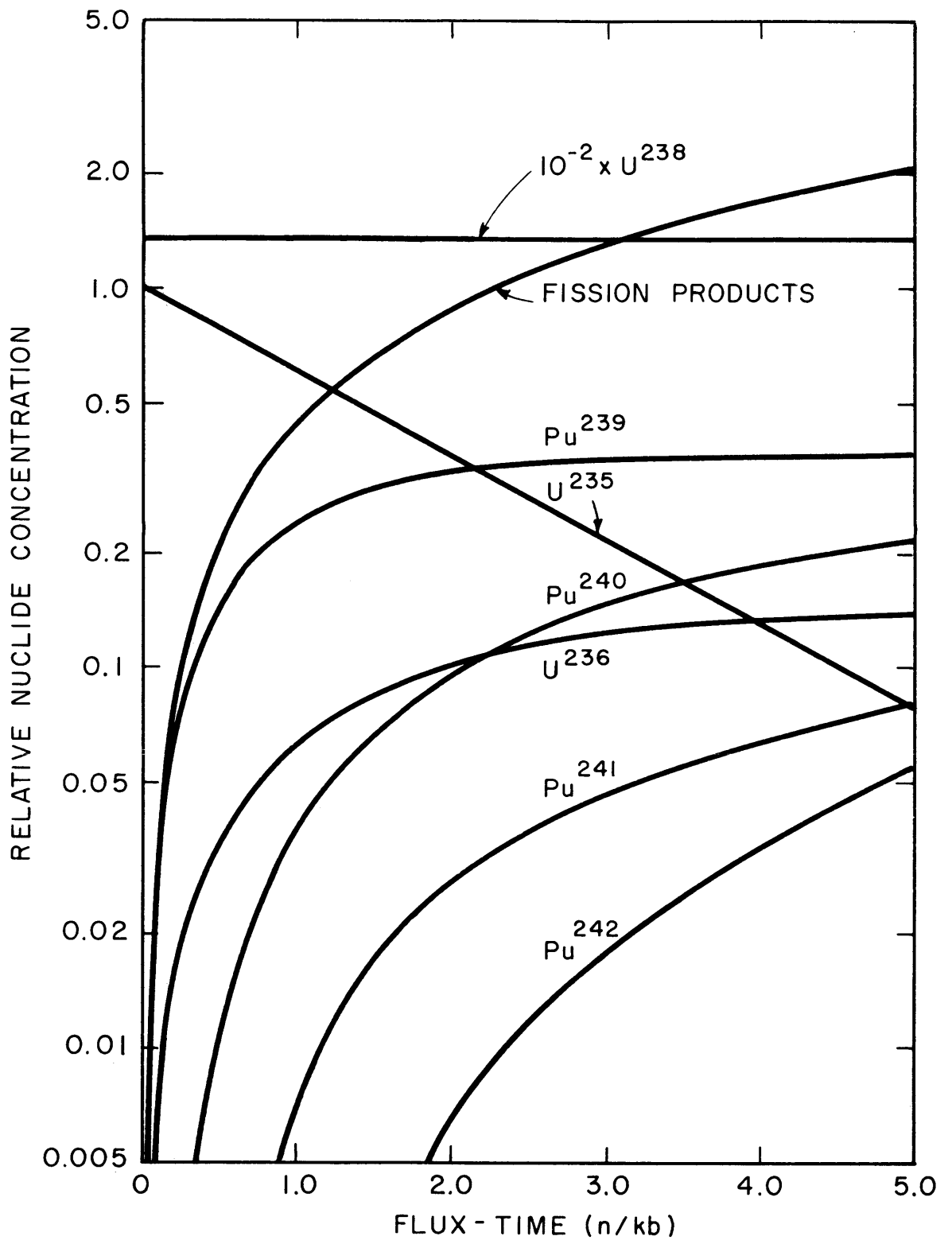
FIG. 6.3 VARIATION OF FUEL COMPOSITION DURING
BURNUP-NATURAL URANIUM CANDU REACTOR
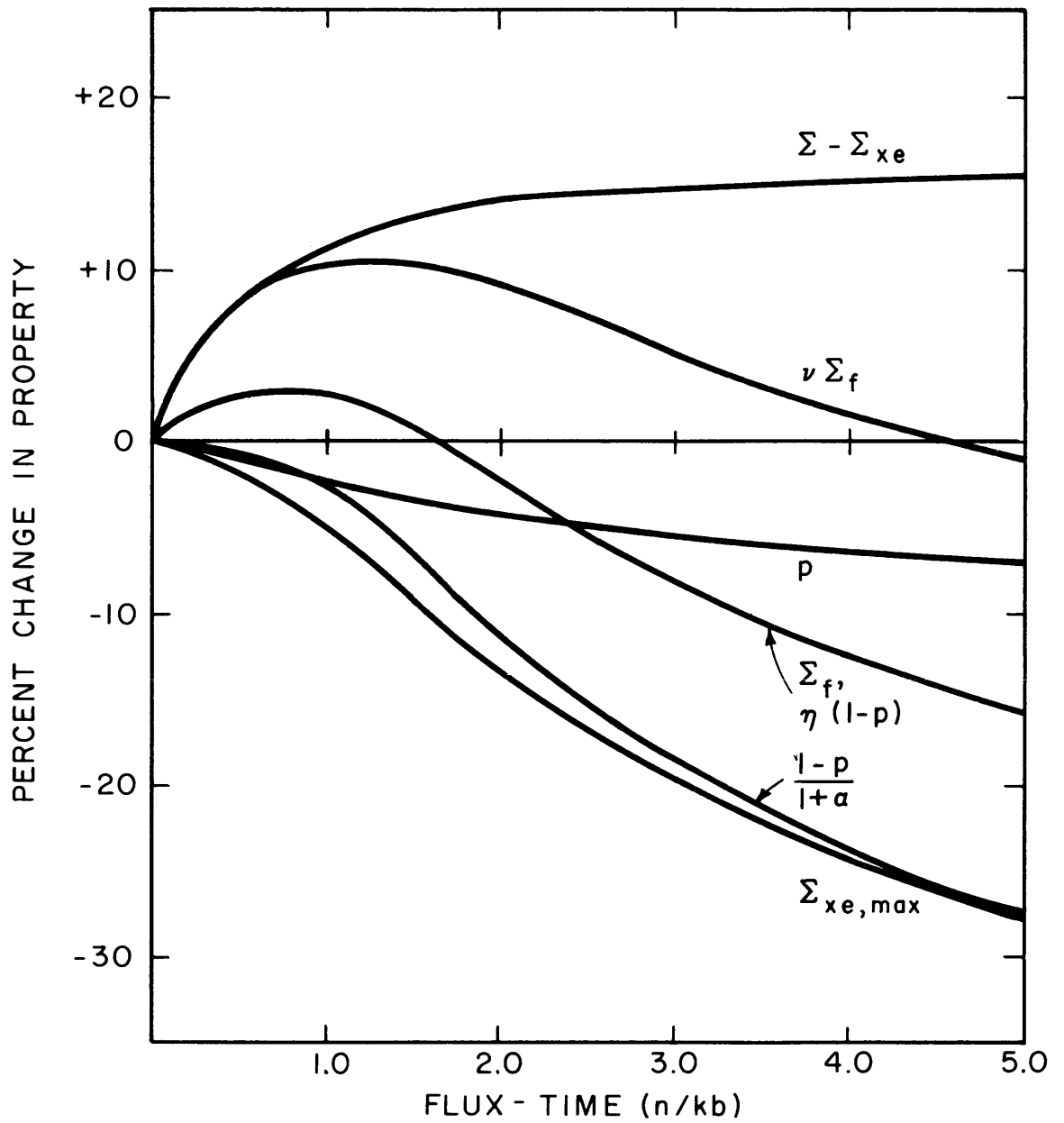
FIG. 6.4   VARIATION OF HOMOGENIZED UNIT CELL
PROPERTIES DURING BURNUP, NATURAL
URANIUM, CANDU UNIT CELL.

$$K_\infty = \frac{\epsilon \, \nu \, \Sigma_f \, p}{(1 - \epsilon \langle \eta (1-p) \rangle)(\Sigma - \Sigma_{xe} + C_5 \Sigma_{xe,max})}$$

C_5 - Xe Fraction BURNED

ENRICHMENT	C_5
NAT	0.90
1.0 %	0.885
1.5 %	0.87
2.5 %	0.84
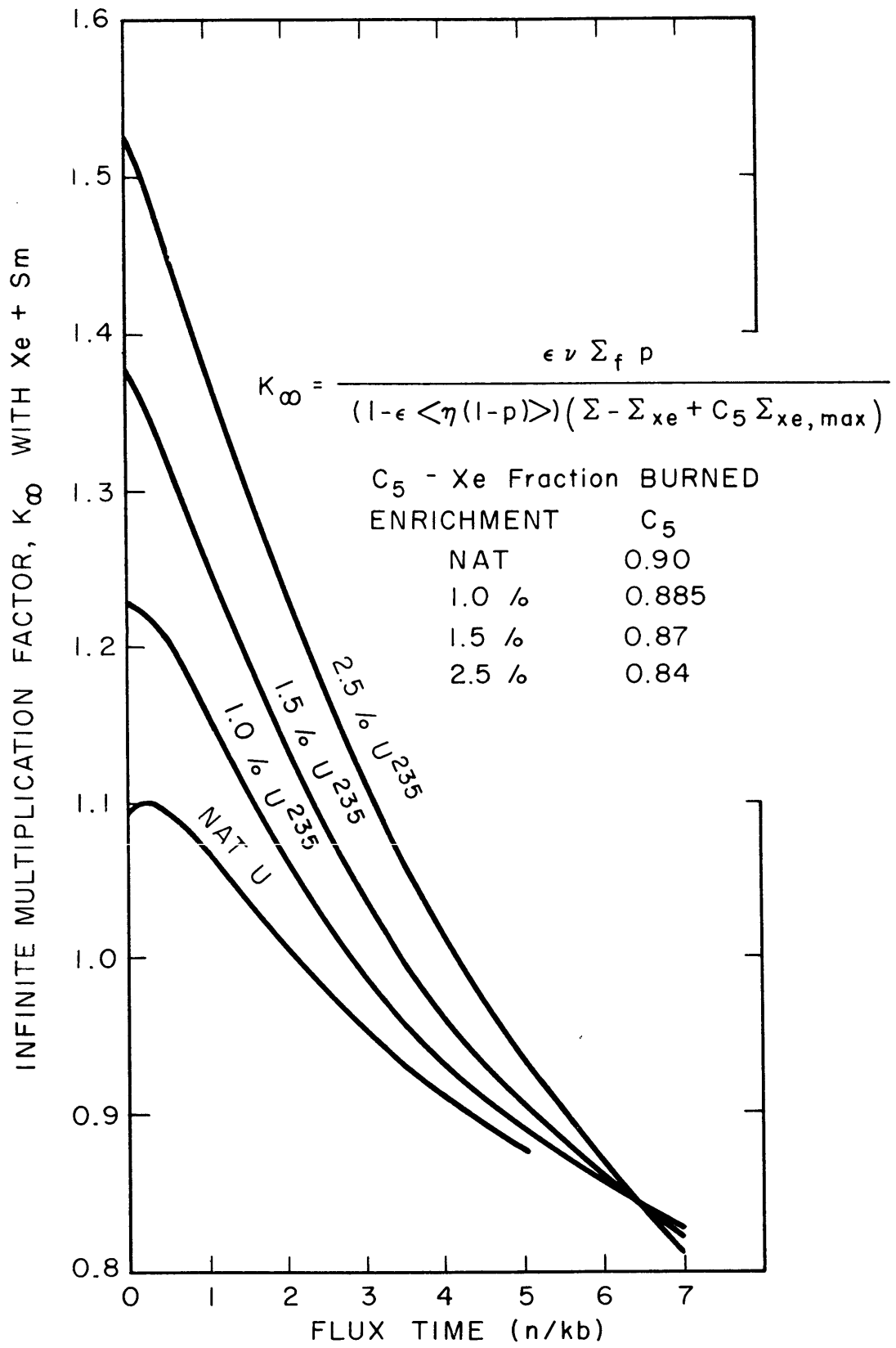
FIG. 6.5   VARIATION OF K_∞ DURING
BURNUP, CANDU REACTOR UNIT
CELL AT VARIUS ENRICHMENTS

211
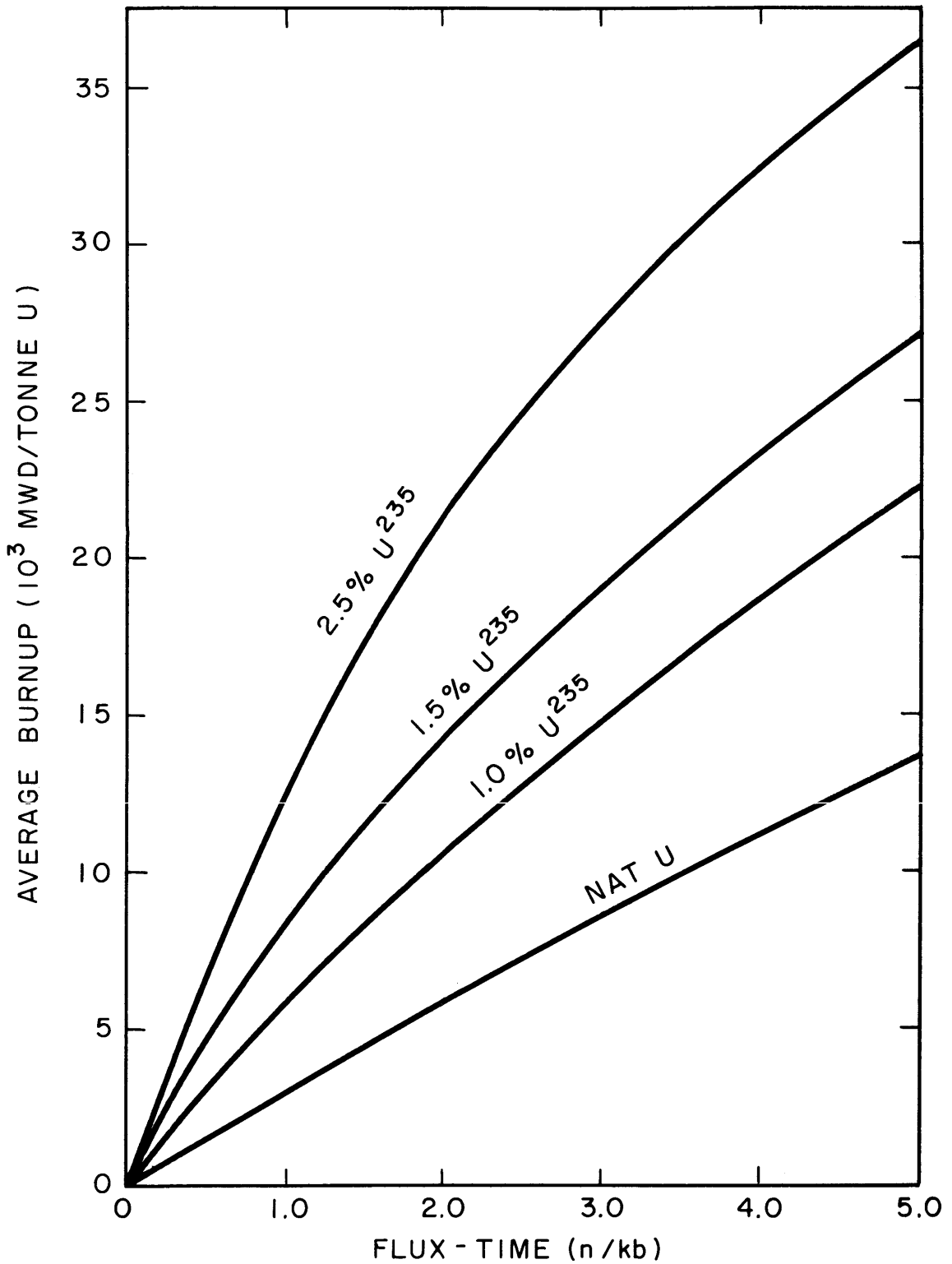
FIG. 6.6   RELATION BETWEEN FLUX-TIME AND
BURNUP AT VARIOUS ENRICHMENTS,
CANDU REACTOR UNIT CELL

212

In addition to the above runs of the FUEL Code, the higher enrichments of the CANDU unit cell were rerun to include a burnable poison. Two magnitudes were chosen for each case, so that the initial k_∞ was either 1.1 or 1.2. The choice of burnable poison cross section merits discussion. It must be greater than that of U^{235}, or the poison will persist too long and cause a sizeable loss of burnup. On the other hand, it must not be so large that it burns out almost immediately, thereby completely failing in its prime objective, that of controlling reactivity over a major part of fuel lifetime. A FUEL Code run using Boron^{10} (σ_0 = 4020) proved it to have much too large a cross section. The best compromises between loss of burnup and long-term control, occur with cross section with the order of σ_0 = 1000 barns, more or less, depending upon individual circumstances. Wolberg (W61), has studied the characteristics of Erbium 167 ($\sigma_0 \approx$ 740b) as a burnable poison. In this study, σ_0 = 945 barns was used, this being the cross section of Li^6.

The use of burnable poisons would be completely unjustified in bidirectional fuel management. It does, however, show promise of lowering the control rod requirements for the discontinuous or batch fuel management procedures, and it puts the reactivity control where it is most needed, right in the fuel. The loss of burnup can be offset by decreased control costs. In cases in which enrichment is determined, not by burnup but by the amount of reactivity control necessary to hold a new core down, burnable poison shows promise of increasing fuel burnup by enabling the use of higher enrichments.

Figure 6.7 illustrates the effect of Li^6 burnable poison on the flux-time behavior of k_∞ for an enrichment of 1.5 a/o. Other enrichments show similar behavior. If the end-of-burnup condition corresponds to k_∞ = 1.05, the use of burnable poison causes a 10%
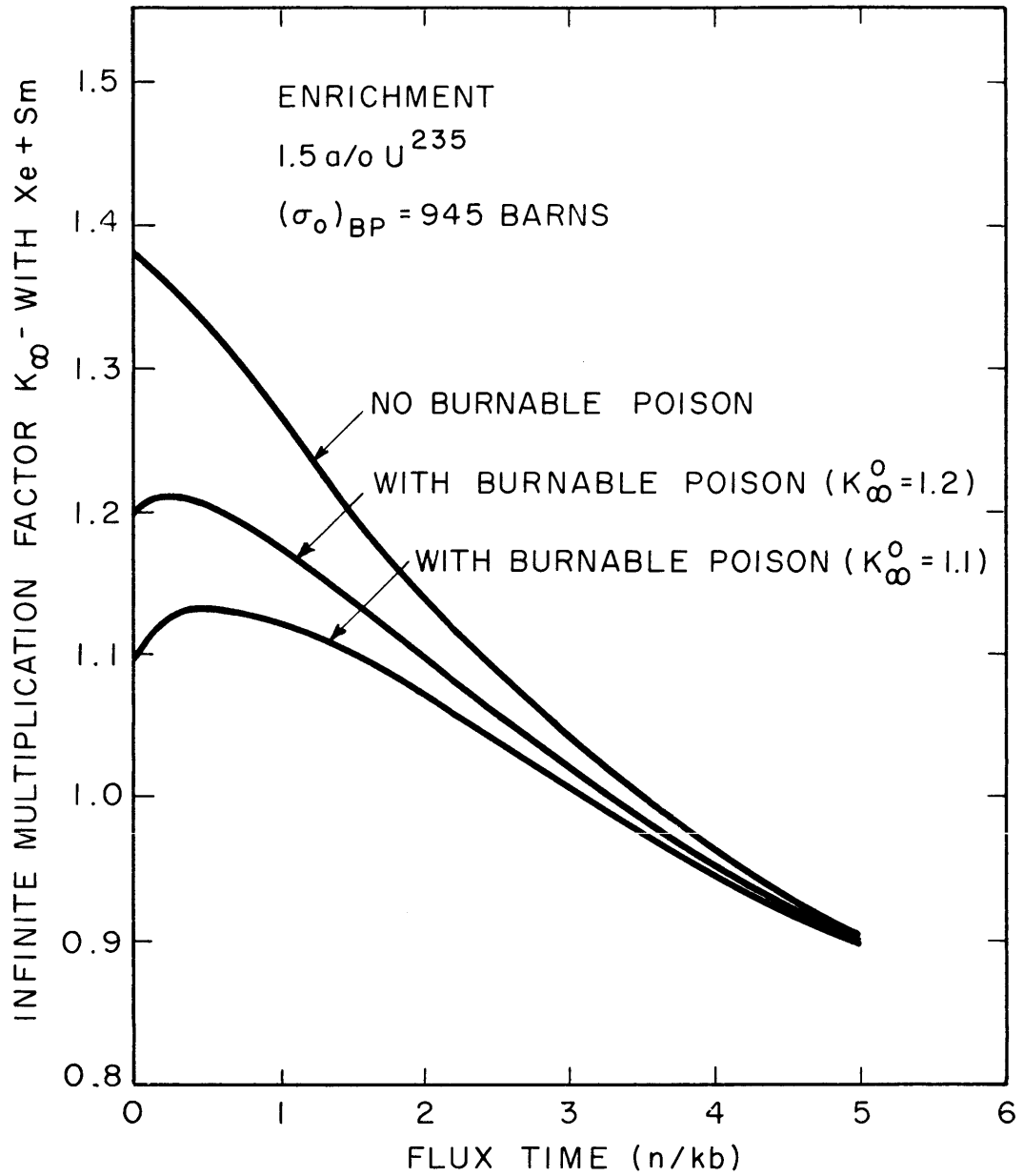
FIG. 6.7   THE FLUX-TIME BEHAVIOR OF K_∞
WITH VARIOUS AMOUNTS OF BURNABLE
POISON AT 1.5 a/o U^{235}

loss of burnup if $k_\infty^O = 1.2$ and a 20% loss of burnup if $k_\infty^O = 1.1$. The control requirement above $k_\infty = 1.05$ in the latter case is only 25% of that when no burnable poison is used.

D. THE FUEL AND POISON MANAGEMENT STUDY

1. Introduction

In Chapter II, the ground rules for fuel and poison management studies with a survey code such as FUELMOVE, were established. In summary, the following points were presented:

1) The particular reactor type is specified.
2) The reactor unit cell design is fixed.
3) A maximum permissible power density which is generally a characteristic of unit cell design is specified.

The third point above is not a necessary condition but will apply in many practical situations. Briefly, its significance is that if a maximum permissible power density is specified, the maximum permissible total power output of a given core, being proportional to the average power density, will be inversely proportional to r, the peak-to-average power density ratio which is a characteristic that varies for different fuel and poison management techniques. Alternatively, if a maximum permissible power density and also a maximum total power output are specified, the necessary core volume will be proportional to r. In either case, a reduction in r reduces the fixed (capital) cost part of the unit energy cost. While there may be some loss of fuel burnup associated with a decrease in r, and a consequent increase in the fuel cost part of the unit energy cost, there is generally an economic incentive to reduce the peak-to-average power density ratio. When a loss of burnup does occur, it is practical to decrease r only to the point at which the incremental unit fixed cost savings equal the incremental unit fuel cost losses. Thus, one objective of a fuel and poison management study

under the constraint of a maximum permissible power density, may be to pick the technique capable of giving the best compromise between fuel burnup and r, the peak-to-average power density ratio.

Also given in Chapter II were the three general classifications, into one of which each fuel and poison management study will fall, depending on its objectives. These were:

1) Fixed core volume, fixed power output: The objective here would be to evaluate minimum fuel cost, or to establish a starting point for either of the two study classifications below.

2) Fixed core volume, variable power output: The objective of this is to reduce unit capital costs associated with the reactor part of the power system by increasing the generating capacity to limits imposed by (i) the maximum permissible power density limit, (ii) the characteristic value of r, and (iii) the core volume.

3) Variable core volume, fixed power output: The objective is to find the fuel and poison management technique which will lead to the smallest core, and hence the smallest reactor capital cost, to within limits imposed by (i) the maximum permissible power density limit, (ii) the characteristic value of r, and (iii) the specified total power output.

The basic problems of fuel and poison management associated with the transient (pre-steady-state) operation of a nuclear power system that will ultimately operate in a continuous or periodic steady-state manner will now be discussed.

Generally, the system will be designed to suit the requirements of steady-state operation, inasmuch as it will operate under these

217

conditions for the majority of its lifetime. Hence, under the limit of a maximum permissible power density, and for a specified total power, the volume of the core will be proportional to the maximum peak-to-average power density ratio, this being a characteristic of the particular steady-state fuel and poison management technique being used. Also, a particular fuel enrichment will have been picked, generally to help satisfy the requirement of minimum total energy cost. In summary then, the system will have been optimized for operation in steady state.

Thus, the problem of transient operation is how to handle the fuel and control poison prior to the steady-state so as to achieve only a minimum of increase in those total energy costs which prevail during steady-state operation.

Generally, there will be the specific requirement that the system must be always capable of operation at full rated output without exceeding the maximum permissible power density limit. This implies that the maximum peak-to-average power density ratio in steady-state operation must not be exceeded during the transient period except possibly in the short (~9 hr.) period during Xe buildup right after startup, when the system will be operating at reduced output. Even if this requirement were relaxed and the reactor were permitted to operate below rated output, energy costs would rise during the period of reduced output, due to the increased fixed costs per unit of energy produced. There is, therefore, an economic incentive to operate at full power throughout the transient period.

Should it be physically impossible during this period to operate at full power without exceeding the steady-state maximum peak-to-average power density ratio, there are two alternatives to that of reducing power. If the nature of the peak permissible power density limit permits, it might be possible to exceed the limit for a short

time under certain conditions. Alternatively, there may be some justification for not operating up to the peak power density limit in steady-state operation. This implies a larger core volume than is necessary in steady state. A small energy cost increase associated with volume increase might be justified as an alternative to decreased power output during startup.

The specific studies in this chapter will be performed on the D_2O moderated and cooled, CANDU reactor whose reference design, 2-79 of H42, has a specified output of 200 Mwe (715.5 Mwt) and is fueled with natural UO_2, using the continuous bidirectional fueling technique. The specific objective of this study, then, will be to examine which of the various fuel and poison management techniques might be capable of improving on the total energy cost of the reference design.

It is both impractical and unnecessary to investigate each of the large number of possible combinations of different fuel and poison management techniques, or to perform each of the three study types listed above on each combination studies. Only those techniques showing the most promise will be evaluated in all aspects.

The fuel management techniques which will be studied are:

1) Continuous bidirectional in steady state.
2) Continuous bidirectional, startup of the reference design.
3) Discontinuous bidirectional, startup and steady-state. This will be compared to some of the steady-state situations.

4) Batch irradiation, both as an individual fuel management procedure, and as the startup of:

5) Discontinous outin, startup and steady state.
6) Continuous outin, steady state.
7) Continous graded, steady state.

219

The most important of the above are (1), (4) and (5), and these will be treated in most detail.

The important poison management techniques that will be investigated for reactivity control and/or power shaping are:

1) Uniform poison removal, corresponding to chemical shim reactivity control.

2) Burnable poison.

3) Radial zone and axial bank poison removal.

4) Fixed absolute poison for control of axial power distribution in continuous bidirectional fuel movements.

2. The Preparation of MOVE Code Input Data

Table 6.3 gives the value of the various items of geometrical input data required by the MOVE Code. The computation of these values is shown in Appendix A. The value of radius listed is that of the outermost core radius.

In addition to the items in Table 6.3, there are a number of control parameters which vary from run to run, depending upon the type of study being performed. Certain of the fuel management procedures also require a small number of input control parameters. All of these are given in Appendix A, along with the input data card formats.

3. The CANDU Reference Design

The CANDU reference design, 2-79 of H42, has a thermal output of 715.5 mw of which 94% or 672.6 mw is transferred to the coolant to result in an ultimate production of 200 Mwe. The power density limit, based on $\int k d\theta = 40$ w/cm and a peak-to-average power density ratio within the 19 rod cluster, of 1.096 (L61), is 17.01 kw/litre, which yields an over-all peak-to-average power density ratio of r = 1.979,

Table 6.3   MOVE Code Input Data for CANDU

Item	Value	Units
R*	230.2	cm
H	500	cm
δR	58.45	cm
δH	2.1	cm
ZSYM	0.	-
DBSQU	1.0845×10^{-4}	cm^{-1}
PFAST	0.9847	-
PDENAV	8.5956	kw/litre
RMAX	1.978	-
ERROR	0.01	-
DELCRT	0.001	-
DELTD	0.0192	years
CRIT	1.000	-

In addition, the control parameters for the particular run are required. See Appendix A.

*This is the outer radius only. In any particular run, it is necessary to specify up to 10 radii, one for each radial mesh point region.

when the average power density is 8.60 kw/litre.

Bidirectional fueling is to be used and for the purpose of power flattening, the core is divided into two radial zones with the fuel in the inner zone being burnt out more than that in the outer zone. The inner zone, with 16% of the core volume, produces 20.1% of the total power and has a discharge burnup 1.35 times that of the outer zone discharge burnup when fueled with natural uranium. The predicted (H42) average burnup of 8850 MWD/T is consistent with an inner zone burnup of 11,320 MWD/T and an outer zone burnup of 8380 MWD/T. The stated (H42) radial flatness of 0.786 corresponds to an axial flatness of 0.643 when the peak-to-average power density ratio is 1.979. This is somewhat less than the $2/\pi$ used as the axial flatness in L61.

The results of the MOVE Code calculation of the reference design are given in Table 6.4. These were obtained using a 10 × 10 uniform mesh, and specifying the same relative discharge flux-times for the two radial zones as are given in H42. The MOVE Code predicts the peak power density to be 3% greater than permissible. The predicted average burnup is about 2.5% greater than that calculated in H42.

A comparison of the relative radial flux shapes at the reactor midplane, for the MOVE Code calculations and those presented in H42, is shown in Figure 6.8. The flux peaking at the interface between the inner and outer zones indicates that the fuel in the inner zone is less reactive than is necessary for a flatter radial distribution of flux. The discrepancy between the MOVE Code prediction of the radial power distribution and that of the reference design may be due to the fact that the reference design curves were obtained, assuming separability of the axial and radial leakages, whereas it is not necessary to make this

Table 6.4   MOVE Code Calculation of the CANDU Reference Design

A. Design Data

Standard Thermal Power, P_o	715.5 MWt
Standard Core Volume, V_o	83.24 m^3
Standard Maximum Power Density, D_o	17.01 kw/l
Relative Discharge Flux-Time	
Radial regions 1-4	1.0
Radial regions 5-10	0.72
Fuel enrichment, a/o U^{235} (Natural)	0.7206 a/o

B. MOVE Code Results

Maximum Power Density		17.56 kw/l
Ratio of Maximum to Average Power Density		2.04
Burnups, MWD/Tonne	Region 1-4	11,620
	Region 5-10	8,590
	Average	9,080
Percent of Power in:	Inner Zone	19.4%
	Outer Zone	80.6%
Full power time of fuel in reactor		1.33 years
Kw he/kg of fuel charged		60,900

C. Material Quantities

Feed rate, kg U/full power year	28,760
Discharge ratio; kg U/full power year	28,350
kg Pu/full power year	123.4
Isotopic Content of Discharged Fuel	
w/o U^{235} in U	0.149
w/o U^{236} in U	0.086
w/o Pu^{239} in Pu	61.27
w/o Pu^{240} in Pu	26.97
w/o Pu^{241} in Pu	8.27
w/o Pu^{242} in Pu	3.49

Table 6.4   (cont'd)

D. FUEL Cycle, and Total Energy Costs

		Cost Basis 1 mills/Kwh	Cost Basis 2 mills/Kwh
1.	Natural UO_2	0.48	0.48
4.	Fabrication	1.42	1.01
5.	Shipping	0.25	0.25
6.	Solvent Extraction	0.34	0.34
9.	Conversion of $Pu(NO_3)_4$ to Pu	0.10	0.10
10.	Sales of Pu to AEC	-0.65	-0.65
12.	Working Capital, Non-Reactor	0.06	0.03
14.	Working Capital, Reactor	0.09	0.06
	Net Fuel Cycle Cost	2.09	1.62
15.	Plant Capital Costs, Reactor	4.47	2.59
16.	Plant Capital Costs, Non-Reactor	3.65	1.91
17.	Operating Costs, Reactor	0.62	0.62
18.	Operating Costs, Non-Reactor	0.40	0.40
	TOTAL ENERGY COST	11.23	7.14

CANDU REACTOR - REFERENCE DESIGN
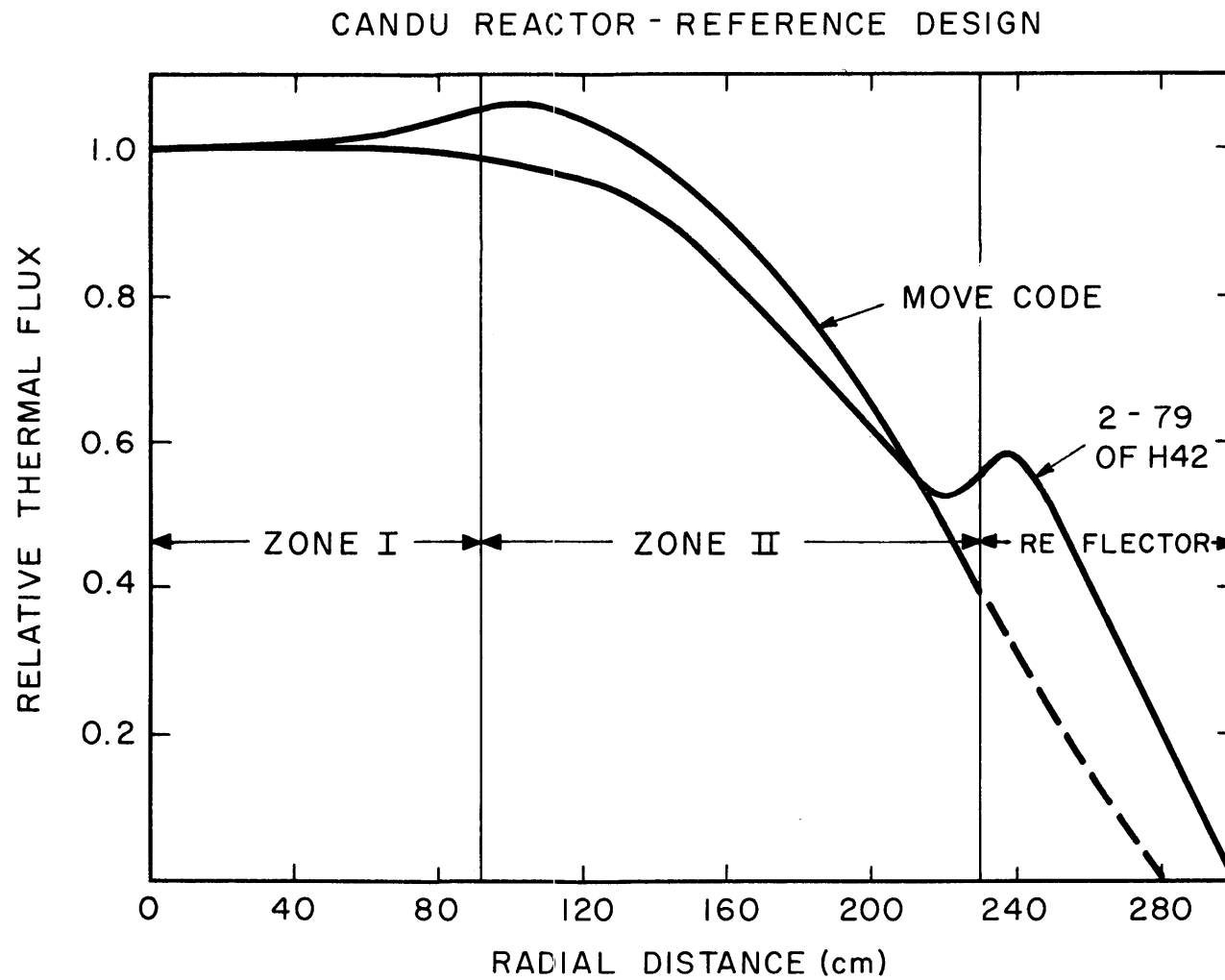
FIG. 6.8 RELATIVE RADIAL FLUX SHAPE AT THE MID-PLANE:
COMPARISON OF MOVE CODE WITH DESIGN PREDICTIONS

225

assumption in the MOVE Code. The lack of a flux peak in the reflector is, of course, due to the reflector savings treatment in the MOVE Code. A contour plot of relative power density, as given in Figure 6.9, also shows the tendency of the power to peak near the zone interface.

In Figure 6.10, the net fuel cycle cost is shown broken down into the various components. The Pu credit more than pays for the material cost of natural UO_2, but the reprocessing cost is actually greater than the Pu credit. This cost, however, includes the shipping charges of \$15.45/kg, equivalent to 0.25 mills/kwh. Actually, it would not pay under the present cost assumptions to reprocess spent fuel if it could be disposed of for less than about \$2.50/kg, which does not seem likely.

4. The Continuous Steady-State Bidirectional Fuel Management Technique

4.1 Introduction

This section presents the study of the effects of various factors on the design of a D_2O reactor system operating in steady state using continuous bidirectional fuel management, this being the specified manner of operating the CANDU. The specific effects to be studied are those of fuel enrichment, radial variation of burnup, zones of different enrichment, fixed poison for axial flux flattening, and reactor core size. Finally, the results of these studies will be combined to specify the designs which will yield the minimum total energy cost.

4.2 The Effects of Enrichment and Radial Variation of Burnup

In this section, the effect on average burnup and power distribution, of varying the discharge burnup of the fuel across the radius of the reactor, is studied at various enrichments. Because this is the
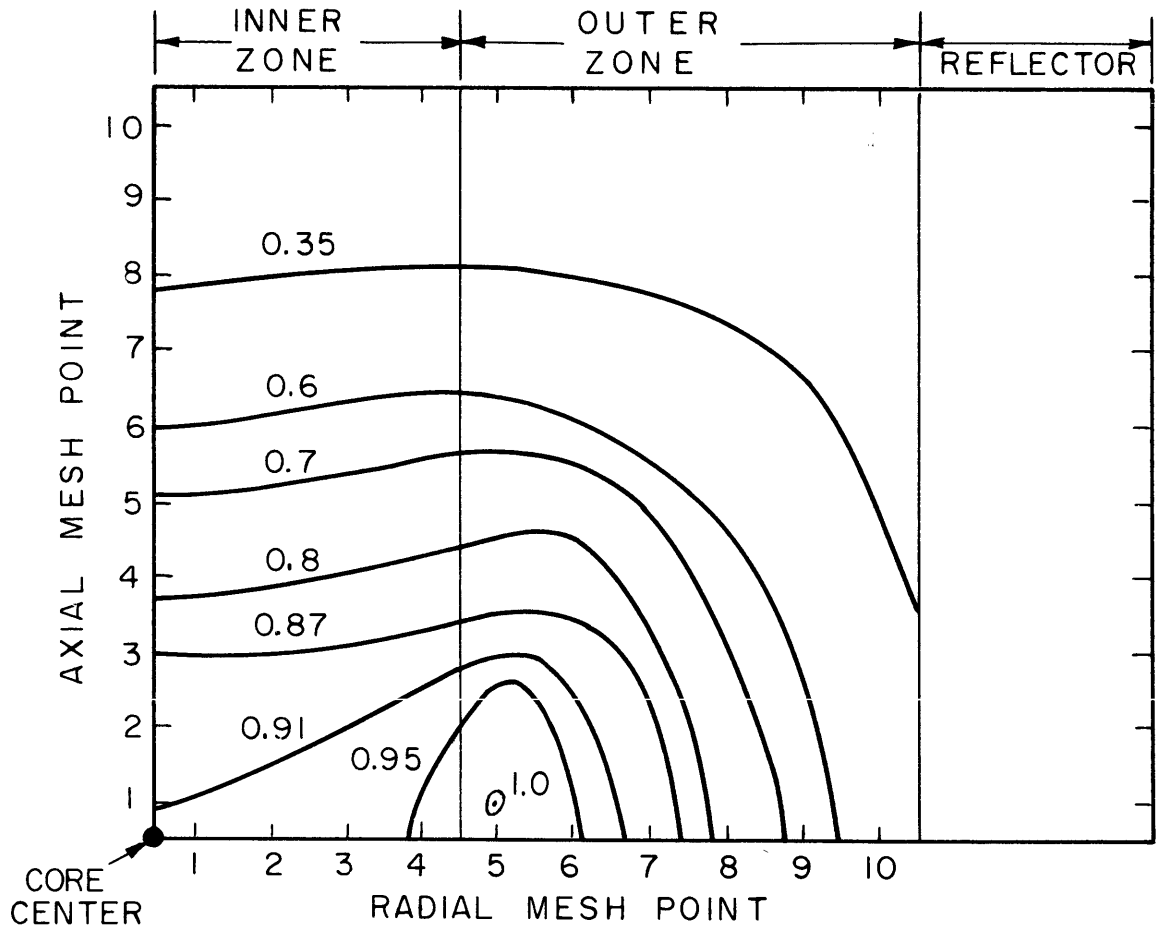
FIG. 6.9 CONTOUR PLOT OF THE RELATIVE POWER DENSITY,
CANDU REFERENCE DESIGN
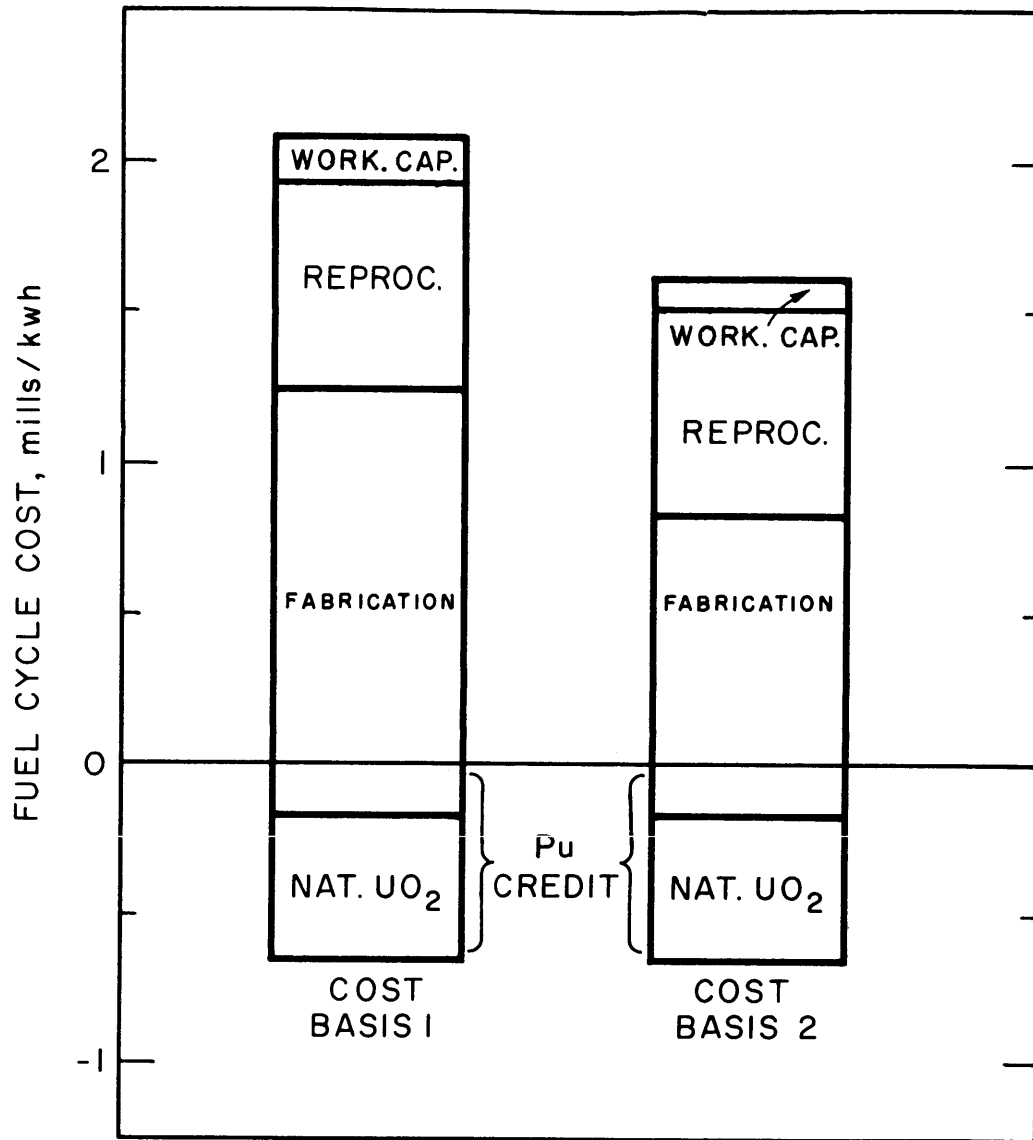
FIG. 6.10   THE COMPONENTS OF NET FUEL
CYCLE COST, CANDU REFERENCE
DESIGN. (NATURAL ENRICHMENT)

228

starting point in the study, the standard (reference) core is operated at standard average power density without applying the constraint of a maximum permissible power density. In addition, the possibility of improving the specified 2-zone radial burnup variation is considered.

In these studies, the functional dependence of discharge burnup is specified in one of three ways. The burnup can be uniform at all radii ($\theta_{d \text{ const.}}$), the relative velocity of the fuel in the axial direction can be uniform at all radii ($V_{z \text{ const.}}$), or the discharge flux-time can be adjusted by trial and error to produce the minimum peak power density ($\theta_{d \text{ min p. d}}$). The enrichments considered are Natural, 1.0 a/o, 1.3 a/o, and 1.5 a/o.

The important results of the parameter survey of radial fuel management and fuel enrichment are presented in Table 6.5, and the radial variation of discharge flux-time is listed for each case in Table 6.6. Specific results are presented graphically.

An indication of the flatness of the power distribution is given by the peak-to-average power density ratio, which is shown in Figure 6.11. It should be noted that the constant axial velocity ($V_{z \text{ const.}}$) technique results in substantial improvement in flatness over the constant discharge burnup situation and comes very close to the minimum power density cases. The three radial fuel management types result in almost identical behavior as a function of enrichment. The main reason for this lies in the axial flux behavior, which is shown in Figure 6.12. This is nearly a cosine for natural U and is considerably flatter for 1.0 a/o U. Above this enrichment, however, the flux tends to peak toward the ends of the core, this peaking becoming more pronounced at higher enrichment. The enrichment for minimum power

229

Table 6.5 Summary of Initial Survey Results for the Bidirectional Fuel Movement

Enrich-ment	θ_d Type	Average burnup in MWD/T	Maximum burnup in MWD/T	Peak power density in KW/L	Maximum to average power density ratio	T_R - Full power time in years	Net fuel cycle cost Mills/Kwh Basis 1	Basis 2	Run no.
Nat	θ_d const.	9450	9450	22.10	2.57	1.38	2.00	1.54	A1.1
	V_z const.	8740	10780	16.87	1.96	1.28	2.18	1.69	A2.1
	θ_d min p.d	7970	12080	15.06	1.75	1.17	2.42	1.88	A6.1
1.0 a/o	θ_d const.	17170	17170	19.70	2.29	2.51	1.39	1.10	A1.3
	V_z const.	16420	18540	14.01	1.63	2.40	1.45	1.15	A2.3
	θ_d min p.d	16070	18660	12.95	1.51	2.35	1.49	1.18	A6.3
1.3 a/o	θ_d const.	23080	23080	23.38	2.72	3.38	1.26	1.05	A1.5
	V_z const.	22430	24530	16.47	1.91	3.28	1.30	1.08	A2.5
	θ_d min p.d	22020	25540	15.31	1.78	3.22	1.32	1.10	A6.5
1.5 a/o	θ_d const.	26550	26550	25.71	2.99	3.89	1.25	1.06	A1.6
	V_z const.	25980	27920	18.92	2.20	3.80	1.27	1.08	A2.6
	θ_d min p.d.	25400	29370	16.95	1.97	3.72	1.30	1.11	A6.6

Table 6.6   The Radial Variation of Discharge Flux-Time for the Bidirectional Fuel Movement

Enrich-ment	Type	θ_c n/kb	Discharge Flux-Time at Each Radial Mesh Point Relative to θ_c							Run No.
			1	2	3	4	5	6	7	
Natural	θ_d const.	3.288	1.00	1.00	1.00	1.00	1.00	1.00	1.00	A1.1
	V_z const.	3.800	1.00	0.996	0.97	0.93	0.865	0.756	0.585	A2.1
	θ_d min p.d	4.310	1.00	0.980	0.940	0.860	0.760	0.620	0.400	A6.1
1.0 a/o	θ_d const.	5.356	1.00	1.00	1.00	1.00	1.00	1.00	1.00	A1.3
	V_z const.	5.900	1.00	0.998	0.988	0.970	0.930	0.845	0.678	A2.3
	θ_d min p.d	5.951	1.00	1.010	1.005	1.000	0.920	0.82	0.620	A6.3
1.3 a/o	θ_d const.	6.610	1.00	1.00	1.00	1.00	1.00	1.00	1.00	A1.5
	V_z const.	7.200	1.00	1.00	0.990	0.98	0.95	0.88	0.715	A2.5
	θ_d min p.d	7.620	1.00	0.994	0.980	0.950	0.90	0.810	0.630	A6.5
1.5 a/o	θ_d const.	7.260	1.00	1.00	1.00	1.00	1.00	1.00	1.00	A1.6
	V_z const.	7.823	1.00	1.00	0.996	0.99	0.960	0.900	0.745	A2.6
	θ_d min p.d	8.430	1.00	0.995	0.980	0.950	0.910	0.810	0.630	A6.6
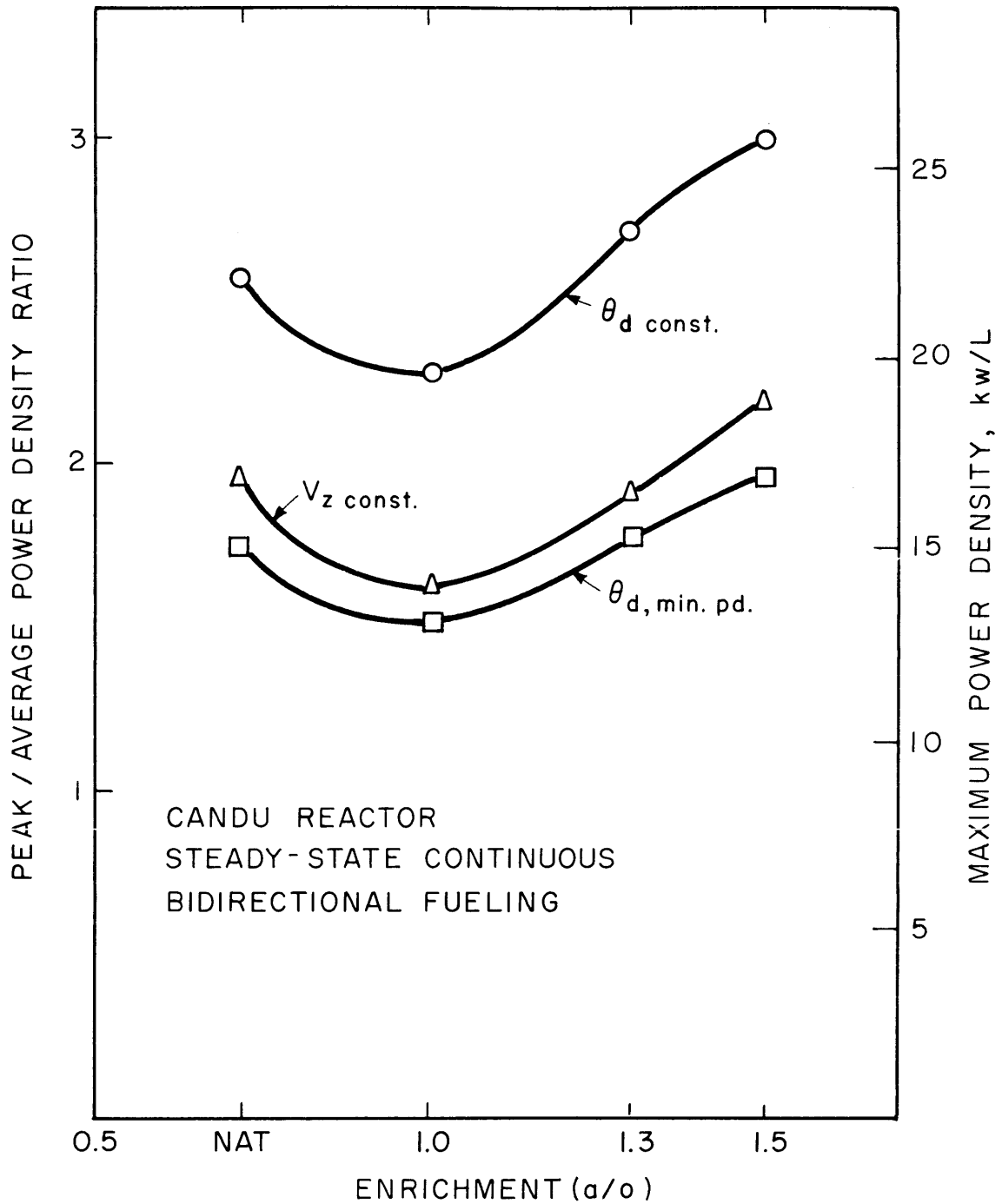
FIG. 6.11 THE PEAK-TO-AVERAGE POWER DENSITY
RATIO IN THE CANDU REACTOR AT
VARIOUS ENRICHMENTS AND RADIAL
SPECIFICATIONS OF DISCHARGE FLUX-TIME

CANDU REACTOR
STEADY-STATE CONTINUOUS
BIDIRECTIONAL FUELING
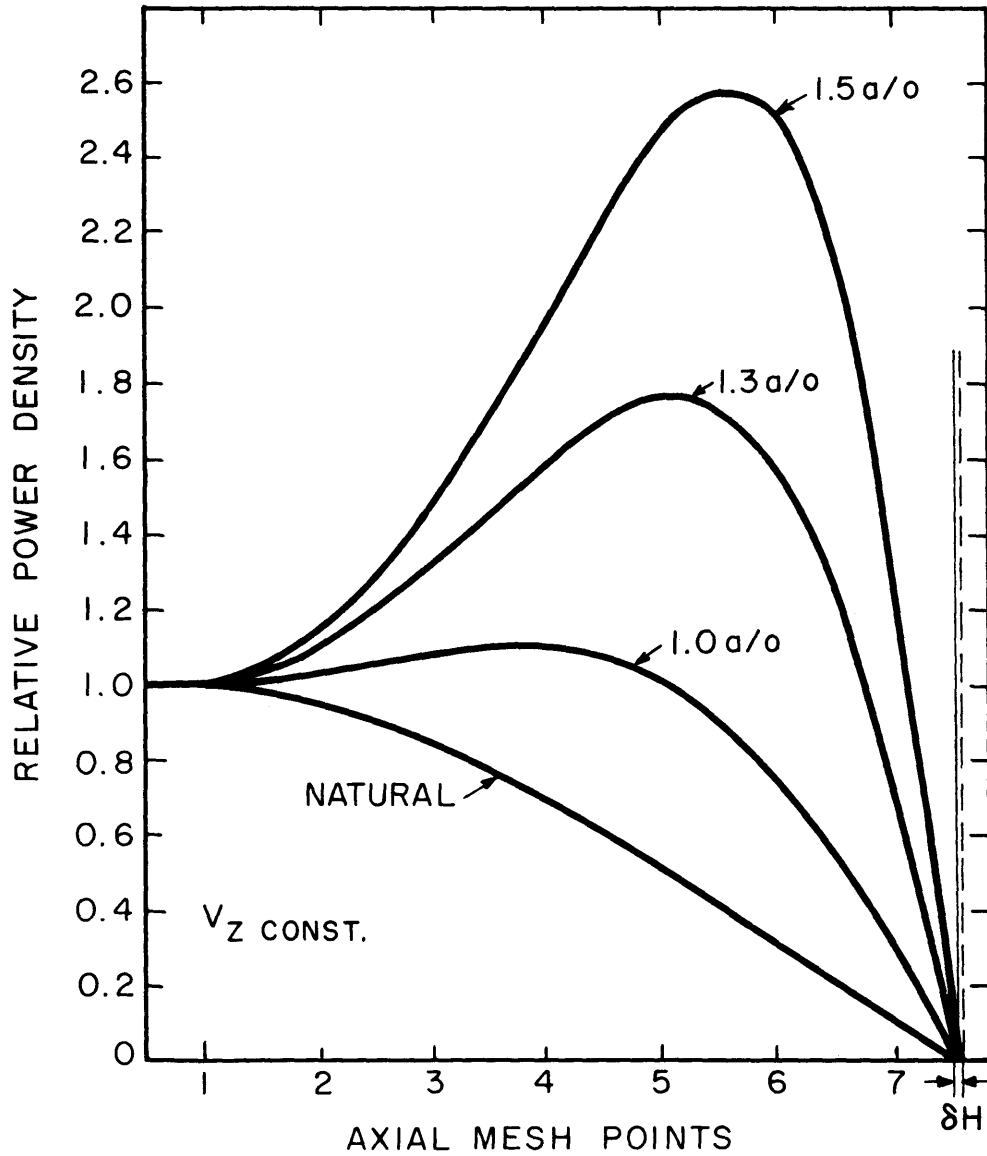
FIG. 6.12   THE AXIAL BEHAVIOR OF RELATIVE
POWER DENSITY AT THE AXIS OF
THE CANDU REACTOR FOR CONSTANT
AXIAL VELOCITY

density is 1.0 a/o for all radial fuel management techniques. Increasing radial flatness with increasing enrichment is evident in the radial behavior of relative power density as shown in Figure 6.13.

One of the consequences of a flat flux distribution is increased neutron leakage. This is the reason for the behavior, at a given enrichment, of the average burnup as shown in Figure 6.14. The best burnup is achieved with the constant discharge burnup situation, which also has the most peaked power and flux distribution. Also, the small additional flattening in going from the $V_{z\ const.}$ curve to the $\theta_{d\ min\ p.d.}$ curve costs almost as much in burnup as going from the $\theta_{d\ const.}$ to the $V_{z\ const.}$ curves, which resulted in substantial improvement in flatness. One additional point should be noted. The burnup loss associated with flux flattening is almost independent of enrichment. Hence, the percentage loss in burnup should decrease substantially with enrichment. In making an economic balance between these factors, increased burnup would be given more weight at lower enrichment and flatter power distribution, more weight at higher enrichment because the fuel burnup cost penalty associated with power flattening will be less significant at higher enrichment.

The use of radial variation of burnup for radial power distribution control results in the behavior of the maximum burnup curves, as shown in Figure 6.15. The $\theta_{d\ const.}$ curve is identical to its namesake on Figure 6.12, since the maximum burnup is equal to the average in this situation. The $V_{z\ const.}$ curve, having larger burnup, and the $\theta_{d\ min.\ p.\ d.}$ curve having the largest, lie in order above the $\theta_{d\ const.}$ curve.

CANDU REACTOR
STEADY-STATE CONTINUOUS
BIDIRECTIONAL FUELING
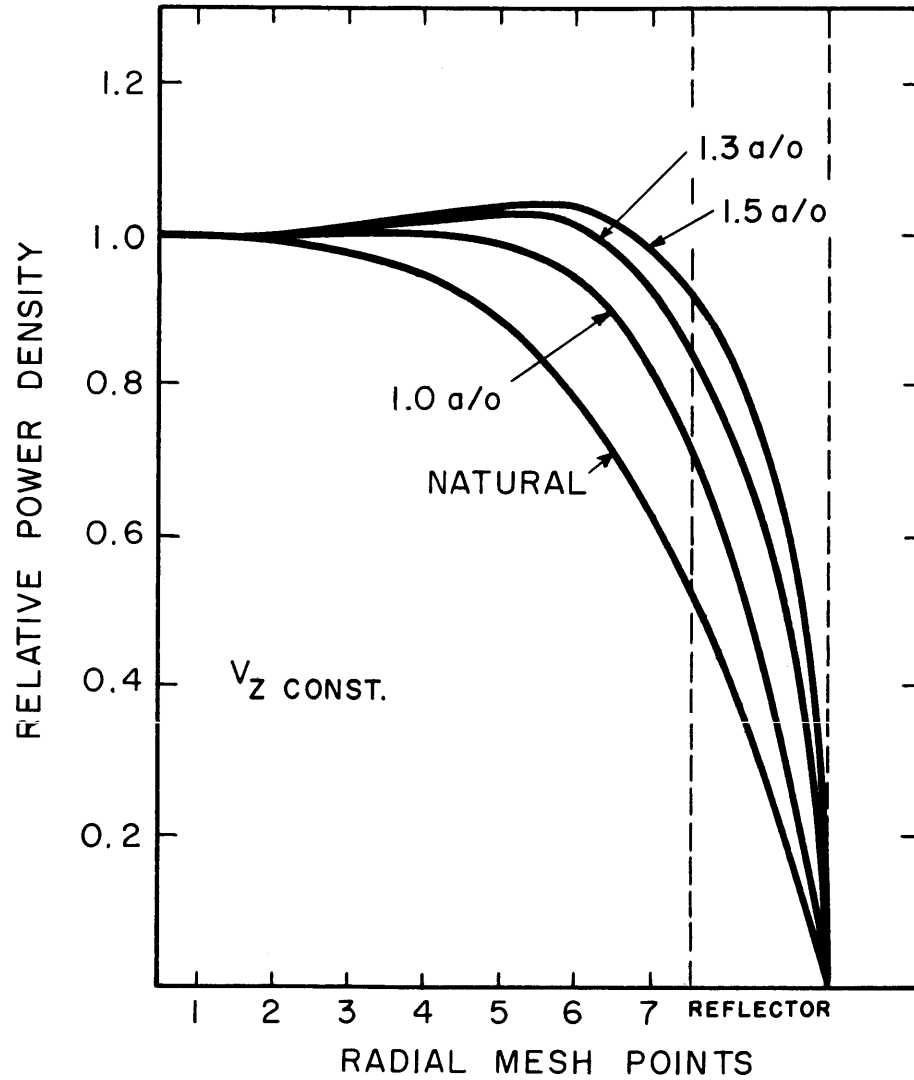
FIG. 6.13   THE RADIAL BEHAVIOR OF RELATIVE
POWER DENSITY AT THE MID-PLANE
OF THE CANDU REACTOR, FOR
CONSTANT AXIAL VELOCITY

235
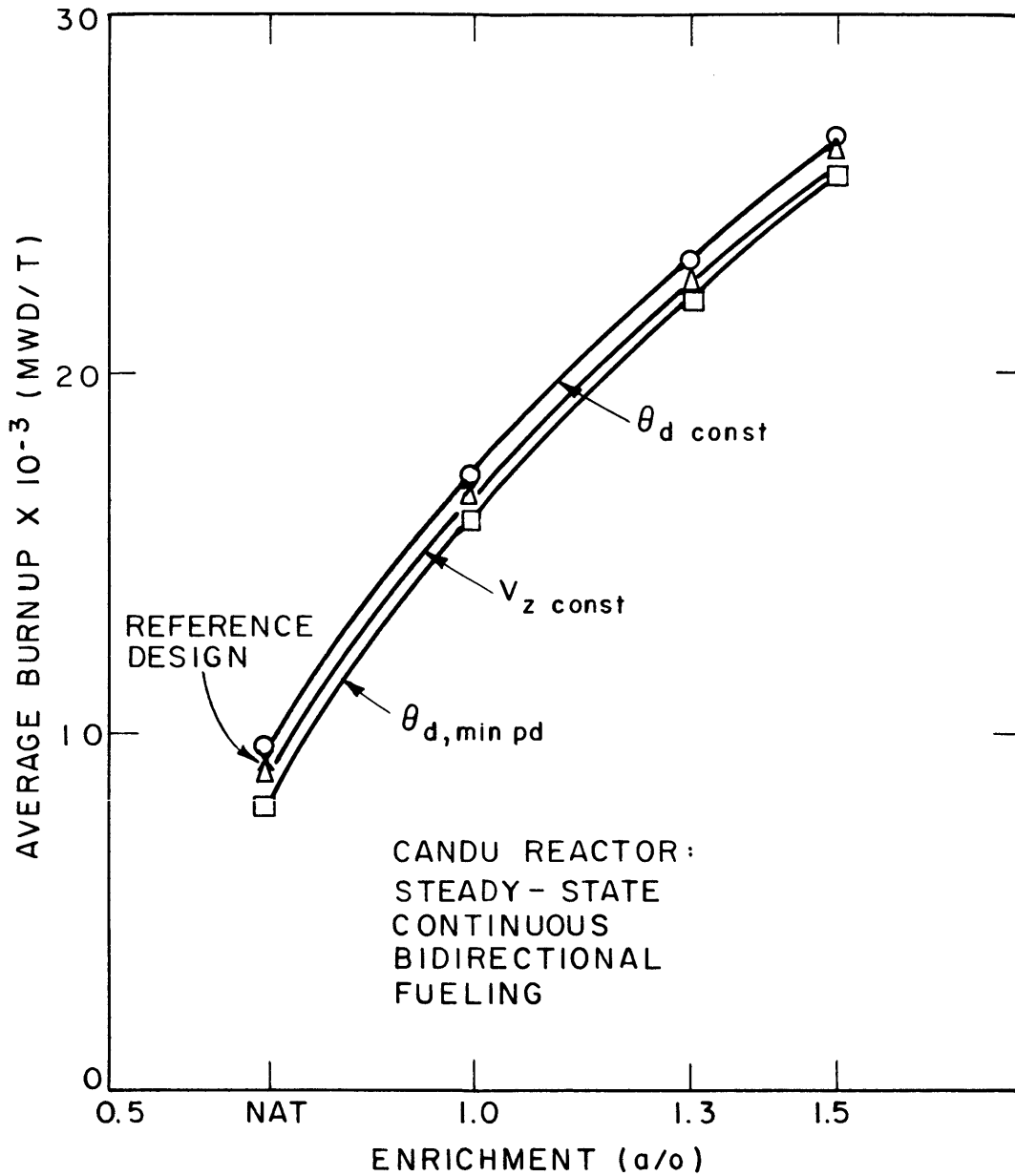
FIG. 6.14 AVERAGE BURNUP IN THE CANDU REACTOR AS A FUNCTION OF ENRICHMENT FOR VARIOUS WAYS OF SPECIFYING THE RADIAL SHAPE OF DISCHARGE FLUX-TIME

236
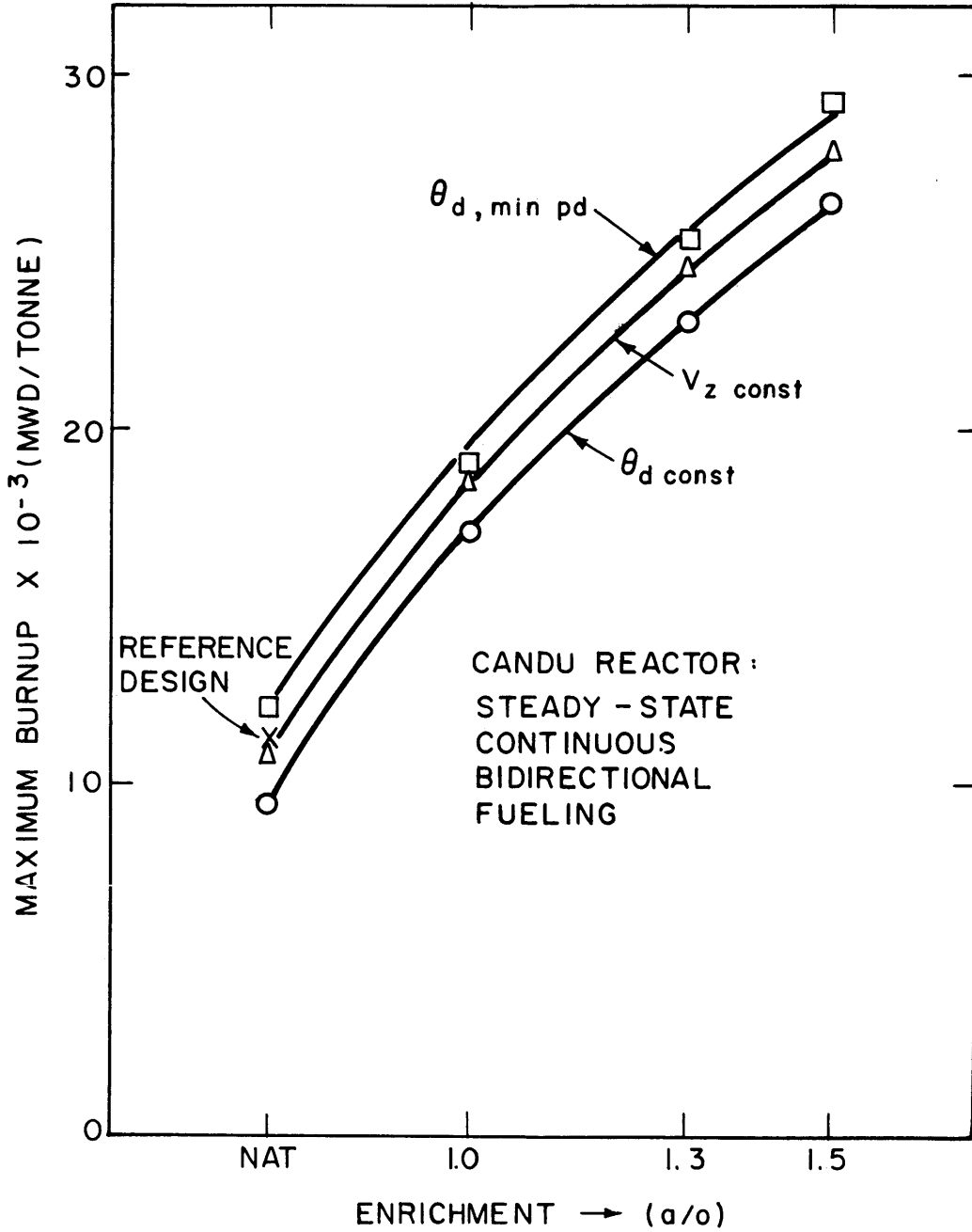
FIG. 6.15 MAXIMUM BURNUP IN THE CANDU REACTOR AS A FUNCTION OF ENRICHMENT FOR VARIOUS WAYS OF SPECIFYING THE RADIAL SHAPE OF DISCHARGE FLUX-TIME

237

Shown in Figure 6.16 is a contour plot of relative power density, showing the flattest power distribution that can be obtained in bidirectional fueling by use of radial variation of discharge burnup. This case, 1.0 a/o, $\theta_{d\ min\ p.\ d.}$ achieves a peak-to-average power density ratio of 1.51.

The net fuel cycle costs for the three radial fuel management techniques are shown in Figure 6.17. Particular notice should be taken of the sensitivity of net fuel cycle cost to the radial fuel management technique at the various enrichments. The natural uranium cases are strongly dependent on the radial discharge flux-time technique, with decreasing importance at higher enrichments. The reason for this behavior is, as pointed out in Figure 6.14, that the percentage burnup loss decreases substantially with enrichment. This, combined with the higher U fuel cost for natural U causes the strong dependence on radial fuel management at this enrichment. A similar dependence would be shown for increased leakage due to smaller core size. Hence, the use of natural uranium will tend to result in larger reactor cores for a given power output in reactors whose output is limited by peak power density, since attempts to flatten the power distribution in order to decrease core volume, will be met with substantial cost penalties associated with burnup losses from both the flattening and the decreased volume. The cost penalties resulting from the same attempts at higher enrichments are much less, and there is reasonable chance that they can be offset by the savings from core volume decrease.

The individual cost components which contribute to the net energy cost are shown in Figure 6.18 for cost basis 1, and in Figure 6.19 for cost basis 2. As is to be expected, the

CANDU REACTOR
STEADY-STATE CONTINUOUS
BIDIRECTIONAL FUELING
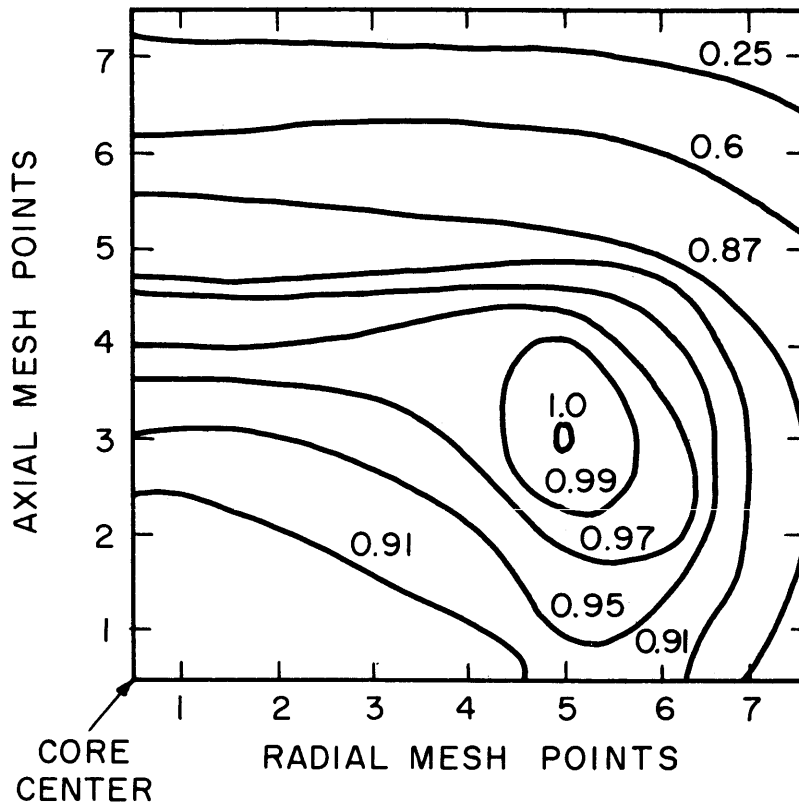
FIG. 6.16   CONTOUR PLOT OF THE RELATIVE
POWER DENSITY, CANDU REACTOR
1.0 a/o   ENRICHMENT, WITH DISCHARGE
BURNUP ADJUSTED FOR MINIMUM
PEAK POWER DENSITY

239

CANDU REACTOR:

STEADY-STATE
CONTINUOUS
BIDIRECTIONAL
FUELING

COST BASIS
1

COST BASIS
2

O $\theta_{d\ min\ pd}$

△ $V_z\ const$
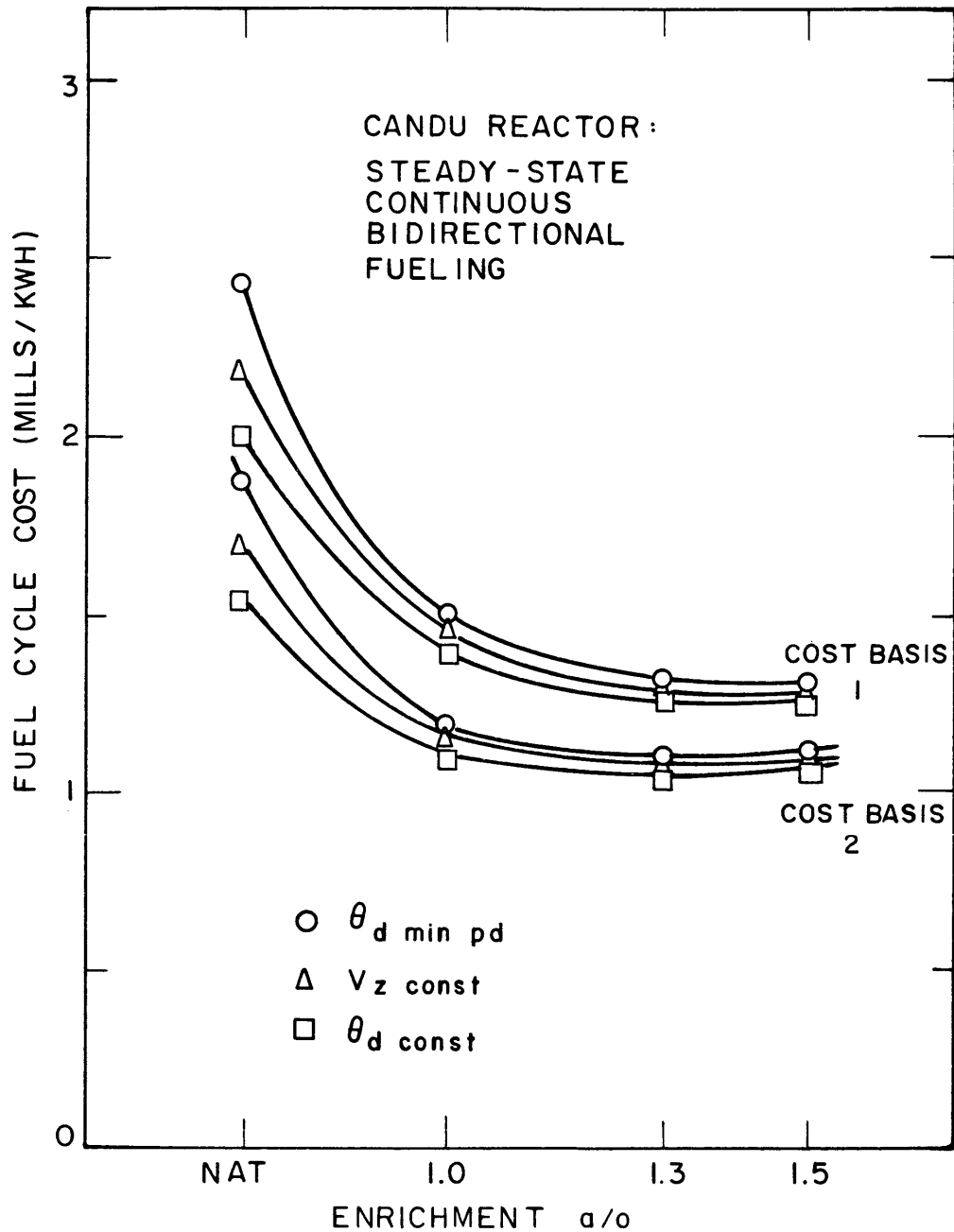
□ $\theta_{d\ const}$

FIG. 6.17 NET FUEL CYCLE COST IN THE CANDU
REACTOR AT VARIOUS ENRICHMENTS AND
RADIAL SPECIFICATIONS OF DISCHARGE
FLUX - TIME

240
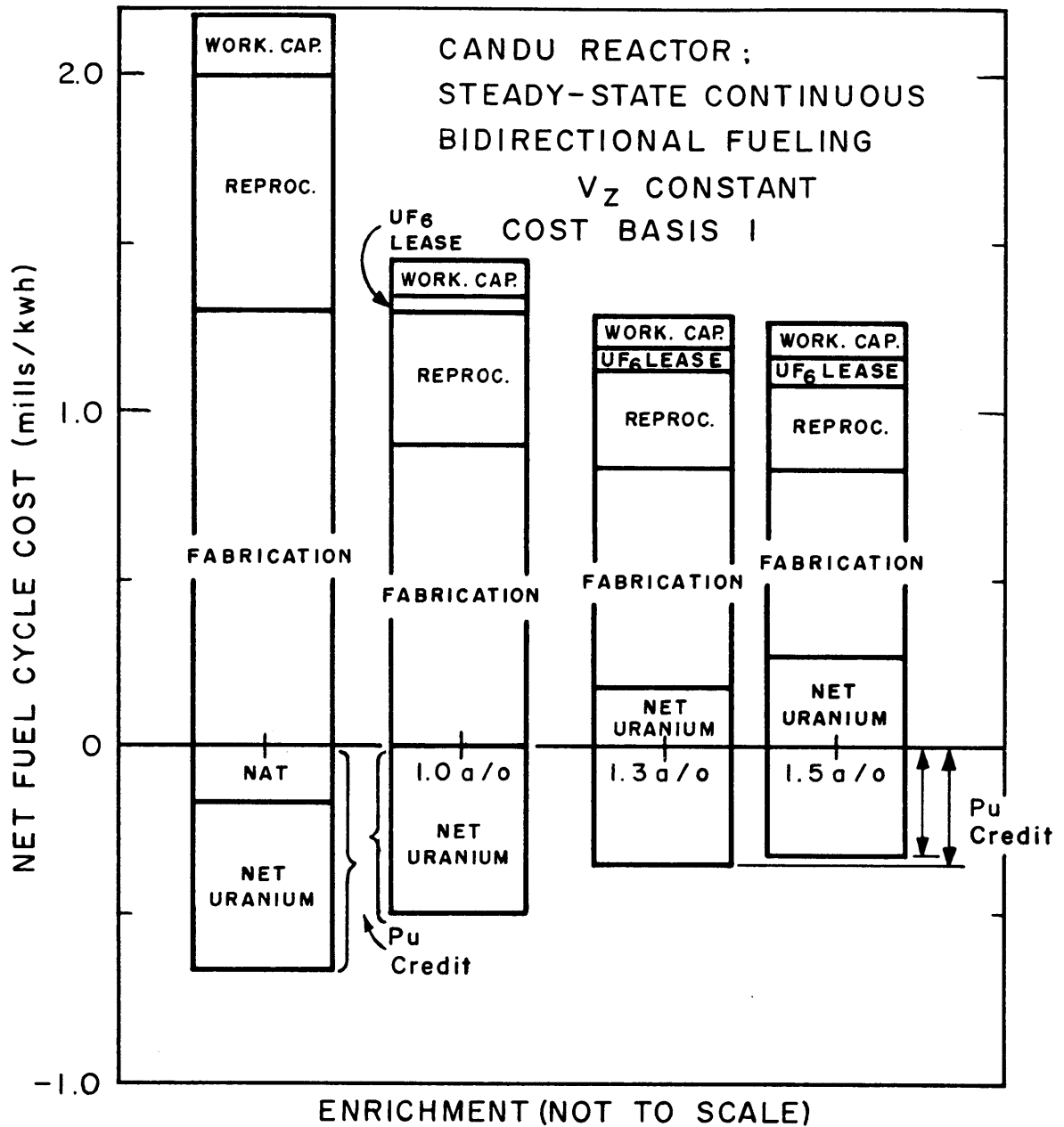
FIG. 6.18 THE COMPONENTS OF THE NET FUEL
CYCLE COST (BASIS I) vs ENRICHMENT.
CANDU REACTOR, CONSTANT AXIAL
VELOCITY
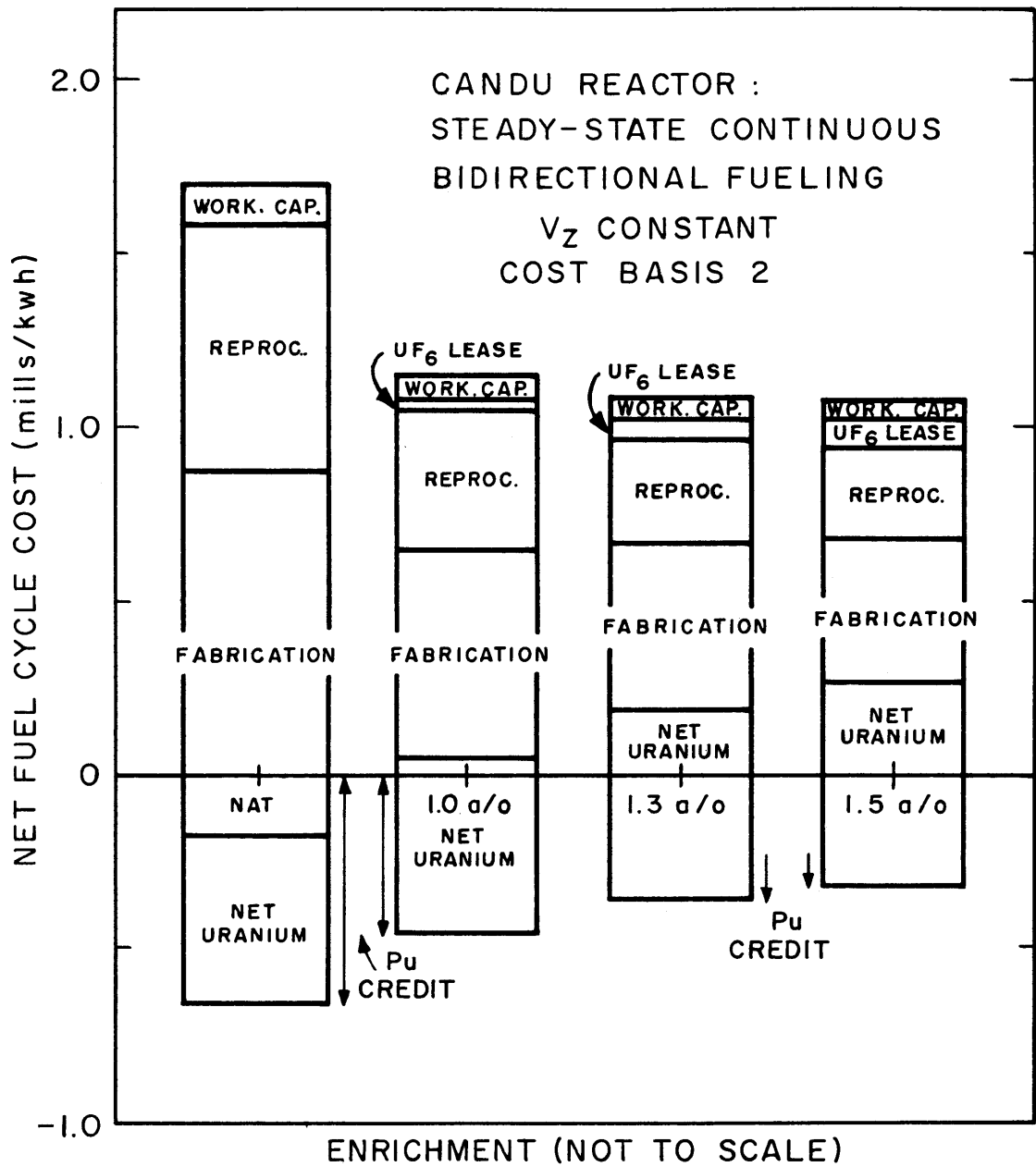
FIG. 6.19 THE COMPONENTS OF THE NET FUEL
CYCLE COST (BASIS 2) vs ENRICHMENT.
CANDU REACTOR, CONSTANT AXIAL
VELOCITY

242

fabrication and reprocessing costs, being inversely proportional to burnup, decrease in an approximate inverse proportionality with enrichment. It is of interest that the Pu credit behaves in much the same manner, implying that Pu reaches a saturation concentration early in irradiation, which is a good approximation to fact, as can be seen from Figure 6.3. The net uranium cost, which in all cases considered here is identical to the initial feed material cost, has very little dependence on enrichment. This implies that the consumption of the more expensive enriched uranium is compensated for by the additional consumption of "free" Pu, that the higher enrichment permits. The sum of working capital plus UF_6 lease charges is also nearly constant, with the UF_6 lease charge increasing slightly with enrichment.

In addition to the general survey of the effects of radial burnup variations and fuel enrichment, three test runs were made using specified discharge burnups similar to those of the reference design, in an attempt to improve on the peak power density or the burnup of the reference design. The results of this investigation, summarized in Table 6.7, show that the power distribution and burnup are not both improved by slight changes in the radial discharge burnup. An improvement in power distribution is made only at the expense of burnup. Hence, it can be concluded that the reference design achieves the maximum burnup that is compatible with its core volume and peak power density limitation.

4.3 The Effect of Mixed Enrichments on Burnup and Power Distribution

The possibility of using two radial zones, each with fuel of different enrichments is considered in this section. This is investi-

Table 6.7 The Effect of Changes on Reference Design Performance.

Run Number	Average Burnup Mwd/T	Maximum Burnup Mwd/T	Peak Power Density Kw/L	Maximum to Average Power Density Ratio	T_R Full Power Time in Years	Net Fuel Cycle Cost Mills/Kwh	
						Cost Basis 1	Cost Basis 2
A5.1 (Reference)	9,080	11,620	17.56	2.04	1.33	2.09	1.62
A3.1.10	9,140	10,650	18.20	2.12	1.34	2.07	1.60
A3.1.7	9,025	11,570	17.29	2.01	1.32	2.10	1.63
A3.1.8	9,010	11,410	17.00	1.98	1.32	2.11	1.63

244

Run Number	θ_c n/kb	Discharge Flux-Time at Each Radial Mesh Point Relative to θ_c									
		1	2	3	4	5	6	7	8	9	10
A5.1 (Reference)	4.130	1.	1.	1.	1.	0.721	0.721	0.721	0.721	0.721	0.721
A3.1.10	3.7481	1.	0.995	0.990	0.970	0.910	0.870	0.820	0.790	0.770	0.770
A3.1.7	3.915	1.	1.010	1.030	1.050	0.800	0.780	0.760	0.750	0.740	0.730
A3.1.8	3.9067	1.	1..010	1.020	1.030	.850	.800	.760	.740	.720	.720

gated because of the potential advantages of flatness that might be achieved. The combination of Natural and 1.0 a/o enrichment was selected for this study. The study was conducted using a 7 × 7 mesh with two radial zones of very nearly equal volume.

The results of this study are summarized in Table 6.8. Also included is the uniform 1.0 a/o enrichment, $\theta_{d \text{ min p. d.}}$ case from the studies of the previous section, for purposes of comparison. The four cases studied with natural uranium in the center show increasing cost trends with increasing flatness, but the costs are substantially above those of the uniform case which is somewhat flatter. The two situations with the 1.0 a/o uranium in the inner zone show slightly lower fuel costs than the uniform case, but there is excessive power peaking.

It is evident that none of the mixed enrichment situations can approach the combined flatness and low fuel cost of the uniformly enriched reactor. As might be expected, the natural uranium is detrimental to the average fuel cost, being a higher cost fuel, as can be seen in Figure 6.17. Its ability to flatten the power distribution in the center is no better and probably worse than if 1.0 a/o fuel were to be used in its place.

The conclusion is that if one compares two fueling procedures which give the same degree of power density flattening, one using fuel of two different enrichments, the other using fuel of the optimum single enrichment with flattening achieved by radial variation of discharge burnup, the single enrichment case leads to the lower fuel cost. Because of this, the use of zones of different enrichment will not be considered further as a possible contributor to the optimum design study.

Table 6.8   The Effect of Mixed Enrichment.

Enrichment			Relative V_z or θ_d		Peak Power Density Kw/L	Avg. Burnup Mwd/T		Net Fuel Cycle Cost Mills/Kwh		Run No.
Inner Zone	Outer Zone	Type	Inner Zone	Outer Zone		Inner Zone	Outer Zone	Basis 1	Basis 2	
Nat	1.0 a/o	V_z Const.	1.0	0.7	14.04	10,760	14,310	1.708	1.333	A4.13.1
			1.0	0.9	14.15	11,450	13,620	1.694	1.324	A4.13.2
Nat	1.0 a/o	θ_d Const.	1.0	1.1	13.94	11.010	14,350	1.682	1.312	A4.13.3
			1.0	0.9	15.27	12,150	13,330	1.671	1.308	A4.13.4
1.0 a/o	Nat	θ_d Const.	0.9	1.0	26.25	16,220	15,100	1.404	1.101	A4.13.5
			1.2	1.0	23.41	16,610	12,000	1.461	1.143	A4.13.6
1.0 a/o		θ_d min p.d	Table 6.6		12.95	16,070		1.49	1.18	A6.3

4.4 The Use of Fixed Poison for Power Flattening and Its Effect on Burnup

In steady-state bidirectional fueling, power flattening in the radial direction is accomplished by means of radial variation of discharge burnup. There is no specific control over axial flattening. In this section, the use of fixed poison for axial flattening is studied. In each case, the spatial poison distribution resulting in the greatest degree of flattening for a given maximum poison magnitude has been obtained by iteration. Only natural and 1.3 a/o were studied to check the feasibility of this technique.

A summary of the basic results of this survey is given in Table 6.9. It is immediately evident that poison use for flattening with natural uranium is completely out of the question, since the cost penalty due to burnup loss is excessive.

However, at 1.3 a/o enrichment, the burnup losses are much less, and there may be justification for use of fixed poison in certain circumstances. Comparison of the poison-flattened 1.3 a/o results with those of the unpoisoned 1.0 a/o results shows, however, that there is nothing to be gained by this technique, even at 1.3 a/o enrichment, since it is possible, using 1.0 a/o and radial burnup control, to achieve equal flatness at lower fuel cost.

The general conclusion then, with regard to the use of fixed poisons for axial power distribution control, is that this technique is unattractive for this central-station nuclear power system. For this reason, no further consideration will be given to this technique as a possible contributor to the optimum design study.

Table 6.9 The Effect of Fixed Poison on Burnup and Power Distribution.

Enrichment	Type	Poison cross section, $\Sigma_{wa,max}$ in $cm^{-1} \times 10^5$	Average Burnup in Mwd/T	Peak Power Density in Kw/L	T_R Full Power Time in years	Net Fuel Cycle Cost in Mills/Kwh		Run No.
						Basis 1	Basis 2	
NAT	$\theta_{d,min\,p.d}$	0	7,970	15.06	1.17	2.42	1.88	A6.1
		30	5,920	13.72	0.866	3.35	2.64	A7.1-30
		60	3,930	12.12	0.574	5.21	4.16	A7.1-60
1.3 a/o	$\theta_{d,min\,p.d}$	0	22,020	15.31	3.22	1.32	1.10	A6.5
		30	20,670	14.49	3.02	1.41	1.18	A7.5-30
		60	19,310	13.33	2.83	1.51	1.26	A7.5-60
		100	18,040	12.41	2.64	1.62	1.36	A7.5-100
1.0 a/o	$\theta_{d,min\,p.d}$	0	16,070	12.95	2.35	1.49	1.18	A6.3

4.5 The Optimized Reactor Designs for Bidirectional Fueling in Steady-State Operation

The results of the bidirectional fueling study up to this point will now be used to specify the various combinations of parameters which result in the minimum total energy cost core design at each fuel enrichment. Having eliminated the use of zones of different enrichment and the use of fixed poison for power distribution control from consideration, only radial variation of burnup and its effect on burnup and power distribution need be considered at each enrichment.

Associated with the choice of an optimum design are the remaining two of the three types of fuel and poison management study. The first type, in which core volume and total output were fixed, has been used in the study of steady-state bidirectional fueling up to this point. However, in order to evaluate the results of the study, it is necessary that the conclusions be based on a common denominator of either fixed core output or, in some cases, fixed core volume, within the constraint of a maximum permissible power density. In the following, most emphasis will be placed on the fixed core energy output basis of comparison, which would be used to establish the design of a new power plant, and this case will be treated first.

If the assumption is made (which is justified by hindsight) that the relative power distribution remains constant with small changes in core volume, a reactor core operating at a specified output, but below its peak power density limit, can be reduced in volume by the ratio of its current maximum power density to the maximum permissible. The resultant core is then operating concurrently at its specified output and at its maximum permissible

power density. Under these circumstances, the volume of the reactor will be proportional to the characteristic peak-to-average power density ratio of the fuel and poison management technique being employed. Hence, there will generally be an economic incentive to reduce the peak-to-average power density ratio. A limit to the degree of flatness will be imposed by one of two factors. It may be physically impossible to increase flatness beyond a certain point with a given fuel management procedure, or it may be that incremental fuel cost increases associated with burnup loss from increasing flatness and decreasing volume will be greater than incremental cost decreases due to the decreasing volume.

When the limit on decreasing core volume is imposed by the physical impossibility of further power distribution flattening, the core volume is characteristic of this maximum flatness. When a compromise between loss of burnup and core volume must be made, it is necessary to use specific cost data in order to evaluate the core volume that will yield minimum total energy cost.

In the CANDU reactor, a large part of the cost of the reactor system is associated with the installation and material cost of the end fittings in each channel. For this reason, the optimum core geometry tends to be a long cylinder. For practical reasons, however, an upper limit of 500 cm. length was assigned (L 61) and this is to be used in this work, and will be held constant when the core volume is varied. With the length constant, both the channel end fitting cost and the cost of D_2O moderator will be proportional to the volume of the reactor.

Using data given in Appendix III of L61, plus the cost of D_2O, both in and out of the core, about \$13,600,000, or \$68/kwe, of the core cost is directly proportional to reactor core volume.

This is expressed in the form

$$C_{15} = 156 + 68\,(V/V_o) \qquad \$ \quad /\text{kwe} \qquad\qquad (6C3)$$

where C_{15} is the plant capital investment associated with the reactor.

The actual design study was performed on the three enrichments, 1.0, 1.3, and 1.5 a/o. The reference design was taken as being representative of the optimum design at natural enrichment. The 1.5 a/o enrichment, because of a combination of circumstances, has the same core volume as the reference design. The volumes of the reactors at 1.0 and 1.3 a/o were reduced until they were operating concurrently at the peak power density limit of 17.0 kw/l and at specified (200 MWE) output. In each case, the limit of volume reduction was imposed by the physical impossibility of additional flattening and not by increased fuel costs. In fact, at 1.3 a/o enrichment the fuel cost actually decreased because the reduction in interest charges due to a higher specific power more than offset the increased cost due to slightly lower burnup. It was therefore unnecessary to make the compromise between burnup and core volume.

The total energy cost for optimized reactors operating at the four enrichments is shown in Figure 6.20. The characteristics of each reactor are given in Table 6.4, 6.10, 6.11, and 6.12 for natural, 1.0, 1.3, and 1.5 a/o, respectively. It is apparent that the optimum enrichment for the 200 Mwe reactor lies in the range between 1.0 and 1.3 a/o.

It is instructive to recall some of the conclusions that were reached in the study of radial variation of burnup and enrichment, and to see how the same factors have influenced the results of the
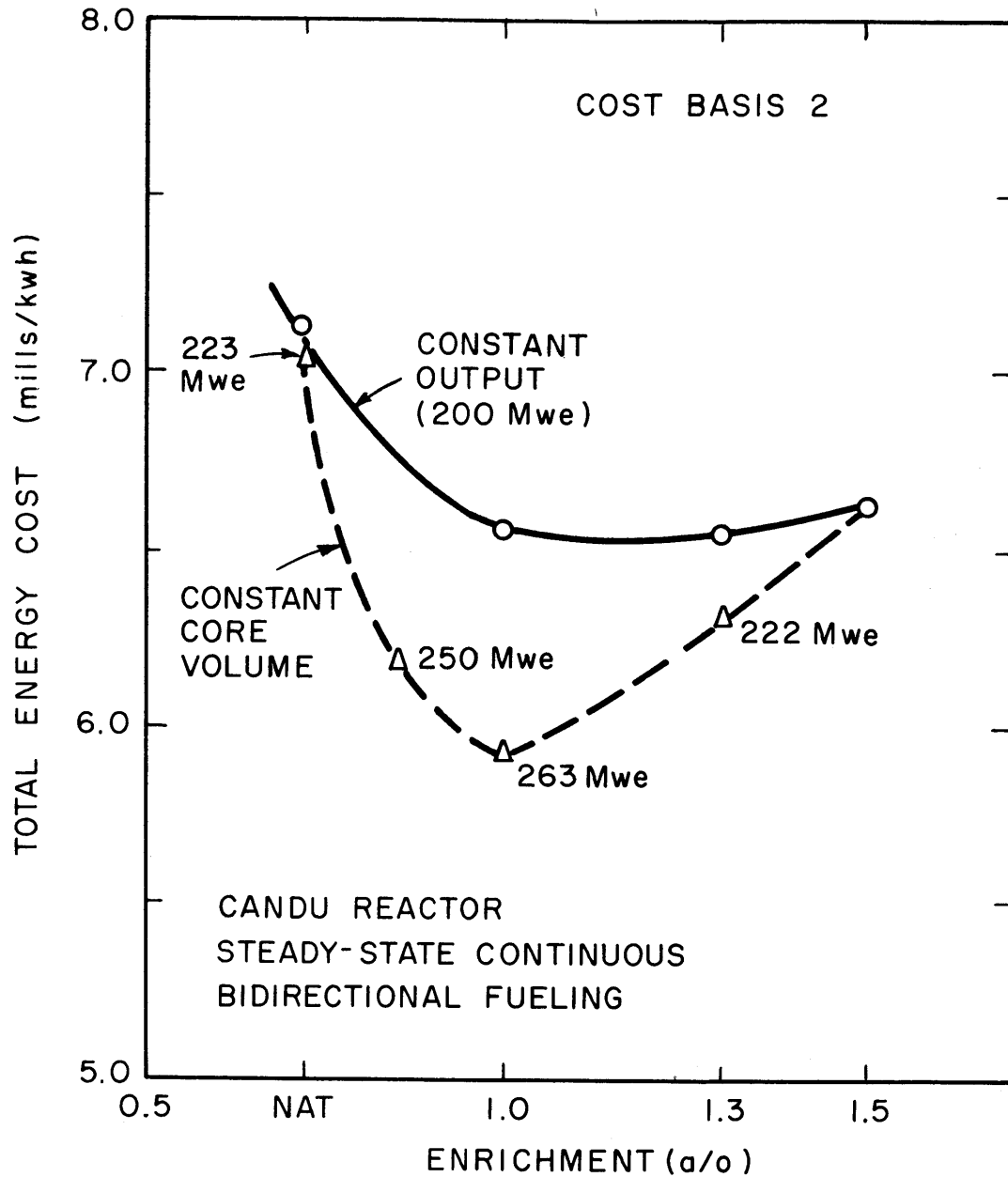
FIG. 6.20 THE VARIATION OF TOTAL ENERGY
COST WITH ENRICHMENT FOR REACTORS
AT CONSTANT OUTPUT OR CONSTANT
VOLUME AND A FIXED PEAK POWER
DENSITY

252

Table 6.10   Characteristics of the Optimum Reactor

at 1.0 a/o Enrichment

A. Design Data

Thermal power	P_o
Core Volume	$0.81\ V_o$
Maximum Power density	17.0 kw/l
Relative Discharge Flux-Time	See Table 6.5
	$(1.0\ a/o\ \theta_{d\ min\ p.\ d})$
Fuel Enrichment a/o U^{235}	1.0 a/o

B. MOVE Code Results (Run No. A8.3)

Maximum Power Density	16.93 kw/l
Ratio of Maximum to Average Power Density	1.97
Average Burnup MWD/T	15,810
Maximum Burnup	18,440
Full Power Time in Reactor	1.87 years
KWhe/kg of fuel charged	106,050

C. Material Quantities

Feed rate kgU/full power year	20,430
Discharge rates	
kgU/full power year	19,970
kgPu/full power year	110
Isotopic Content of Discharged Fuel	
w/o; U^{235} in U	0.096
U^{236} in U	0.134
Pu^{239} in Pu	51.57
Pu^{240} in Pu	30.53
Pu^{241} in Pu	10.05
Pu^{242} in Pu	7.85

253

Table 6. 10 (cont'd)

D. Fuel Cycle, and Total Energy Costs

		Cost Basis 1 mills/Kwh	Cost Basis 2 mills/Kwh
1.	Natural UO_2	0	0.17
2.	UF_6 From AEC	0.47	0.35
3.	UF_6 to UO_2	0.12	0.05
4.	Fabrication	0.82	0.58
5.	Shipping	0.15	0.15
6.	Solvent Extraction	0.19	0.19
9.	Conversion of $Pu(NO_3)_4$ to Pu	0.07	0.07
10.	Sale of Pu to AEC	-0.46	-0.46
11.	UF_6 Lease, Non-reactor	0.01	0.01
12.	Working Capital, Non-reactor	0.03	0.02
13.	UF_6 Lease, Reactor	0.03	0.02
14.	Working Capital, Reactor	0.06	0.04
	Net Fuel Cycle Cost	1.49	1.19
15.	Plant Capital Costs, Reactor	4.21	2.44
16.	Plant Capital Costs, Non-reactor	3.65	1.91
17.	Operating Costs, Reactor	0.62	0.62
18.	Operating Costs, Non-reactor	0.40	0.40
	TOTAL ENERGY COST	10.37	6.56

Table 6.11   Characteristics of the Optimum Reactor

at 1.3 a/o Enrichment

A. Design Data

Thermal Power	P_o
Core Volume	$0.9 \, V_o$
Maximum Power Density	17.0 kw/l
Relative Discharge Flux-Time	See Table 6.6
	$(1.3 \text{ a/o } \theta_{d \text{ min p. d}})$
Fuel Enrichment a/o U^{235}	1.3 a/o

B. MOVE Code Results (Run No. A8.5)

Maximum Power Density	16.97 kw/l
Ratio of Maximum to Average Power Density	1.97
Average Burnup in MWD/T	21,920
Maximum Burnup	25,400
Full Power Time in Reactor	2.89 years
Kwhe/kg of fuel charged	147,040

C. Material Quantities

Feed Rate kgU/Full power year	13,230
Discharge rates	
kgU/Full power year	12,830
kgPu/Full power year	75
Isotopic Content of Discharged Fuel	
w/o U^{235} in U	0.07
U^{236} in U	0.18
Pu^{239} in Pu	46.52
Pu^{240} in Pu	31.63
Pu^{241} in Pu	10.48
Pu^{242} in Pu	11.37

255

Table 6.11 (cont'd)

D. Fuel Cycle, and Total Energy Costs

		Cost Basis 1 mills/Kwh	Cost Basis 2 mills/Kwh
1.	Natural UO_2	0.00	0.04
2.	UF_6 from AEC	0.55	0.53
3.	UF_6 to UO_2	0.09	0.07
4.	Fabrication	0.59	0.42
5.	Shipping	0.10	0.10
6.	Solvent Extraction	0.14	0.14
9.	Conversion of $Pu(NO_3)_4$ to Pu	0.06	0.06
10.	Sale of Pu to AEC	-0.36	-0.36
11.	UF_6 Lease, Non-Reactor	0.01	0.01
12.	Working Capital, Non-Reactor	0.02	0.01
13.	UF_6 Lease, Reactor	0.05	0.04
14.	Working Capital, Reactor	0.07	0.04
	NET FUEL CYCLE COST	1.32	1.10
15.	Plant Capital Costs, Reactor	4.34	2.52
16.	Plant Capital Costs, Non-Reactor	3.65	1.91
17.	Operating Costs, Reactor	0.62	0.62
18.	Operating Costs, Non-Reactor	0.40	0.40
	TOTAL ENERGY COST	10.33	6.55

Table 6.12   Characteristics of the Optimum Reactor

at 1.5 a/o Enrichment

A. Design Data

    Thermal Power P_o

    Core Volume V_o

    Maximum Power Density   17. 0 kw/l

    Relative Discharge Flux-Time   See Table 6.6

                                             (1. 5 a/o $\theta_{d\ min\ p.\ d}$)

    Fuel Enrichment a/o U^{235} 1. 5 a/o

B. MOVE Code Results (Run No. A6.6)

    Maximum Power Density   16. 95 kw/l

    Ratio of Maximum to Average Power Density   1. 97

    Average Burnup in MWD/T   25, 400

    Maximum Burnup in MWD/T   29, 370

    Full Power Time in Reactor   3. 72 years

    Kwhe/kg of fuel charged   170, 390

C. Material Quantities

    Feed Rate kgU/Full power year   10, 270

    Discharge rates

        kgU/Full power year   9, 920

        kgPu/Full power year   54

    Isotopic Content of Discharged Fuel

    w/o: U^{235} in U   0. 06

           U^{236} in U   0. 21

           Pu^{239} in Pu   44. 57

           Pu^{240} in Pu   31. 79

           Pu^{241} in Pu   10. 52

           Pu^{242} in Pu   13. 12

Table 6.12 (cont'd)

D. Fuel Cycle, and Total Energy Costs

		Cost Basis 1 mills/Kwh	Cost Basis 2 mills/Kwh
2.	UF_6 from AEC	0.60	0.60
3.	UF_6 to UO_2	0.07	0.07
4.	Fabrication	0.51	0.36
5.	Shipping	0.09	0.09
6.	Solvent Extraction	0.12	0.12
9.	Conversion of $Pu(NO_3)_4$ to Pu	0.05	0.05
10.	Sale of Pu to AEC	-0.32	-0.32
11.	UF_6 Lease, Non-reactor	0.02	0.02
12.	Working Capital, Non-reactor	0.02	0.01
13.	UF_6 Lease, Reactor	0.07	0.06
14.	Working Capital, Reactor	0.08	0.05
	Net Fuel Cycle Costs	1.31	1.11
15.	Plant Capital Costs, Reactor	4.47	2.60
16.	Plant Capital, Non-Reactor	3.65	1.90
17.	Operating Costs, Reactor	0.62	0.62
18.	Operating Costs, Non-Reactor	0.40	0.40
	TOTAL ENERGY COSTS	10.45	6.63

optimization study. The use of natural uranium results in higher fuel costs than the other enrichments. In addition, however, it was shown to be more sensitive to factors affecting leakage, such as power distribution flatness and reactor volume. This combination of a higher fuel cost plus the economic inability to increase flatness and reduce volume will result in a higher total energy cost, and a larger core volume than if a higher enrichment were used.

The use of 1.0 a/o enrichment starts off with several advantages over natural uranium. It yields basically lower fuel costs. Also, its power distribution is less sensitive to the leakage factors, such as radial burnup variation and core volume. The result is a reactor operating with about 80% of the reference design core volume with a consequent saving of about $2.5 million in capital costs and also lower fuel costs than natural uranium.

The dominant factor which results in the minimum core volume near 1.0 a/o enrichment is the axial flatness, which is a maximum near 1.0 a/o. Beyond 1.0 a/o, the axial flatness starts decreasing and this will result in a trend to larger cores. However, 1.3 a/o enrichment still results in basically lower fuel costs than 1.0 a/o and it is less sensitive to leakage factors. The net result of these two opposing effects is a virtual standoff with the increased capital cost being slightly less than decrease in fuel cost from 1.0 a/o. The relative power distribution at 1.3 a/o enrichment is shown in Figure 6.21.

Beyond 1.3 a/o enrichment, fuel costs start a slight trend upward and because axial flatness decreases, capital costs also increase, resulting in increased total energy cost.

The curve shown on Figure 6.20 for constant core volume brings out the effect of maximum flatness that occurs at 1.0 a/o enrichment.

CANDU REACTOR
STEADY-STATE CONTINUOUS
BIDIRECTIONAL FUELING
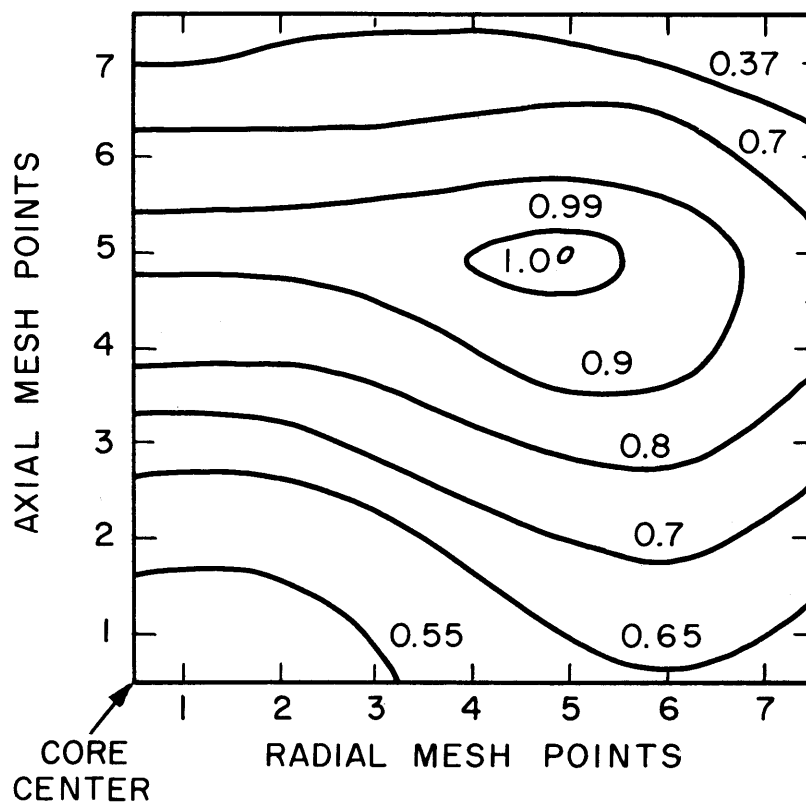
FIG. 6.21 CONTOUR PLOT OF THE RELATIVE
POWER DENSITY, MINIMUM CORE
VOLUME AT 1.3 a/o ENRICHMENT

260

This curve was obtained by holding the core volume constant and increasing the output until the maximum permissible power density was reached. All unit costs were assumed to be identical to those at the 200 Mwe output, except that costs associated with the reactor part of the capital and operating costs, plus the "on stream" fuel interest charges were reduced by the factor by which the output was increased. The constant core volume curve would be significant only if the reference design reactor were to run at 1.0 or 1.3 a/o enrichment at increased output, after having been initially designed and presumably optimized for use with natural uranium.

The conclusion that is reached with regard to steady-state bidirectional fuel management is that, under the current cost assumptions, the optimum enrichment is in the range between 1.0 and 1.3 a/o for the CANDU reactor when operating at 200 Mwe. It would take fairly large changes in the cost assumptions to change this optimum range. Lower fabrication costs would tend to favor the lower enrichment, whereas lower UF_6 prices would tend to favor the higher enrichment, and would actually be detrimental to natural uranium, since Pu credit would be decreased. This would be significant only up to the point at which it no longer paid to reprocess spent fuel. Increases in interest rates or capital costs would tend to favor 1.0 a/o whereas decreases would favor both natural and 1.3 a/o enrichment.

Inasmuch as there is a trend with time to lower fabrication costs, lower UF_6 costs, and generally lower capital costs, the overall picture will remain somewhat as is given, using the current cost assumptions.

5. The Transient Bidirectional Fuel Movement

In this section, some of the characteristics of the presteady-
state, bidirectional fuel movement will be given for the period immedi-
ately following batch irradiation in the startup of the CANDU Reference
Design. Because of the similarity between the continuous bidirectional,
and the discontinuous bidirectional with a large number of "zones", this
particular study will not be done in detail. The basic trends will be
very similar to those for the "multi-zoned" discontinuous bidirectional
fuel movement which is treated in detail in the next section.

The results shown in Figures 6.22-24 were obtained by speci-
fying the reference design relative axial fuel velocity for the situation
immediately following batch irradiation. Initially (the first two velocity
iterations) discharged fuel was recycled. After this, new fuel was
charged and spent fuel discharged, with a fuel cycle cost analysis being
performed on the spent fuel. The burnup of the spent fuel discharged
at various times is shown in Figure 6.22. This burnup is low initially
because the fuel that is being discharged comes from the end of the core
where it has not been as fully irradiated as the material closer to the
center. The burnup rises as this material closer to the center is
moved axially toward the ends where it is discharged. Figure 6.23
also shows the effect of this more highly irradiated central fuel being
pushed toward the discharge ends of the reactor. This figure shows
that the peak-to-average power density ratio of the core increases
with time. The initial flatness of the core is due to the presence of
the most irradiated fuel closest to the center. As this fuel is pushed
outward, the flux tends to increase in the central region.

In Figure 6.24, the fuel cycle cost is given for the fuel that is
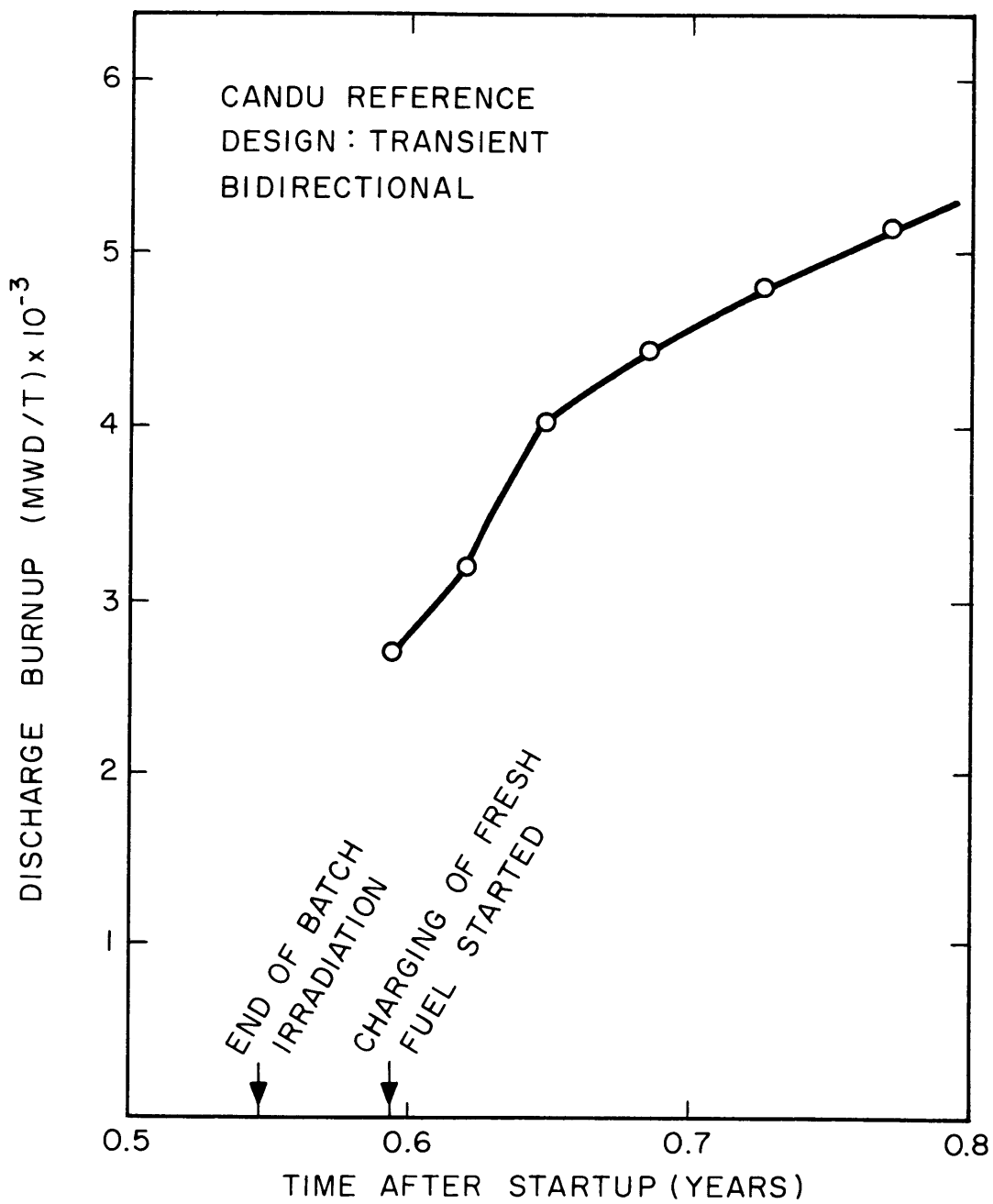
FIG. 6.22   BURNUP AT VARIOUS TIMES OF FUEL
BEING DISCHARGED CONTINUOUSLY

263
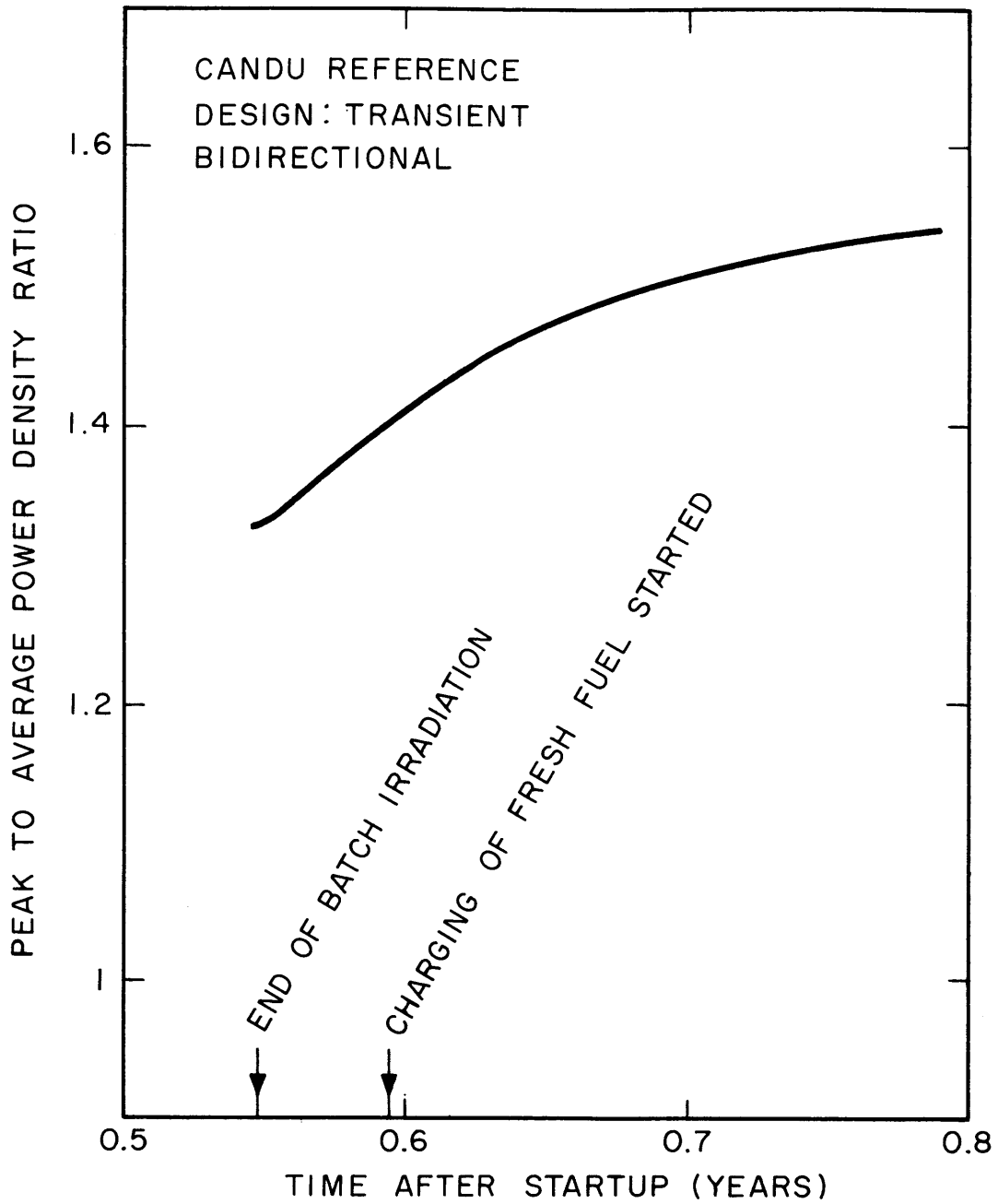
FIG. 6.23   INITIAL BEHAVIOR OF THE RATIO OF
PEAK TO AVERAGE POWER DENSITY
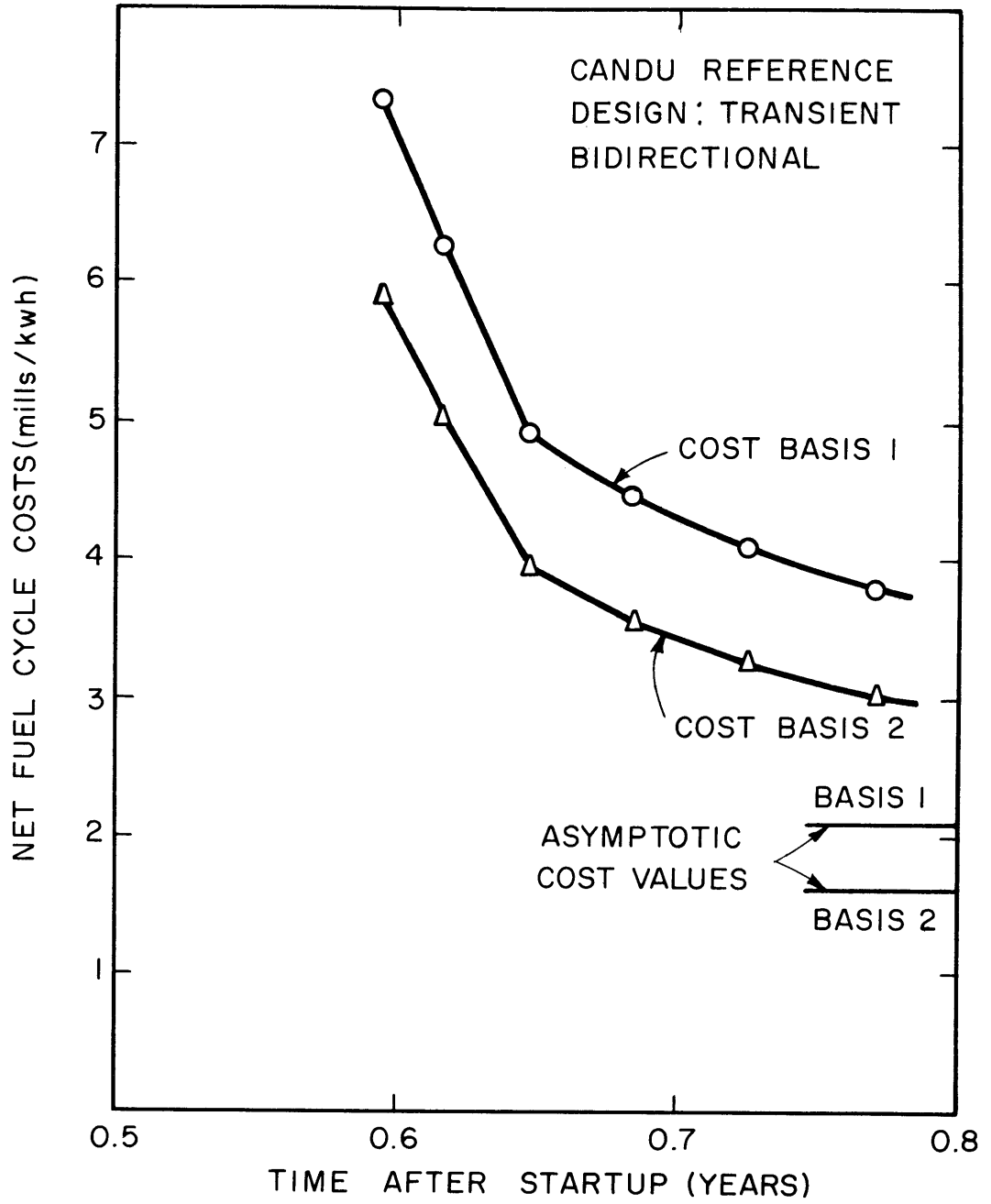
FIG. 6.24   FUEL CYCLE COST FOR FUEL
            DISCHARGED AT VARIOUS TIMES
            AFTER STARTUP

265

discharged at various times following startup of the reactor. It should be recalled that both this curve, and that of burnup, Figure 6.22, are actually continuous curves, since fuel is being moved continuously along the channels. The cost shows the decreasing trend that is to be expected from increasing burnup. Shown for comparison on Figure 6.24, are the fuel cost asymptotes which apply to the CANDU Reference Design.

One can conclude with the help of the results from the discontinuous bidirectional study given in the following section that both the fuel burnup and the peak-to-average power density ratio will increase in time, up to the point at which somewhere over one-half of the initial fuel has been discharged, at which point the most burnt-up fuel will have been removed. It would also appear to be possible to recharge spent fuel for a longer time following batch irradiations than was done in this study. It also seems likely, again in view of the discontinuous study results, that it will not be too difficult to stay within the peak power density limit while maintaining full output. Some sacrifice of fuel burnup might be necessary, however.

6. The Discontinuous Bidirectional Fuel Management Technique

This technique is similar to the continuous bidirectional fuel movement in that fuel is moved in opposite directions in adjacent channels. However, the fuel is moved only in steps rather than continuously, and is batch-irradiated between steps, so that it is necessary to use control poison. The loss of burnup that will result depends upon the amount of excess reactivity that is added each time the fuel is moved. There will be some incentive, then, to

reduce this excess, and this will involve an increase in the number of axial zones. Here a zone is defined by the axial length of fuel charged at any one time. Hence this fuel length must be a rational fraction of the total channel length.

In this section, the characteristics of 2, 3, 5, and 16 zone discontinuous bidirectional fuel movement will be presented, for both startup and steady state, and their steady-state values will be compared with the continuous (∞ zone) situation. Because of computer time limitations, it was necessary to limit the scope of this study to natural uranium, and to consider only those situations in which new fuel is added in equal quantities at all radial points at each reactor shutdown. The general trends should be revealed in spite of this limitation, however. The addition of equal amounts of new fuel at all radii is equivalent to the constant axial velocity situation in continuous bidirectional fuel management, and comparisons with the continuous asymptotes will be made on this basis.

Shown in Figure 6.25 is the time behavior of average discharge burnup for the 2, 3, 5, and 16 zone situations, along with the end-of-batch burnup and the continuous steady-state average burnup. The damped oscillatory behavior is noteworthy. The burnup peaks occur when the most irradiated fuel from the initial batch loading is discharged. There are two effects which determine when this most-irradiated fuel will be discharged. These are 1) the end-of-batch burnup distribution with the peak burnup generally occurring near the reactor center and 2) the additional time which each particular fuel element spends in the reactor following the end-of-batch irradiation. The first effect would favor the occurrence of the peak burnup in, for example, element 8 of a 16 zone core, whereas the
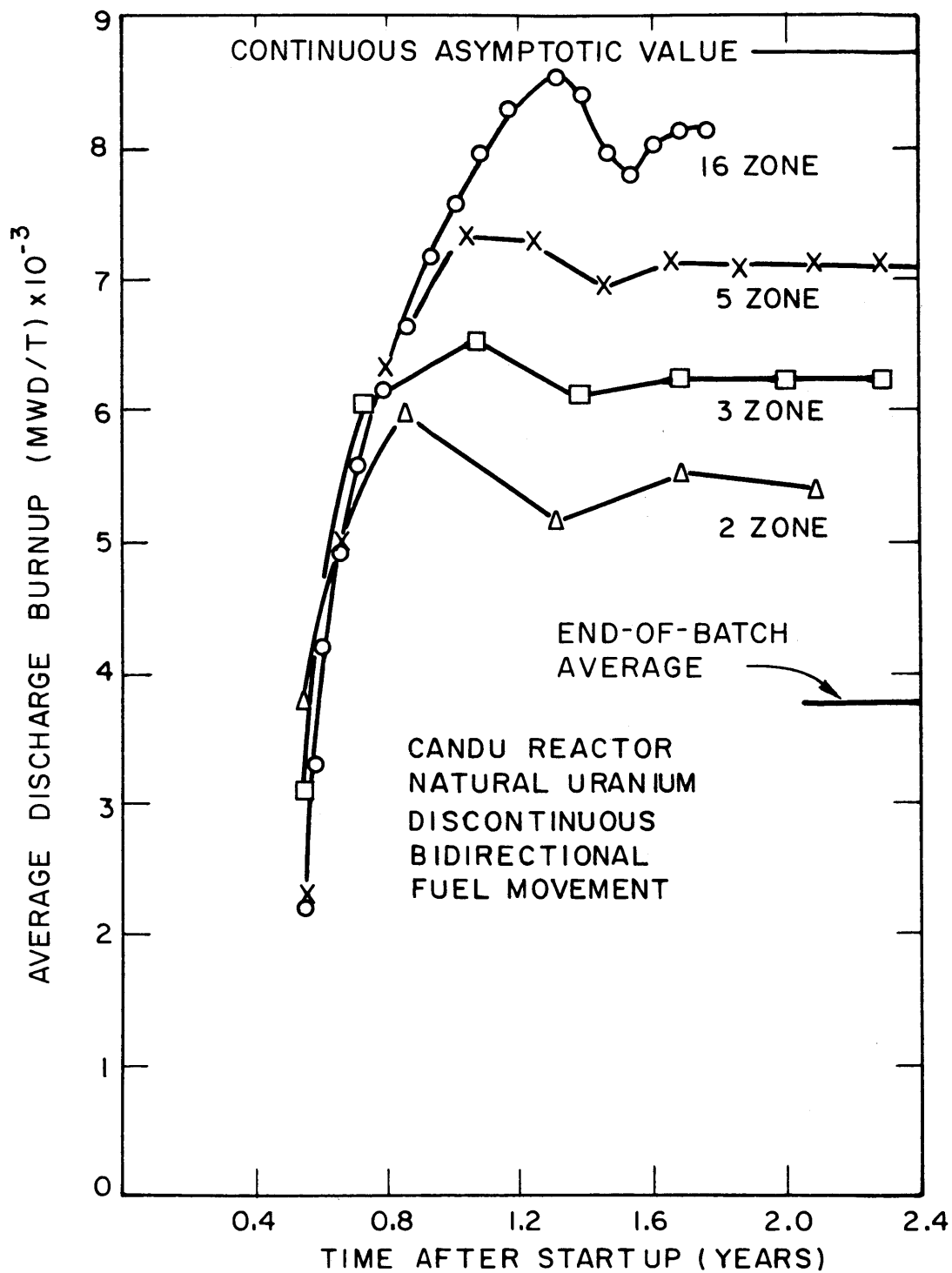
FIG. 6.25 AVERAGE BURNUP OF DISCHARGED FUEL AT
VARIOUS TIMES AFTER STARTUP

second effect would favor element 16, this being the last element of the original batch loading to be discharged. The net result of combining the two effects is that the peak occurs at the 2nd discharge in the 2 zone situation, the 3rd discharge in the 3 zone, the 4th discharge in the 5 zone, and the 13th in the 16 zone situation.

The behavior of the peak-to-average power density ratio during the startup period is shown in Figure 6.26 for 2 and 16 zones. The extreme peaking in the 2 zone situation immediately following the first fuel change is due to the fact that spent fuel, formerly at the center, has been pushed through to the edge, and the relatively fresh fuel, formerly at the edge is now at the center. Hence, the flux peaks at the center. This cycle repeats itself each time fuel is moved. The same behavior occurs for 3 and 5 zones, although with somewhat decreasing severity. In the 16 zone case, there is little difference in power distribution between changes. The peak which gradually builds up in the 16 zone situation occurs around the 10th step when the highly irradiated initial fuel charge has arrived at the edge of the reactor, causing the flux to peak toward the center. The extreme peaking which occurs with the 2, 3, and 5 zone reactors makes them unacceptable for use with uniform control poison removal. Alternative control poison techniques could undoubtedly improve performance, but these wide swings of reactivity are indicative of potential difficulty.

The net fuel cycle costs shown in Figure 6.27 show the expected behavior of approximate inverse proportionality to burnup. Because no fuel was recharged in the 16 zone case, the initial fuel costs are much higher than is necessary, since the first three or four zones could probably have been recharged without creating difficulty.
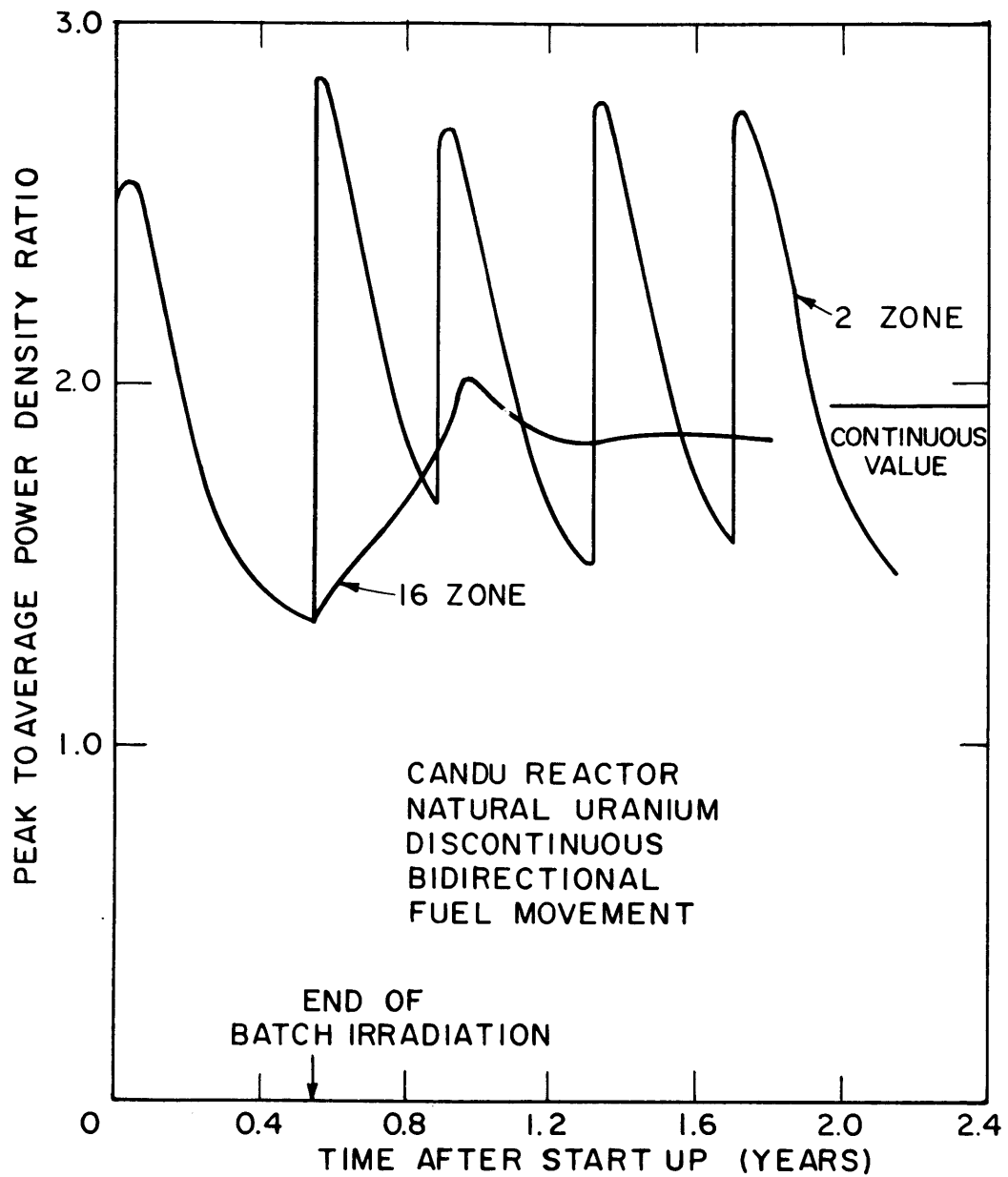
FIG. 6.26 THE VARIATION OF PEAK TO AVERAGE POWER
DENSITY RATIO
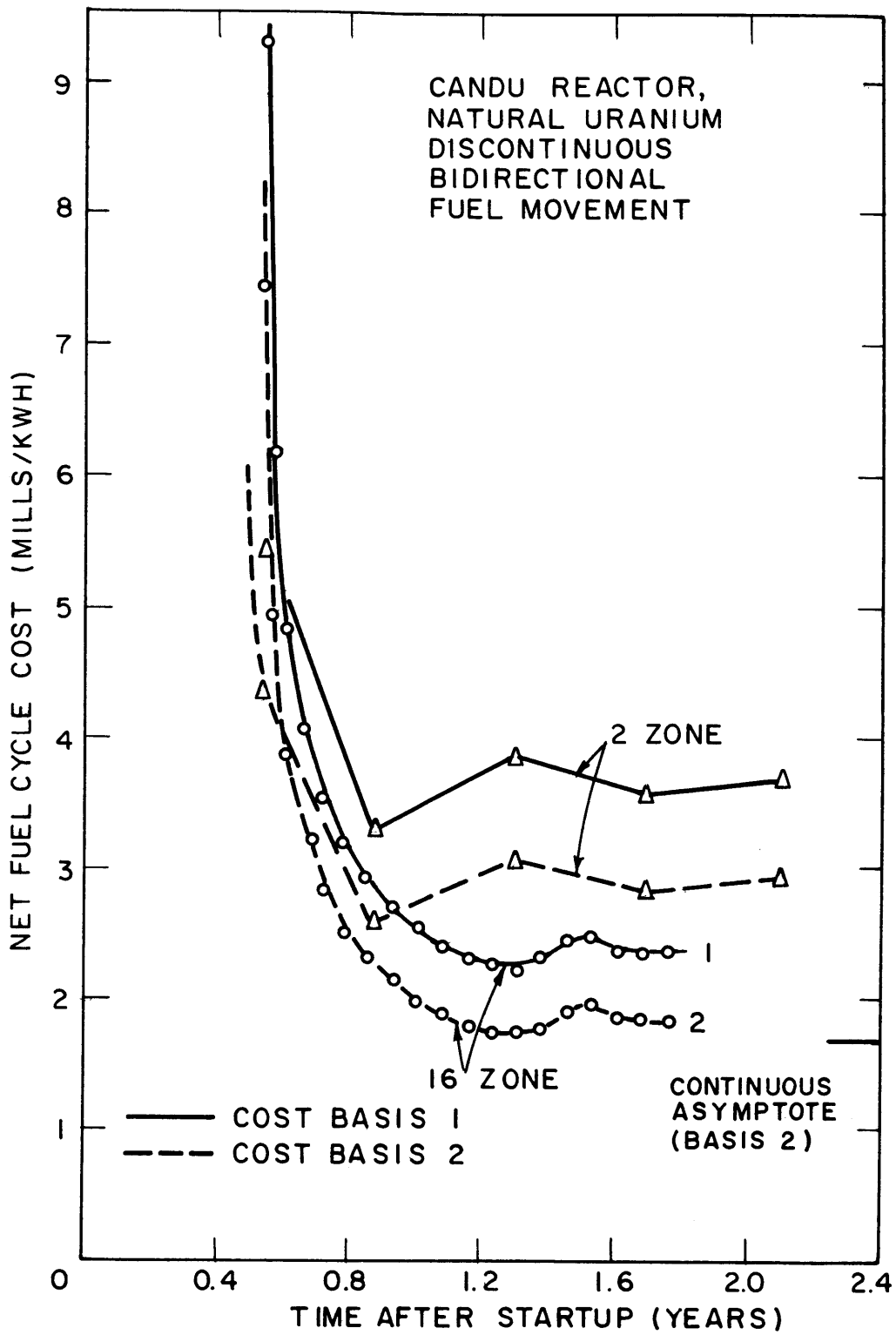
FIG. 6.27 NET FUEL CYCLE COST FOR FUEL DISCHARGED
AT VARIOUS TIMES

271

It is apparent that the 16 zone case is well behaved with regard to both power distribution and burnup, and approaches quite closely the low fuel cost attained in the continuous constant axial velocity bidirectional fuel movement. This result would seem to indicate that the startup in continuous bidirectional would be reasonably straightforward.

7. Batch Irradiation

7.1 Introduction

Batch irradiation is one of the most important of the fuel irradiation techniques, inasmuch as it is the procedure used during startup of the other techniques. The basic objective is, as always, to determine the combination of fuel enrichment and control poison technique that will result in lowest energy cost.

In this work, studies have been made of the effect of enrichment and enrichment distribution, of control poison distribution and removal including the use of burnable poison, and finally, the effect on fuel costs of core volume changes. The particular order of presentation will be as follows. First, the results of an enrichment survey using uniform initial enrichment and uniform initial control poison concentration will be presented, along with a study of three poison removal techniques, uniform removal, radial zone, and axial bank control poison removal. Also, the potential usefulness of burnable poison will be investigated. Following this, various combinations of enrichment and control poison distribution will be studied systematically in an effort to evaluate the preferred combinations. Finally, the effect of volume changes on fuel costs will be examined and the

results used to specify the optimum combination of core volume and poison removal for each enrichment, for a reactor system of 200 Mwe power output.

7.2 Batch Enrichment Survey

Table 6.13 gives the results of the straight enrichment survey for Batch Irradiation. Because of excessive flux and power peaking, it was possible to use the radial zone and axial bank poison removal techniques only with natural enrichment. This indicates that control poison must be present near all fuel with any appreciable amount of excess reactivity. Hence, practical control rod removal programs will be better represented by uniform poison removal than by the other techniques available in the MOVE Code, and this technique will show the desired trends and be capable of showing the most desirable control poison distribution. These capabilities are sufficient for a general parameter survey such as is being presented here. More detailed control poison removal could be written into the MOVE Code for studies of certain specific reactor designs but this would add another variable and thereby compound the computer time requirement for a parameter study.

Details of the important data presented in Table 6.13 are given in Figures 6.28-30. In Figure 6.28, the peak-to-average power density ratio is plotted for batch-irradiated natural uranium with initially uniform control poison, for the three poison removal techniques. The initial value with no Xe or Sm group poisoning is the same in each case (2.52). The behavior of the uniform poison removal curve is typical of an initially uniform core in which the reactivity of the fuel in the center where the flux is highest, first gains

Table 6.13   Enrichment Survey for Batch Irradiation: Uniform Initial Control Poison

Enrich-ment a/o	Poison Removal Technique	Ratio of Peak to Average Power Density			Average Burnup MWD/T	Time in Reactor, Years	Fuel Cycle Cost (mills/Kwh)		Run No.
		Initial*	Maximum	Final			Basis 1	Basis 2	
Nat	Uniform	2.44	2.55	1.32	3,760	0.558	5.49	4.40	D1.1-1
	Radial Zone	1.83	2.72	2.72	4,110	0.602	4.98	3.98	D1.1-2
	Axial Bank	4.31	4.31	2.93	4,580	0.668	4.45	3.55	D1.1-3
1.30	Uniform	2.39	2.39	1.12	11,040	1.648	2.69	2.29	D1.5
1.75	Uniform	2.35	2.35	1.07	15,800	2.372	2.40	2.11	D1.7
2.50	Uniform	2.29	2.29	1.06	23,190	3.500	2.30	2.08	D1.9

*with equilibrium Xe and Sm

274
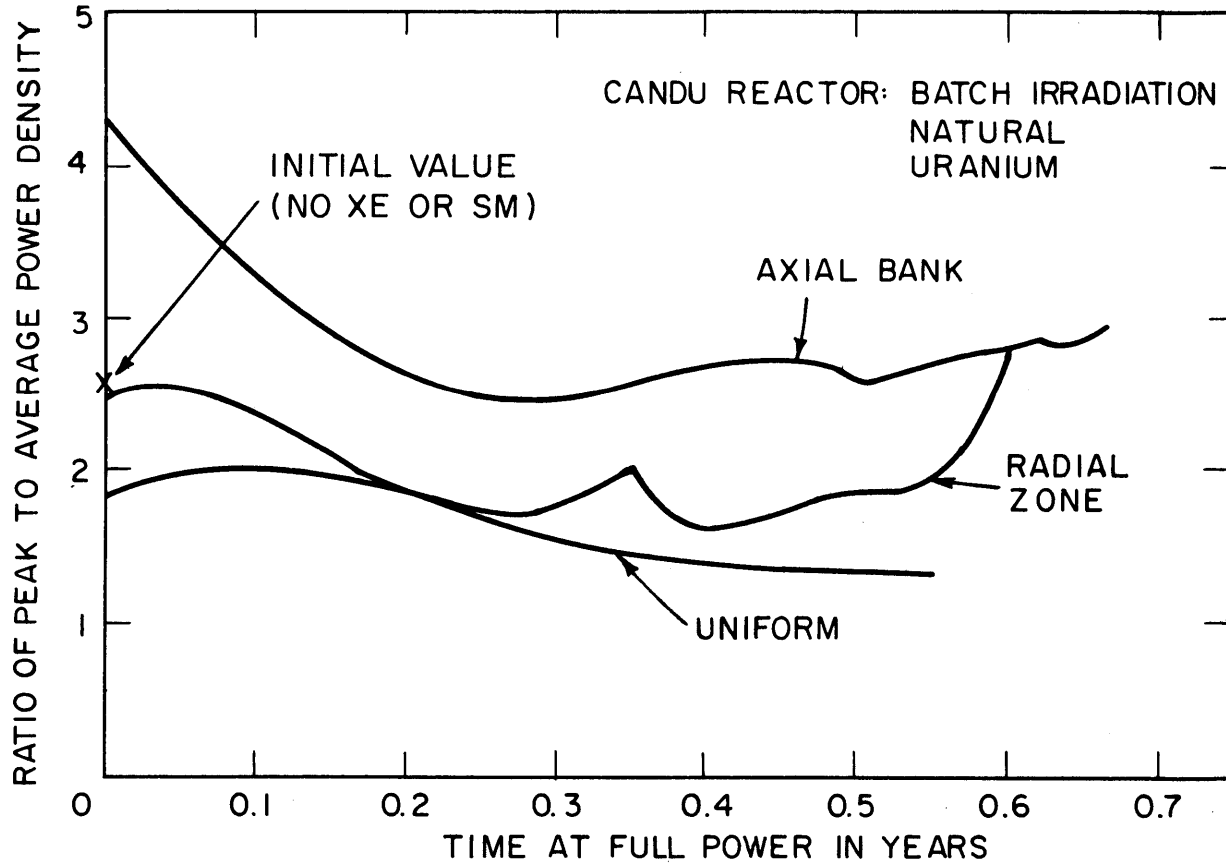
FIG. 6.28 THE BEHAVIOR OF THE PEAK-TO-AVERAGE POWER DENSITY
RATIO FOR VARIOUS CONTROL POISON REMOVAL TECHNIQUES.

reactivity due to Pu^{239} buildup and then loses it due to U^{235} depletion and fission product poisoning. The gain in reactivity in the center causes the flux, and power to peak there, followed by a decrease in central flux, due to lowered reactivity, with a consequent flattening of the power distribution. In both the radial zone, and axial bank poison removal schemes, the flux and power tend to peak in the parts from which the control poison has been removed. Hence, in radial zone control, the flux peaks at the outer edge initially, causing the peak-to-average ratio to drop substantially from the hot, clean value. At the end of life, however, when the remaining poison is removed from the center, the peaking occurs there, causing a sharp rise in the peak-to-average ratio near the end-of-life. The use of axial bank poison removal is virtually ruled out by the extreme peaking which occurs initially at the unpoisoned end of the core.

Figure 6.29 illustrates the peak-to-average behavior of the four enrichments which were studied using uniform control poison removal. The behavior is similar to that of natural as described above, except that for the higher enrichments there is no initial peak in the peak-to-average ratio, due to the fact that fuel reactivity at the higher enrichments always decreases with irradiation, since U^{235} depletion dominates Pu^{239} buildup.

The net fuel cycle cost as a function of enrichment is shown in Figure 6.30. It can be seen that a broad minimum exists from about 1.5 a/o to upwards of 2.5 a/o enrichment. Because the reactivity that is held down by control poison is very large at the higher enrichments, further studies will not include the 2.5 a/o enrichment. The enrichments which will be given most attention will therefore be 1.3, 1.5, and 1.75 a/o.
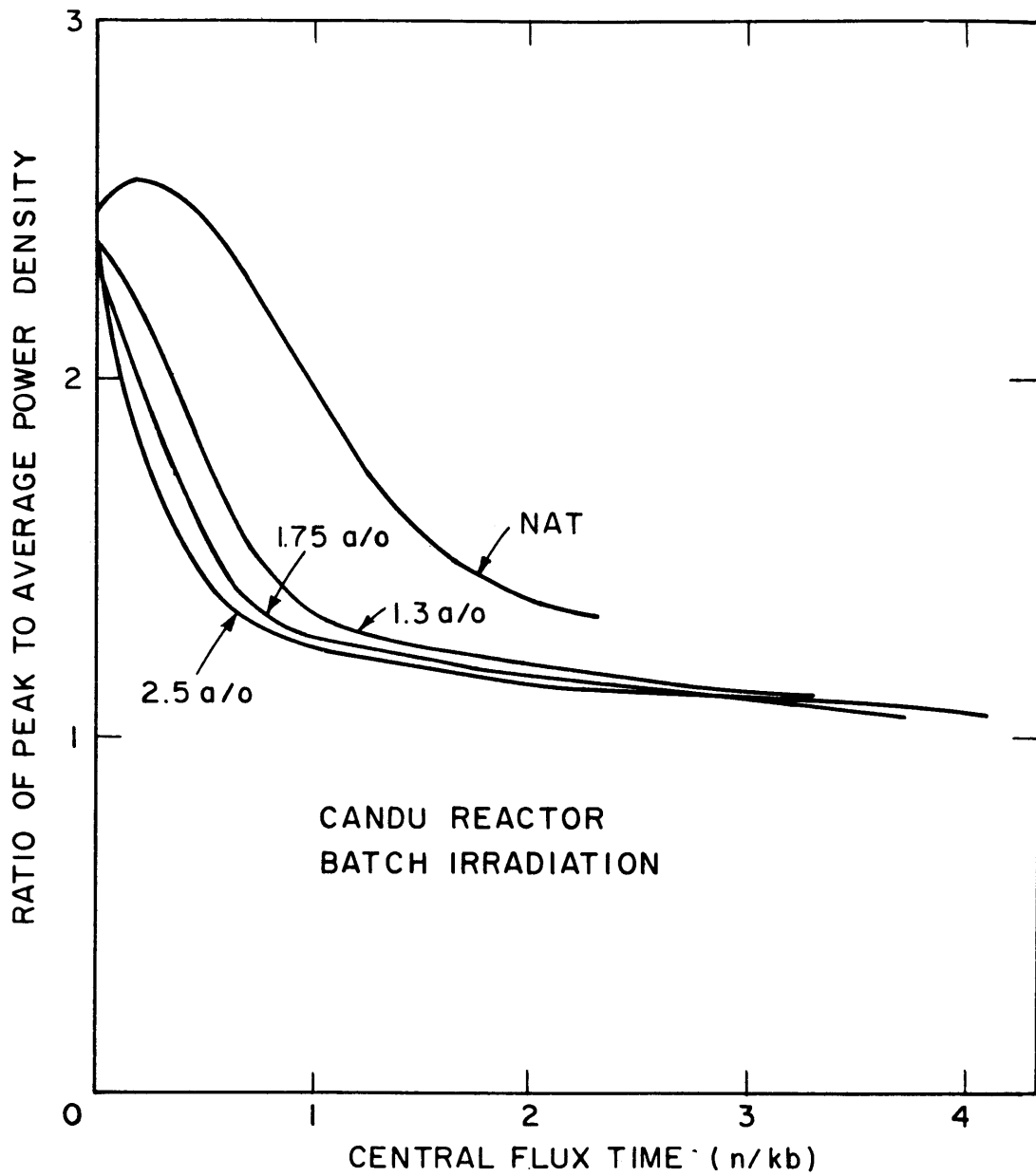
FIG. 6.29 THE BEHAVIOR OF THE PEAK-TO-AVERAGE POWER
DENSITY RATIO FOR VARIOUS ENRICHMENTS WITH
UNIFORM POISON REMOVAL
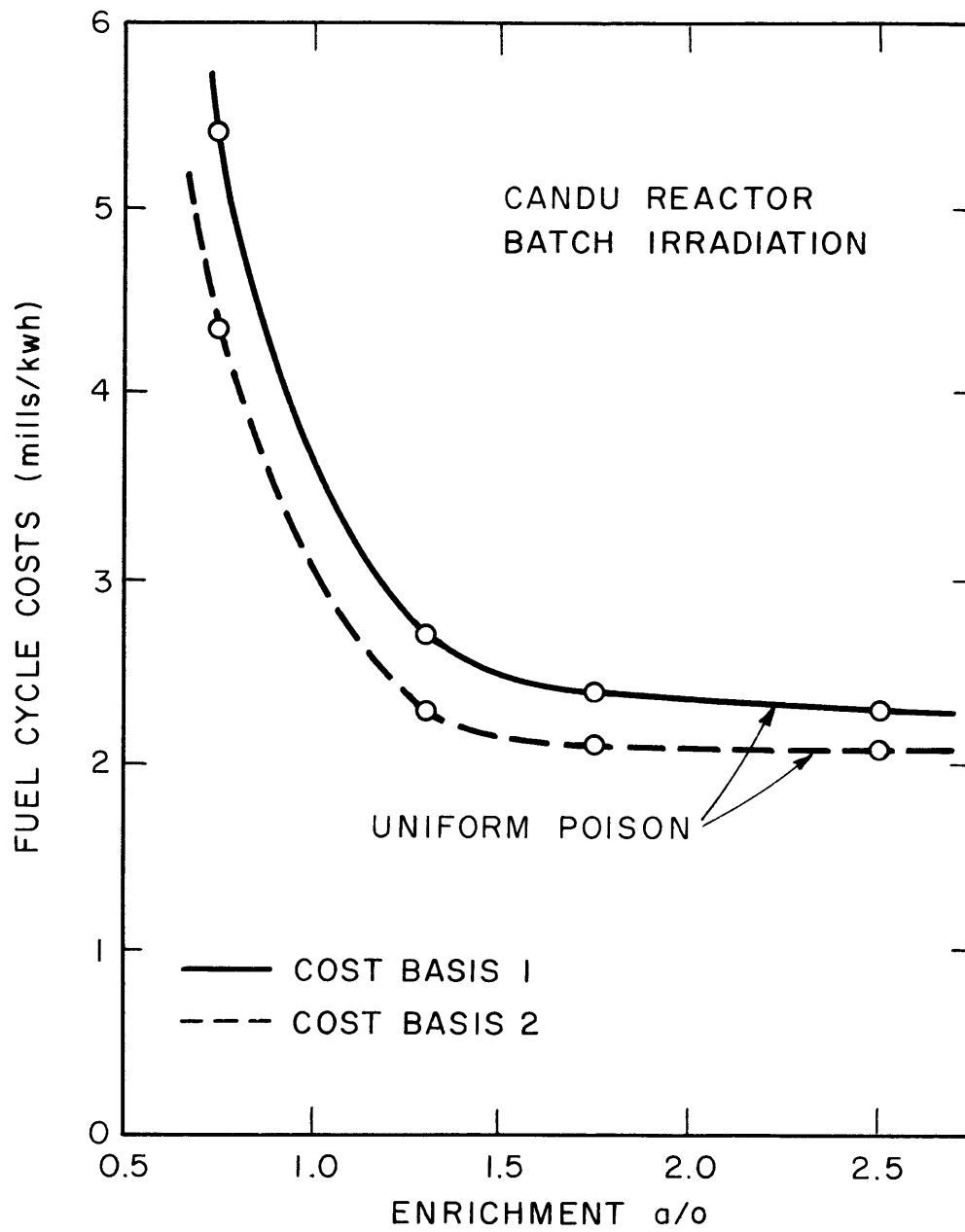
FIG. 6.30   NET FUEL CYCLE COST AS A
FUNCTION OF ENRICHMENT

7.3 The Use of Burnable Poison

The potential use of burnable poison can be evaluated from the data given in Table 6.14. The loss of burnup which is a necessary consequence of the use of burnable poison can be justified only under certain conditions. The merit in its use is the reduced control requirement. Hence, if the loss of burnup can be more than compensated by decreased control costs, then burnable poison would be justified. Alternatively, if the enrichment of reactor fuel is limited by control requirements to a value substantially below the value for minimum fuel cost, there might be something to be gained by using a more enriched fuel with burnable poison to reduce the direct control requirement.

The values of the maximum control poison requirement shown in Table 6.14 indicate a factor of 3 reduction at a penalty of about 20% in burnup. This penalty amounts to 0.5 mills/kwh at 1.3 a/o enrichment and 0.4 mills/kwh at 1.75 a/o. At 7000 hours per year and 200 Mwe, 0.4 mills /kwh due to burnup loss is $560,000 per year. Even at an interest rate of 14% per annum for fixed charges on the control system, the initial savings on reduced control requirement would have to be $4,000,000. Hence, it is improbable that burnable poison could be justified on the grounds of reduced capital expenditure.

The use of burnable poison in control-limited situations is more promising, however. Because it is difficult to interpolate between the numbers given in Table 6.14, a graph of these results is shown in Figure 6.31. The ordinate of this graph is the maximum control requirement of the various situations plotted. The upper curve represents the fuel cycle costs that are obtained at various enrichments. It is apparent from this curve that if a given reactor

Table 6.14   The Use of Burnable Poison in Batch Irradiation with Uniform Poison Removal. $(\sigma_o)_{BP}$ = 945 Barns.

Enrichment a/o	Initial k_∞	Ratio of Peak to Average Power Density			Average Burnup	Fuel Cycle Cost mills/kwh		Maximum Control Poison	Run No.
		Initial*	Maximum	Final	(MWD/T)	Basis 1	Basis 2	cm^{-1} × 10^3	
1.3	1.330 (No B.P.)	2.39	2.39	1.12	11,040	2.69	2.29	3.574	D1.5
	1.2	2.38	2.38	1.17	10,090	2.94	2.51	2.402	D2.5.2
	1.1	2.38	2.63	1.25	9,000	3.28	2.81	1.330	D2.5.1
1.75	1.429 (No B.P.)	2.35	2.35	1.07	15,800	2.40	2.11	5.717	D1.7
	1.2	2.34	2.41	1.16	14,210	2.64	2.32	3.129	D2.7.2
	1.1	2.34	2.70	1.27	13,020	2.84	2.50	1.715	D2.7.1
0.85	1.164 (No B.P.)	2.43	2.43	1.23	5,613	4.11	3.25	1.367	D1.2
1.0	1.230 (No B.P.)	2.41	2.41	1.18	7,521	3.33	2.71	2.111	D1.3
1.15	1.284 (No B.P.)	2.40	2.40	1.15	9,327	2.92	2.44	2.847	D1.4

*with equilibrium Xe and Sm.
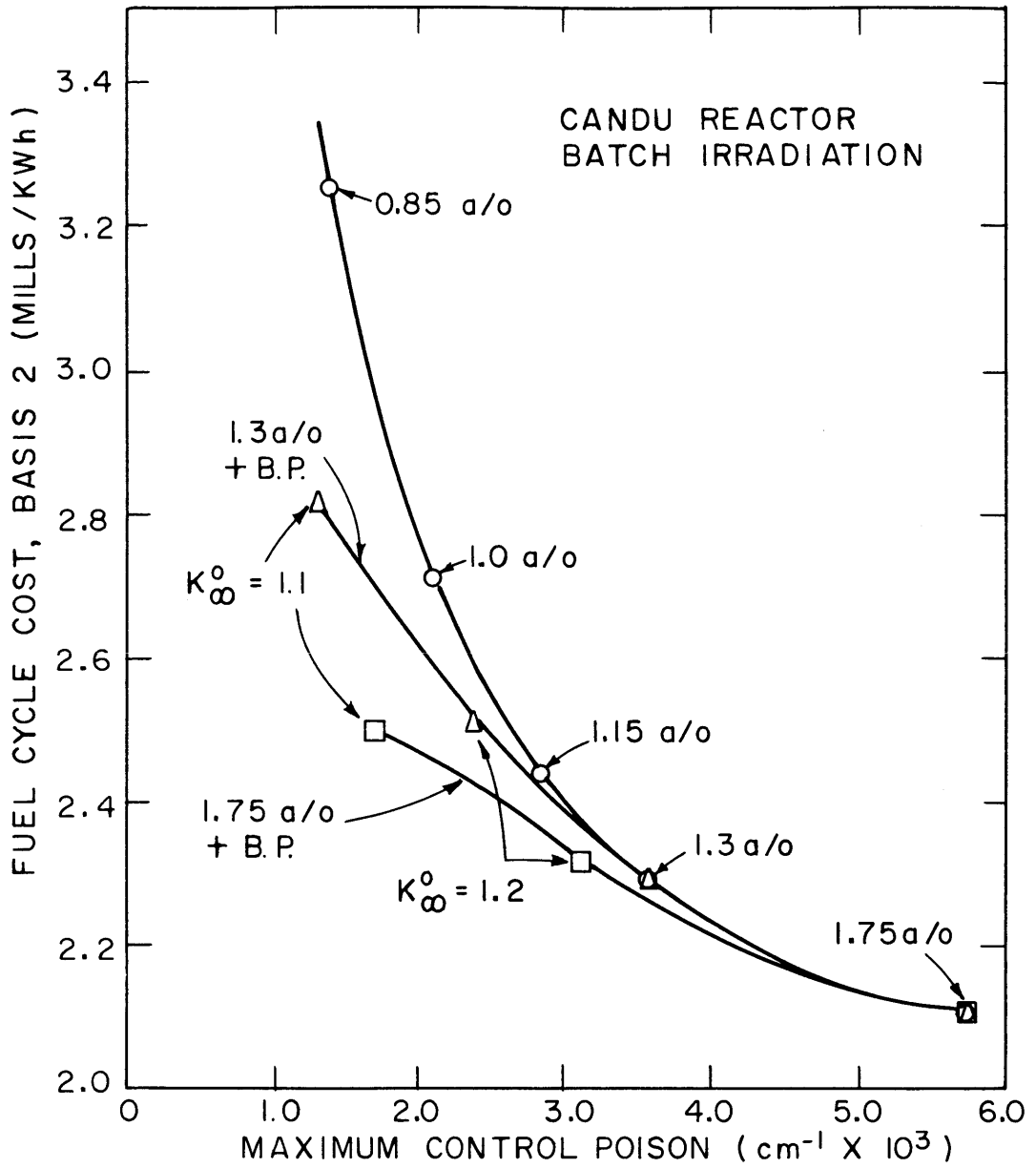
FIG. 6.31 GRAPH ILLUSTRATING THE USE OF BURNABLE POISON IN CONTROL LIMITED REACTORS

281

core is control-limited to an enrichment below that at which it could achieve minimum fuel cost, lower fuel costs can be achieved by using a higher enrichment plus burnable poison instead of using the enrichment which results in the limiting control requirement. The results in Figure 6.31 are plotted for Cost Basis 2. The advantages of burnable poison are even more pronounced under Cost Basis 1.

7.4 Variation of Radial Zone Poison and Enrichment

In order to flatten the power distribution in the initial stages of batch irradiation with uniform poison removal, it is advisable to use higher concentrations of poison in the central regions of a reactor core. In this study, the reference design reactor core has been divided into two equal-volume radial zones and the relative magnitude of control poison in each zone varied in order to achieve power flattening.

The results given in Table 6.15 show that there is a definite economic incentive to flatten the power inasmuch as burnup increases somewhat with increased flattening. The reduction in core volume which can be achieved in peak-power-density-limited reactors operating at a specified output is also, of course, an advantage, although there would be some burnup loss associated with reducing volume which would work against the burnup increase achieved by power flattening.

The increased burnup with increasing flatness is due to an effect which is not always evident in fuel management studies inasmuch as it is usually less important than other effects. For example, it was shown that in the continuous bidirectional fuel movement, increasing flatness led to increased neutron leakage and hence, lowered burnup. In batch irradiation, however, the excess neutrons are not put to profitable use,

Table 6.15   The Use of Radial Zone Poison Variation with Uniform Enrichment in Batch Irradiation.

Enrichment	Ratio of Outer to Inner Zone Poison	Ratio of Peak to Average Power Density			Average Burnup MWD/T	Fuel Cycle Cost mills/kwh		Maximum Inner Zone Control Poison (cm^{-1}×10^3)	Run No.
		Initial*	Maximum	Final		Basis 1	Basis 2		
Nat	1.0	2.44	2.55	1.32	3,760	5.49	4.40	0.719	D1.1
	0.85	2.32	2.38	1.35	3,750	5.44	4.35	0.758	D3.1-1
	0.70	2.19	2.21	1.40	3,770	5.42	4.33	0.802	D3.1-2
	0.60	2.11	2.11	1.44	3,780	5.40	4.32	0.832	D3.1-3
	0.50	2.01	2.01	1.49	3,800	5.37	4.29	0.866	D3.1-4
1.3 a/o	1.0	2.39	2.39	1.12	11,040	2.69	2.29	3.570	D1.5
	0.80	1.65	1.65	1.23	11,030	2.69	2.29	3.851	D3.5-2
	0.70	1.86	1.86	1.30	11,080	2.68	2.28	3.991	D3.5-3
1.75 a/o	1.0	2.35	2.35	1.07	15,800	2.40	2.11	5.717	D1.7
	0.90	1.79	1.79	1.12	15,810	2.40	2.11	5.923	D3.7-1
	0.87	1.67	1.67	1.14	15,820	2.40	2.11	5.988	D3.7-2

*with equilibrium Xe and Sm.

283

as they are in the continuous fuel movements. It makes little difference to the final burnup whether a neutron is absorbed in control poison or leaks out of the reactor. The end-of-batch irradiation is therefore determined mostly by the reactivity distribution which prevails at that time with the practical preferred situation being that in which reactivity distribution is as nearly uniform as possible. There is, therefore, an advantage in batch irradiation, to operating with as flat a flux as possible, since the resulting reactivity distribution at the end of life would also tend to be uniform. The more peaking that occurs in the central regions of the reactor, the more non-uniform will be the reactivity distribution towards the end-of-life, thereby reducing lifetime.

In conclusion, then, flux flattening by means of radial variation of control poison magnitude is beneficial for two reasons. It enables use of smaller core volumes, and it improves burnup by improving the end-of-life reactivity distribution.

An additional survey was performed, using the two equal-volume zones with lower enrichment in the inner zone and with different relative magnitudes of control poison in each zone. The results as presented in Table 6.16 show that nothing can be gained, either in additional flux flattening or lowered fuel costs, by using a lowered enrichment in the inner zone. The reason for this is similar to that given for the same result using mixed enrichment in the steady-state continuous bidirectional fuel movement. The use of zones of different enrichment with one of the enrichments yielding basically higher fuel costs cannot improve on the performance of the same reactor operating with the uniform lower fuel cost enrichment.

7.5 The Optimized Reactor Designs for Batch Irradiation

The results of the batch irradiation study up to this point can now be used to specify the combination of parameters which will result in the minimum energy cost reactor design at each enrichment, for reactors operating at 200 Mwe output, and not limited by a maximum control requirement.

284

Table 6.16 The Effect of Radial Variation of Enrichment and Initial Control Poison Distribution.

Enrichment a/o		Relative Σ_w		Peak-to-Average Power Density Ratio			Average Burnup MWD/T		Fuel Cycle Cost mills/Kwh		Run No.
Central	Outer	Central	Outer	Initial*	Maximum	Final	Central	Outer	Basis 1	Basis 2	
1.75		1.0	1.0	2.35	2.35	1.07	16,820	14,780	2.40	2.11	D1.7
1.75		1.0	0.9	1.79	1.79	1.12	16,680	14,940	2.40	2.11	D3.7-1
1.75		1.0	0.87	1.62	1.62	1.14	16,640	15,000	2.40	2.11	D3.7-2
1.50	1.75	0.9	1.0	1.62	1.62	1.11	14,350	14,600	2.45	2.14	D4.7-1
1.50		0.8	1.0	2.21	2.21	1.15	14,500	14,420	2.45	2.14	D4.7-2
1.30		0.75	1.0	1.78	1.78	1.18	12,470	14,390	2.50	2.17	D4.7-3
1.30		0.65	1.0	1.95	1.95	1.22	12,680	14,220	2.50	2.16	D4.7-4

*with equilibrium Xe and Sm.

Table 6.16 (cont'd)

Enrichment a/o		Relative Σ_w		Peak-to-Average Power Density Ratio			Average Burnup MWD/T		Fuel CycleCost mills/Kwh		Run No.
Central	Outer	Central	Outer	Initial*	Maximum	Final	Central	Outer	Basis 1	Basis 2	
1.5		1.0	1.0	2.37	2.37	1.09	14,160	12,170	2.53	2.18	D1.6
1.5		1.0	0.9	1.88	1.88	1.14	14,050	12,330	2.52	2.18	D3.6-1
1.5		1.0	0.85	1.62	1.62	1.17	13,990	12,420	2.51	2.17	D3.6-2
1.3	1.5	0.9	1.0	1.68	1.68	1.13	12,180	12,060	2.59	2.23	D4.6-1
.1.3		0.8	1.0	2.20	2.20	1.17	12,330	11,900	2.59	2.22	D4.6-2
1.0		0.7	1.0	2.08	2.08	1.23	9,040	11,740	2.79	2.35	D4.6-3
1.0		0.6	1.0	1.90	1.90	1.27	9,240	11,560	2.78	2.34	D4.6-4
1.3		1.0	1.0	2.39	2.39	1.12	11,040	11,040	2.69	2.29	D1.5
1.3	1.3	1.0	0.85	1.74	1.74	1.19	11,010	11,010	2.69	2.29	D3.5-1
1.3		1.0	0.8	1.65	1.65	1.23	11,740	10,330	2.69	2.29	D3.5-2

*with equilibrium Xe and Sm.

The effect of core volume on power distribution, burnup and fuel cost is shown in Table 6.17 for the three most important enrichments, 1.3, 1.5, and 1.75 a/o. Results are compared in this table for the reference design volume, V_o, and 0.9 V_o. Two compensating effects result in practically no change in fuel cost. The slight loss of burnup is almost exactly balanced by the decreased interest costs on UF_6 and working capital due to the increased specific power of the fuel. The assumption of constant power distribution with volume change is correct to within 4%, with the smaller core having the somewhat greater peak power density. It is therefore justifiable to use the results obtained at core volume V_o, and reduce core volume to the point at which the maximum permissible power density is reached for the specified output of 200 Mwe. The resulting reactor specifications are given in Table 6.18 for the enrichments natural, 1.3, 1.5, and 1.75 a/o. It is evident that the minimum energy cost occurs at 1.75 a/o or possibly somewhat higher, as can be seen in Figure 6.32. The factors which contribute to this minimum are burnup, which results in lowest fuel cost, and reduced core volume and increased fueling load factor which enable both the fixed capital charges and operating costs to be the lowest at this enrichment.

In summary, the above study of batch irradiation has shown that very adequate power distribution flattening can be achieved by the use of two radial zones containing different amounts of control poison, the relative magnitudes being dependent upon the particular enrichment used. The use of mixed enrichments cannot improve on the performance of uniform enrichment, and is detrimental to the fuel cost if the comparison is based on a uniform distribution of the lower fuel cost enrichment.

The use of burnable poison could not be justified on the grounds that it saves more on the control rod requirement than it costs in fuel burnup, since burnup losses are of the order of 10 to 20% of the unpoisoned burnup. On the other hand, it was shown that the use of burnable poison in control-limited situations can improve fuel cycle cost while staying within the specified control limit. This particular

Table 6.17 The Effect of Core Volume Change on the Fuel Cycle Cost for Batch Irradiation. V_o = Core Volume of Reference Design.

Enrichment a/o	Core Volume	Ratio of Outer to Inner Zone Σ_w	Peak-to-Average Density Ratio		Average Burnup MWD/T	Fuel Cycle Cost mills/kwh		Run No.
			Initial*	Final		Basis 1	Basis 2	
1.3	V_o	0.8	1.65	1.23	11,030	2.690	2.289	D3.5-2
	0.9 V_o	0.8	1.62	1.23	10,960	2.696	2.297	D5.5
1.5	V_o	0.85	1.62	1.17	13,200	2.514	2.174	D3.6-2
	0.9 V_o	0.85	1.68	1.17	13,130	2.515	2.177	D5.6
1.75	V_o	0.87	1.62	1.14	15,820	2.398	2.106	D3.7-2
	0.9 V_o	0.87	1.67	1.14	15,740	2.392	2.103	D5.7

*with equilibrium Xe and Sm.

Table 6.18 Characteristics of the Optimum Reactors for Batch Irradiation at Various Enrichments.

	Enrichment (a/o)			
A: Design Data	Nat	1.3	1.5	1.75
Thermal Power	P_o	P_o	P_o	P_o
Core Volume	$1.02\ V_o$	$0.82\ V_o$	$0.84\ V_o$	$0.84\ V_o$
Maximum Power Density (Kw/l)	17.0	17.0	17.0	17.0
Ratio of Outer to Inner Zone Σ_w	0.5	0.8	0.85	0.87
B. MOVE Code Results				
Maximum Power Density (Kw/l)	17.0	17.0	17.0	17.0
Ratio of Peak to Average Power Density				
a) Initial[*]	1.98	1.62	1.68	1.68
b) Final	1.49	1.23	1.17	1.14
Average Burnup (MWD/T)	3,800	11,030	13,200	15,820
Maximum Burnup (MWD/T)	6,310	13,680	15,950	18,640
Full Power Time in Reactor (years)	0.558	.1.350	1.660	1.994
Kwhe/kg of Fuel Charged	25,490	73,989	88,546	106,121
Fuelling Load Factor	0.972	0.990	0.992	0.993

[*]with equilibrium Xe and Sm.

Table 6.18 (cont'd)

C: Material Quantities	Enrichment (a/o)			
	Nat	1.3	1.5	1.75
Feed Rate (kgU/Full Power Year)	6.846×10^4	2.830×10^4	2.302×10^4	1.916×10^4
Discharge Rates				
1. kgU/Full Power Year	6.801×10^4	2.782×10^4	2.257×10^4	1.872×10^4
2. kgPu/Full Power Year	167	116	101	89
Isotopic Content of Discharged Fuel				
w/o U^{235} in U	.390	.359	.361	.387
U^{236} in U	.050	.144	.173	.209
Pu^{239} in Pu	78.2	63.4	61.3	59.5
Pu^{240} in Pu	17.1	24.5	25.2	25.7
Pu^{241} in Pu	4.0	8.6	9.2	9.8
Pu^{242} in Pu	.7	3.5	4.3	5.0
D: Fuel Cycle and Total Energy Costs Cost Basis 2 (Mills/Kwh)				
Net Material	1.142	0.604	0.696	0.794
Fabrication	2.410	0.970	0.838	0.699
Reprocessing	0.605	0.566	0.478	0.429
UF_6 Lease	0.0	0.077	0.096	0.121
Working Capital	0.137	0.072	0.066	0.063
NET FUEL CYCLE COST	4.295	2.289	2.174	2.106
Plant Capital Costs	4.650	4.405	4.414	4.408
Operating Costs	1.049	1.029	1.028	1.026
TOTAL ENERGY COSTS	9.994	7.723	7.616	7.540
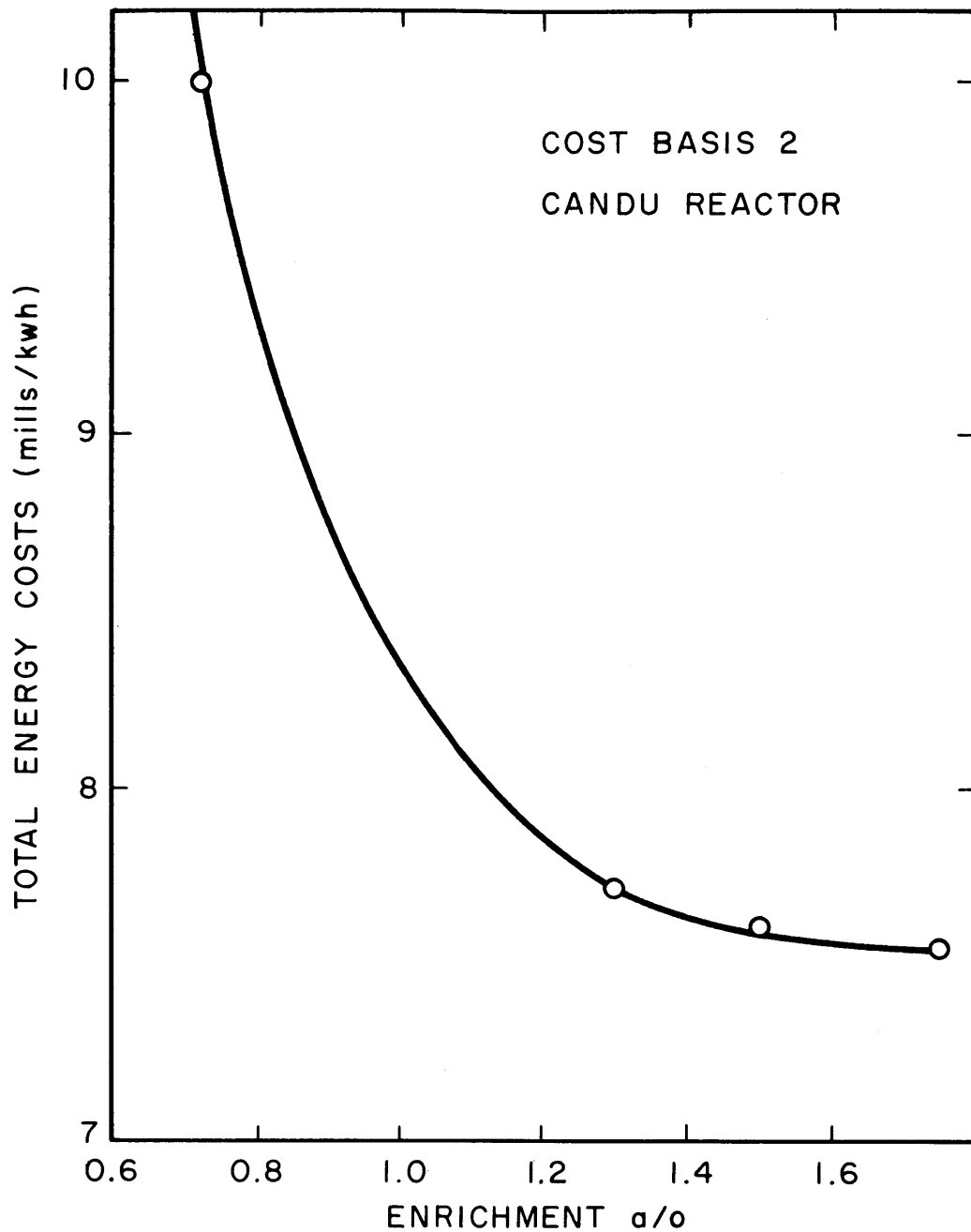
FIG. 6.32   TOTAL ENERGY COST AS A FUNCTION
OF ENRICHMENT FOR THE CANDU
REACTOR OPTIMIZED FOR BATCH
IRRADIATION AT 200 MWE OUTPUT
AND AT FIXED PEAK POWER DENSITY

291

advantage of burnable poison would be lost if control limitations could be removed by the use of chemical control poison such as boric acid dissolved in the moderator.

The enrichment at which minimum energy cost can be achieved in batch irradiation is at, or slightly above 1.75 a/o, although there is some doubt as to whether a reactor would be run with the large initial reactivity that such an enrichment would imply in a D_2O reactor.

8. DISCONTINUOUS OUTIN FUEL IRRADIATION

8.1 Introduction

In the discontinuous outin fueling, the reactor is divided into a number of radial zones of equal volume. The fuel is irradiated batch-wise until the reactor ceases to be critical. It is then shut down and the fuel in the central zone is discharged. The fuel in the remaining zones is moved one zone closer to the center, and new fuel is charged to the outer zone. There are two basic problems in the operation of such a system. One is to determine the enrichment and control poison removal technique that will result in minimum energy cost during steady-state operation. The other is the problem of how to arrive at the steady state.

The first of these problems is more straightforward than the second. It involves finding the radial zone poison distribution and removal technique which yields the best degree of flatness compatible with low fuel cost at any particular enrichment. Particular system requirements may complicate the solution of the second problem, that of operating technique during the startup and approach to the steady state.

As was pointed out in the introduction to Section D of this chapter, there is an economic incentive in being capable of operation at full output during this transient period, and this will complicate the startup problem. In addition, it is generally necessary on startup to control an amount of reactivity that is substantially greater than during steady state in which the fuel in the central zones has been considerably

depleted. This implies an additional expenditure for the part of the control system that will be required only during the initial startup. The alternative is to use only the steady-state control system on startup and in a particular inner zone use an enrichment which is equivalent in reactivity to the partially spent fuel that would be charged to that zone in steady-state operation. This use of lower enrichments in the inner zones, however, will increase fuel costs during startup. Hence, a comparison must be made of the cost of extra control and the increased fuel costs. In the study that follows, both the extra control requirement and the increased burnup costs will be evaluated.

There are several options available in the discontinuous outin fuel movement. The question of the use of axial inversion will be evaluated specifically. The fuel will always be transferred (IMOVE option), and the radial flux-time gradient will also always be transferred. This will produce a flatter power distribution than if the average flux-time is transferred, since the more irradiated fuel in any zone will always be kept closest to the center of the reactor. Control poison management will be in the form of uniform removal of an initial poison distribution consisting of equal magnitudes within radial zones, but with relative magnitudes differing from zone to zone. It was pointed out in the Batch Irradiation study that this represents what a practical control rod removal program should accomplish.

In the cost analysis of the discontinuous outin fuel movement, it has been assumed that it takes seven days to refuel the reactor. This number is used to evaluate the fueling load factor which is part of the over-all load factor, and therefore affects primarily the capital and operating costs. Increases in this assumed seven-day downtime will be less detrimental to the techniques which require fewer fuel changes.

The results of the study of the discontinuous outin fuel movement are presented in the following order. The question of whether to specify axial inversion of fuel is examined, along with the influence on operating characteristics of the number of radial zones. An enrichment and poison distribution survey is then used in the evaluation of the

optimum steady-state reactors at various enrichments. The problem
of how to achieve the steady-state is then considered.

8.2 The Effect of Axial Inversion and the Number of Radial Zones

In order to reduce the number of possible variables, it is
desirable to conduct an initial survey of the effect of axial inversion on
power distribution and energy costs. In addition, it is convenient to
fix the number of radial zones at a value that might be representative
of a practical operating reactor system.

For the purposes of this study, the CANDU reactor was divided
into two or three radial zones and operated with a fuel of natural enrich-
ment. The control poison technique specified was the uniform removal
of an initially uniform poison distribution. The important results of
this study are given in Figures 6.33 to 6.35. In Figure 6.33, the
behavior of the peak-to-average power density ratio and the average
burnup of discharge fuel is shown as a function of full power time for
two radial zones. Figure 6.34 shows the behavior for the same study
using three radial zones. The results of this study clearly indicate
the advantages and disadvantages of axial inversion. There is a gain
of 8 to 10% in burnup. This gain, however, has been achieved from
reduced leakage which is a consequence of peaking in the central part
of the reactor. Hence, it would require a larger peak-power-density-
limited reactor core to produce the same output as a reactor operating
without axial inversion.

The differences between the two-zone and the three-zone situ-
ations should also be noted. The larger number of zones enables the
attainment of a fuel burnup which is higher by about 10%. As is usual,
however, there is a compensating factor that tends to offset this
advantage. If the burnups in the two cases had been equal, the three-
zone reactor would require 50% more shutdowns for refuelling in a
given time than would the two-zone reactor. This implies economic
penalties due to a reduced load factor, and also involves handling
almost 50% more irradiated fuel in a given period of time than would
be necessary with two zones. While it is difficult to attach a dollar
sign to the latter factor, it would undoubtedly increase the down-time
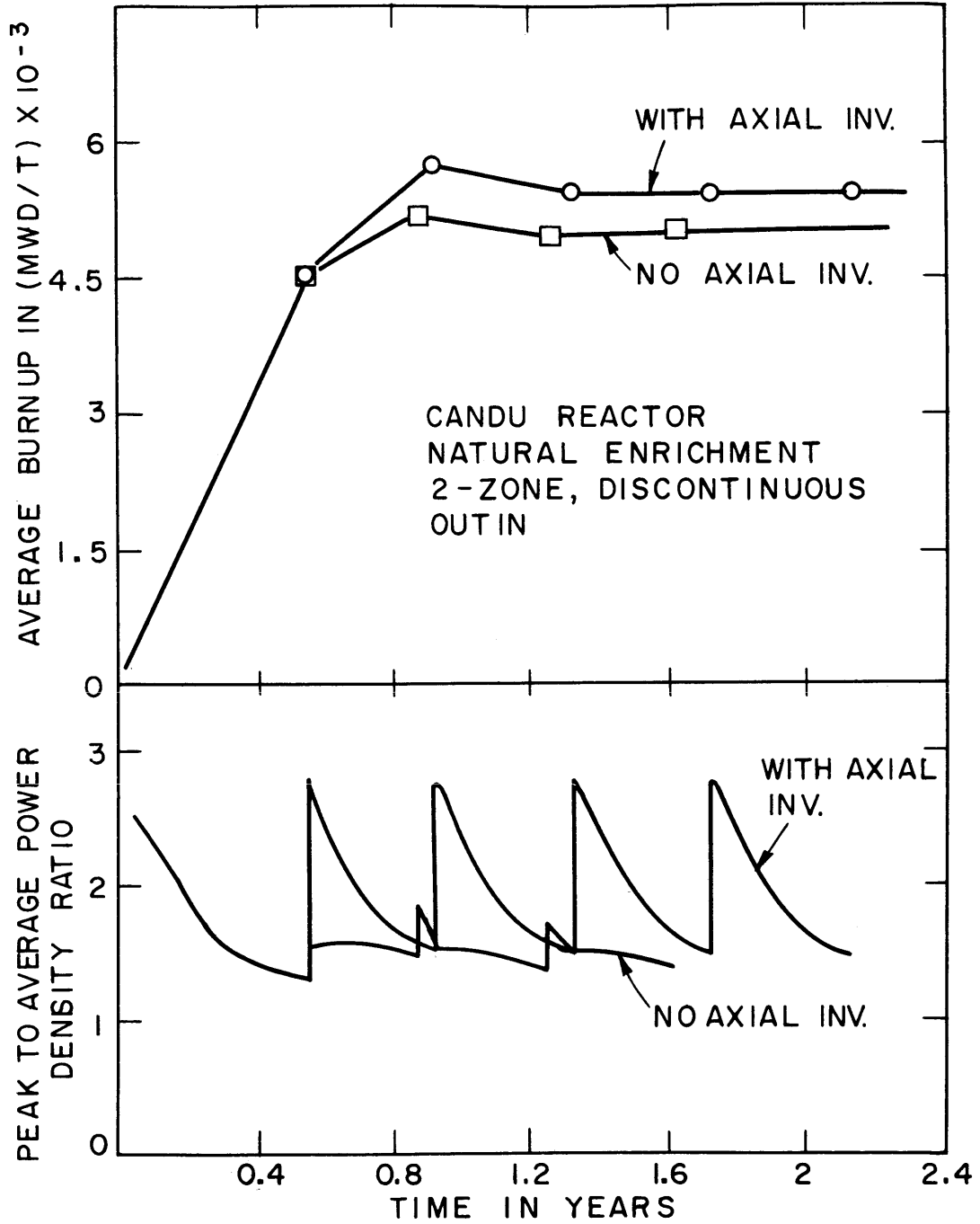
FIG. 6.33 THE TIME BEHAVIOR OF AVERAGE BURNUP
AND THE PEAK - TO - AVERAGE POWER DENSITY
RATIO WITH 2 RADIAL ZONES

295
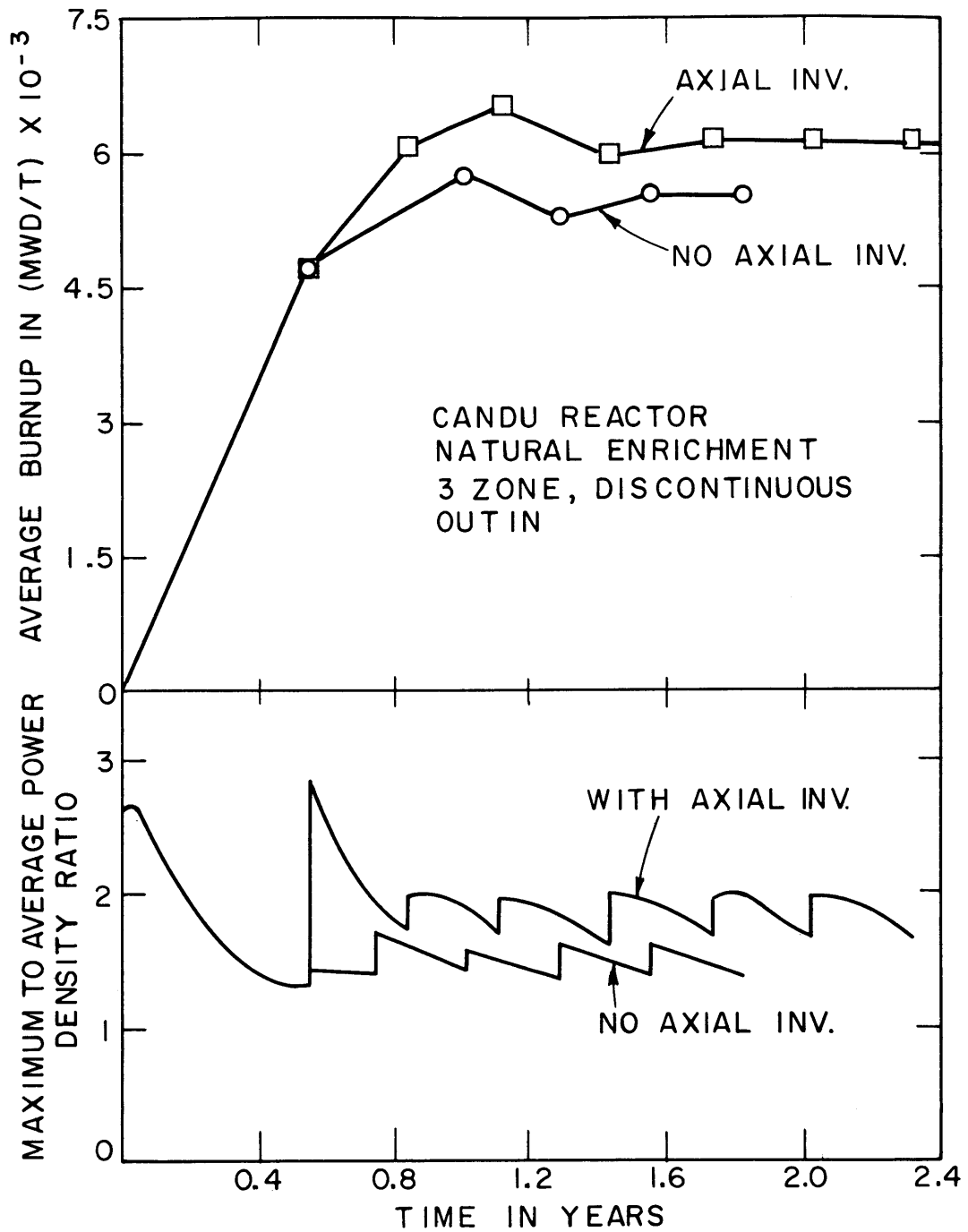
FIG. 6.34 THE TIME BEHAVIOR OF AVERAGE BURNUP
AND THE PEAK-TO-AVERAGE POWER DENSITY
RATIO WITH 3 RADIAL ZONES

needed for refuelling, and would increase any expenses associated directly with the refuelling procedure.

The severity of flux peaking in the three-zone reactor using axial inversion is substantially less in the steady state than it is using two zones. The reason for this is that when there are only two zones, the relatively undepleted fuel at the ends of the outer zone is transferred to the center of the inner zone, and is right at the center of the reactor, where it causes large peaking. With three zones, however, the fuel at the ends in the outer zone is transferred to the center of the middle zone, which is only about half way radially toward the center of the reactor. Following irradiation in the middle zone, this fuel will have a relatively uniform burnup distribution, axially, and will not provide an excess of reactivity when it is transferred to the central region. The peaking which does occur following the first fuel change in the three-zone reactor could have been reduced by not inverting the fuel which was in the middle zone during Batch irradiation.

Shown in Figure 6.35 is the total energy cost for both cost bases, using two and three zones, with and without axial inversion, during the approach to steady-state operation. This graph shows costs for reactors which are not peak-power-density limited and does not, therefore, show the true penalty associated with the peaking that occurs when axial inversion is used. Consideration of this factor would exclude the use of a two-zone reactor with axial inversion from consideration. The three-zone reactor with axial inversion does show definite promise as a practical operating technique.

It was the purpose of this particular study to reduce the number of variables to a more tractable quantity. While the three-zone reactor with axial inversion during fuel transfer shows definite promise, this study will proceed on the assumption that axial inversion will not be used. Furthermore, in spite of potential gains in burnup that can be realized with a greater number of zones, the two-zone reactor will be used in the rest of this study, since it will have generally greater load factors and less frequent fuel transfers and associated complication. Also, the results obtained using two zones will show trends that can
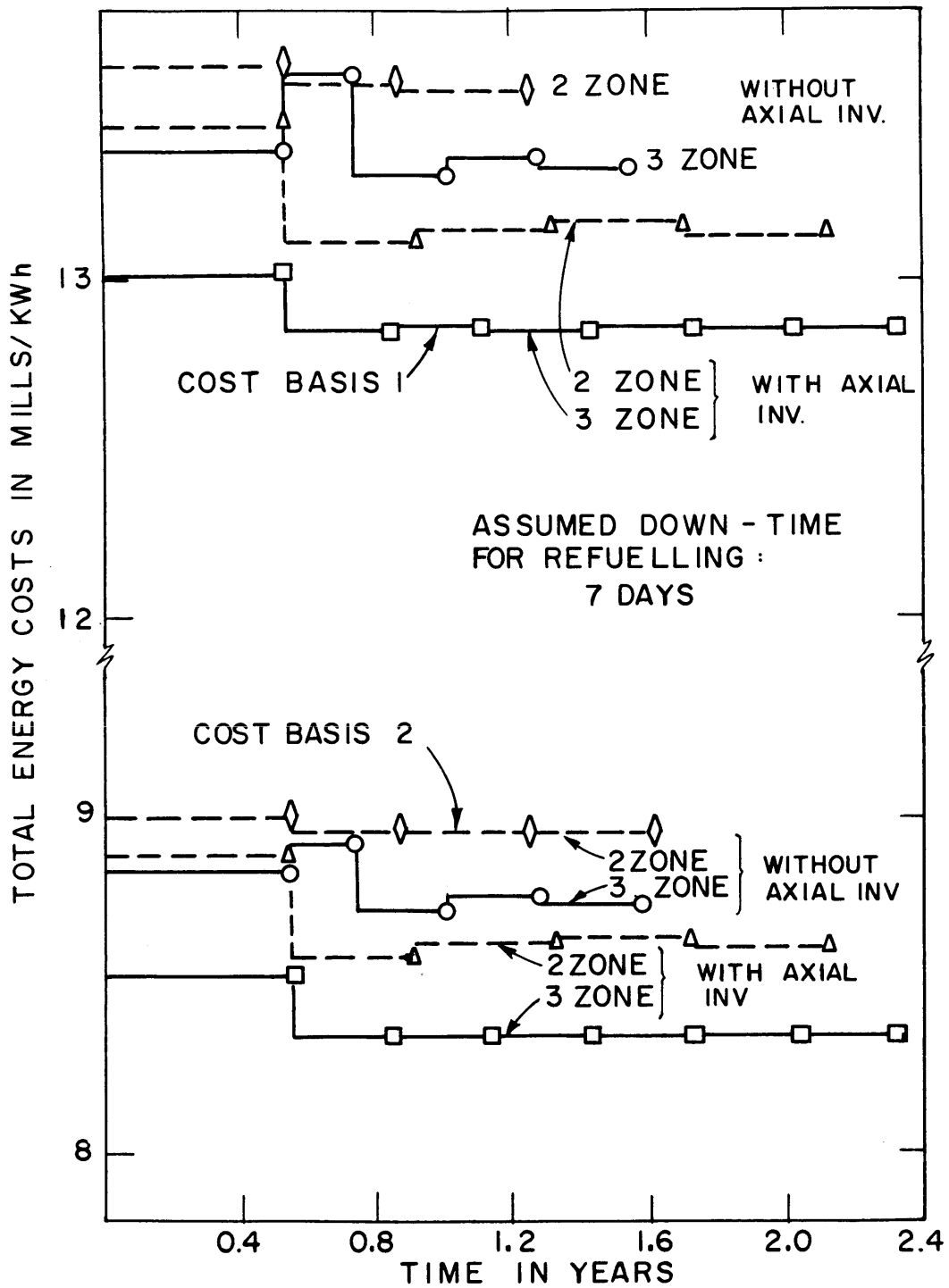
FIG. 6.35 THE TOTAL ENERGY COST DURING THE STARTUP
PERIOD OF 2-AND 3-ZONE CANDU REACTORS,
WITH AND WITHOUT AXIAL INVERSION OF FUEL.
ENRICHMENT: NATURAL

generally be extrapolated to a greater number of zones.

8.3 The Effect of Poison Management and Enrichment on the Steady-State Reactor Design

Because a reactor system will spend the majority of its lifetime operating with steady-state fuel management, the next step in the study of the discontinuous outin fuel movement is to obtain the poison management technique and enrichment that will result in the production of energy at minimum cost. First, results of a combined survey of enrichment and radial zone poison distribution will be presented. As was done for Batch Irradiation, the effect of core volume on burnup, fuel cost and power distribution will be examined. These results can then be used to specify the reactor design capable of producing energy at minimum cost for the specified output of 200 Mwe.

The results summarized in Table 6.19 show the importance to power density distribution of matching the control poison in a given zone to the reactivity of the fuel in that zone. The study was performed on a two-zone reactor at reference design volume, using uniform poison distribution within a zone, but varying the relative magnitudes between the two zones. The results predict that a very adequate degree of power distribution flattening can be achieved and maintained throughout fuel lifetime, by making judicious choice of the relative control poison magnitude between the two zones.

Also presented in Table 6.19 are the results of a run using a core volume of 0.9 of the reference design core volume. This indicates an identical trend to that shown in Table 6.17 for Batch Irradiation. In summary, in both cases there is a slight burnup loss which when translated into fuel costs is more than offset by decreased interest charges on UF_6 lease and working capital. The reduced core volume causes a slight improvement in the power distribution at 1.3 a/o, but has a small influence in the opposite direction for 1.5 and 1.75 a/o. The results of Table 6.19 have been used to obtain the data presented in Table 6.20 for the optimized steady-state reactors operating with discontinuous outin fuel management with two zones. The results in

Table 6.19   Radial Zone Poison Distribution: Steady State, Two Zone, Discontinuous Outin.

Enrich-ment a/o	Ratio of Inner to Outer Zone Control Poison Σ_w	Peak to Average Power Density Ratio			Average Burnup MWD/T	Time in Reactor Years	Fuel Cycle Cost mills/KWh		Maximum Control Σ_w cm$^{-1} \times 10^3$	Run No.
		Initial*	Maximum	Final			Basis 1	Basis 2		
1.0	0.4	1.42	1.59	1.47	10,020	1.499	2.450	1.980	1.964	E2.3-.40
	0.45	1.51	1.63	1.45	9,910	1.484	2.479	2.005	1.838	E2.3-.45
	0.25	1.38	1.63	1.53	14,470	2.184	2.034	1.719	2.981	E2.5-.25
1.3	0.3	1.58	1.68	1.51	14,293	2.162	2.059	1.741	3.275	E2.5-.30
	0.3**	1.51	1.63	1.50	14,288	1.943	2.046	1.732	3.305	E3.5.2
1.5	0.25	1.60	1.70	1.55	16,970	2.574	1.951	1.677	4.210	E2.6-.25
	0.3	1.78	1.78	1.50	16,730	2.560	1.980	1.702	3.946	E2.6-.30
1.75	0.25	1.81	1.81	1.56	19,890	3.064	1.913	1.672	5.102	E2.7-25

*with equilibrium Xe and Sm.

**Core Volume = 0.9 V_o

Table 6.20   The Characteristics of the Optimum Reactor for Discontinuous Outin Irradiation with Two Radial Zones.

A: Design Data	Enrichment (a/o)			
	1.0	1.3	1.5	1.75
Thermal Power	P_o	P_o	P_o	P_o
Core Volume	$0.8\ V_o$	$0.8\ V_o$	$0.87\ V_o$	$0.93\ V_o$
Maximum Power Density (Kw/L)	17.0	17.0	17.0	17.0
Ratio of Inner to Outer Zone Σ_w	0.4	0.25	0.25	0.25
Fuelling Load Factor	0.979	0.985	0.988	0.990
B: MOVE Code Results				
Maximum Power Density	17.0	17.0	17.0	17.0
Ratio of Peak to Average Power Density				
a) Initial[*]	1.60	1.60	1.74	1.86
b) Final	1.47	1.53	1.55	1.56
Average Burnup (MWD/T)	10,020	14,470	16,970	19,890
Maximum Burnup (MWD/T)	12,100	16,950	19,800	23,110
Full Power Time in the Reactor (years)	1.199	1.747	2.239	2.849
Kwhe/kg of Fuel Charged	67,214	97,065	113,835	133,422

[*]with equilibrium Xe and Sm.

Table 6.20 (cont'd)

C: Material Quantities	Enrichment (a/o)			
	1.0	1.3	1.5	1.75
Feed Rate (kgU/Full Power Year)	3.187×10^4	2.187×10^4	1.707×10^4	1.341×10^4
Discharge Rates				
a) kgU/Full Power Year	3.139×10^4	2.142×10^4	1.667×10^4	1.305×10^4
b) kgPu/Full Power Year	131	103	84.7	69.6
Isotopic Content of				
Discharged Fuel				
w/o U^{235} in U	0.268	0.250	0.253	0.260
U^{236} in U	1.111	0.159	0.189	0.226
Pu^{239} in Pu	62.9	57.7	55.8	54.0
Pu^{240} in Pu	25.4	27.3	27.9	28.2
Pu^{241} in Pu	8.2	9.5	9.9	10.3
Pu^{242} in Pu	3.5	5.5	6.4	7.5

Table 6.20 (cont'd)

D: Fuel Cycle and Total Energy Costs Cost Basis 2 mills/Kwh	Enrichment (a/o)			
	1.0	1.3	1.5	1.75
Net Material	0.248	0.400	0.493	0.618
Fabrication	0.989	0.740	0.651	0.556
Reprocessing	0.624	0.442	0.379	0.326
UF$_6$ Lease	0.039	0.071	0.090	0.112
Working Capital	0.082	0.068	0.063	0.061
NET FUEL CYCLE COST	1.982	1.720	1.676	1.673
Plant Capital Costs	4.440	4.410	4.457	4.495
Operating Costs	1.041	1.034	1.032	1.030
TOTAL ENERGY COST	7.463	7.164	7.165	7.198

terms of total energy cost are presented in Figure 6.36. While the minimum fuel cost occurs at around 1.75 a/o enrichment, it is a very broad minimum, and the better power distribution available at 1.3 a/o permits operation at this enrichment with a smaller core volume, thereby yielding minimum total energy cost at this point, although, here again, there is a very broad minimum. It should be recalled that these designs do not take into consideration the possible changes that might have to be made to accommodate the startup and transient periods prior to the onset of steady-state. The compromises that may be necessary are evaluated in the following section.

8.4 The Startup and Pre-Steady-State Operation of Discontinuous Outin

It was pointed out in the introduction to Section D of this chapter that there is an economic incentive to being always capable of operation at full capacity. This implies that the power distribution during the pre-steady-state period must never be more peaked than in the steady state. If this is physically impossible, there are three alternatives: 1) Redesign the steady-state- optimized reactor, 2) Exceed the specified maximum power density limit (the feasibility of this would depend upon the type of limit, and the particular circumstances) , 3) Decrease the power output.

In the startup of the discontinuous outin fuel irradiation technique, there are two alternatives, as mentioned in Section 8.1. One of these is to accept the steady-state control poison distribution and to use in the inner zones, fuel whose enrichment is equivalent in reactivity to the partially spent fuel that would be charged to those zones in steady-state operation. This use of fuel of lower enrichment on startup will result in higher fuel costs than if the reactor were charged uniformly with the enrichment that is charged to the reactor in steady-state. In the latter case, however, additional control must be provided, that will be used only once, on startup. Hence, the cost of this control must be balanced against the increased fuel cost when lower enrichments are used. It may be that one of the two alternatives will be preferred due to better power distribution.
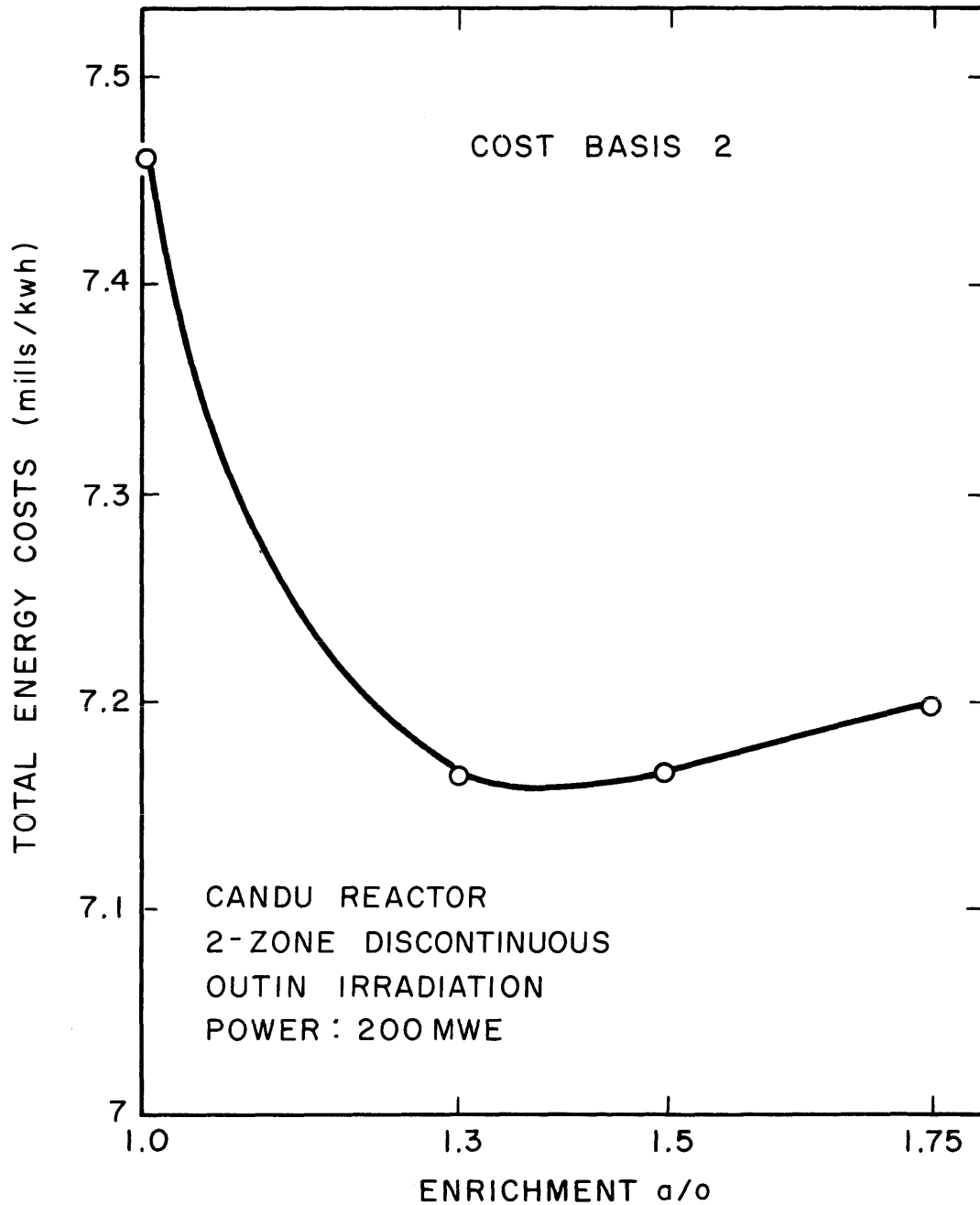
FIG. 6.36 THE VARIATION OF TOTAL ENERGY COST
WITH ENRICHMENT FOR REACTORS AT
CONSTANT OUTPUT AND FIXED PEAK
POWER DENSITY IN STEADY
STATE OPERATION

305

These two alternatives have been examined. When a decreased enrichment is required in the inner zone of a two-zone loading for this reactor, natural uranium gives the best power distribution when used in conjunction with the steady-state control poison distribution for 1.0 or 1.3 a/o enrichment. An enrichment somewhat higher than natural would probably be preferable when 1.5 or 1.75 a/o is used in the outer zone. The results are summarized in Table 6.21, Parts A to D, for the four enrichments, 1.0, 1.3, 1.5, and 1.75 a/o, respectively, all starting with their steady-state control poison distributions and with natural uranium in their central zones. Also included for comparison is one uniform enrichment case, Part E at 1.3 a/o, which is started off with an initial control poison distribution that corresponds to that obtained in Batch Irradiation at optimum flatness. After the first fuel is discharged, the control distribution reverts to the steady-state control poison distribution.

It is instructive to compare the two 1.3 a/o startup cases, Parts B and E. The situation fuelled initially with uniform enrichment (Part E) and requiring extra control produces energy at 7.51 mills/kwh for 1.47 years, while the other reactor using natural uranium and no additional control (Part B) produces energy at 7.62 mills/kwh for 1.15 years and at 7.32 mills following this time, for an average of 7.55 mills/kwh over the 1.47 year period. The difference of 0.04 mills/kwh for 1.47 years at 200 Mwe amounts to $103,000. The cost of additional control can be compared to this quantity. The uniformly fuelled case, Part E, will require approximately four times as much control in the center zone in the first operating period as is needed for the steady-state operation; this amounts to about 60% more control in the whole core. The use of natural uranium in the central zone on startup is therefore probably cheaper than providing for the additional control needed only on startup with uniform enrichment.

The remaining factor that must be considered is that of power distribution during the approach to the steady-state. It is apparent that without exception, the startup peak-to-average power density ratios exceed those that prevail in steady-state, and the discrepancy

306

Table 6.21   The Startup of 2-Zone Discontinuous Outin   Part A

Specification: 1.0 a/o, Natural Center; $\dfrac{\Sigma_w \text{ center}}{\Sigma_w \text{ outer}} = 0.4$; $V = V_o$

Cost Basis 2, Run E 2.3 - .40

		Batch		Step 1		Step 2		Step 3	
		Initial*	Final	Initial*	Final	Initial*	Final	Initial*	Final
Time (years)		0	.85	0.85	1.58	1.58	2.33	2.33	3.08
Average Burnup (MWD/T)	Inner	0	5660 (nat)	5,910	10,080	5,530	10,020	5,580	10,020
	Outer	0	5,910	0	5,530	0	5,580	0	5,580
Peak to Average Power Density Ratio		1.86	1.39	1.64**	1.48	1.58**	1.46	1.59**	1.46
Cost of Fuel Discharged (mills/kwh)		2.79		1.97		1.98		1.98	
Average Energy Cost (mills/kwh)	Fuel	2.39		1.98		1.98		1.98	
	Total	8.02		7.62		7.62		7.62	

*with equilibrium Xe and Sm.

**Maximum

Table 6.21 (cont'd)   Part B

Specification: 1.3 a/o, Natural Center; $\dfrac{\Sigma_{w\ center}}{\Sigma_{w\ outer}} = 0.25$; $V = V_o$

Cost Basis 2, Run E 2.5 - .25

Item		Batch		Step 1		Step 2		Step 3	
		Initial*	Final	Initial*	Final	Initial*	Final	Initial*	Final
Time (years)		0	1.15	1.15	2.24	2.24	3.33	3.33	4.42
Average Burnup (MWD/T)	Inner	0	6,530 (nat)	8,950	14,550	8,710	14,470	8,660	14,470
	Outer	0	8,950	0	8,710	0	8,660	0	8,660
Peak to Average Power Density Ratio		1.95	1.47	1.67**	1.54	1.63**	1.53	1.63	1.53
Cost of Fuel Discharge (mills/kwh)		2.38		1.71		1.72		1.72	
Average Energy Costs (mills/kwh)	Fuel	2.02		1.72		1.72		1.72	
	Total	7.62		7.32		7.32		7.32	

*with equilibrium Xe and Sm.

**Maximum

308

Table 6.21 (cont'd) Part C

Specification: 1.5 a/o, Natural Center; $\dfrac{\Sigma_w \text{ center}}{\Sigma_w \text{ outer}} = 0.25$; $V = V_o$

Cost Basis 2, Run E 2.6 - .25

Item		Batch		Step 1		Step 2		Step 3	
		Initial*	Final	Initial*	Final	Initial*	Final	Initial*	Final
Time (years)		0	1.33	1.33	2.60	2.60	3.90	3.90	5.20
Average Burnup (MWD/T)	Inner	0	6,740 (nat)	11,090	17,020	10,730	16,970	10,810	16,970
	Outer	0	11,090	0	10,730	0	10,810	0	10,810
Peak to Average Power Density Ratio		2.15	1.48	1.71	1.54	1.70**	1.55	1.70**	1.55
Cost of Fuel Discharged (mills/kwh)		2.30		1.67		1.68		1.68	
Average Energy Costs (mills/kwh)	Fuel	1.95		1.68		1.68		1.68	
	Total	7.54		7.27		7.27		7.27	

*with equilibrium Xe and Sm.

**Maximum

309

Table 6.21 (cont'd)   Part D

Specification: 1.75 a/o, Natural Center; $\dfrac{\Sigma_{w\ center}}{\Sigma_{w\ outer}} = 0.25$; $V = V_o$

Cost Basis 2,   Run E 2.7 - .25

Item		Batch Initial*	Batch Final	Step 1 Initial*	Step 1 Final	Step 2 Initial*	Step 2 Final	Step 3 Initial*	Step 3 Final
Time (years)		0	1.53	1.53	3.04	3.04	4.58	4.58	6.11
Average Burnup (MWD/T)	Inner	0	6,915 (nat)	13,600	19,940	13,240	19,885	13,260	19,890
	Outer	0	13,600	0	13,240	0	13,260	0	13,260
Peak to Average Power Density Ratio		2.31	1.47	1.89	1.56	1.81	1.54	1.81	1.54
Cost of Fuel Discharged (mills/kwh)		2.25		1.67		1.67		1.67	
Average Energy Costs (mills/kwh)	Fuel	1.90		1.67		1.67		1.67	
	Total	7.49		7.25		7.25		7.25	

*with equilibrium Xe and Sm.

Table 6.21 (con'td) Part E

Specification: 1.3 a/o Uniform; $\dfrac{\Sigma_{w \ center}}{\Sigma_{w \ outer}} = \begin{cases} \dfrac{1}{0.85} & \text{Batch} \\ \\ 0.25 & \text{Other Steps} \end{cases}$; $V = 0.9 \, V_o$

Cost Basis 2, Run E 3.5.1

Item		Batch		Step 1		Step 2		Step 3	
		Initial*	Final	Initial*	Final	Initial*	Final	Initial*	Final
Time (year)		0	1.47	1.47	2.37	2.37	3.36	3.36	4.34
Average Burnup (MWD/T)	Inner	0	11,745	10,130	14,830	8445	14,485	8555	14,470
	Outer	0	10,130	0	8445	0	8555	0	
Peak to Average Power Density Ratio		1.79	1.19	1.83	1.55	1.58**	1.52	1.58**	1.52
Cost of Fuel Discharged (mills/kwh)		2.13		1.68		1.70		1.71	
Average Energy Costs (mills/kwh)	Fuel	1.93		1.69		1.71		1.71	
	Total	7.43		7.24		7.24		7.24	
Total at V = V_o		7.51		7.32		7.32		7.32	

*with equilibrium Xe and Sm.

**Maximum

increases at higher enrichment, although this condition might be improved by the use of slightly enriched uranium in the center zone instead of natural. The problem of whether to increase core volume or run at reduced power can be resolved if the system requirement does not prohibit reduced power operation. An increase in core volume of 10% will cost about 0.08 mills/kwh, whereas a reduction of 10% in core power will cost about 0.57 mills/kwh, a factor of seven greater. Generally, however, the reduced power operation would last only a short time, the order of a month or so, whereas the increase in core volume would, of course, be effective over the whole lifespan of the reactor. It would therefore seem evident that reduced power operation would be the more economical way to deal with the excess peaking that occurs on startup.

8.5 Conclusions

The discontinuous outin fuel management technique permits the attainment of substantial increases in fuel burnup over those possible in batch irradiation. It permits a large degree of flexibility with respect to the compromises that can be made between fuel burnup, power distribution and fuelling down-time.

The above studies have shown that the flattest power distributions are obtained without the use of axial inversion, but increased burnup can be attained if axial inversion is used. The choice of the number of radial zones is also a matter of compromise. The two-zone reactor will have the least handling of irradiated fuel, but it will not attain the fuel burnup that is possible with a greater number of zones.

Reactor systems using discontinuous outin fuel management can be designed for operation in the steady-state. The correct combination of control poison distribution and fuel enrichment can result in a very satisfactory degree of flattening and hence a high average power density at a specified output. During the startup and pre-steady-state operation of the system, it will probably be necessary to reduce power for short periods so as to stay within a maximum permissible power density limit. Provided the initial control poison technique and fuel enrichment have

been well chosen, reducing power would be cheaper than designing the reactor for startup conditions when most of its energy will be produced at steady state.

9. CONTINUOUS GRADED AND OUTIN FUEL IRRADIATION

The continuous graded and outin fuel management techniques, unlike the continuous bidirectional, would not be practical for use in a nuclear power system, because of excessive interference with operation. They are, however, of interest as the asymptotes of discontinuous irradiation techniques. Continuous outin is the limiting case of discontinuous outin with an infinite number of radial zones. Discontinuous graded irradiation, which is not studied in this work, is a possible and practical way of operating a reactor.

The study of these continuous techniques is similar to that used for continuous bidirectional, although optimum reactor designs will not be specified here. It will be recalled that in the continuous fuelling techniques, it is assumed that no time is lost in the fuelling operation, since this is presumably done while the reactor system is at full power. The extent of the enrichment survey of continuous outin was limited by the inability of the MOVE Code to converge on the correct flux shapes for enrichments greater than 1.0 a/o. The reason for this is the extreme peaking which occurs in the new fuel being charged to the periphery of the reactor. Radial variation of burnup for power distribution flattening has been used in the graded irradiation study, with the radial dependence of discharge flux-time being identical with those used in bidirectional to obtain maximum flatness.

The results of this study are given in Table 6.22, and the important characteristics are shown individually in Figures 6.37 to 6.39. It is interesting to note that the use of radial burnup variation in graded irradiation results in the same type of behavior as was obtained under similar circumstances with the continuous bidirectional fuelling technique. Figure 6.37 shows that the flattening causes a burnup loss which is virtually independent of burnup, and hence its percentage effect on fuel cost should decrease with enrichment. The

Table 6.22   The Characteristics of Continuous Outin and Graded Fuel Irradiations.

Enrich-ment a/o	Type of FUEL MOVE	θ_d type	Average Burnup MWD/T	Maximum Burnup MWD/T	Peak Power Density KW/l	Maximum to Average Power Density Ratio	T_R Full Power Time Years	Net Fuel Cycle Costs mills/kwh*		Run No.
								Basis 1	Basis 2	
NAT	O U T I N	-	6,800	8,770	13.33	1.55	0.99	2.88	2.26	G1.1
0.85		-	10,010	12,250	14.71	1.71	1.46	2.21	1.70	G1.2
1.0		-	13,130	15,610	17.21	2.00	1.92	1.84	1.47	G1.3
NAT	G R A D E D	θ_d Const	7,770	9,990	17.73	2.06	1.14	2.33	1.85	F1.1
		θ_d min p.d	6,480	11,680	12.46	1.45	0.95	2.98	2.23	F2.1
1.0		θ_d Const	15,340	18,040	16.27	1.89	2.24	1.42	1.14	F1.3
		θ_d min p.d	14,270	19,110	11.22	1.30	2.09	1.82	1.38	F2.3
1.3		θ_d Const	21,860	24,770	15.48	1.80	3.20	1.34	1.12	F1.5
		θ_d min p.d	20,380	27,800	10.51	1.22	2.98	1.43	1.20	F2.5

*Without allowance for down time during fueling.
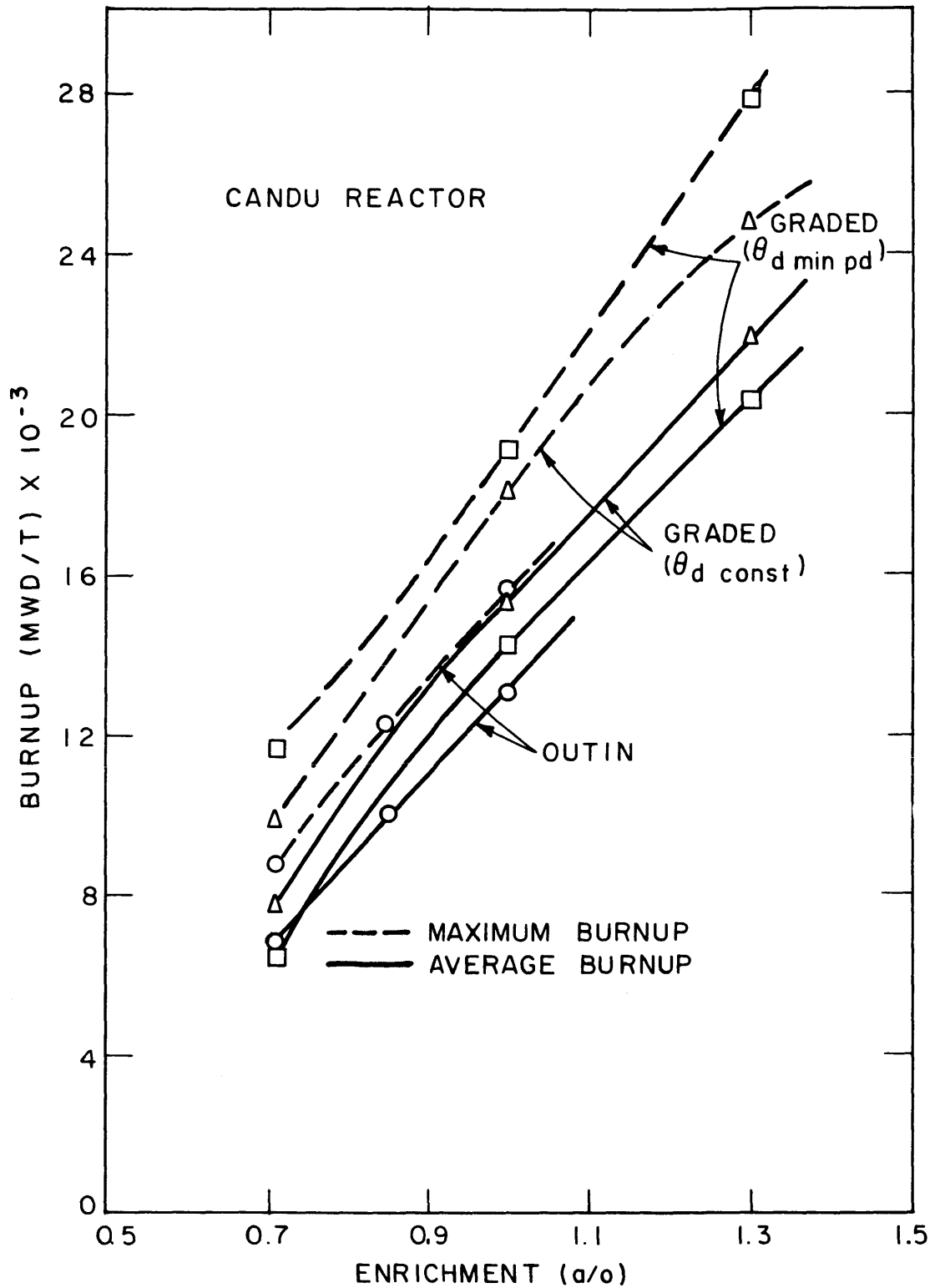
FIG. 6.37 THE VARIATION WITH ENRICHMENT OF MAXIMUM
AND AVERAGE BURNUP, FOR CONTINUOUS OUTIN
AND GRADED IRRADIATIONS

315

degree of flattening attainable by radial burnup variation is evident in Figure 6.38. This does not show the radial and axial flux shape dependence that was evident in bidirectional, so that flatness keeps increasing with enrichment increase. The peak-to-average power density ratio for outin increases with enrichment due to the increased peaking at the outer edge where new fuel is being continuously charged. The fuel cycle cost data shown on Figure 6.39 shows a minimum for graded irradiation in the vicinity of 1.3 a/o enrichment, and a value which compares quite favorably with that achieved in continuous bidirectional irradiation.

An examination of the results of the continuous outin enrichment study points out two important facts with respect to power and reactivity distribution in fuel and poison management. First, if bad peaking must occur, it is advantageous to have it occur in the outer zones where the volume weighting is highest. When this occurs, the peak power density cannot get too far away from the average due to the high volume weighting of the region where the peak occurs. For example, at 1.0 a/o fuel enrichment where the peak-to-average ratio is 2.00, the ratio of peak to core-center power density is close to 9.

The second point shown to advantage in the continuous outin fueling is this. If fuel whose infinite multiplication factor is less than unity, is present in a reactor, it must be supplied with neutrons which can be provided only by developing a neutron density gradient. Gradients, however, tend to be detrimental to power distributions. In the continuous outin irradiation, the depleted fuel at the reactor center is being driven by the gradient developed by the large peak at the outer edge. The conclusion that is to be drawn from this point is that excess reactivity should be controlled as much as possible at its source rather than permitting development of the flux peaks which are necessary to rid a region of its excess neutrons. One should distinguish here between short range neutron transfer (less than a migration length, say) and longer range diffusion. Short range neutron transfer is assumed to occur between adjacent channels in bidirectional and between adjacent fuel elements in graded irradiation, whereas the longer range diffusion

316
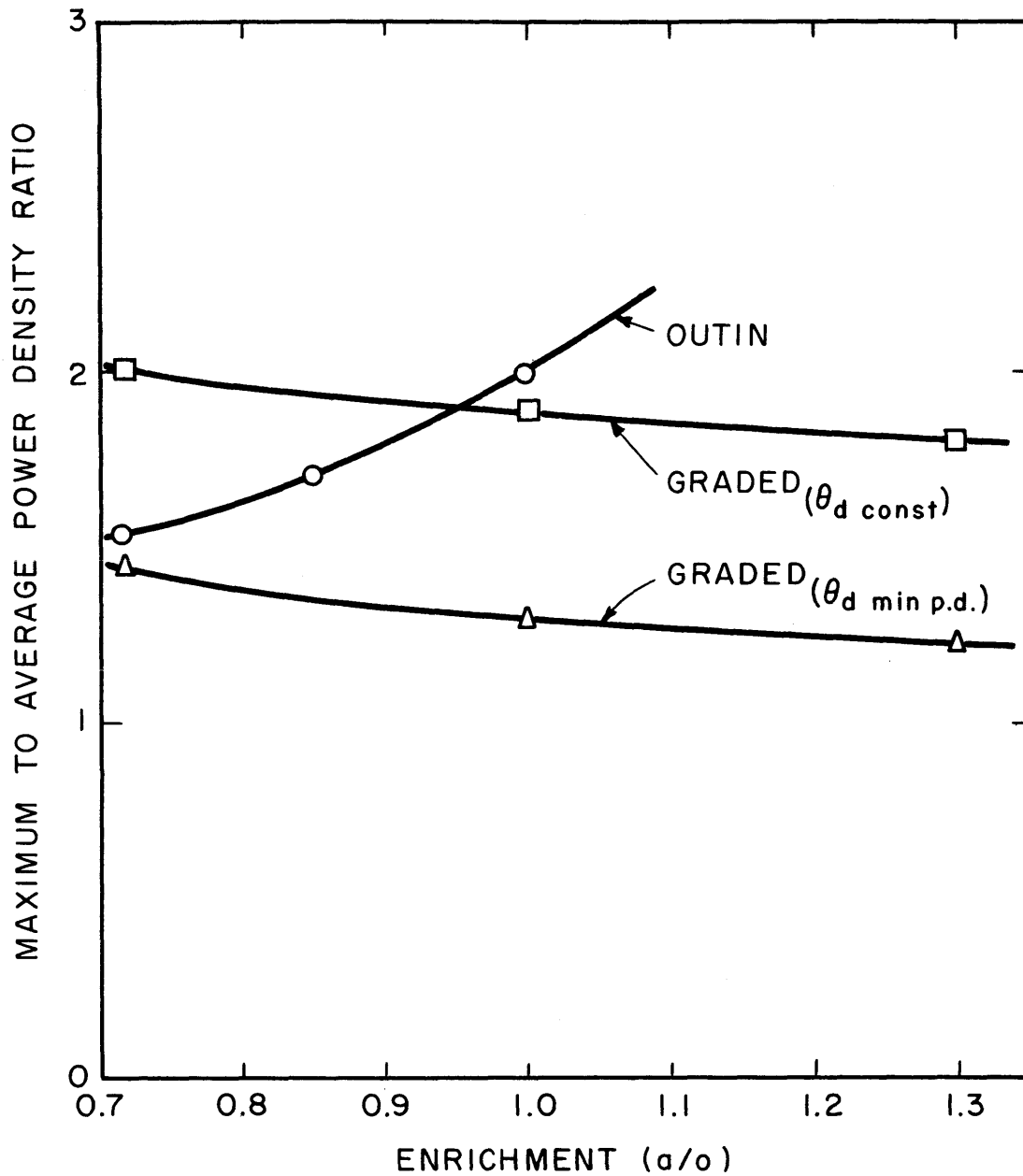
FIG. 6.38 THE VARIATION WITH ENRICHMENT OF THE
PEAK-TO-AVERAGE POWER DENSITY RATIO
FOR CONTINUOUS OUTIN AND GRADED
IRRADIATIONS

317
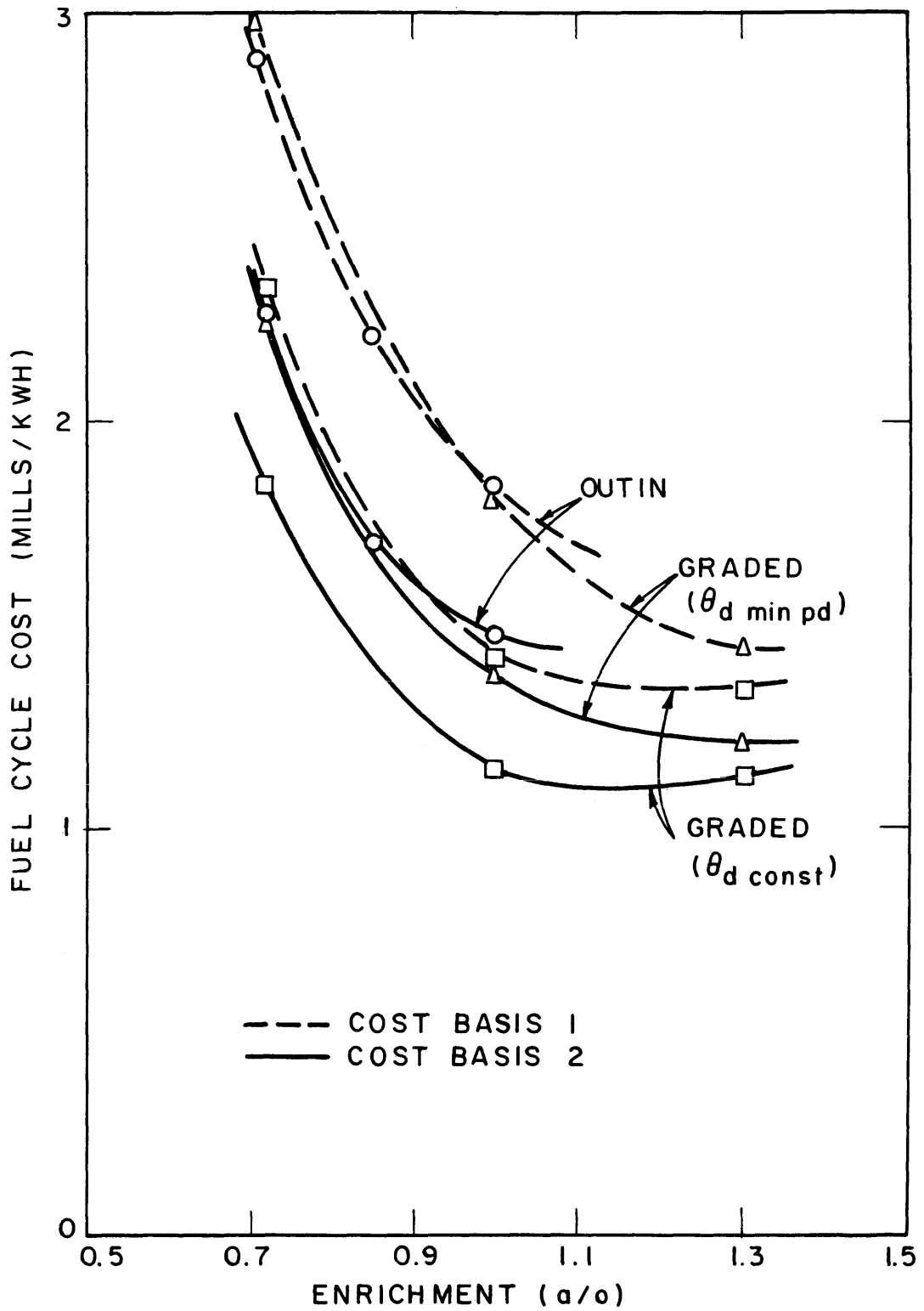
FIG. 6.39 THE VARIATION WITH ENRICHMENT OF NET FUEL
CYCLE COST FOR CONTINUOUS OUTIN AND
GRADED IRRADIATIONS

318

occurs in outin irradiation. Both of these utilize excess neutrons in depleted fuel but, in outin irradiation, severe flux peaking is required to drive the neutrons.

E. SUMMARY AND GENERAL CONCLUSIONS

Of the fuel and poison management techniques studied in the previous section, the three most important are 1) Batch Irradiation, 2) Discontinuous Outin, and 3) Continuous Bidirectional Irradiation. In each case, the objective of the study has been to analyze those factors that are under the control of fuel and poison management, and which influence the cost of energy produced.

The results of the analyses have been used to specify the combination of fuel enrichment, control poison technique and core volume which would produce energy at minimum cost, under the constraint of a maximum permissible power density and a specified total core output. An additional assumption that has been made throughout the analysis is that the end of fuel life is determined by criticality considerations rather than by radiation damage limitations.

It is the purpose of this section to summarize the results of the previous section, to compare the relative merits of the techniques studied, and finally to correlate the specific results in a manner that illustrates the general principles of fuel and poison management in nuclear power systems.

In Batch Irradiation, one of the major variables is the use of control poison. The choice of a particular poison removal technique will be based mostly on the effect it has on power distribution during reactor core lifetime. The relative merit of the three control poison techniques available in the MOVE Code can be evaluated using this criterion. The use of radial zone poison removal appears quite promising when used with natural uranium in the CANDU reactor, but at the higher enrichments which are economically preferable, excess peaking in the outer zones limits its usefulness. Axial bank poison removal is definitely impractical due to the excessive peaking in the regions from which control poison has most recently been removed. The conclusion that can be made is that the use of a uniform poison removal technique provides the best over-all performance with respect to power distribution during reactor core lifetime. In a

320

practical situation, uniform poison removal adequately represents the use of a soluble chemical control poison dissolved in the moderator, with concentration varied to maintain reactor criticality. There are obvious limitations to representing removal of finite control rods by means of uniform poison removal, but programming of control rod removal should attempt to do basically just that.

A complement to removable control poison is the use of burnable poison as an integral part of the fuel. This has the advantage of providing reactivity control where it is needed, right in the fuel. On the other hand, it is impossible to achieve both adequate long-term reactivity control and virtually zero residual poison at end-of-life. Hence, there will be a burnup loss associated with the use of burnable poison. It is doubtful that the reduced control requirement can compensate, costwise, for the burnup loss sustained when burnable poison is used. On the other hand, should fuel enrichment be limited by a maximum amount of attainable reactivity control, there is a definite advantage in using a higher enrichment plus the amount of burnable poison required to satisfy the maximum control criterion.

This study shows that in Batch Irradiation, the use of zones of different enrichment is not justified, since the same degree of flatness can be attained with radial variation of control poison, and lower fuel costs can be obtained using a single optimum enrichment. The use of a reduced amount of control poison in the outer regions of the core allows flux gradient changes to occur primarily in the outer regions rather than over the whole core and thereby enables the attainment of flatter power distributions.

Because Discontinuous Outin Irradiation is similar to Batch, the same general conclusions with regard to control poison removal will apply in both cases. However, the somewhat depleted fuel in the central regions of the core will require less reactivity control than the outer regions when the reactor is in steady-state operation. This use of spatially non-uniform control poison implies that chemical poison,which will be spatially uniform, must be supplemented in the outer zones by control rods, if it is to be used with the Discontinuous Outin fueling technique.

The startup of the Discontinuous Outin creates additional problems. From a fuel cost point of view, the enrichment of the fuel in the central zones should be the same as that in the outer zone. This, however, requires substantially more reactivity control than is necessary in steady- state operation.

The alternative is to use fuel enrichments in the inner zones which are equivalent in reactivity to the fuel which will be charged to those zones in steady-state. Using this approach, the steady-state control system is adequate for startup, and the steady-state condition is reached somewhat earlier than if a uniform loading were used. Fuel costs for the startup period will be somewhat higher when the non-uniform initial loading is used, but the savings in control requirement will generally be in excess of these fuel cost losses.

The Discontinuous Outin fueling technique provides a fair degree of flexibility with respect to the possible compromises between fuel burnup, the amount of control required, the amount of acceptable spent fuel handling, and the amount of reactor downtime for refueling. This flexibility is provided by the optional use of axial inversion during fuel transfer plus the number of radial zones which may be chosen. In general, the use of axial inversion increases average fuel burnup, but also increases the peak power density, in some cases to an intolerable level. If axial inversion were to be used, at least three radial zones must also be employed, since with two zones, virtually fresh fuel will be placed at the center of the reactor, causing excessive flux and power density peaking.

The choice of the number of radial zones to employ will be based on the following factors. Fuel burnup will increase and the reactivity control requirement will decrease as the number of radial zones is increased. However, since each reactor refueling shutdown will require a finite number of days, a large number of zones will require a sizeable total downtime per year. Also, each fuel element will have to be moved once for each zone, making the amount of handling of irradiated fuel proportional to the number of radial zones. In addition, a large number of zones would complicate the control rod programming.

322

Consideration of the above factors will tend to limit the number of zones to two or three. With a greater number of zones, the incremental fixed charge increase will have an increasing tendency to exceed the incremental fuel cost savings from increased burnup.

The Bidirectional Irradiation technique enables the highest degree of excess neutron utilization of all the fuel management techniques studied. It is unlikely that even the promising spectral shift reactors can attain the burnups that are possible with bidirectional fueling when compared at a specified enrichment, although it is difficult to compare the two types on a common basis, since their moderators are different with the spectral shift moderator having variable properties.

The most important single factor next to fuel enrichment in bidirectional irradiation, is the radial variation of discharge burnup. When discharge burnups are equal at all radii, the fuel cost tends to be a minimum, but power distributions are more peaked than is desirable. Considerable improvement can be obtained by specifying that the axial fuel velocity be constant at all radii. This is equivalent to specifying equal charging rates at all points on the radius of the reactor core. Some additional flattening can be achieved by reducing the charging rate in the central region.

The choice of fuel enrichment depends on the comparative power distributions and fuel burnups that can be obtained. In the CANDU reactor using natural uranium, attempts to flatten the power distribution are somewhat unsuccessful due to the large percentage changes in burnup that occur. Hence, it is necessary when designing for a specified output, to make a compromise between incremental fuel cost increases and the incremental savings from reduced core volume. Because of this sensitivity to power distribution, and the necessity of maintaining high burnup with natural uranium, core volumes will be larger than if enriched uranium were used. With higher enrichments, percentage burnup losses are smaller and hence the amount of flatness turns out to be limited, not by burnup considerations, but by the physical impossibility of further improvement.

This flatness limit is a function of fuel enrichment. While the radial flatness can be controlled by radial variation of discharge burnup,

the axial flatness is a function of the fuel behavior as it moves axially through the reactor, and is therefore dependent upon enrichment. In the CANDU reactor, 1.0 a/o enrichment has the best inherent axial flatness and hence will generally lead to the smallest reactor core at a specified output. It is also likely that further savings can be made by using enriched uranium. Because of the declining importance of leakage at the higher enrichments, the optimum reflector thickness could probably be reduced somewhat, although flatness might suffer if the reflector were reduced too much.

The use of fixed poison to control axial flatness is not justified due to the fact that burnup losses exceed the gains from any axial flattening. Also, the use of radial zones of different enrichment for purposes of radial flattening, at best, cannot improve upon the over-all performance of the system operated at an optimum enrichment, and will generally lead to higher fuel costs than those attained with the single enrichment.

The problem of comparing Batch, Discontinuous Outin and Bidirectional irradiations is difficult for the reason that a reactor system can be optimized to fit the fuel and management procedure. The CANDU reactor has been optimized for Bidirectional Fueling. If, however, a comparison is made using the CANDU reactor, with only the core volume adjusted to fit the particular requirements of the fuel management procedure, the comparison of the three tech-niques can be made on the basis of the total energy cost for the optimized designs as a function of enrichment as presented in Figures 6.20, 6.32, and 6.36. Figure 6.40 is a composite of the results given on these. It is immediately apparent that the bidirectional irradiation technique can achieve a cost advantage of about 0.65 mills/kwh over the two-zone discontinuous outin and about 1.0 mills/kwh over the batch ir-radiation, the majority of the difference in each case being due to fuel cost differences, and hence burnup differences. The high degree of neutron economy in bidirectional irradiation is evident from the fact that at 1.3 a/o enrichment, 1.84 fissions per initial fissile atom have occurred in the discharged fuel. Indicative of the lower degree of neutron economy in batch, is the 0.98 fissions per initial fissile

324
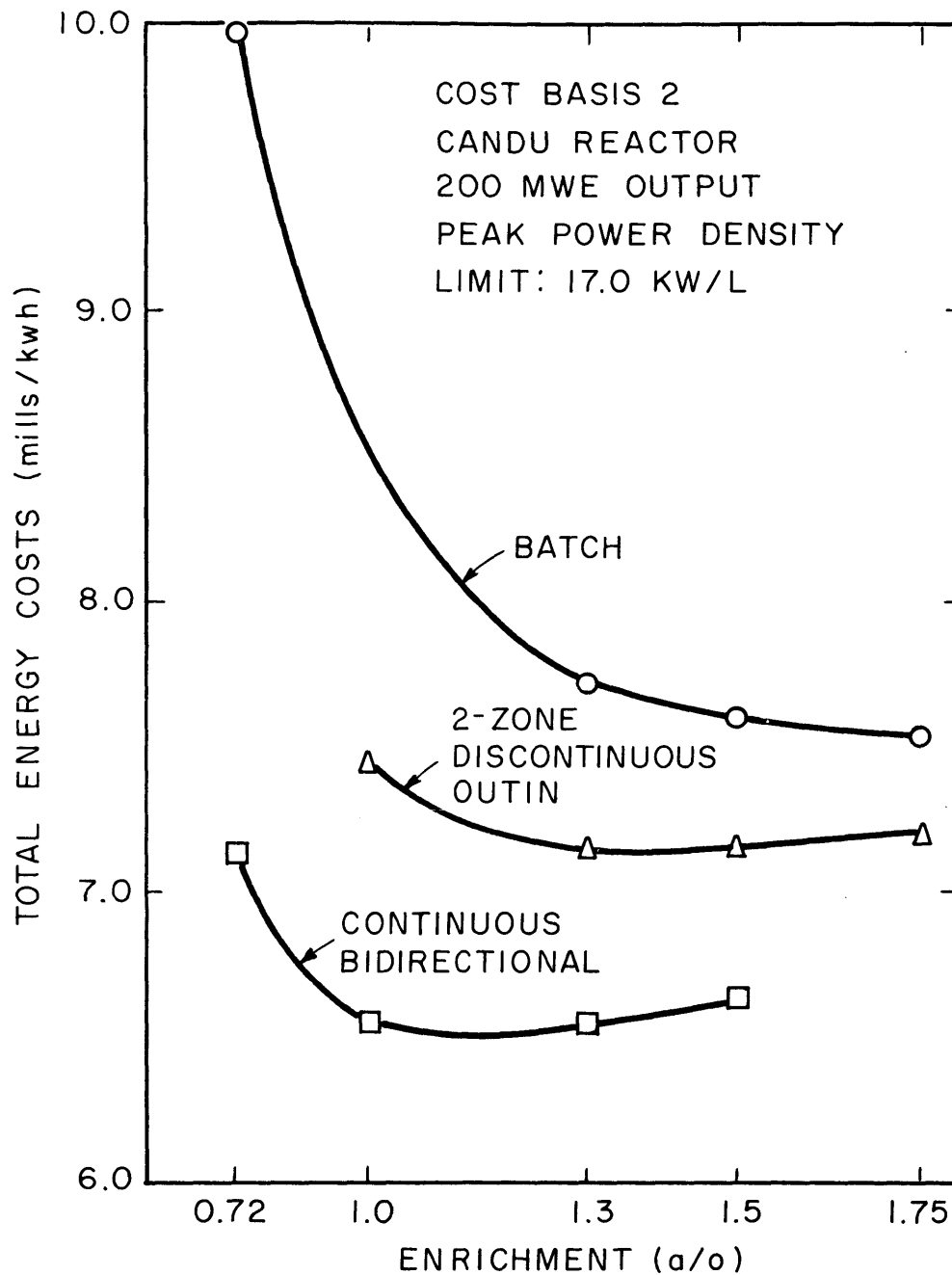
FIG. 6.40 THE TOTAL ENERGY COST AS A
FUNCTION OF ENRICHMENT FOR
VARIOUS FUEL AND POISON
MANAGEMENT TECHNIQUES

325

atom attained at 1.75 a/o enrichment.

In addition to the energy cost, there are several other factors to consider when comparing the batch-type irradiations, Batch and Discontinuous Outin, with the Bidirectional Irradiation. The batch irradiation could be accomplished in a pressure vessel, and long fuel rods could be used instead of the short slugs required in bidirectional fueling. Because of the relatively low power densities attainable with D_2O, as compared to H_2O, pressure vessel size might be a limiting factor, whereas the pressure tube concept, which is a necessity with bidirectional irradiation, will not be limited by size. The coolant leakage problem, which is particularly important in a D_2O reactor, will be greater in a pressure tube reactor due to the large number of welds, joints, and fittings. In addition, restrictions are imposed by neutron economy considerations, on the amount of pressure tube material that can be permitted in-core. Hence, there is an incentive to reduce safety factors in pressure-tube design. This effect would not be as important at higher enrichments as it is with natural uranium because the percentage burnup loss would not be as great at the higher enrichments.

In continuous bidirectional irradiation, it is necessary to have an on-line fueling machine. The main advantage of this machine is, therefore, that it permits on-line fueling and the fuel cost advantages that are attained thereby. An additional consequence of continuous on-line fueling is that no control rods are required. The fuel charging rate is adjusted to maintain criticality with the fine adjustment being accomplished, in the CANDU reactor, by means of moderator level control. A further advantage is that because the fuel slugs must be short, the fueling machine, while somewhat complex, can be relatively small. Hence, the amount of clearance around the reactor does not have to be as large as if full-length fuel elements had to be handled. Reactor containment and building volume can therefore be reduced, with some saving in capital cost.

The major disadvantages of bidirectional fueling are associated with the on-line fueling machine. The reliability of such a machine under

the severe conditions of on-line refueling is as yet uncertain. It is necessary that coolant flow and pressure be maintained with only limited D_2O leakage when both ends of a channel are opened to make fuel changes, which for the CANDU reactor would be from four to ten times a day, depending upon fuel enrichment. The actual cost of this fueling machine will be greater than for a machine equipped only for fuel changes with the system shut down. However, this cost will be somewhat reduced because of the smaller size of the on-line fueling equipment. The fuel cost saving of 0.6 mills/kwh with on-line fueling is equivalent to about $10 million in capital investment, which is of course substantially more than the cost of the on-line fueling equipment.

An additional disadvantage with on-line fueling is the lack of readily available excess reactivity for Xe-override. Special equipment to help override Xe will, of course, add to the capital cost requirement.

The above discussion summarizes the relative advantages and disadvantages of continuous bidirectional fuel irradiation as compared to the batch-type irradiation, Batch and Discontinuous Outin. The comparison of Batch with Discontinuous Outin was given in detail with the presentation of the Discontinuous Outin design study. In summary, the Batch irradiation is the simplest fuel management procedure, but results in higher fuel costs and requires the largest amount of reactivity control. In contrast, Discontinuous Outin achieves higher fuel burnups, and hence lower fuel costs, and requires less reactivity control than Batch, but requires more fuel changes and more irradiated fuel handling. The plant load factor will be somewhat lower than with Batch, due to the increased fueling downtime.

One of the assumptions in this study up to this time has been that the end-of-fuel life is governed by reactivity considerations. An alternative limit may be imposed by a maximum permissible fuel burnup, this limit being set, for example, by the sharply increased probability of fuel failure above a certain burnup level. Figure 6.41 shows the summary cost data presented in Figure 6.40, except that
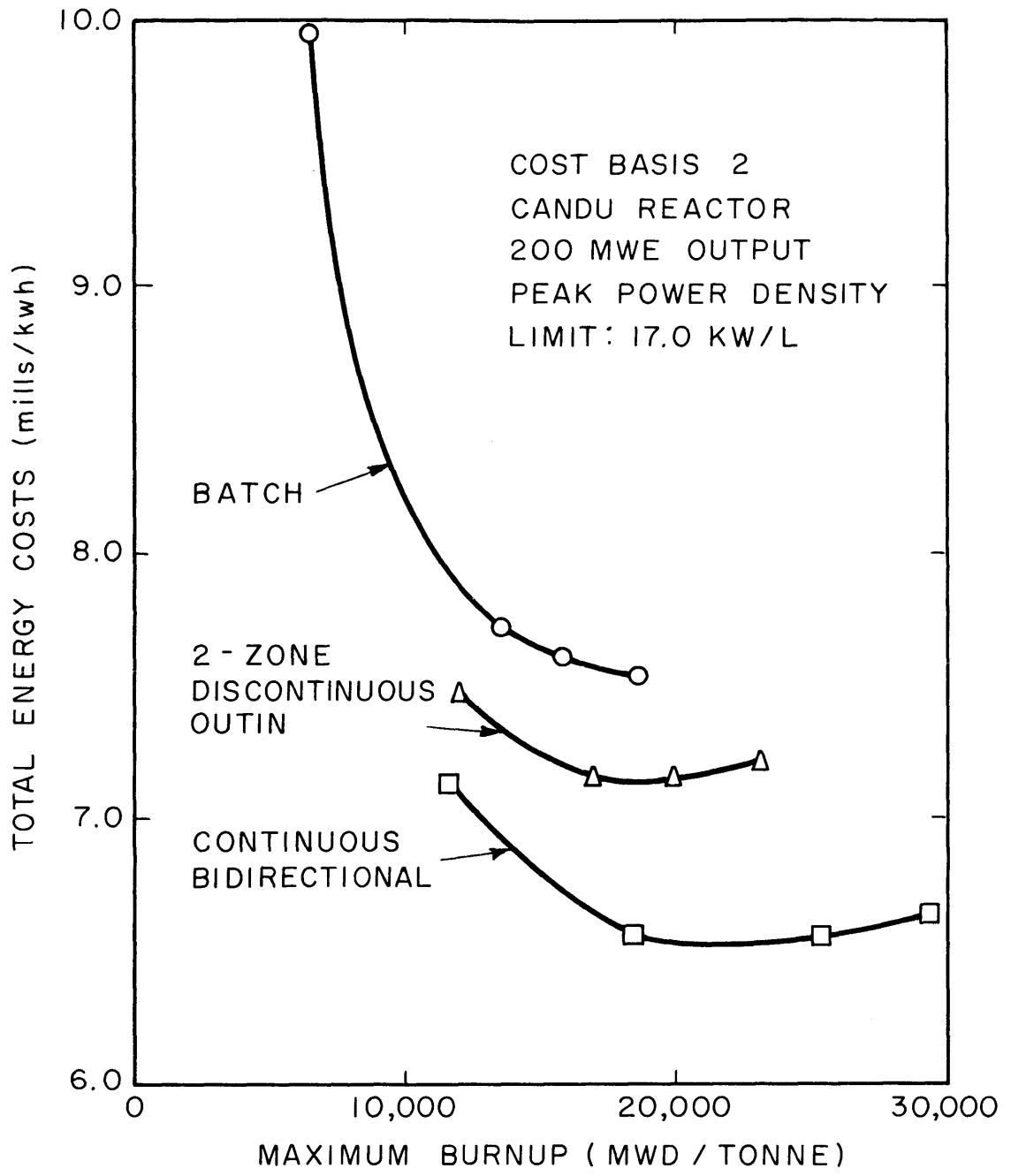
FIG. 6.41 TOTAL ENERGY COST AS A FUNCTION OF MAXIMUM BURNUP FOR VARIOUS FUEL AND POISON MANAGEMENT TECHNIQUES

total energy cost is presented as a function of maximum burnup for the three most important fuel management techniques. It is evident from Figure 6.41 that the relative advantages of bidirectional fueling are maintained. It may not be possible to operate at optimum enrichment, however. In spite of this, at any specified maximum burnup, the bidirectional fueling yields minimum total energy cost, and, in general, all comparisons between the three techniques will be similar, whether fuel lifetime is limited by criticality or by a maximum permissible burnup. This assumes, of course, that when a maximum burnup is specified, an appropriate enrichment is chosen so that the criticality end-of-life will coincide with the maximum burnup end-of-life.

A common basis for comparison of fuel and poison management techniques is the manner in which excess neutrons are utilized. In a reactor operating at constant power, the excess neutrons in a given region must either be absorbed in control poison, or leak away. Those leaking away can either be absorbed in a region with a deficiency of neutrons or can escape from the reactor entirely. This latter group are those that provide the flux gradient changes necessary to satisfy the boundary conditions on the reactor, and are therefore common to all fuel and poison management techniques. It is the balance between the remaining excess neutrons (those absorbed in poison and those which leak into neutron-deficient regions) which results in the variation in fuel performance with the various techniques. Hereafter, "excess neutrons" refers to those which are absorbed in poison or which leak into neutron-deficient regions.

An idealized illustration of the effect on fuel burnup and reactivity control requirement of changes in the distribution of excess neutrons between control poison absorptions and leakage into neutron-deficient areas, is shown in Figure 6.42, for Batch, two-zone Discontinuous and Continuous Irradiations. The model for this illustration, which was suggested by Arnold (A62), assumes a linear variation of the neutron excess with fuel burnup. Part I of Figure 6.42 shows the Batch case in which all excess neutrons are absorbed in control poison with the end of life occurring at burnup B. Part II shows the gain in
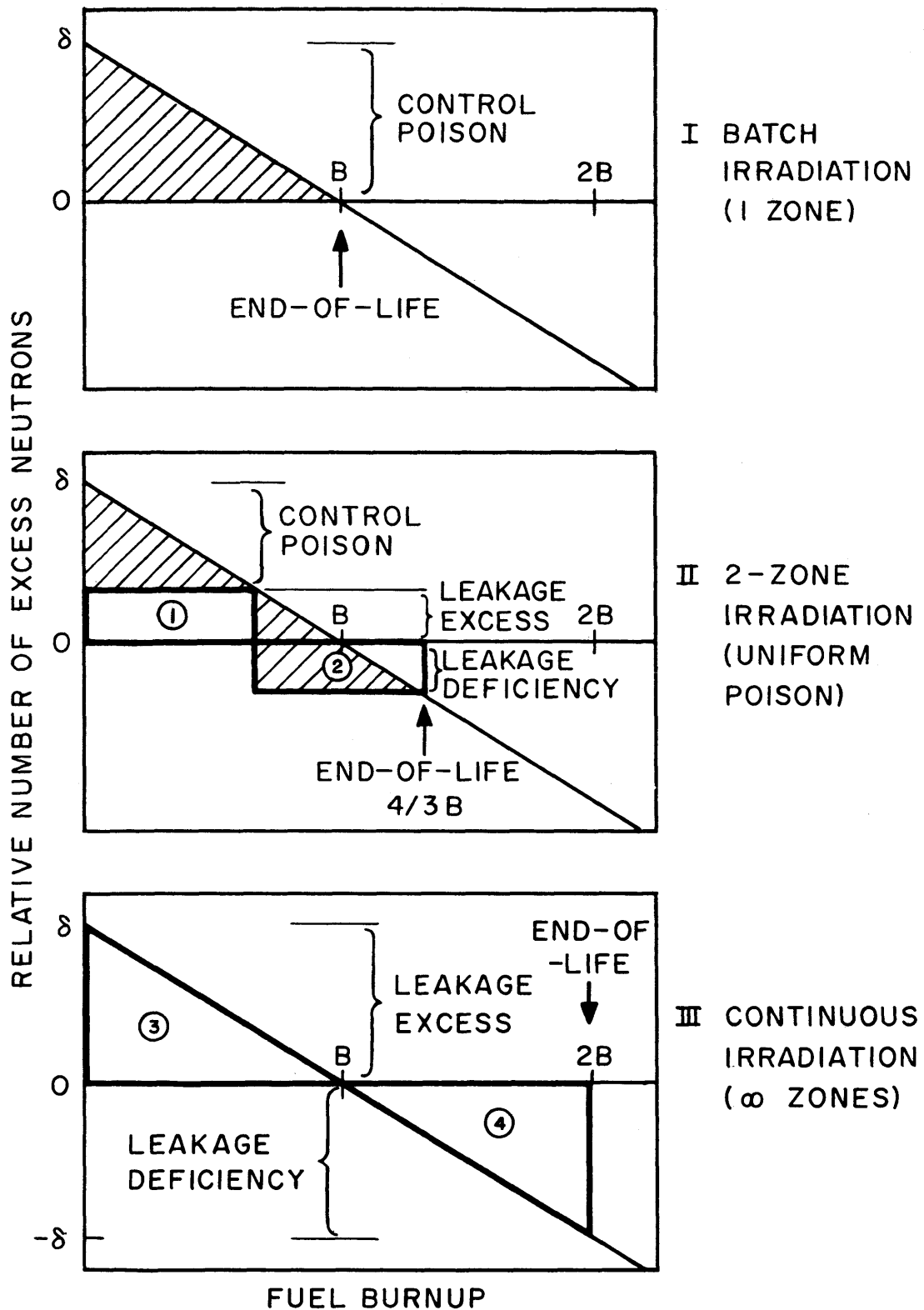
FIG. 6.42 THE EFFECT OF VARIOUS DEGREES OF EXCESS NEUTRON DISTRIBUTION BETWEEN CONTROL POISON AND LEAKAGE

330

burnup and the decreased control requirement when some of the excess neutrons, (1), are allowed to leak from the region of surplus to the region of deficit neutrons. Note that the deficit neutron region, (2), is deficient for the first part of the irradiation only, due to the presence of control poison which is assumed to be uniform. In Part III, all neutrons in the surplus region, (3), leak into the deficit region, (4), with no control poison absorptions. Note that the fuel burnup is double the batch burnup.

Referring to Part II, the manner in which the end-of-life burnup is obtained for the multi-zone irradiations will be developed. The criterion for criticality is that the area of surplus above the $\delta = 0$ line, (1), must equal the area of deficiency below the $\delta = 0$ line, (2). If b is the end-of-life burnup with two zones,

$$\frac{b}{2}\left(\frac{\delta b}{B} - \delta\right) = \frac{b}{2}\left(\delta - \frac{\delta b}{2B}\right)$$

or $\quad b = \frac{4}{3} B$

In general, for n zones,

$$b = 2B \frac{n}{n + 1}$$

In summary, the major point shown in Figure 6.42 is the increasing fuel burnup and decreasing control requirement that results when an increasing number of the excess neutrons in a surplus region are permitted to leak into a neutron-deficient region. Qualitatively, this conclusion agrees with that obtained using the MOVE Code. Quantitatively, the agreement is not so good, due to the idealized nature of the model. In particular, the burnup behavior of natural uranium differs somewhat from the linear dependence assumed. Also, the leakage of neutrons from surplus to deficient regions may involve flux gradients, which are generally undesirable from a power-density distribution point of view. This is not true of short-range leakage, such as occurs between the adjacent channels in bidirectional fueling but becomes a major factor in the continuous outin fueling, which relies on longer-range neutron diffusion and may also be important in the discontinuous outin fuel management procedure.

CHAPTER VII

CONCLUSIONS AND RECOMMENDATIONS

A. THE VERIFICATION OF THE FUEL CODE NEUTRON BEHAVIOR MODEL

The most complete available experimental data on measurements
of concurrent nuclide concentrations and reactivity changes during fuel
irradiation (W51) have been used in a comparison with the predictions of
the FUEL Code in an analysis of the behavior of uranium metal rods ir-
radiated in the NRX Reactor. The comparison of nuclide concentration
data showed excellent agreement except at the highest flux-times
(0.79 n/kb) where the higher Pu isotopes show a trend which indicates
insufficient Pu^{240} buildup in the FUEL Code predictions. This implies
that for uranium metal, the technique used for calculating resonance dis-
advantage factors underestimates the amount of self-shielding which occurs
in the large Pu^{240} resonance. This factor can be adjusted to yield better
agreement with experiment for the higher Pu isotopes at the highest flux-
times. Experimental data indicates that no adjustment of the Pu^{240}
resonance disadvantage factor is needed for UO_2 fuel (C42).

The comparison of experimental and FUEL Code reactivity changes
shows a constant discrepancy amounting to 0.6% in reactivity, but excellent
correspondence, otherwise. Since this discrepancy has been noted, using
a different neutron behavior model (W41), there is a good possibility that
the models may not be wholly responsible for the discrepancy. An error
in fission product yields has been postulated to explain this effect.

If this constant discrepancy is removed, the experimental and
FUEL Code reactivities agree very well, and when the uncertainty in the
FUEL Code value is obtained from uncertainties in the basic nuclear data,
the experimental values fall well within this uncertainty range.

Considering the above factors, the FUEL Code is capable of calculating the irradiation behavior of nuclear fuels to within accuracy limitations imposed primarily by uncertainties in basic nuclear data.

B. THE FUEL AND POISON MANAGEMENT STUDY

The inherent relationship between neutron economy, fuel burnup and control requirement is the basic reason for the relative importance of the various fuel and poison management techniques studies in this work. In order of increasing importance, these are: Batch Irradiation, Discontinuous Outin, and Bidirectional. There is a difference in fuel cost of about 1 mill/kwh between the Batch and the Bidirectional techniques, with the control requirement and fuel cost being a minimum and the fuel burnup and neutron economy being a maximum with Bidirectional, regardless of whether the fuel is criticality-limited or maximum-burnup-limited.

If there is a technical limitation which prevents the use of bidirectional fueling, the Discontinuous Outin technique is capable of performance superior to that of Batch irradiation, achieving better fuel burnups and requiring less reactivity control.

When Bidirectional fueling is used, the following factors favor the use of enriched uranium over natural.

1) Lower fuel costs

2) Smaller core volumes for the same power output

3) More conservative pressure tube design

4) Fewer on-line fuel changes

Conversely, the following disadvantages are encountered.

1) Higher fuel burnups are necessary.

2) Operation during the startup period is more difficult, due primarily to control requirements.

334

C. RECOMMENDATIONS FOR FUTURE WORK

The following potential uses of the FUELMOVE Code are suggested.

1. The Startup Problem in Bidirectional Fueling

A detailed investigation of the effect of various parameters on the bidirectional startup could be investigated. Specifically, the following points might be studied for the CANDU reactor.

1) The effect on power distribution of varying fuel charging rates radially.

2) How long to recharge discharged fuel before starting to charge new fuel.

3) The effect of higher enrichments on the power distribution and fuel costs during the transient period.

2. The Study of Fuel and Poison Management in Control Limited Reactors

The results presented in this work indicate that burnable poison can be used to lower fuel costs in control-limited reactors when operated batchwise. The reduced control requirement of discontinuous outin will also enable improvements over batch irradiation under control-limited situations. The use of burnable poison with the discontinuous fueling might offer even further advantages.

3. The Study of Discontinuous Graded Fuel Irradiation

One of the disadvantages of the discontinuous outin fueling technique is that for an "n" zone reactor, irradiated fuel must be handled "n" times before it is finally discharged. A further disadvantage is the flux and power peaking which tends to occur in the outer zone. A fuel management technique which does not have these disadvantages, but which is capable of equivalent performance otherwise, is the discontinuous graded technique in which the most irradiated fuel in a group of fuel elements is replaced by fresh fuel. Each group of fuel elements in the reactor has the same rational fraction of its fuel replaced, and the fuel is irradiated batchwise between fuel changes. A MOVE Code subroutine could be written to facilitate a study of this fuel management procedure.

APPENDIX A

OPERATIONAL INFORMATION

1. Input Data Card Formats

The **FUELMOVE** Code uses the three standard Fortran II input data forms 1) <u>Hollerith</u> for transmitting alphanumeric identification information; 2) <u>Integer</u> for transmitting integer numerical information; and 3) <u>Floating</u> point for transmitting floating point (decimal) information.

In the **FUELMOVE** Code, the Hollerith information when it is used, occupies the full width (72 spaces) of the standard IBM Card. On the card, the first character, which controls the output spacing, should be left blank, or made zero. Integer information is generally transmitted 24 per card, with 3 spaces per integer field, with the integers always being as far to the right of the field as possible. Floating point information can be transmitted in various equivalent ways, with or without the E designation. When used, the exponent field must be moved to the far right. As an example, the following forms give the value 1·2, assuming a field width of 8:

```
1  2  3  4  5  6  7  8
               1  ·  2
      1  ·  2
      ·  1  2     E  1
   ·  1  2     E  +  0  1
      1  2  ·  E  -  1
```

2. The FUEL Code

2.1 Input Data Preparation

A typical calculation of input data for the FUEL Code is given below. Specifically the CANDU unit cell is calculated from data given in Section VI B, Table 6.1.

N_5^O: Initial U^{235} concentration

$$N_5^O \; \frac{atoms}{barn \; cm.} = \frac{atom \; fraction \; x \; density \; x \; N_o \; x \; 10^{-24}}{Mol. \; wt.}$$

$$= \frac{.007206 \; x \; 10.2 \; x \; .6025}{270.10}$$

$$= 1.6396 \; x \; 10^{-4} \; atoms/barn \; cm. \; of \; fuel$$

N_6^O: Initial U^{236} concentration $N_6^O = 0.$

N_7^O: Initial fission product concentration $N_7^O = 0.$

N_8^O: Initial U^{238} concentration

$$N_8^O = \frac{.9928 \; x \; 10.2 \; x \; .6025}{270.10}$$

$$= 2.259 \; x \; 10^{-2} \; atoms/barn \; cm.$$

$N_9^O - N_{12}^O$:   Initial Plutonium isotope concentration

$$N_9^O = N_{10}^O = N_{11}^O = N_{12}^O = 0$$

337

EVCUT: the cutoff energy at the upper end of the thermal region in electron volts. The resonance integral data in the FUEL Code is consistent with EVCUT = 0.45ev

$$EVCUT = 0.45ev$$

SDP: the slowing down power of the non-fuel part of the unit cell in cm^{-1}

$$SDP = \xi \Sigma_s = \frac{\sum\limits^{\text{non-fuel}} \xi_i \sigma_{si} N_i V_i}{\sum\limits_{\text{non-fuel}} V_i} \qquad \dagger$$

$$= 0.16135 \ cm^{-1} \ (\text{of non-fuel})$$

TMOD: the average moderator temperature in Centigrade. In a cold moderator, hot coolant unit cell, the average is obtained by volume-flux weighting.

$$TMOD = \frac{(V \cdot \psi)_C T_C + (V \cdot \psi)_M \cdot T_M}{(V \cdot \psi)_C + (V\psi)_M}$$

$$= 85.27^{\circ}C.$$

PSI1(8): the resonance disadvantage factor for U^{238}. This quantity is best obtained by means of a trial run in which a desired initial conversion ratio is obtained. For an ICR of 0.77,

$$P_8 = 0.8925$$

$$PSI1(8) = \frac{-C_1 N_8^o I_8}{\ln P_8}$$

$$= \frac{0.3335 \times .02259 \times 282.}{0.11373}$$

$$= 18.68$$

$\dagger$　See Table A.1

Table A.1 FUEL Code Input Data Calculations

(Based on cross sections from Table 6.1)

Item	$N \times 10^{-24}$	V	ψ	$V\psi$	$\sigma NV\psi$	$\sum \sigma_s NV$	$\sigma_{tr} NV\psi$
Fuel	0.02275	27.96	1.000	27.96	------	------	10.18
Cladding	0.0429	4.08	1.003	4.09	0.0369	0.031	1.43
Coolant	0.0254	21.48	1.1	23.63	0.0014	2.949	6.33
Press Tube	0.0429	11.28	1.265	14.26	0.1285	0.086	4.98
Gap	0.	16.26	1.31	(21.31)*	------	------	------
Cal. Tube	0.0429	4.60	1.357	6.23	0.0561	0.035	2.17
Moderator	0.0324	461.89	1.823	842.13	0.0614	80.734	287.57
Totals	-------	①547.55	-----	③(939.61)	------	------	⑦312.66
Totals, non-fuel	-------	②519.59	-----	④890.34	⑤0.2843	⑥83.835	------

* This term included only in ③ for calculation of **D**

$$\text{SDP} = \frac{⑥}{②} = 0.16135 \qquad \text{PSI} = \frac{④}{②} = 1.7135$$

$$\text{SIGOMD} = \frac{⑤}{④} = 3.19 \times 10^{-4} \qquad \text{D} = \frac{1}{3} \cdot \frac{③}{⑦} = 1.002$$

C_1:   constant term in the resonance escape probability in cm.

$$C_1 = \frac{V_{fuel}}{\Sigma_s \times V_{non-fuel}} = \frac{27.958}{0.16135 \times 519.59}$$

$$= 0.3335 \text{ cm.}$$

EPSI: fast fission effect = 1.0173

P1IN: fast non-leakage probability

$$P1IN = \frac{1}{1 + B_g^2 \tau}$$

$$= \frac{1}{1 + 1.08 \times 10^{-4} \times 143.5} = 0.9847$$

SIGOMD: the unhomogenized 2200 m/s macroscopic cross section of the non-fuel region, in cm^{-1}

$$SIGOMD = \frac{\sum\limits_{non-fuel} N_i \sigma_i \psi_i V_i}{\sum\limits_{non-fuel} \psi_i V_i} = 3.19 \times 10^{-4} cm^{-1} \quad †$$

SGOXEG: the microscopic 2200 m/s Xe cross section, times its Westcott "g factor" at T_{MOD}, in barns

$$SGOXEG = \sigma_{xe}^o \cdot g_{T_{MOD}}$$

$$= 2.40 \times 10^6 \times 1.2628 = 3.03 \times 10^6 \text{ barns}$$

VFL: the fraction of the unit cell volume which is fuel.

---

† See Table A.1

340

$$VFL = \frac{\sum\limits_{fuel} V_i}{\sum\limits_{fuel} V_i + \sum\limits_{non\text{-}fuel} V_i} = 0.05106$$

PSI: the ratio of average flux in the non-fuel region to the average flux in the fuel.

$$PSI = \frac{\sum\limits_{non\text{-}fuel} V_i \times \psi_i}{\sum\limits_{non\text{-}fuel} V_i} = 1.7136 \qquad \dagger$$

POWERD: the average core power density in kw/1 of core

$$POWERD = \frac{\text{Total Thermal Power in MW}}{\text{Total core volume in } m^3}$$

$$= \frac{715.5}{\pi \times 2.302^2 \times 5.} = 8.5956 \text{ kw/1}$$

ZETA: the flux-time step size used in the step-wise solution of the nuclide concentration equations, in neutrons/barn. For accuracy, this step size should not be much greater than .0003 n/b.

ZETA = .00025 n/barn

SGMSFL: the macroscopic fast scattering cross section of the fuel region, in cm^{-1}

---

†   See Table A.1

341

$$\text{SGMSFL} = \frac{.6025 \times 10^{24} \times 10.2 \times 15.8}{270.1}$$

$$= 0.3595 \text{ cm}^{-1}$$

(based on $\sigma_s = 8.3b$ for U, and $\sigma_s = 3.75b$ for 0)

ANBP: the concentration of burnable poison in atoms/barn cm. In the code $N_{13}{}^o$ is set equal ANBP.

      ANBP = 0.

SIGOBP: the microscopic 2200 m/s cross section of burnable poison, in barns.

      SIGOBP = 0.

SGOIN7:   the microscopic 2200 m/s cross section of initial fission products, in barns.

      SGOIN7 = 47.67 barns

      (this value is consistent with the initial value of the built-in fission product cross section which is used every flux-time step past the first)

TAU: the Fermi Age = 143.5 cm^2

D: the diffusion length in cm

$$D = \frac{1}{3\Sigma_{tr}} = \frac{1}{3} \frac{\sum\limits_{all} V_i \psi_i}{\sum\limits_{all} N_i \sigma_{tr,i} V_i \psi_i} \dagger$$

$$= 1.002 \text{ cm.}$$

$\dagger$ See Table A.1

342

PDNLIM: the maximum permissible power density rating of the fuel in kw/l.

Based on $kd\theta$ = 40 w/cm = 505 w/cm length, transferred to coolant or $\frac{505}{.94}$ = 537 w/cm total power produced, and a peak to average power density ratio within the cluster of 1.096:

$$PDNLIM = \frac{.537 \frac{kw}{cm} \times 19 \text{ rods/unit cell}}{1.096 \times .5475 \text{ 1/cm}} = 17.00 \text{ kw/l}$$

RIUFP: the resonance integral for fission products from uranium fissions, in barns

RIUFP = 181 barns

RIPFP: the resonance integral for fission products from plutonium fissions, in barns

RIPFP = 264 barns

FPFCTR: an arbitrary factor which multiplies the built-in fission product cross section

FPFCTR = 1.0

APSI: the constant of proportionality used to vary the thermal disadvantage factor, PSI, with flux-time. Its units are: fractional change per flux-time step.

APSI = 0.

RIBP: the resonance integral of the burnable poison, in barns

RIBP = 0.

OMPMOD: the resonance capture probability of the non-fuel region of the unit cell.

343

$$\text{OMPMOD} = 1 - p_{\text{MOD}} \approx C_1 \sum_{\text{non-fuel}} \frac{V_i}{V_{\text{fuel}}} \frac{N_i \, \text{RI}_i^{\infty}}{\psi_{1,i}}$$

$$= C_1 \left[\frac{V_{D_2O}}{V_{\text{fuel}}} N_{D_2O} \, \text{RI}_{D_2O} + \frac{V_{zr}}{V_{\text{fuel}}} N_{zr} \, \text{RI}_{zr} \right]$$

$$= .3335 \, [0.59 \times 10^{-3} + 18.41 \times 10^{-3}]$$

$$= 6.34 \times 10^{-3}$$

IL: the number of velocity points in the Wilkins thermal flux spectrum, between 0 and EVCUT, inclusive of the two end points. Must be an odd integer less than 100

      IL = 49

NUMPOZ: the number of flux-time steps at which nuclide concentrations and properties are to be obtained, including zero flux-time. The final flux-time that will be reached in the calculations will be ZETA (NUMPOZ-1)

      NUMPOZ = 31   (Must be < 61)

NUMSPA: the number of flux-time solution points per fit point. The quantity, $\text{JAY} = 1 + \dfrac{(\text{NUMPOZ-1})}{\text{NUMSPA}}$, must be an integer less than 16.

      NUMSPA = 3.

IPSI: the resonance disadvantage factor control parameter: if IPSI = 0, the Crowther-Weil treatment of resonance disadvantage factors is used; if IPSI = 2, factors are read-in which multiply the Crowther-Weil factors; if IPSI = 1,

constant read-in factors are used, or if IPSI < 0, the disadvantage factors are set equal unity. In all cases above the U^{238} resonance disadvantage factor, PSI1 (8), is kept unchanged from its input magnitude.

IPSI = 0

ISKIP: the binary output tape position control parameter. If MOVE Code output data is to be transferred to the FUEL Code via binary tape, ISKIP controls the tape position so that new data going onto the tape need not erase data already put on the tape. Specifically, ISKIP is the number of data groups (i.e., different enrichments) that are to be skipped before the new data is recorded on the binary output tape. Each data group is made up of four binary records.

IPRNT: a written output control parameter. If IPRNT ≠ 0, the final summary of results is printed out. Generally, IPRNT = 1.

NOT: Output Tape logical number. NOT = 2 at MIT.

NPT: Punch Tape logical number. BCD tape is written for subsequent punching of cards off-line. These cards will be used by the MOVE Code as input data. At MIT, NPT = 3. If punched-card output is not desired, set NPT = 0.

NWT: Write Tape logical number. Binary tape is written, using ISKIP for tape positioning, for subsequent use as input by the MOVE Code. If binary tape output is not desired, set NWT = 0.

IPRT1: a written output control parameter, generally set = 0. If IPRT1 ≠ 0, cross sections at each velocity point are

printed out.

IPRT2:   a written output control parameter, generally set = 0. If IPRT2 $\neq$ 0, the results computed by each subroutine are printed out, at each flux-time step.

IPRWLK: a written output control parameter, generally set = 0. If IPRWLK $\neq$ 0, the flux magnitude and the hardening parameter are printed out at each velocity point, at each flux-time step.

The following tables give the specific location on the input cards for the above information. The three input types H, for Hollerith, F for floating point (decimal) information and I for integer, are specified in each case.

Table A. 2 FUEL Code Input Data Card Formats

Card No.	Column No.	Type	Item	Compatible Units
1	1-72	H	Identification	-
2	1-12	F	N_5^o	atoms/barn cm of fuel
2	13-24	F	N_6^o	"
2	25-36	F	N_7^o	"
2	37-48	F	N_8^o	"
2	49-60	F	N_9^o	"
2	61-72	F	N_{10}^o	"
3	1-12	F	N_{11}^o	"
3	13-24	F	N_{12}^o	"
3	25-36	F	EVCUT	ev
3	37-48	F	SDP	cm^{-1}
3	49-60	F	TMOD	^oC
3	61-72	F	PSI1(8)	-
4	1-12	F	C_1	cm
4	13-24	F	EPSI	-
4	25-36	F	P1IN	-
4	37-48	F	SIGOMD	cm^{-1} of moderator
4	49-60	F	SGOXEG	barns
4	61-72	F	VFL	-

Table A.2 FUEL Code Input Data Card Formats

Card No.	Column No.	Type	Item	Compatible Units
5	1-12	F	PSI	-
5	13-24	F	POWERD	kw/
5	25-36	F	ZETA	neutrons/barn
5	37-48	F	SGMSFL	cm^{-1} of fuel
5	49-60	F	ANBP	atoms/barn cm of fuel
5	61-72	F	SIGOBP	barns
6	1-12	F	SGOIN7	barns
6	13-24	F	TAU	cm^2
6	25-36	F	D	cm
6	37-48	F	PDNLIM	kw/
6	49-60	F	RIUFP	barns
6	61-72	F	RIPFP	barns
7	1-12	F	FPFCTR	-
7	13-24	F	APSI	fraction per flux-time step
7	25-36	F	RIBP	barns
7	37-48	F	OMPMOD	-
8	1-3	I	IL	-
8	4-6	I	NUMPOZ	-
8	7-9	I	NUMSPA	-
8	10-12	I	IPSI	-

348

Card No.	Column No.	Type	Item	Compatible Units
8	13-15	I	ISKIP	-
8	16-18	I	IPRNT	-
8	19-21	I	NOT	-
8	22-24	I	NPT	-
8	25-27	I	NWT	-
8	28-30	I	IPRT1	-
8	31-33	I	IPRT2	-
8	34-36	I	IPRWLK	-
Note:	the following are used only if IPSI > 0			
9	1-12	F	PSI1(5)	-
9	13-24	F	PSI1(6)	-
9	25-36	F	PSI1(7)	-
9	37-48	F	PSI1(9)	-
9	49-60	F	PSI1(10)	-
9	61-72	F	PSI1(11)	-
10	1-12	F	PSI1(12)	-
10	13-24	F	PSI1(13)	-

2.2 Assembly of the FUEL Code FORTRAN Source Deck

The use of the SHARE program RKY3 for the step-by-step integration of the nuclide concentrations deserves mention. In order to avoid using a long transfer vector in the RKY3, the following must be done to the NUCON binary deck following assembly.

(1) Insert a correction card changing "GO TO 40" to "GO TO 60" (See NUCON Source deck)

(2) Add an entry point to the NUCON program card, to be called DERIV1. This entry point is to correspond to the FORTRAN statement, "CALL DERIV"

(3) Add an entry point to the RKY3 program card, to be called RETRKY, corresponding to the location RETRKY in the program listing.

In addition to the above, it should be noted that COMMON storage in the 704 FORTRAN starts at 32,562 while it is one lower in the 709 and 7090 FORTRAN. Since the transfer of data takes place between subprograms by using COMMON, the specified absolute location at the end of the RKY3 program listing should agree with the FORTRAN system being used.

3. Data Transfer from the FUEL Code to the MOVE Code

3.1 Introduction

The MOVE Code, which performs the fuel and poison management studies, requires as part of its input, the properties of various types and/or enrichments of fuel, as functions of flux-time. Specifically there are five blocks of magnetic core memory reserved for the storage of the properties during burnup of up to five different fuel types, for use by the MOVE Code.

These properties can be transmitted from the FUEL Code to the MOVE Code in one of two ways, either by card or binary tape.

When card transfer is used, a group of cards containing the flux-time history of a given fuel type is punched out by the FUEL Code. Subsequently, up to five of these groups of cards, each describing a different fuel type or enrichment, are loaded into the blocks of MOVE Code memory in the order in which they are presented to the MOVE Code as input. When tape transfer is used, a series of binary tape records is made up by the FUEL Code, each group of four records describing the burnup history of one fuel type. The MOVE Code is told to select certain of these groups on the tape and to load this information into the specified blocks of MOVE Code memory.

3.2 Card Transfer

Table A.3 lists the card format which the FUEL Code punches out, and which is used by the MOVE Code as input. The first two cards contain parameters which are, with three exceptions, input data for the FUEL Code. The three exceptions are: 1) JAY = 1 + $\dfrac{NUMPOZ - 1}{NUMSPA}$ which is the number of Lagrangian fit points for the flux-time fitting of the seven homogenized properties and the nuclide concentrations, 2) C5P = λ_{xe}/σ_{xe} in (barn sec)$^{-1}$, and 3) SIGMSM, the initial homogenized Sm group cross section.

Following these first two cards, are "JAY" groups of three cards each. Each group of cards contains the seven properties, and the nuclide concentrations at one flux-time point. Also included are TZ, the flux-time for this group of cards, normalized to ZETA, and ALAG, the denominator of the Lagrangian coefficient for the group.

3.3 Tape Transfer

The same data that is transferred by card may be transferred by binary tape, with one tape containing FUEL Code results for any number of different fuel types or enrichments. The positioning of the

Table A. 3 FUEL Code Output Data Card Formats

Card No.	Column No.	Type	Item Description	FORTRAN Symbol
1	1-12	I	JAY	JAY
1	13-24	F	ZETA	ZETA
1	25-36	F	EPSI	EPSI
1	37-48	F	VFL	VFL
1	49-60	F	C5P	C5P
1	61-72	F	TAU	TAU
2	1-12	F	D	D
2	13-24	F	PDNLIM	PDNLIM
2	25-36	F	SIGMSM	SIGMSM
Note:	the following group of 3 cards is repeated JAY times			
1	1-12	F	θ/ZETA	TZ
1	13-24	F	$\Sigma_{Xe, max}$	SGXMTZ
1	25-36	F	$\Sigma_{TOT} - \Sigma_{Xe}$	SGM1TZ
1	37-48	F	Σ_f	C53TZ
1	49-60	F	$\nu\Sigma_f$	C10TZ
1	61-72	F	$(1-p)/(1+\alpha)$	C54TZ
2	1-12	F	$<\eta(1-p)>$	C11TZ
2	13-24	F	p	PLTZ
2	25-36	F	−	ALAG
2	37-48	F	N_5	ANTZ(5)
2	49-60	F	N_6	ANTZ(6)
2	61-72	F	N_7	ANTZ(7)
3	1-12	F	N_8	ANTZ(8)
3	13-24	F	N_9	ANTZ(9)
3	25-36	F	N_{10}	ANTZ(10)
3	37-48	F	N_{11}	ANTZ(11)
3	49-60	F	N_{12}	ANTZ(12)
3	61-72	F	N_{13}	ANTZ(13)

tape by use of ISKIP, prior to recording a new set of results by the FUEL Code was detailed in the previous section. The positioning of the tape by the MOVE Code to obtain certain sets of FUEL Code results will be described. Inasmuch as the tape has been made up with no specific identification, it is necessary to know the relative location on tape of the desired fuel properties, for example, to know that the desired fuel is the seventh of the various fuel types on the tape. The five parameters which control the tape input, LOCPRP (1) to LOCPRP (5), are part of the MOVE Code input data. When LOCPRP (3) is assigned the value, 7, this implies that the seventh group of tape records is to be transmitted to the third block of MOVE Code storage. There is no restriction on numerical order of the values assigned to LOCPRP (1) to LOCPRP (5). However, the MOVE Code will stop if a value of LOCPRP is greater than 50.

4. The MOVE Code

4.1 Input Data Preparation

The factors entering into the preparation of MOVE Code input data will be discussed. The numbers used are for the CANDU Reactor whose core is divided into two equal volume radial zones.

R(1) to R(10): the outer radii for each radial mesh area. Referring to Fig. 4.2, it can be seen that the mesh point is midway between two adjacent radii. Generally, these radii will be equally spaced. However, when equal volume zones are required, it is necessary that the radii be chosen for this requirement. Whatever the requirement, an attempt should be made to keep the mesh spacing as uniform as possible, and there should not be more than 30% difference between adjacent mesh spacings. The following are recommended choices for the number of mesh points per equal volume zone.

1 zone: 3 to 10
2 zones: 5 (inner) + 2 or 7 + 3
3 zones: 2 (inner) + 1 + 1 or 4 + 2 + 2
4 zones: 2 (inner) + 1 + 1 + 1 or 4 + 2 + 2 + 2
5 zones: 2 (inner) + 1 + 1 + 1 + 1

For the particular example of two equal volume zones with five mesh points in the inner zone plus two in the outer:

R(1) = 32.555
R(2) = 65.110
R(3) = 97.665
R(4) = 130.221
R(5) = 162.776   (end of first zone)
R(6) = 196.488
R(7) = 230.2 cm   (outer core radius)
R(8) = 0.
R(9) = 0.
R(10) = 0.

H:	the axial height of the core
	H = 500 cm
δR:	the radial reflector savings. This was obtained from the stated (L61) geometrical buckling of
	$$B^2 = \left(\frac{2.405}{R+\delta R}\right)^2 + \left(\frac{\pi}{H+2\,\delta H}\right)^2 = 1.0824 \text{ m}^{-2}$$
	and an unreflected axial extrapolation of
	$0.71\,\lambda_{tr} = 2.13D = 2.1$ cm:
	$\delta R = 58.45$ cm
δH:	the axial reflector savings
	$\delta H = 2.1$ cm (above)
ZSYM:	the axial symmetry control. If ZSYM = 0., the reactor core is assumed to be axially symmetric about the mid-plane.
	ZSYM = 0.
DBSQU:	the initial thermal leakage estimate in cm^{-1}
	DBSQU = D $\cdot$ B^2 = 1.002 x 1.08 x 10^{-4}
	= 1.08 x 10^{-4} cm^{-1}
PFAST:	the initial fast non-leakage probability estimate:
	$$\text{PFAST} = \frac{1}{1 + B^2 \tau} = 0.9847$$
PDENAV:	the core average power density in kw/l
	PDENAV = $\dfrac{\text{Total thermal output}}{\text{Total core volume}}$
	= 8.5956 kw/l
RMAX:	the maximum permissible peak-to-average power density ratio. (Not used in the current version of FUELMOVE)
ERROR:	the criterion for flux iteration convergence. When $(\Delta\phi/\phi) <$ ERROR at all points in the core, the flux is assumed to be converged.
	ERROR = 0.01 or 0.005

355

DELCRT: the end-of-irradiation criterion. When the criticality, $C = CRIT \pm DELCRT$, the burnup calculations are stopped and a cost analysis is performed on the discharged fuel

DELCRT = 0.0015

DELTD: the down-time in years required for unloading and recharging a reactor core.

DELTD = 7 days = 0.0192 years

CRIT: the desired end-of-irradiation unpoisoned criticality, which is normally unity.

CRIT = 1.

At this point the control parameters for the MOVE Code will be listed. There are three types: 1) logical control, 2) output control, and 3) input control. In general, when any of these are zero, an option is _not_ used, output is _not_ given, or input is _not_ desired. Also, the input controlled by the six input options will be read in, in the same sequence as these options appear on the input data cards.

NZONE(1) to NZONE(5):

    the number of radial mesh points per radial zone.
    NZONE(1) = 5
    NZONE(2) = 2
    NZONE(3) = NZONE(4) = NZONE(5) = 0

LOCPRP(1) to LOCPRP(5):

    the relative location on binary tape of FUEL Code data, which is to go into MOVE Code storage, blocks 1 to 5. This was described in the previous section.

    LOCPRP(1) to LOCPRP(5) = 0, since the FUEL Code input in this example will be by card, not tape.

IPROP(1) to IPROP(5):

    the MOVE Code block storage location containing the FUEL properties that are to be used in radial zones

356

1 to 5. For example, if IPROP(2) is set equal to 4, this implies that the fuel properties for radial zone 2 are located in the MOVE Code block storage location 4. Block storage location 4 had obtained these properties from the FUEL Code either by card or binary tape.

IPROP(1) = 1
IPROP(2) = 1
IPROP(3) = IPROP(4) = IPROP(5) = 0

IRL: the total number of radial mesh points. This must be consistent with the numbers specified by IZONE(1 to 5), and be less than 11.

IRL = 7

JZL: the total number of axial mesh points. This is generally (though not necessarily) set equal to IRL, and must be less than 16.

JZL = 7

IZONE: the number of radial zones. This must be consistent with NZONE(1 to 5) and less than 6.

IZONE = 2

NLOAD: the input control parameter for the input of FUEL Code results. This specifies the number of blocks of FUEL Code data that are to be read from cards or tape, and must be less than 6.

NLOAD = 1

NOT: logical number of the output tape. At MIT,

NOT = 2

NRT: logical number of the read tape containing FUEL Code results. If NRT = 0, the results are to be obtained by card reading.

NRT = 0

IMUV: the fuel management control parameter.

If ISSCNT = 0: IMUV = 1 Batch irradiation

= 2 Discontinuous outin, startup

= 3 Discontinuous outin, steady state

= 4 Continuous bidirectional, startup

= 5 Discontinuous bidirectional

If ISSCNT ≠ 0: IMUV = 1 Continuous outin and/or graded

IMUV = 2 Continuous bidirect; discharge flux-time, θ_d, specified

IMUV = 3 Continuous bidirect; axial velocity, V_z, specified

IPOIS: the poison management control parameter (cf. Sect. IV, C3.1).

IPOIS = 0 no control poison

IPOIS = 1 uniform poison removal

IPOIS = 2 radial zone poison removal

IPOIS = 3 axial bank poison removal

NPOISR: the number of radial mesh points, starting at the outer edge containing no control poison. This is normally zero.

NPOISZ: the number of axial mesh points, starting at the end, containing no control poison. This is normally zero.

NSTEP: the number of distinct fuel changes that are to be made in the discontinuous irradiations.

ISSCNT: the control parameter for steady-state continuous fuel irradiations. If ISSCNT = 0, the steady state continuous fuel movements are not desired. (See IMUV)

IBATCH: the control parameter for batch fuel irradiation. If IBATCH = 0, batch irradiation of the fuel does not take place.

IGNORR: an unused control parameter.

ITRATE: the parameter which controls the maximum of iteration loops to obtain the correct value of control poison ($C_w = 1 \pm .005$)

IPRT1:   the print option controlling the printing of the flux shape and power density shape. If IPRT1 = 0, the flux and power shapes are printed out <u>only</u> at the start and end of batch irradiation, or for the final (C = 1.) continuous steady-state irradiations.

IPRT2:   the print option used only on program checkout. This option controls the printout of all the detailed calculations of all subroutines. Once the program is working, IPRT2 = 0, always.

IPSPPR: the print option controlling the output of the subroutine PTPROP. If IPSPPR $\neq$ 0, the values of the seven properties are printed out at each mesh point. IPSPPR = 0, normally.

IPSGMW: the print option controlling the control poison cross-section print-out. If IPSGMW $\neq$ 0, the control poison cross section at each point is printed out.

IPOWD: the power density input control. If IPOWD $\neq$ 0, the relative power density is read in at each mesh point, and the subsequent irradiation will proceed at constant power density.

INORMP: the normalized control poison input control. If INORMP > 0, the normalized control poison, Σwn, is read in at each point. If INORMP = 0, Σwn is set = 1.0 at each point. If INORMP < 0, the current values of Σwn go unaltered.

IABSP: the absolute (fixed) poison input option. If IABSP > 0, the absolute poison, Σwa, is read in at each point. If IABSP = 0, Σwa is set equal zero at each point, and if IABSP < 0, the current values of Σwa go unaltered.

ITHET: the flux-time input option. If ITHET > 0, the flux-time
           in n/kb is read in at each point, followed by the time,
           in years. If ITHET = 0, the flux-time at each point and
           the time in years are set equal zero, and if ITHET < 0,
           the current flux-time values and the time go unaltered.

ICSTRD: the cost-data input option. If ICSTRD ≠ 0, ICSTRD sets
           of cost data are read in. After the read-in, ICSTRD is
           set equal to zero.

In addition to the above input, the individual fuel movements,
with the exception of batch irradiation, require input on the first time
entry is made into them, and the continuous steady-state fuel move-
ments require input every time entry is made.

When entry is made to the continuous steady-state fuel move-
ments (ISSCNT ≠ 0), an identification card, plus the following input are
required.

THETA1:   the first estimate of the characteristic discharge flux-
           time.

THETA2:   the second estimate of the characteristic discharge
           flux-time.

DAMP1:   the damping factor between successive flux-time esti-
           mates. Normally, DAMP1 = 0.5.

EFF: the fraction by which the mid-plane flux-time in bi-
           directional differs from one half of the discharge flux-
           time. This is normally set = 0.

ERROR: the flux convergence criterion. When, for all points in
           the core, the fractional flux change between two suc-
           cessive iterations $(\Delta \phi/\phi) \leq$ ERROR, the flux is assumed
           to have converged.

           ERROR = 0.01 or 0.005

DELCNV: the convergence criterion on criticality. When the
           criticality changes by less than DELCNV between two

successive iterations, the criticality is assumed to have converged, and its value is assumed to be characteristic of the flux-time estimate which led to this criticality. This is normally set at .001 or .0005, and should be less than DELCRT.

LPMX: the number of iteration loops on Σwa to obtain the flattest power distribution. When IABSP = 0 (and hence Σwa = 0), LPMX will be set equal to zero. Otherwise, it requires from three to five loops to obtain the Σwa distribution which yields the flattest power.

NEXT: the control parameter for the next run within CONSTS. If NEXT = 0, an exit is made back to the MAIN program. If NEXT ≠ 0, IMUV is set = NEXT, and a new series of continuous steady-state runs can be performed without returning to MAIN.

FCTR(1) to FCTR(10):
When IMUV = 1(graded and/or outin), FCTR(I) governs whether the particular radial mesh point, I, is to be run graded, or outin. If FCTR(I) = 0, it is to be run outin. Otherwise, it is run as graded with the midplane maximum graded flux-time given by FCTR(I) · THETAC where THETAC is the current characteristic flux-time. When IMUV > 1(bidirectional), FCTR(I) is either the flux-time relative to THETAC (IMUV = 2) or the relative axial velocity (IMUV = 3).

When entry is made to the batch-type fuel movements (ISSCNT = 0), the following input is required.

ZET2:   the central flux-time step for batch irradiation.

If IMUV = 2 or 3 (discontinuous outin):

INVERT(1) to INVERT(5):The axial inversion control parameter. If INVERT(2) ≠ 0, fuel in the second zone (before transfer) will be inverted. Inversion can take place only with axial symmetry (ZSYM = 0).

361

IMOVE: If IMOVE = 0, no fuel will be transferred (or dis-
           charged). Normally, IMOVE ≠ 0.

IGRAD: If IGRAD = 0, the average flux-time at any axial
           height is transferred. If IGRAD ≠ 0, the radial
           flux-time gradient is transferred. In this work,
           IGRAD ≠ 0.

IPR: this is the IPROP (fuel type) of the new fuel being
           charged to the outer zone.

NSHUF: this is the number of fuel shuffling operations that
           are to be carried out using the current control
           parameters. For example, if NSHUF = 1, the
           control parameters given above will be used only
           once, and then new ones must be read in. This is
           set equal to 99 if no changes are desired.

If IMUV = 4 (continuous bidirectional startup):

NMOVES: this is similar in operation to NSHUF, above. It is
           the number of times axial velocity calculations are
           to be made using the current control parameters.
           NMOVE can be set at 99 if no changes are desired.

NBAT: the number of iterations required to evaluate the
           end-of-batch conditions so as to be consistent with
           the tighter convergence criteria necessary for this
           fuel movement.

IP: a print control option. If IP ≠ 0, the flux-times are
           printed out after each velocity calculation has been
           made.

ILOAD(1) to ILOAD(10):
           the reload control parameters at each radius. If
           ILOAD = 0, fuel discharged from the adjacent channel
           is recharged. If ILOAD ≠ 0, new fuel is charged.

362

VREL(1) to VREL(10):

the relative velocities at each radius. Because of normalization, at least one of these should be unity.

THRECH(1) to THRECH(10):

the recharge flux-time criterion. No discharged fuel will be recharged if its flux-time in n/kb exceeds THRECH.

ERROR, DELCRT, and DELCNV have the same significance as previously.

FDAMP: the damping factor between successive flux-time estimates during any one velocity iteration. Generally, FDAMP = 0.5.

If IMUV = 5 (discontinuous bidirectional):

NPOINT: the number of axial points which are to represent one fuel element. This number must be a factor of 2xJZL, and hence JZL and NPOINT must be chosen for compatibility.

NSHUF: this is identical to NSHUF for IMUV = 2 or 3.

ILOAD(1) to ILOAD(10):

the reload control parameter at each radius. If ILOAD = 0, no fuel is moved or recharged. If ILOAD = 1, new fuel is charged. If ILOAD = -1, discharged fuel is recharged with the end toward the end, and if ILOAD = -2, discharged fuel is recharged with the end toward the center.

THRECH(1) to THRECH(10):

identical to THRECH for IMUV = 4.

When control is returned to MAIN from any of the above subroutines, a new run can be started. The first card to be read in is an identification card, followed by the NEXRUN card. If NEXRUN = 1, all new data is read in. If NEXRUN = 2, all new control data is read

in. If NEXRUN = 3, the following is read in: IPROP(1) to IPROP(5), IMUV, IPOIS, ISSCNT, and IBATCH. Control is then transferred to the part of the code immediately following the FUEL Code input. Hence, care must be taken to ensure that the old values of IPOWD, INORMP, IABSP, and ITHET are adequate for the new run. If they are not, NEXRUN = 2 should be used.

In Table A.4 the grouping of the cards, and their relative positions in the input data are given, along with their conditions of use. Table A.5 gives the specific data on card formats required for each case mentioned above. Also included in Table A.5 are the card formats for the COST Cards. For the meaning of the symbols, refer to Fig. 4.2.

TABLE A.4 THE SEQUENCE OF MOVE CODE INPUT DATA CARDS

	Cards	Number of Cards	Condition of Use — Initially	Condition of Use — On NEXRUN (non-initial)
1	Identification	1	Always used	Never
2	Geometry	4	Always used	If NEXRUN = 1
3	Control	2	Always used	If NEXRUN = 1 or 2
4	Fuel property cards	NLOAD x (2+3·JAY)	Only if NRT=0 and NLOAD>0	If NEXRUN = 1 or 2, and NRT = 0 with NLOAD > 0
5	POWD	JZL	Only if IPOWD≠0	NEXRUN=1,2 or 3, IPOWD≠0
6	SIGMWN	JZL	Only if INORMP>0	NEXRUN=1,2 or 3, INORMP>0
7	SIGMWA	JZL	Only if IABSP > 0	NEXRUN=1, 2 or 3, IABSP > 0
8	THETA	JZL	Only if ITHET > 0	NEXRUN=1, 2 or 3, ITHET > 0
9	YEARS	1	Only if ITHET > 0	NEXRUN=1, 2 or 3, ITHET > 0
10	COST	3(ICSTRD+1)	Only if ICSTRD>0	NEXRUN=1, or 2, ICSTRD > 0
11	ZET2	1	Always if ISSCNT = 0	NEXRUN=1, 2 or 3, ISSCNT=0

IF ISSCNT ≠ 0: (Continuous Steady-State)

	Number of Cards	Condition of Use
Identification	1	ISSCNT ≠ 0. These may be repeated if
CONSTS Control	2	NEXT ≠ 0; see text.

IF ISSCNT = 0: (Batch-type irradiation)

	Number of Cards			
SHUFFL Control	1	IMUV = 2 or 3		These may be repeated; see text.
TRNSNT Control	4	IMUV = 4	ISSCNT = 0	
DISCNT Control	2	IMUV = 5		

START OF NEW RUN

	Number of Cards	Condition of Use
Identification	1	Always used
NEXRUN	1	Always used
N3	1	Used if NEXRUN = 3

TABLE A.5 MOVE CODE INPUT DATA CARD FORMATS

Card	Column Number	Type	Item	Comments
1	1-72	H	Identification	
2	1-12	F	R(1)	Units: cm
2	13-24	F	R(2)	"
2	25-36	F	R(3)	"
2	37-48	F	R(4)	"
2	49-60	F	R(5)	"
2	61-72	F	R(6)	"
3	1-12	F	R(7)	"
3	13-24	F	R(8)	"
3	25-36	F	R(9)	"
3	37-48	F	R(10)	"
3	49-60	F	H	"
3	61-72	F	δR	"
4	1-12	F	δH	"
4	13-24	F	ZSYM	-
4	25-36	F	DBSQU	cm^{-1}
4	37-48	F	PFAST	-
4	49-60	F	PDENAV	kw/1
4	61-72	F	RMAX	-
5	1-12	F	ERROR	-
5	13-24	F	DELCRT	-
5	25-36	F	DELTD	years
5	37-48	F	CRIT	-
6	1-3	I	NZONE(1)	
6	4-6	I	NZONE(2)	
6	7-9	I	NZONE(3)	
6	10-12	I	NZONE(4)	
6	13-15	I	NZONE(5)	
6	16-18	I	LOCPRP(1)	

TABLE A.5 (Cont.)

Card	Column Number	Type	Item	Comments
6	19-21	I	LOCPRP(2)	
6	22-24	I	LOCPRP(3)	
6	25-27	I	LOCPRP(4)	
6	28-30	I	LOCPRP(5)	
6	31-33	I	IPROP(1)	
6	34-36	I	IPROP(2)	
6	37-39	I	IPROP(3)	
6	40-42	I	IPROP(4)	
6	43-45	I	IPROP(5)	
6	46-48	I	IRL	
6	49-51	I	JZL	
6	52-54	I	IZONE	
6	55-57	I	NLOAD	
6	58-60	I	NOT	
6	61-63	I	NRT	
6	64-66	I	IMUV	
6	67-69	I	IPOIS	
6	70-72	I	NPOISR	
7	1-3	I	NPOISZ	
7	4-6	I	NSTEP	
7	7-9	I	ISSCNT	
7	10-12	I	IBATCH	
7	13-15	I	IGNORR	
7	16-18	I	ITRATE	
7	19-21	I	IPRT1	
7	22-24	I	IPRT2	
7	25-27	I	IPSPPR	
7	28-30	I	IPSGMW	
7	31-33	I	IPOWD	
7	34-36	I	INORMP	

TABLE A.5 (Cont.)

Card	Column Number	Type	Item	Comments
7	37-39	I	IABSP	
7	40-42	I	ITHET	
7	43-45	I	ICSTRD	
POWD	1-7	F	POWD(1, J)	This card is repeated from J = 1 to J = JZL
	8-14	F	" (2, J)	
	15-21	F	" (3, J)	
	22-28	F	" (4, J)	
	29-35	F	" (5, J)	
	36-42	F	" (6, J)	
	43-49	F	" (7, J)	
	50-56	F	" (8, J)	
	57-63	F	" (9, J)	
	64-70	F	" (10, J)	
SIGMWN	1-7	F	SIGMWN(1, J)	This card is repeated from J = 1 to J = JZL
	8-14	F	" (2, J)	
	15-21	F	" (3, J)	
	22-28	F	" (4, J)	
	29-35	F	" (5, J)	
	36-42	F	" (6, J)	
	43-49	F	" (7, J)	
	50-56	F	" (8, J)	
	57-63	F	" (9, J)	
	64-70	F	" (10, J)	
SIGMWA	1-7	F	SIGMWA (1, J)	This card is repeated from J = 1 to J = JZL
	8-14	F	" (2, J)	
	15-21	F	" (3, J)	
	22-28	F	" (4, J)	
	29-35	F	" (5, J)	

TABLE A.5 (Cont.)

Card	Column Number	Type	Item	Comments
SIGMWA	36-42	F	SIGMWA (6, J)	
	43-49	F	" (7, J)	
	50-56	F	" (8, J)	
	57-63	F	" (9, J)	
	64-70	F	" (10, J)	
THETA	1-7	F	THETA (1, J)	This card is repeated from J = 1 to J = JZL
	8-14	F	" (2, J)	
	15-21	F	" (3, J)	
	22-28	F	" (4, J)	
	29-35	F	" (5, J)	
	36-42	F	" (6, J)	
	43-49	F	" (7, J)	
	50-56	F	" (8, J)	
	57-63	F	" (9, J)	
	64-70	F	" (10, J)	
YEARS	1-12	F	YEARS	This single card must follow the THETA Cards
C_1 (of Cost)	1-6	F	$f(1)$	$f(1)-f(10)$ are the material adjustment factors
	7-12	F	$f(2)$	
	13-18	F	$f(3)$	
	19-24	F	$f(4)$	
	25-30	F	$f(5)$	
	31-36	F	$f(6)$	
	37-42	F	$f(7)$	
	43-48	F	$f(8)$	
	49-54	F	$f(9)$	
	55-60	F	$f(10)$	
	61-66	F	γ	Net efficiency
	67-72	F	SPPDAV	

TABLE A.5 (Cont.)

Card	Column Number	Type	Item	Comments
C_2	1-12	F	x_o	
	13-24	F	C_E	
	25-36	F	WTF	
	37-48	F	FLOAD	
	49-60	F	D_6	
	61-72	F	$D_{7,1}$	
C_3	1-12	F	$D_{7,2}$	
	13-24	F	TUPR	
	25-36	F	TWPR	
	37-48	F	TPOST	

Note: Cards C_4, C_5, and C_6 are to be repeated "ICSTRD" times.

Card	Column Number	Type	Item	Comments
C_4	1-12	F	C(1, J)	C(1, J) to C(18,J) are the unit costs 1 to 18 of cost set "J"
	13-24	F	C(3, J)	
	25-36	F	C(4, J)	
	37-48	F	C(5, J)	
	49-60	F	C(9, J)	
	61-72	F	C(10, J)	
C_5	1-12	F	C(15, J)	
	13-24	F	C(16, J)	
	25-36	F	C(17, J)	
	37-48	F	C(18, J)	
	49-60	F	FU(J)	
	61-72	F	FW(J)	
C_6	1-12	F	FCAPR(J)	
	13-24	F	FCAPNR(J)	
	25-36	F	XOPT(J)	
ZET2	1-12	F	ZET2	Central flux-time step

TABLE A.5 (Cont.)

Card	Column Number	Type	Item	Comments
Note: the following are used by CONSTS (ISSCNT ≠ 0)				
CON1	1-72	H	Identification	These cards may be repeated if NEXT ≠ 0. See text.
CON2	1-10	F	THETA1	
	11-20	F	THETA2	
	21-30	F	DAMP1	
	31-40	F	EFF	
	41-50	F	ERROR	
	51-60	F	DELCNV	
	61-66	I	LPMX	
	67-72	I	NEXT	
CON3	1-7	F	FCTR(1)	
	8-14	F	FCTR(2)	
	15-21	F	FCTR(3)	
	22-28	F	FCTR(4)	
	29-35	F	FCTR(5)	
	36-42	F	FCTR(6)	
	43-48	F	FCTR(7)	
	49-56	F	FCTR(8)	
	57-63	F	FCTR(9)	
	64-70	F	FCTR(10)	
Note: the following card is for SHUFFL (ISSCNT = 0, IMUV = 2 or 3)				
SHUF	1-3	I	INVERT(1)	This card may be repeated, depending upon NSHUF. See text.
	4-6	I	INVERT(2)	
	7-9	I	INVERT(3)	
	10-12	I	INVERT(4)	
	13-15	I	INVERT(5)	
	16-18	I	IMOVE	
	19-21	I	IGRAD	

TABLE A.5 (Cont.)

Card	Column Number	Type	Item	Comments
SHUF	22-24	I	IPR	
	25-27	I	NSHUF	
Note: the following four cards are for TRNSNT (ISSCNT = 0, IMUV = 4)				
TRN1	1-3	I	NMOVES	These cards may be repeated, depending upon NMOVES. See text.
	4-6	I	NBAT	
	7-9	I	IP	
	10-12	I	ILOAD(1)	
	13-15	I	" (2)	
	16-18	I	" (3)	
	19-21	I	" (4)	
	22-24	I	" (5)	
	25-27	I	" (6)	
	28-30	I	" (7)	
	31-33	I	" (8)	
	34-36	I	" (9)	
	37-39	I	" (10)	
TRN2	1-7	F	VREL(1)	
	8-14	F	" (2)	
	15-21	F	" (3)	
	22-28	F	" (4)	
	29-35	F	" (5)	
	36-42	F	" (6)	
	43-49	F	" (7)	
	50-56	F	" (8)	
	57-63	F	" (9)	
	64-70	F	" (10)	
TRN3	1-7	F	THRECH(1)	
	8-14	F	" (2)	

TABLE A.5 (Cont.)

Card	Column Number	Type	Item	Comments
TRN3	15-21	F	THRECH (3)	
	22-28	F	" (4)	
	29-35	F	" (5)	
	36-42	F	" (6)	
	43-49	F	" (7)	
	50-56	F	" (8)	
	57-63	F	" (9)	
	64-70	F	" (10)	
TRN4	1-7	F	ERROR	
	8-14	F	DELCRT	
	15-21	F	DELCNV	
	22-28	F	FDAMP	

Note: the following two cards are for DISCNT (ISSCNT = 0, IMUV = 5)

Card	Column Number	Type	Item	Comments
DISC1	1-3	I	NPOINT	These cards may be repeated, depending upon the value of NSHUF.
	4-6	I	NSHUF	
	7-9	I	ILOAD(1)	
	10-12	I	" (2)	
	13-15	I	" (3)	
	16-18	I	" (4)	
	19-21	I	" (5)	
	22-24	I	" (6)	
	25-27	I	" (7)	
	28-30	I	" (8)	
	31-33	I	" (9)	
	34-36	I	" (10)	
DISC2	1-7	F	THRECH (1)	
	8-14	F	" (2)	
	15-21	F	" (3)	

TABLE A.5 (Cont.)

Card	Column Number	Type	Item	Comments
DISC2	22-28	F	THRECH (4)	
	29-35	F	" (5)	
	36-42	F	" (6)	
	43-49	F	" (7)	
	50-56	F	" (8)	
	57-63	F	" (9)	
	64-70	F	" (10)	
Note: the following cards are the start of a new run.				
-	1-72	H	Identification	
NEXRUN	1-3	I	NEXRUN	
N3	1-3	I	IPROP (1)	Required only if NEXRUN = 3
	4-6	I	" (2)	
	7-9	I	" (3)	
	10-12	I	" (4)	
	13-15	I	" (5)	
	16-18	I	IMUV	
	19-21	I	IPOIS	
	22-24	I	ISSCNT	
	25-27	I	IBATCH	

4.2 General Comments on Flux Iteration Convergence

As a general rule, the more non-uniform a core is reactivity-wise, the more difficult will be the flux convergence. The cause of this is simply that an excess or deficiency of reactivity must be compensated for by leakage. This leakage will occur only if large flux gradients are developed, which in turn will result in badly peaked power distributions. The MOVE Code has the most convergence difficulty with those outin fuel movements which in spite of control poison have large reactivity differences between the new fuel at the outer radius and the spent fuel near the axis.

However, this convergence difficulty does not necessarily limit the usefulness of the MOVE Code. This is because the badly peaked power distributions which are usually synonymous with the difficulty are of little use in a practical reactor system and are therefore generally of academic interest only. In fact, if a non-convergent situation arises, it suggests that inadequate spatial control of reactivity exists, and alternative methods should be devised and analysed.

4.3 Possible Changes to the FUELMOVE Code

1) Other Machines: FUELMOVE is written in FORTRAN for use on an IBM 709 or 7090. When tape input is not desired, the "READ INPUT TAPE" instructions should be changed to "READ", and in the FUEL Code, the instruction "WRITE OUTPUT TAPE NPT" (for off line punching) could be changed to "PUNCH".

2) Thorium FUEL Code: The FUEL Code could be written to include the Thorium-U^{233} cycle, if the flux dependence of the Thorium cycle were removed by assuming an average flux. The spatial flux routines of the MOVE Code would not need to be altered, but the parts of the MOVE Code associated with the cost analysis would have to be changed to include the $Th + U^{233}$ nuclide concentrations. This would involve the

transfer of more nuclide concentrations from the FUEL Code to the MOVE Code.

3) <u>New Fuel and Poison Management Techniques</u>: Poison management is written into SPFUN. New fuel movements could be included by either calling them by the same name as existing fuel movements, and making a direct substitution, or the MAIN program could be re-written to include a new entry point for the new routine. If new sub-routines are written, it should be noted that the bulk of calculational and control data is stored in COMMON to avoid the use of long trans-fer vectors. Care must be exercised to ensure that the new sub-routines are identical in the universal part of COMMON.

4) <u>Different Mesh Limits</u>: The FUELMOVE Code is written for 10 radial by 15 axial mesh points. These dimensions could be increased if some of the fuel movements were to be sacrificed. A change from 10 x 15 to 15 radial x 10 axial may be desirable, again at the expense of certain fuel movement subroutines. The 15 x 10 spacing required more space than the 10 x 15, because the routine SPACFX reserves a block of magnetic core storage $(2 \times IRL + 1) \cdot IRL \cdot JZL$ which is 6300 locations with 10 x 15, but 9300 at 15 x 10.

4.4 Program Stops in FUELMOVE

Program stops in the FUEL Code are identified directly on the output tape. MOVE Code stops are to be identified using Table A.6.

TABLE A.6   PROGRAM STOPS IN THE MOVE CODE

Stop Number	In Program	Reason
1	MAIN	Desired properties not found in first 50 records on tape NRT (FUEL tape).
2	-	Not currently used.
3	SPACFX	No flux convergence in 15 loops.
4	SPFUN	IPOIS < 0, or machine error.
5	MAIN	Criticality, $C < CRIT$, with no Xe or Sm on first step of batch-type irradiation.
6	COST	Too many cost sets (ICSTRD > 4).
7	CONPWD	Negative control poison before first flux-time step.
8	CONSTS	$\theta_1 = \theta_2$; equal input flux-time estimates.
9	PTPROP	$\sum_1^N$ ALAG $\neq 1 \pm .005$. The Lagrangian fit is being attempted outside its range.
10	AVPROP	More than two different enrichments are being used in graded irradiation.
11	TRNSNT	The correct axial velocity has not been found in ten iterations.
12	TRNSNT	The axial velocity is negative.

5. Sample Test Cases

Listed in Table A. 7 is the input data for the FUEL Code test case. The results of this run, on punched cards, are listed in Table A. 8. Table A. 9 lists the input data for the MOVE Code test case. The results of this test case should indicate a burnup of 3711 MWD/T for the Batch irradiation, and 9468 MWD/T for the Bi-directional irradiation.

Table A.7 Input Data for the FUEL Code Test Case

```
0    FUEL CODE TEST CASE    CANDU REACTOR   -    NATURAL ENRICHMENT
1.63955 E-04                              2.25887 E-02
0.           0.            .45            .16135        85.27         18.68
.3335        1.0173        .9847          3.19      E-04 3.03     E+06 .05106
1.71366      8.59566       0.0003         .3595         0.            0.
47.53        143.5         1.002          17.01         181.2         264.
1.           0.            0.             6.34      E-03
  49 13  2  0  0  1  2  3  0  0  0  0
```

Table A.8 The FUEL Code Punched Card Output

```
           7 3.00000E-04 1.01730E 00 5.10600E-02 9.24840E-12 1.43500E 02
1.00200E 00 1.70100E 01 6.30112E-05
0.           2.37951E-04 6.94768E-03 3.48032E-03 8.52678E-03 1.18858E-02
2.93493E-02 8.77186E-01 4.60800E 04 1.63955E-04-0.          -0.
2.25887E-02-0.          -0.           0.           0.           0.
2.00000E 00 2.33092E-04 7.53504E-03 3.60609E-03 9.29198E-03 1.19515E-02
3.07492E-02 8.67552E-01-7.68000E 03 1.20915E-04 6.65062E-06 4.44565E-05
2.25482E-02 2.91539E-05 2.83667E-06 3.39071E-07 1.70892E-08 0.
4.00000E 00 2.22528E-04 7.80107E-03 3.55246E-03 9.44239E-03 1.14242E-02
3.02047E-02 8.54857E-01 3.07200E 03 8.91586E-05 1.14922E-05 8.92237E-05
2.25074E-02 4.49069E-05 8.41842E-06 1.74653E-06 1.89836E-07 0.
6.00000E 00 2.11141E-04 7.92494E-03 3.44220E-03 9.35587E-03 1.07994E-02
2.91824E-02 8.44145E-01-2.30400E 03 6.57358E-05 1.49909E-05 1.32903E-04
2.24666E-02 5.31914E-05 1.44463E-05 3.78309E-06 6.73906E-07 0.
8.00000E 00 2.00697E-04 7.98139E-03 3.32061E-03 9.18024E-03 1.02185E-02
2.81172E-02 8.35865E-01 3.07200E 03 4.84652E-05 1.74987E-05 1.75084E-04
2.24261E-02 5.73933E-05 2.00829E-05 5.88951E-06 1.51415E-06 0.
10.00000E 00 1.91780E-04 8.00866E-03 3.20714E-03 8.98459E-03 9.72180E-03
2.71545E-02 8.29509E-01-7.68000E 03 3.57336E-05 1.92776E-05 2.15759E-04
2.23859E-02 5.93956E-05 2.50575E-05 7.78177E-06 2.67818E-06 0.
1.20000E 01 1.84496E-04 8.02655E-03 3.10957E-03 8.80173E-03 9.31649E-03
2.63428E-02 8.24559E-01 4.60800E 04 2.63489E-05 2.05211E-05 2.55091E-04
2.23461E-02 6.02341E-05 2.93240E-05 9.37377E-06 4.10455E-06 0.
```

Table A.9 Input Data for the MOVE Code Test Case

```
0  CANDU REACTOR  MOVE CODE TEST CASE   BIDRCT,NATURAL,BURNUP=9468 MWD/T
32.8857        65.7714        98.6571        131.5428        164.4286        197.3143
230.2          0.             0.             0.              500.            58.45
2.1            0.             1.0845  E-04 .9847             8.59563         1.98
.01            .001           .02            1.
   7  0  0  0  0  0  0  0  0  0  1  0  0  0  0  7  7  1  1  2  0  2  0  0
   0  0  1  0  0  0  1  0  0  0  0  0  0  0  2

XXXXX      INSERT FUEL CARDS HERE      XXXXX

1.015 1.018 1.018 1.015 1.000 0.990 0.987 0.987 0.980 0.980 .2795 18.725
0.00277        37.287         38210.         0.8            17100.          5.60
 32.           0.60           0.50           2.33
28.70          12.50          85.30          15.45          1500.           9500.
224.           183.           4.37           2.78           .0475           .06
0.14           0.14           .0
28.70          12.50          60.60          15.45          1500.           9500.
224.           183.           4.37           2.78           .045            .045
.0813          .0731          .0142
0  CANDU REACTOR  MOVE CODE TEST CASE   BIDRCT,NATURAL,BURNUP=9468 MWD/T
.00329    .00332    .7        0.            .005           .0005                0        0
1.     1.     1.     1.      1.     1.      1.
0  CANDU REACTOR  MOVE CODE TEST CASE   BATCH,NATURAL,BURNUP=3711 MWD/T
   3
   1  0  0  0  0  1  1  0  1
```

APPENDIX B

THE GENERAL TREATMENT OF THE
STEADY-STATE BIDIRECTIONAL FUEL MOVEMENT

The steady-state bidirectional fuel movement is represented in the MOVE Code by the mathematical model given below, of which the description in Section C3. 3 of Chapter IV is a special case.

In the following, the flux-times in adjacent channels are evaluated in terms of flux and the discharge flux-time. The effect of flux differences in adjacent channels is also treated. Subscript 1 refers to the channel with fuel moving toward the midplane of the reactor, and subscript 2 refers to the adjacent channel with fuel moving away from the center.

The fluxes in adjacent channels are

$$\phi_1 = \phi + \Delta\phi$$

$$\phi_2 = \phi - \Delta\phi$$

where ϕ is the average flux, and $\Delta\phi$ is assumed to be of the form

$$\Delta\phi = a\phi\Delta\theta \tag{B1}$$

where $\Delta\theta$ is the flux-time difference between channels,

a is a constant of proportionality.

The flux-time at the midplane, θ_c, is given in terms of the

discharge flux-time, θ_d, by

$$\theta_c = \frac{1 + F}{2} \cdot \theta_d \tag{B2}$$

where F is an input number, to which a can be related.

By definition:

$$\theta_d = \frac{1}{V_z} \int_{-H/2}^{H/2} \phi\,dz = \frac{2}{V_z} \int_0^{H/2} \phi\,dz \tag{B3}$$

$$\theta_1(z) = \theta_c - \frac{1}{V_z} \int_0^z \phi_1\,dz \tag{B4}$$

$$\theta_2(z) = \theta_c + \frac{1}{V_z} \int_0^z \phi_2\,dz \tag{B5}$$

$$\Delta\theta = \theta_2 - \theta_1 = \frac{1}{V_z} \int_0^z (\phi_2 + \phi_1)\,dz \tag{B6}$$

$$= \frac{2}{V_z} \int_0^z \phi\,dz \tag{B7}$$

$$\theta_c = (1 + F)\frac{\theta_d}{2} = \frac{1}{V_z} \int_0^{H/2} \phi_1\,dz \tag{B8}$$

$$= \frac{\theta_d}{2} + \frac{1}{V_z} \int_0^{H/2} \Delta\phi\,dz \tag{B9}$$

Hence,

$$\frac{F \cdot \theta_d}{2} = \frac{1}{V_z} \int_0^{H/2} \Delta\phi\,dz \qquad (B10)$$

$$= \frac{2a}{V_z^2} \int_0^{H/2} \phi(z) \int_0^z \phi(x)dx \cdot dz \qquad (B11)$$

$$= \frac{a}{V_z^2} \left[\int_0^{H/2} \phi\,dz \right]^2 \qquad (B12)$$

$$= \frac{a}{4} \theta_d^2 \qquad (B13)$$

and $\qquad a = \frac{2F}{\theta_d} \qquad (B14)$

Finally, the computational forms needed are:

$$\int_0^z \Delta\phi\,dz = F \frac{\left[\int_0^z \phi\,dz \right]^2}{\int_0^{H/2} \phi\,dz} \qquad (B15)$$

384

$$\theta_1(z) = \frac{\theta_d}{2} \left\{ 1 + F - \left(\frac{\int_0^z \phi dz + \int_0^z \Delta\phi dz}{\int_0^{H/2} \phi dz} \right) \right\} \qquad \text{(B16)}$$

$$\theta_2(z) = \theta_1(z) + \theta_d \frac{\int_0^z \phi dz}{\int_0^{H/2} \phi dz} \qquad \text{(B17)}$$

$$\frac{\Delta\phi}{\phi}(z) = 2F \frac{\int_0^z \phi dz}{\int_0^{H/2} \phi dz} \qquad \text{(B18)}$$

To obtain the average properties of adjacent channels, the thermal properties are weighted with their fluxes, and the non-thermal properties are weighted with their slowing-down densities.

APPENDIX C

SAMPLE COST CALCULATION

A sample cost analysis for the CANDU reference design (2-79 of H42) is presented in this Appendix. The method of cost analysis has been outlined in Section IV C4, and this is illustrated below, using cost basis 2.

The non-interest fuel cycle cost contribution, $\overline{C}_i'$ in \$/kg is given by:

$$\overline{C}_i' = f_i W_i C_i \qquad 1 \leq i \leq 10$$

where the values of f_i and C_i are those given in Table 4.2.

The factor W_i, which is the mass ratio of "material i" to the fuel fed to the reactor, is obtained from the initial and discharge nuclide concentrations. To convert $\overline{C}_i'$ in \$/kg into $\overline{C}_i'$, mills/kwh, the factor G is used:

$$G = \frac{10^3}{24\overline{B}\gamma} \qquad \frac{mills/kwh}{\$/kg}$$

where

$\overline{B}$ = average burnup in MWD/Tonne

γ = net thermal efficiency

For this example, the reference design average burnup of 9078 MWD/Tonne, and the net efficiency of 0.2795, gives:

$$G = \frac{10^3}{24 \times 9078 \times 0.2795}$$

$$= 0.016423 \quad \frac{mills/kwh}{\$/kg}$$

1. Cost of Natural UO_2

$$\overline{C}_1' = f_1 W_1 C_1$$

$$= 1.015 \times 1 \times 28.70 = \$29.13/kg$$

$$\overline{C}_1' = G \cdot \overline{C}_1' = 0.4784 \text{ mills/kwh}$$

2. <u>UF$_6$ from AEC</u> $\quad\quad\quad\quad = 0$

3. <u>UF$_6$ to UO$_2$ Conversion</u> $\quad\quad = 0$

4. <u>Fabrication</u>

$$\overline{C}_4' = 1.015 \times 1 \times 60.60 = \$61.51/\text{kg}$$

$$\overline{C}_4' = G \cdot \overline{C}_4' = 1.0102 \text{ mills/kwh}$$

5. <u>Shipping</u>

$$\overline{C}_5' = 1 \times 1 \times 15.45 = \$15.45/\text{kg}$$

$$\overline{C}_5' = G \cdot \overline{C}_5' = 0.2534 \text{ mills/kwh}$$

6. <u>Solvent Extraction</u>

$$C_6 = \frac{D_6}{\text{WTF}} \left(\frac{\text{WTF}}{1000} + 8 \right)$$

$$= \frac{\$17,100}{38,120} (38.12 + 8)$$

$$= \$20.68/\text{kg}$$

$$\overline{C}_6' = 0.99 \times 1 \times 20.68 = \$20.47/\text{kg}$$

$$\overline{C}_6 = G \cdot \overline{C}_6' = 0.3362 \text{ mills/kwh}$$

7. <u>Conversion of UO$_2$(NO$_3$)$_2$ to UF$_6$</u> = 0

8. <u>Return of UF$_6$ to AEC</u> $\quad\quad\quad = 0$

9. Conversion of $Pu(NO_3)_4$ to Pu

$$W_9 = \frac{\sum\limits_{m=9}^{m=12} (230+m)N_m}{235N_5{}^\circ + 238N_8{}^\circ}$$

$N_5{}^\circ = 3.9817 \times 10^{-4} \quad \text{atoms/b cm}$

$N_8{}^\circ = 223.55 \times 10^{-4} \quad \text{"}$

$N_9 = .5949 \times 10^{-4} \quad \text{"}$

$N_{10} = .2607 \times 10^{-4} \quad \text{"}$

$N_{11} = .0797 \times 10^{-4} \quad \text{"}$

$N_{12} = .0334 \times 10^{-4} \quad \text{"}$

$$W_9 = \frac{232.0 \times 10^{-4}}{541.4 \times 10^{-2}} = 0.00429$$

$\overline{C}_9{}' = 0.98 \times .00429 \times 1500 = \$6.30/kg$

$\overline{C}_9 = G \cdot \overline{C}_9{}' = 0.1035 \text{ mills/kwh}$

10. Sale of Pu to AEC

$\overline{C}_{10}{}' = 0.98 \times (-0.00429) \times 9500 = -\$39.89/kg$

$\overline{C}_{10} = G \cdot \overline{C}_{10}{}' = -0.6551 \text{ mills/kwh}$

11. Non-Reactor UF_6 Lease $= 0$

12. Non-Reactor Working Capital

$\overline{C}_{12}{}' = \left[\overline{C}_1{}' + \overline{C}_3{}' + \overline{C}_4{}'\right] \text{TWPR} \cdot \text{FW}$

$\qquad = \left[29.13 + 0 + 61.51\right] \times 0.5 \times 0.045 = \$2.04/kg$

$\overline{C}_{12} = G \cdot \overline{C}_{12}{}' = 0.0335 \text{ mills/kwh}$

13. Reactor Time UF$_6$ Lease = 0

14. Reactor Time Working Capital

$$\overline{C}_{14}' = (\overline{C}_1' + \overline{C}_3' + \overline{C}_4') \, TR \cdot FW/2Lo$$

$$= (29.13 + 0 + 61.51) \times 1.3287 \times 0.045/2 \times 0.8 = \$3.39/kg$$

$$\overline{C}_{14} = G \cdot \overline{C}_{14}' = 0.0557 \text{ mills/kwh}$$

Net Fuel Cycle Cost $= \displaystyle\sum_{i=1}^{14} \overline{C}_i'$

$$= \$98.40/kg$$

$$G \cdot \sum_{i=1}^{14} \overline{C}_i' = 1.62 \text{ mills/kwh}$$

15. Reactor Capital Costs

$$\overline{C}_{15} = \frac{C_{15} \cdot FCAPR}{8.766 \, L}$$

$$= \frac{224 \times 0.0813}{8.766 \times 0.8} = 2.60 \text{ mills/kwh}$$

16. Non-Reactor Capital Costs

$$\overline{C}_{16} = \frac{C_{16} \cdot FCAPNR}{8.766 \, L}$$

$$= \frac{183 \times 0.0731}{8.766 \times 0.8} = 1.91 \text{ mills/kwh}$$

17. Reactor Operating Costs

$$\overline{C}_{17} = \frac{C_{17}}{8.766L} = \frac{4.37}{8.766 \times 0.8} = 0.62 \text{ mills/kwh}$$

18. Non-Reactor Operating Costs

$$\overline{C}_{18} = \frac{C_{18}}{8.766L}$$

$$= \frac{2.78}{8.766 \times 0.8} = 0.40 \text{ mills/kwh}$$

$$\underline{\text{Net Energy Cost}} = \sum_{i=1}^{18} \overline{C}_i = 7.15 \text{ mills/kwh}$$

APPENDIX D

FUELMOVE SUBPROGRAMS

In the following sections, the computer logic flow charts of the FUELMOVE subroutines are presented. The flow charts of the FUEL and MOVE Code MAIN programs and the symbols used have been given in Section IV. E.

In addition to the subroutines given below, the code requires the standard Fortran II input-output routines and loader, plus EXP and SQRT (FUEL Code only) or LOG (MOVE Code only). The main programs, as assembled at M.I.T., use the M.I.T. post mortem and floating point overflow routines F2PM and FPT. The M.I.T. routines CLOCK and TIME are also used. These write the date and time during running of the code. The M.I.T. routines WTPE and GETPE can be used in the MOVE Code and because of their usefulness have been described with the MOVE Code subroutines.

1. The FUEL Code
   1. MAIN   (given in Section IV. E)
   2. TIMECK
   3. HALT
   4. PTCS
   5. CONST
   6. RESPRB
   7. AVGCS2
   8. WILK2

9. FLF2

10. CSF2

11. NUCON

12. RKY3

13. DERIV

EXP
SQRT
LOADER
INPUT-OUTPUT } Standard Fortran II Subroutines.

TIME
CLOCK
F2PM
FPT } M. I. T. Subroutines which are optional.

2. TIMECK

Purpose: to write the time and identify the location in the program (for timing different parts of the code). (Time check)
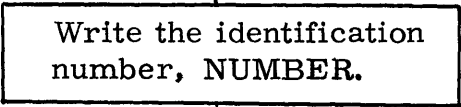
Input arguments: NUMBER

Output parameters: none ·

Subprograms called: TIME, (INPUT-OUTPUT)

Space required: 39

Discussion: A "real time" clock must be connected.

Step	Flow Chart	Comments	Fortran Statement Number
1.	△ 2 TIMECK		
2.	Write the identification number, NUMBER.		10

393

Step	Flow Chart	Comments	Fortran Statement Number

3.　/TIME\　Write the time.

4.　/Return\

3. HALT

Purpose: to write the identification of a program error stop and transfer control to the Fortran Monitor System.

Input arguments: NUMBER

Subprograms called: EXIT, (INPUT-OUTPUT)

Space required: 39

Discussion: For IBM 704 operation, the transfer to EXIT is changed to an HPR.

Step	Flow Chart	Comments	Fortran Statement Number

1.　/3 HALT\

2.　Write the identification number, NUMBER　　5

3.　◇EXIT◇　Transfer to FMS.

4.　/Return\　Return is needed for FORTRAN assembly.

394

4. PTCS

<u>Purpose</u>: to calculate and tabulate the microscopic cross sections of the fuel nuclides at different velocities in the thermal range. (Point cross sections)

<u>Input arguments</u>: IL, μ_v, IPRT1

<u>Output parameters</u>: $\sigma_{i, m}$, for $1 \leq i \leq IL$

$$m = 5; 6; 8 \text{ to } 12; f, 9; f, 11$$

<u>Subprograms called</u>: (INPUT-OUTPUT)
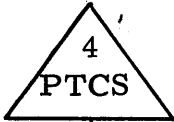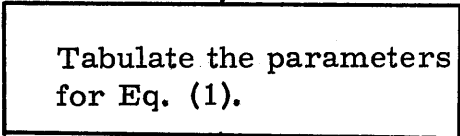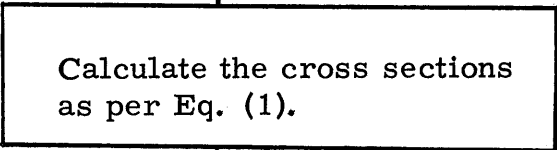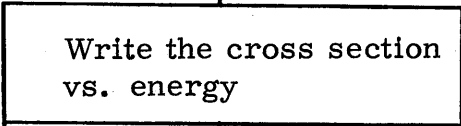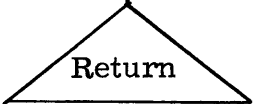
<u>Space required</u>: 639+530 common

<u>Discussion</u>: The cross sections are calculated at the velocities $i\mu_v v_o$, where μ_v is the spacing normalized to v_o, and i takes values from unity to IL. (IL must be odd and less than 100.)

The method used is to calculate the cross sections at each velocity point using the equations given by Westcott, W41. The fit equation is:

$$\sigma(E) = E^{-1/2} \left\{ a + \sum_{j=1}^{n} \frac{c_j}{b_j + (E - e_j)^2} \right\} \qquad (1)$$

The parameters a, b_j, c_j, and e_j are tabulated in W41 for the nuclides required. These terms are the resolved resonance parameters for energies near resonances and are chosen so that the sum of "resonance type" terms fits the BNL-325 curves in regions away from the resonances. Normalization values for the cross sections have been listed in Table 4.1.

Step	Flow Chart	Comments	Fortran Statement Number

1.

```
    /\
   / 4\
  /PTCS\
 /_____\
```

2.   Tabulate the parameters for Eq. (1).   10-160

3.   Calculate the cross sections as per Eq. (1).   Taking velocity steps of $\mu_v v_o$.   170-300

4.   Write the cross section vs. energy   Bypassed if IPRT1 = 0.   310-320

5.   Return

5. CONST

Purpose: to tabulate the nuclear constants which are invariant for all cases. (Constants)

Input arguments: none

Output parameters: ν_m, a_m, η_m, $y_{Xe,m}$, $y_{Sm,m}$, for m = 5, 8, 9, 11

λ_{Xe}, I_m^∞, for m = 5, 6, 8-12

Subprograms called: (INPUT-OUTPUT)

Space required: 263

Discussion: The value of λ_{11} is tabulated in NUCON. η's and a's are averages for the resonance region, except for U238 for which they are fast fission terms. The values used for these parameters have been listed in Table 4.1.

Step	Flow Chart	Comments	Fortran Statement Number
1.	$\triangle$ 5 CONST		
2.	Tabulate nuclear constants.		10-30
3.	Write nuclear constants.		40-90
4.	Return		

6. RESPRB

Purpose: to calculate resonance escape probabilities for the fuel nuclides.

Input arguments: N_m, I_m^∞, ψ_{1m}, C_1, $\Sigma_{s,fl}$, IPRT2
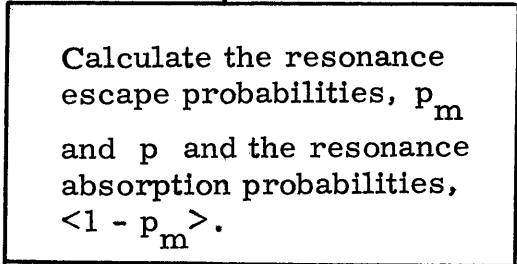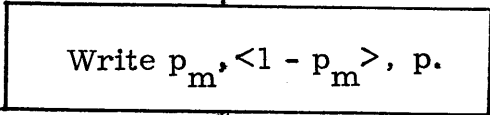
Output arguments: p_m, $<1 - p_m>$, p

$$m = 5 \text{ to } 13$$

Subprograms called: EXP, (INPUT-OUTPUT)

Space required: 282

Discussion: Equations for the resonance escape probabilities are given in Section IV. B. 4.

Step	Flow Chart	Comments	Fortran Statement Number
1.	$\triangle$ 6 RESPBR		
2.	Calculate the resonance escape probabilities, p_m and p and the resonance absorption probabilities, $<1 - p_m>$.		10-40
3.	Write p_m, $<1 - p_m>$, p.	Bypassed if IPRT2 = 0.	50-60
4.	$\triangle$ Return		

7. AVGCS2

Purpose: to calculate average thermal cross sections for the fuel
nuclides (Average cross sections, 2nd revision).

Input arguments: T, $\sigma_{i,m}$, $\oint\Sigma_s$, N_m, N_{8p}, ψ, V_{fl}, μ_v, IL, IPRWLK

Output parameters: σ_m,   for m = 5; 6; 8 to 12; f, 5; f, 9; f, 11

Subprograms called: WILK2, FLF2, CSF2, (INPUT-OUTPUT)

Space required: 456

Discussion: N_{8p} is a term proportional to the concentration of
fission products which when multiplied by the microscopic cross
section of U238 will give the proper effect of fission products in
hardening the thermal neutron spectrum. The reason for treating
fission products in this way is that the cross sections of fission
products, like U238, are assumed to be inversely proportional to
velocity, and the 1/v dependence of the U238 cross section is avail-
able to this subprogram.

Step	Flow Chart	Comments	Fortran Statement Number
1.	(triangle: 7 AVGCS2)		
2.	Calculate the equivalent additional pseudo amount of U-238 to give Σ_{md} a 1/v behavior (energy wise).	Requires an estimate of σ_8.	10-30

398
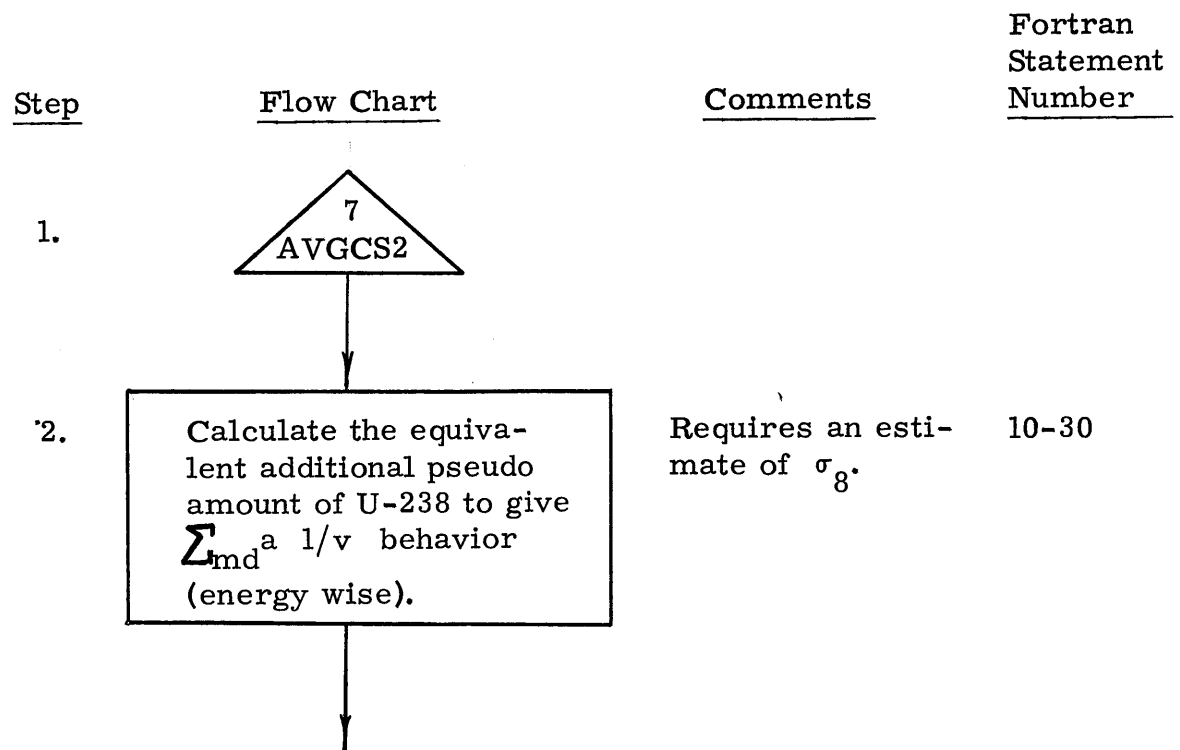
Step	Flow Chart	Comments	Fortran Statement Number
3.	Calculate the cell average absorption cross section versus velocity, Σ_i.	i is the velocity step index.	10-30
4.	Calculate the hardening parameter $A_i = \dfrac{\Sigma i}{\int \Sigma s}$ versus velocity.		10-30
5.	8 WILK2	Calculate the energy spectrum.	
6.	9 FLF2	Calculate the integrated flux, ϕ.	
7.	10 CSF2	Calculate the cross sections, σ_m.	46
8.	Y ← Any more cross sections to be calculated?		50
	N		
9.	Write ϕ and A_i.	Bypassed if IPRWLK=0.	60
10.	Write the thermal cross sections, σ_m.		70
11.	Return		

8. WILK2

Purpose: to solve for the energy distribution of the thermal flux according to Wilkins equation. (Wilkins)

Input arguments: T, IL, μ_v, A_i, IPRWLK

Output parameters: $Y_i = \dfrac{d\phi}{dx}$

Subprograms called: EXP, SQRT, HALT, (INPUT-OUTPUT)

Space required: 514 + 519 common

Discussion: The equations used to generate the Wilkins spectrum are given in Appendix A of Shanstrom (S41).

Step	Flow Chart	Comments	Fortran Statement Number
1.	$\triangle$ 8 WILK2		
2.	$\triangle$ 8 →		
3.	Calculate the flux per unit velocity, Y_i, for i = 1, 4 by the Wilkins startup series. Also calculate y_i and y_i .	Eqs. (3), (4) and (19) from Appendix A of Shanstrom (S41).	10-50
4.	Does the series converge? —Y— $\triangle$ 7		

400

Step	Flow Chart	Comments	Fortran Statement Number

（N）

5.

Write "no convergence in Wilkins startup," list the last term in the series and the sum of terms.

35

6.

3
HALT 1

Stop No. 1 for no convergence.

7.

4

8.

Have we completed the four startup calculations?

（N）

2

（Y）

9.

Calculate Y_i for $i = 5$ to IL by the Milne method: also calculate y_i', y_i'', the truncation error estimate, and the cumulative truncation error estimate.

Eqs. (3), (4), (5) (6), and (22) from Appendix A, Shanstrom (S41).

60-80

10.

Write the flux per unit velocity, Y_i, the truncation error, F_T, and the cumulative truncation error, F_{cum}, versus energy.

Bypassed if IPRWLK=0.

90-100

11.

Return

9. FLF2

Purpose: to integrate the flux per unit velocity, Y_i, giving the magnitude of the flux (i. e. , the integrated weighting function for averaging thermal cross sections). (Flux function, 2nd revision)

Input arguments: IL, μ_v, Y_i, $(T_o/T_{md})^{1/2}$

Output parameters: ϕ
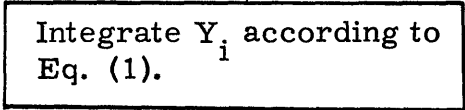
Discussion: The parabolic rule is used for integration of Y.

$$\phi = \int_0^{x_{max}} Y(x)dx = \frac{\mu}{3}(Y_1 + 4Y_2 + 2Y_3 + 4Y_4 + \ldots + 4Y_{IL-1} + Y_{IL}) + 0(\mu^5)$$

(1)

where μ is the spacing in x, given by,

$$\mu = \mu_v(T_o/T_{md})^{1/2}$$

(2)

Since the parabolic rule is used, IL must be odd (and < 100).

Step	Flow Chart	Comments	Fortran Statement Number
1.	9 FLF2		
2.	Integrate Y_i according to Eq. (1).		10-30
3.	Return		

10. CSF2

<u>Purpose</u>: to calculate the average thermal cross section for nuclide m, given Y_i and ϕ. (Cross section function, 2nd revision)
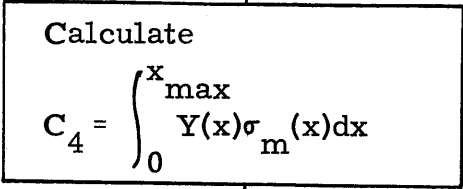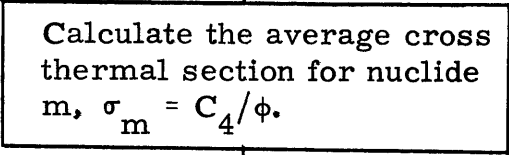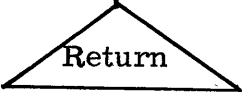
<u>Input arguments</u>: m, ϕ, IL, μ_v, Y_i, $\sigma_{i,m}$, $(T_o/T_{md})^{1/2}$

<u>Output parameters</u>: σ_m, for given input value of m

<u>Space required</u>: 169

<u>Discussion</u>: The parabolic rule is used for integration.

$$\sigma_m = \frac{1}{\phi} \int_0^{x_{max}} \sigma_m(x)Y(x)dx = \frac{\mu}{3\phi}[\sigma_{1,m}Y_1 + 4\sigma_{2,m}Y_2 + \dots + \sigma_{IL,m}Y_{IL}]$$

$$+ O(\mu^5) \tag{1}$$

Step	Flow Chart	Comments	Fortran Statement Number
1.	$\triangle$ 10 CSF2		
2.	Calculate $C_4 = \int_0^{x_{max}} Y(x)\sigma_m(x)dx$		10-30
3.	Calculate the average cross thermal section for nuclide m, $\sigma_m = C_4/\phi$.	ϕ comes from FLF2.	
4.	Return		

403

11. NUCON

Purpose: to solve for the nuclide concentrations one flux time step, ζ, advanced from the known values, to calculate escape probabilities, macroscopic Sm group cross section and the average macroscopic Xe cross section. (Nuclide concentrations)

Input arguments: $N_{m,\theta}$, σ_m, $<1-p>_m$, $C_5 = \dfrac{\sigma_{Xe}\bar{\phi}}{\sigma_{Xe}\bar{\phi} + \lambda_{Xe}}$

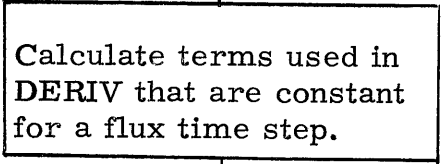$\bar{P}_1$, ϵ, ν_m, a_m, η_m, $y_{Xe,m}$, $y_{Sm,m}$,
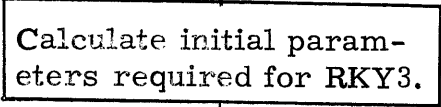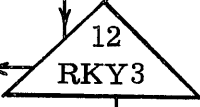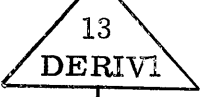
$\zeta = \delta\theta$, I_m^∞, $\psi_{1,m}$, $C_1 = \dfrac{V_{fl}}{\zeta\Sigma_s V_{md}}$, $\Sigma_{s,fl}$, IPRT2
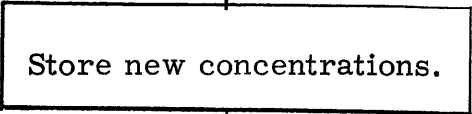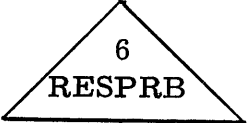
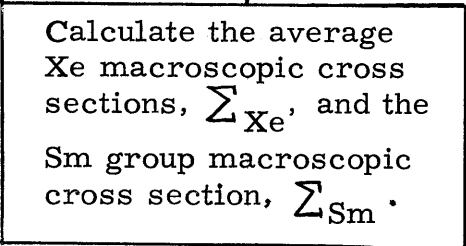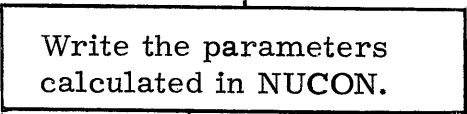**Output parameters:** $N_{m,\theta+\zeta}$, Σ_{Xe}, Σ_{Sm}, p_m, p

Subprograms called: RKY3, DERIV, RESPRB, (RETRKY), (INPUT-OUTPUT)

Space required: 483 + 36 common

Discussion: NUCON is coded in a manner to preserve the relocable features of its subprograms, while allowing a SAP subprogram, RKY3, to be used for the numerical integrations. The numerical integration is by a fourth order Runge-Kutta method, as modified by Gill. The entry to DERIV for the derivative calculation is via the entry point called DERIV1 in NUCON. Return after the derivative calculation is to the entry point in RKY3 called RETRKY.

Step	Flow Chart	Comments	Fortran Statement Number
1.	**11 NUCON**		
2.	Calculate initial parameters required for RKY3.	$N_{m,\theta} \rightarrow$ XRKY3 $N_{m,\theta} \rightarrow$ YRKY3 $0 \rightarrow$ QRKY3	10-20
3.	Calculate terms used in DERIV that are constant for a flux time step.	(a_m), (e_m) $(\sigma_f))_m$	30-35
4.	**12 RETRKY**	2nd entry point for RKY3.	
5.	**12 RKY3**	Numerical solution of the nuclide concentration differential equations.	
6.	Deriv Exit / Final Exit	There are four derivative exits for each final exit.	
7.	**13 DERIV1**	2nd entry point of Nucon, provides input data for DERIV.	
8.	**13 DERIV**	Calculate derivatives.	40

405

Step	Flow Chart	Comments	Fortran Statement Number

9.   Store new concentrations. $XRKY3 \rightarrow N_{m, \theta + \zeta}$

10.   6 / RESPRB   Calculate resonance escape probabilities using the new concentrations.

11.   Calculate the average Xe macroscopic cross sections, Σ_{Xe}, and the Sm group macroscopic cross section, Σ_{Sm}.   80-100

12.   Write the parameters calculated in NUCON.   Bypassed if IPRT2=0

13.   Return

12. RKY3

Purpose: to solve numerically the set of first order differential equations for the nuclide concentrations one flux time advanced from the last values. (Runge-Kutta)

Input parameters: ζ(flux time step) (also needs initial values of XRKY3, YRKY3, and QRKY3 which were stored in common by NUCON and $\dfrac{dN_m}{d\theta}$, or YRKY3, stored in common by DERIV)

Output parameters: $N_{m,\,\theta+\zeta}$(XRKY3 in SAP)

Subprograms called: DERIV (via DERIV1 in NUCON)

Space required: 155 + 36 common

Discussion: This is a standard SAP subprogram only modified to make it compatible with the connected relocatable Fortran programs. The method used is a fourth order Runge-Kutta process as modified by Gill (see G42).

13. DERIV

Purpose: to calculate the flux time derivatives of the nuclide concentrations. (Derivatives)
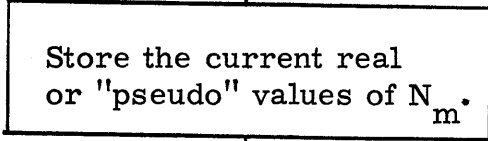
Input arguments: η_m, I_m^{∞}, $\psi_{1,\,m}$, C_1, $\Sigma_{s,\,fl}$, a_m, e_m, $(\sigma_f \mathcal{V})_m$, σ_m, N_m(XRKY3), IPRT2
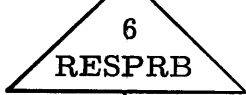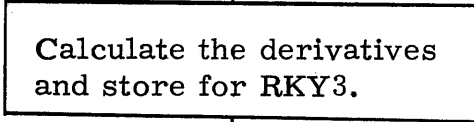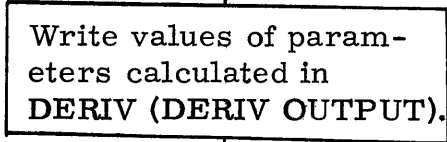
Output parameters: $\dfrac{dN_m}{d\theta}$ (VRKY3) ("pseudo" values at partial flux time steps are also stored for N_m, p_m, $<1-p_m>$, and p for the RKY3 Runge-Kutta solution)

Subroutines called: RESPRB, (INPUT-OUTPUT)

Space required: 318 + 16 common

Discussion: Equations for the derivatives have been given in Section IV. A. 3.   Combinations of terms in these equations that are considered constant for a flux time step are combined in NUCON, into the term a_m, e_m, and $(\sigma_f \nu)_m$, prior to entry into RKY3 and DERIV.

Step	Flow Chart	Comments	Fortran Statement Number
1.	13 DERIV		
2.	Store the current real or "pseudo" values of N_m.	$XRKY3 \rightarrow N_m$.	10-20
3.	6 RESPRB	Calculate the real or pseudo p_m for use in the derivative equations.	
4.	Calculate the derivatives and store for RKY3.	$\dfrac{dN_m}{d\theta} \rightarrow VRKY3$.	30-90
5.	Write values of parameters calculated in DERIV (DERIV OUTPUT).	Bypassed if IPRT2=0.	95
6.	Return		

2. The MOVE Code

1.	MAIN	(Given in Section IV. E)	
2.	TIMECK		(Given with FUEL Code)
3.	HALT		
4.	SPACON		
5.	PTPROP		
6.	SPACE2		
7.	SPFUN	LOG	Standard Fortran
8.	SPACFX	INPUT-OUTPUT	II Subroutines
9.	SPFUN2	LOADER	
10.	FIPRNT	TIME	Optional M. I. T.
11.	NCGTHV	CLOCK	Subroutines
12.	COST	F2PM	
13.	CPF	FPT	
14.	CONPWD		
15.	CONSTS		
16.	GROUTN		
17.	AVPROP		
18.	BIDRCT		
19.	SHAPE		
20.	SHUFFL		
21.	TRNSNT		
22.	DISCNT		
23.	WTPE and GTTPE (M. I. T. Routines)		

4. SPACON
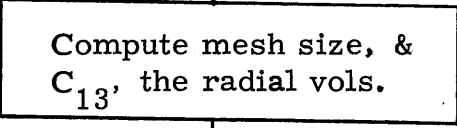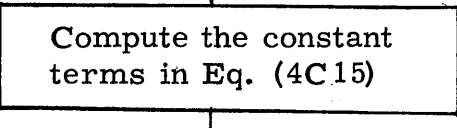
Purpose: to calculate the parameters for the spatial subprogram (SPACE2) which are constant for a given problem. (Space constants).

Input arguments: R, H, δR, δH, D, γ, ZSYM, IRL, JZL

Output parameters: $V_r = C_{13}$, the volume of each radial region; $C_{15's}$ and $C_{17's}$, the thermal and fast diffusion constants.

Space required: 317

Discussion: The terms calculated are the time-invariant components in Eq. (4C15).

Step	Flow Chart	Comments	Fortran Statement Number
1	$\triangle$ 4 SPACON		
2	Compute mesh size, & C_{13}, the radial vols.		5-17
3	Compute the constant terms in Eq. (4C15)		20-80
4	$\triangle$ RETURN		

5. PTPROP

Purpose: to calculate at each mesh point in a given radial zone the seven homogenized "Point Properties" required by the spatial subroutine, SPACE2.

Input arguments: IJ, IN, JZL, N, plus all the data transferred from the FUEL Code for the given enrichment (See Appendix A). Flux-times at each mesh point are also required. IJ and IN define the limits of the radial zone. N designates the group of properties to be used.

Output parameters: The seven homogenized properties at each mesh point in the specified zone: $\sum_{Xe, max}$, $(\sum - \sum_{Xe})$, $\sum_f$, $\nu\sum_f$, $(\frac{1-p}{1+\alpha})$, $<\eta(1-p)>$, p.
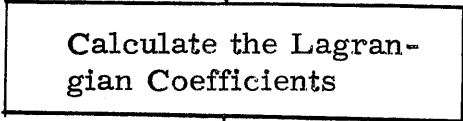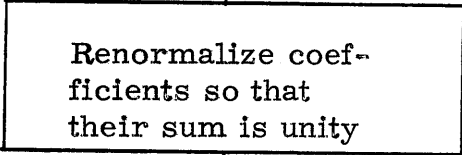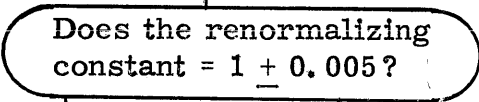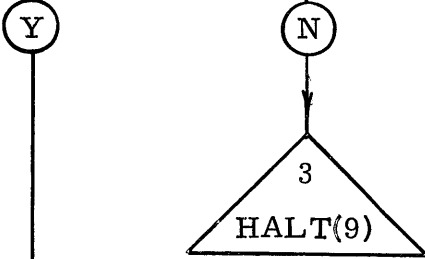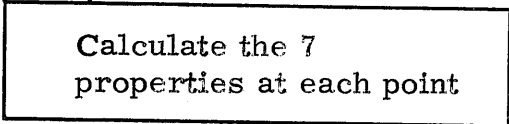
Subprograms called: HALT, (INPUT-OUTPUT)

Space required: 228

Discussion: The properties at a point are obtained from the specified flux-time at the point by means of a Lagrangian fit (see Section IVC2.4) at up to 15 fit points to yield up to a 14th degree polynomial fit.

Step	Flow Chart	Comments	Fortran Statement Number
1	$\triangle$ 5 PTROP		

Step	Flow Chart	Comments	Fortran Statement Number

2 — Calculate the Lagrangian Coefficients — The denominators of these terms have been transferred from the FUEL Code. — 420-431

3 — Renormalize coefficients so that their sum is unity — — 433

4 — Does the renormalizing constant = 1 ± 0.005? — —

Y   N

5 — HALT(9) — — 435

6 — Calculate the 7 properties at each point — — 440-450

7 — RETURN

6. SPACE 2

<u>Purpose</u>: to connect and control the subroutines which calculate the spatial flux and power distribution, the criticality, the control poison, and other reactor properties.

<u>Input arguments</u>: at each mesh point, the 7 properties obtained in PTPROP, the spatial constants from SPACON, IRL, JZL, PDENAV, $-D\nabla^2$, P_1, and flux shape. The last three are used as initial estimates.

<u>Output parameters</u>: $\phi_{r,z}$, $\dfrac{\phi_{r,z}}{\phi_{1,1}}$ $(-D\nabla^2)_{r,z}$, $P_{1,r,z}$, C, $\overline{P_1}$,

$$C_5 = \frac{\overline{\phi}}{\overline{\phi} + (\frac{\lambda}{\sigma})_{Xe}}.$$

<u>Subprograms called</u>: SPFUN, SPACFX, SPFUN2, (INPUT-OUTPUT)

<u>Space Required</u>: 614

Step	Flow Chart	Comments	Fortran Statement Number
1	△ 6 SPACE2		
2	△ 10	Entry point for control poison iteration.	5
3	△ 7 SPFUN	Calculate the d and e matrices of Eq. (4C15)	5

Step	Flow Chart	Comments	Fortran Statement Number

4   IPRT2 = 0 ?   Input control parameter

    Y   N

5   Write out the d and e matrices   Normally bypassed   7

6   8 SPACFX   Calculate the spatial flux distribution   25

7   9 SPFUNι Calculate criticality and other parameters at each mesh point, also core averages

8   IPOIS = 0 ?

    Y   N

9   Is control poison correct or have ITRATE loops been made ?   40-55

    Y   N

10   RETURN   2   60
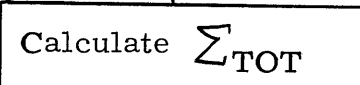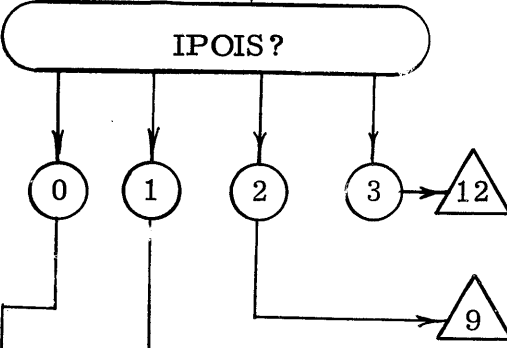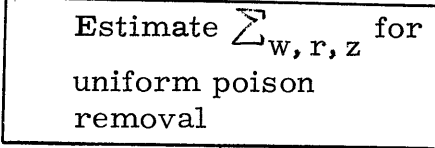
7. SPFUN

Purpose: to calculate the coefficient matrices d and e of Eq. (4C15), for use by SPACFX.

Input Arguments: at each mesh point, the :7 properties obtained in PTPROP, the spatial constants from SPACON, IRL, JZL, $-D\nabla^2$, P_1, $(\Sigma_w)_{r,z}/(\Sigma_w)_{1,1}$, $\phi_{r,z}$.

Output Parameters: $d_{r,z,u}$, $e_{r,z}$, $C_{20_{r,z}} = \Sigma_{r,z} + \Sigma_{w,r,z}$

Space Required: 690

Step	Flow Chart	Comments	Fortran Statement Number
1	$\triangle$ 7 SPFUN		
2	Calculate Σ_{TOT}	$\Sigma_{TOT} = \Sigma_1 + \dfrac{\phi\sigma_{Xe}}{\phi\sigma_{Xe} + \lambda_{Xe}} \cdot \Sigma_{Xe,max}$	20
3	IPOIS?	Input control parameter	26
	0 1 2 3 → $\triangle$12	Axial bank poison removal	
	→ $\triangle$9	Radial zone poison removal	
4	Estimate $\Sigma_{w,r,z}$ for uniform poison removal	Uniform poison removal	27

415

Step	Flow Chart	Comments	Fortran Statement Number
5	Set $\sum_{w,r,z} = 0$	No poison control	28
6	△ 11, 14	Reentry point for axial bank and radial zone poison control.	29
7	Calculate d and e matrices		29-200
8	RETURN		
9	△ 3		300
10	Compute $\sum_{w,r,z}$ for radial zone removal		300-320
11	△ 6		
12	△ 3		400
13	Compute $\sum_{w,r,z}$ for axial bank removal		400-440
14	△ 6		

8. SPACFX

Purpose: to calculate the spatial flux distribution.
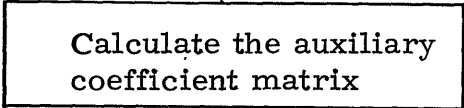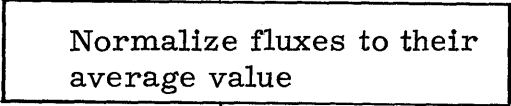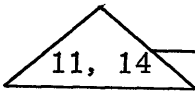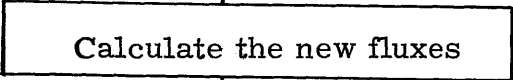
Input arguments: IRL, JZL, d, e

Output parameters: $\phi_{r,z}/\phi_{1,1}$

Subprograms called: HALT, (INPUT-OUTPUT)

Space required: 1028 + 9007 common. This subroutine occupies the largest amount of common storage.

Discussion: The iteration method has been given in Section IV C 2. 5. The modified Crout reduction that is used is described in S_{41}.

Step	Flow Chart	Comments	Fortran Statement Number
1	△ 8 SPACFX		
2	Calculate the auxiliary coefficient matrix		10-200
3	Normalize fluxes to their average value		205-210
4	△ 11, 14	Entry point in iteration loop	215
5	Calculate the new fluxes		215-325

Step	Flow Chart	Comments	Fortran Statement Number

6 — Renormalize fluxes to their average value — 325-330

$\dfrac{\Delta\phi}{\phi} < ERROR$? — 330-340

7 — Have the fluxes converged?

Y

△15

N

ERROR is input data

8 — Have > 15 loops been made? — 350

N

Y

3

9 — △HALT(3) — 355

10 — Can Aiken δ^2 flux extrapolation be used? — Used for all odd-numbered loops after the 4th.

Y

N

11 — △4

Step	Flow Chart	Comments	Fortran Statement Number

| 12 | Make extrapolation of fluxes using the Aiken δ^2 process | | 375-380 |

| 13 | Renormalize fluxes to their average | | 380-390 |

| 14 | △4 | Start new flux iteration loop | |

| 15 | △8 | Final exit | 400 |

| 16 | Normalize fluxes to $\phi_{1,1}$ | | 420-430 |

| 17 | Write out the number of iteration loops required for convergence | | |

| 18 | RETURN | | 440 |

9. SPFUN2

<u>Purpose</u>: to calculate at each mesh point and also the core averages of: the criticality factor, C; the fast non-leakage probability, P_1; the thermal neutron production term, $(q/\phi)P_1 p$; the thermal leakage term $(-D\nabla^2)$; and the power densities. In addition, the reactor criticality factor with control poison, C_W, the flux magnitudes, $\phi_{r,z}$, and the maximum to average power density ratio are obtained.

<u>Input arguments</u>: $\phi_{r,z}/\phi_{1,1}$, SPACON output, $C_{20,r,z}$, $(\nu\Sigma_f)_{r,z}$, $\Sigma_{f,r,z}$, $<\eta(1-p)>_{r,z}$, $\left(\frac{1-p}{1+a}\right)_{r,z}$, ϵ , C5P, IRL, JZL

<u>Output parameters</u>: $\phi_{r,z}$, $V_r\phi_{r,z} = C_{28,r,z}$, $(-D\nabla^2)_{r,z} = C_{36,r,z}$
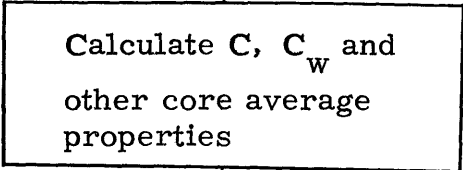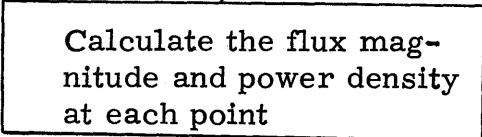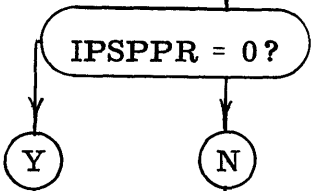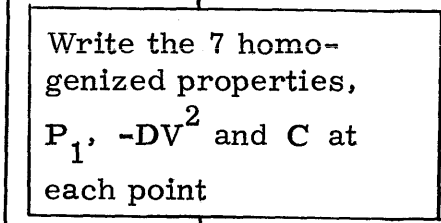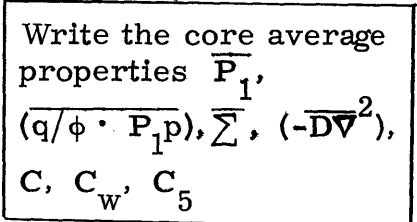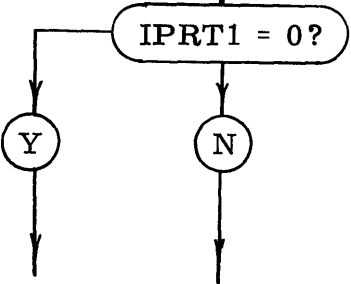
$P_{1,r,z}$, C, C_W, $\overline{P_1}$, $C_5 = \dfrac{\overline{\phi}}{\overline{\phi} + C5P}$

<u>Subprograms called</u>: (INPUT-OUTPUT)

<u>Space required</u>: 816

<u>Discussion</u>: The core averaging method was discussed in Section IVC2.6

Step	Flow Chart	Comments	Fortran Statement Number
1	△ 9 SPFUN2		
2	Calculate thermal and fast leakage terms at each mesh point		10-30

Step	Flow Chart	Comments	Fortran Statement Number

3 — Calculate C, C_W and other core average properties — 30

4 — Calculate the flux magnitude and power density at each point — 42-64

5 — IPSPPR = 0? — Input control parameter

Y   N

6 — Write the 7 homogenized properties, P_1, $-DV^2$ and C at each point — Normally bypassed — 67

7 — Write the core average properties $\overline{P_1}$, $\overline{(q/\phi \cdot P_1 p)}$, $\overline{\sum}$, $(-\overline{D\nabla}^2)$, C, C_w, C_5 — 75

8 — IPRT1 = 0?

Y   N

Step	Flow Chart	Comments	Fortran Statement Number
9	**10** FIPRNT	Writes out the flux and power density at each point	85
10	Write the peak-to-average power density and flux ratios		147
11	IPSGMW = 0 ? Y N		
12	Write out $\sum'_w$ at each point		204
13	RETURN		
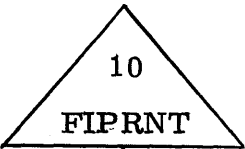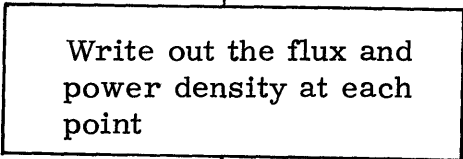
10. FIPRNT

<u>Purpose</u>: to write out the flux and power density at each point in the reactor.

<u>Input arguments</u>: $\phi_{r,z}$, $POWD_{r,z}$, IRL, JZL

<u>Subprograms called</u>: (INPUT-OUTPUT)

<u>Space required</u>: 144

Step	Flow Chart	Comments	Fortran Statement Number
1	△ 10 FIPRNT		
2	Write out the flux and power density at each point		90-145
3	RETURN		

11. NCGTHV

Purpose: to calculate the nuclide concentration at a specified flux-time

Input arguments: θ, the specified flux-time; N, which designates the enrichment desired; plus the nuclide concentration data and other parameters transferred from the FUEL Code.

Output parameters: $N_m(\theta)$ for m = 5, 12

Subprograms called: (INPUT-OUTPUT)

Space required: 156

Discussion: The use of Lagrangian polynomials is identical to that used in PTPROP.

Step	Flow Chart	Comments	Fortran Statement Number
1	△ 11 NCGTHV		
2	Calculate the Lagrangian coefficients and the nuclide concentrations		20-60
3	(IPRT2 = 0 ?) Y N		
4	Write out the nuclide concentrations		65-70
5	△ RETURN		75

424

12. COST
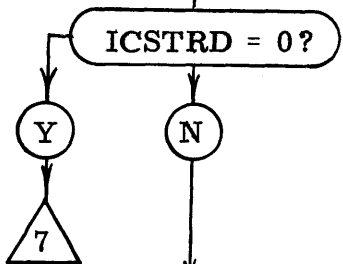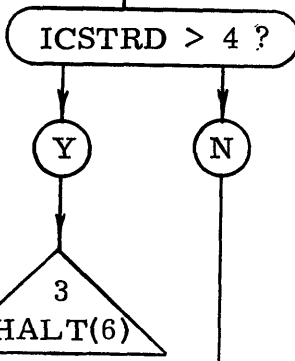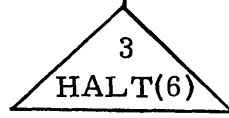
__Purpose:__ to calculate the fuel cycle and total energy cost using up to four sets of cost parameters

__Input arguments:__ the initial and discharge nuclide concentrations, N_m^o and N_m; the reactor "on stream" time, TR; the real "full power" time since startup, years; and the average burnup, $\overline{B}$.
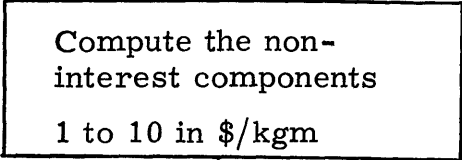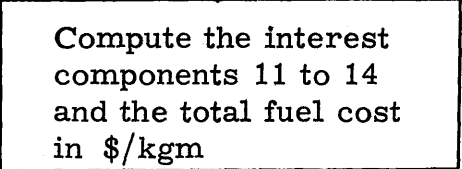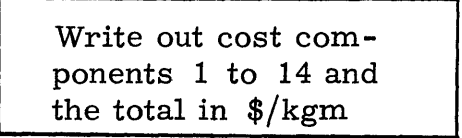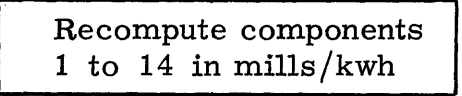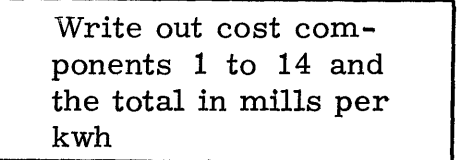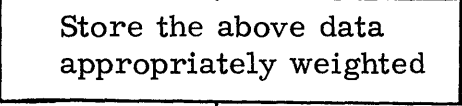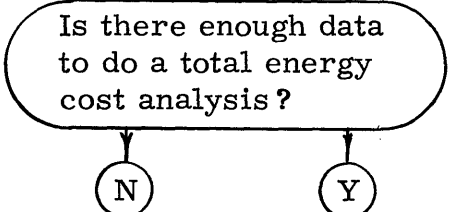
__Subprograms called:__ CPF, HALT, (INPUT-OUTPUT)
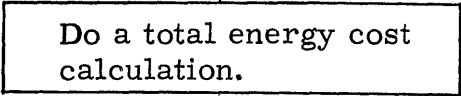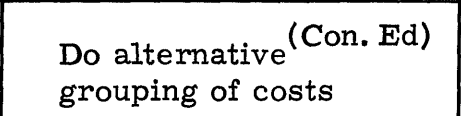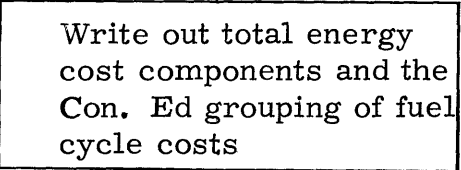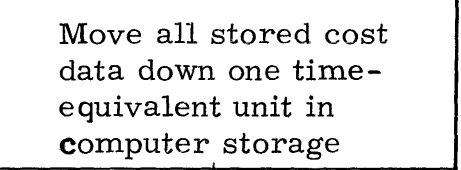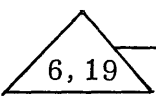
__Space required:__ 3262

__Discussion:__ the cost analysis is described in Section IVC4.

Step	Flow Chart	Comments	Fortran Statement Number
1	$\triangle$ 12 COST		
2	ICSTRD = 0? Y → 7, N	On the first entry to COST, only the cost sets are read in. No cost calculations are performed.	
3	ICSTRD > 4 ? Y, N		5
4	Y → 3 HALT(6)	Stop for too many cost sets.	8

425

Step	Flow Chart	Comments	Fortran Statement Number
5	Read in ICSTRD sets of cost data Set JCOSTL = ICSTRD ICSTRD = 0		10-15
6	△24	Return to the MAIN program	
7	△3	Entry point for cost analysis	18
8	INCOST = 0?	Cost control parameter for initialization of cost calculation.	18
	N Y		
9	Write out cost input data		19-22
10	Set up initial conditions for the cost analysis		
11	Compute the W terms, also C_2, C_8 △13 CPF		29-105

Step	Flow Chart	Comments	Fortran Statement Number

| 12 | Compute the non-interest components 1 to 10 in $/kgm | | 105-118 |

| 13 | Compute the interest components 11 to 14 and the total fuel cost in $/kgm | | 118-119 |

| 14 | Write out cost components 1 to 14 and the total in $/kgm | | |

| 15 | Recompute components 1 to 14 in mills/kwh | | 120 |

| 16 | Write out cost components 1 to 14 and the total in mills per kwh | | |

| 17 | Store the above data appropriately weighted | | 123-150 |

| 18 | Is there enough data to do a total energy cost analysis? | | 199 |

N

Y

| 19 | 24 | | |

Step	Flow Chart	Comments	Fortran Statement Number
20	Do a total energy cost calculation.		205-220
21.	Do alternative (Con. Ed) grouping of costs		220-225
22	Write out total energy cost components and the Con. Ed grouping of fuel cycle costs		230-280
23	Move all stored cost data down one time-equivalent unit in computer storage		280-299
24	6, 19		300
25	RETURN		

428
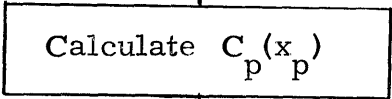
13. CPF

<u>Purpose:</u> to calculate the unit price of UF_6.

<u>Input arguments:</u> the fractional enrichment x_p; the optimum waste composition, x_o; and the unit cost of separative duty, C_E.

<u>Output parameter:</u> the unit price of UF_6, C_p

<u>Space required:</u> 93

Step	Flow Chart	Comments	Fortran Statement Number
1	△ 13 CPF		
2	Calculate $C_p(x_p)$	Equations given in Section IVC4. 4	
3	RETURN		

429

14. CONPWD

Purpose: to compute the spatial flux and control poison shape when a power density shape and the 7 properties at each mesh point are specified.

Input arguments: the 7 homogenized properties, the power density at each point, PFAST and PDENAV
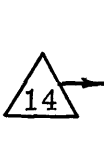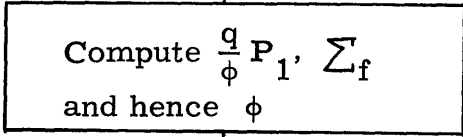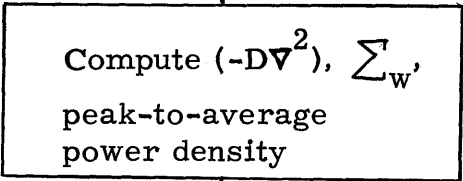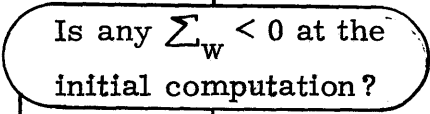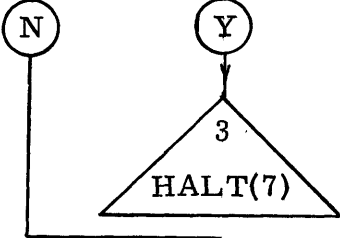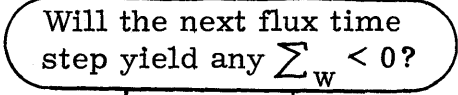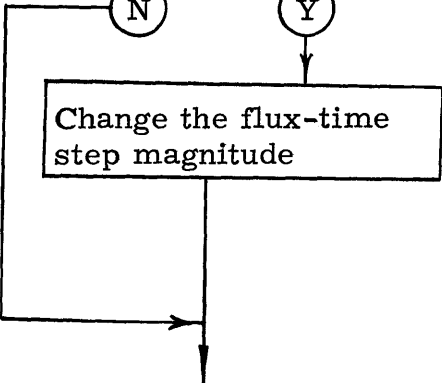
Output parameters: $\phi_{r,z}$, $(-D\nabla^2)_{r,z}$, $P_{1,r,z}$, C, $V_r\phi_{r,z}$

Subprograms called: HALT, (INPUT-OUTPUT)

Space required: 1077

Discussion: The equations used in this subroutine are described in Section IV C3.1

Step	Flow Chart	Comments	Fortran Statement Number
1	△ 14 CONPWD		
2	Set P_1 = PFAST and store previous control poison values		1
3	INCON = 0 ?		
	N ← Y		
4	Scale the input power density to produce the specified average power density, PDENAV		2-4

430

Step	Flow Chart	Comments	Fortran Statement Number

5 — △14 — 15

6 — Compute $\frac{q}{\phi} P_1$, $\sum_f$ and hence ϕ — 15–18

7 — Compute $(-D\nabla^2)$, $\sum_w$, peak-to-average power density — 18–120

8 — Is any $\sum_w < 0$ at the initial computation? — 120–130

N   Y

9 — △ 3 HALT(7) — 125

10 — Will the next flux time step yield any $\sum_w < 0$? — 145

N   Y

11 — Change the flux-time step magnitude — 150

Step	Flow Chart	Comments	Fortran Statement Number

12 — Is this the second iteration? — 200

Y   N

13 — Compute $P_{1, r, z}$ — 205-290

14 — /5/ — Start second iteration

15 — Compute the core average properties (see SPFUN2) — 310-340

16 — Write out $\phi_{r, z}$, $\Sigma_{w, r, z}$ and the core average properties — 340

17 — IPSPPR = 0? — Input control parameter

Y   N

18 — Write $\frac{q}{\phi} P_1$, P_1, p, $-D\nabla^2$, and Σ at each mesh point — Normally bypassed — 375

19 — RETURN — 390

15. CONSTS

Purpose: to make the fuel management calculations for the continu-
ous steady-state fuel movements, and perform the cost
analysis.

Input arguments: flux estimates at each point, plus all of the data
required by PTPROP and SPACE2.
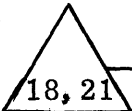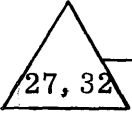
Output parameters: Flux and flux-time distributions, discharge burn-
ups, and cost results, plus the standard SPACE2 output.

Subprograms called: BIDRCT, COST, FIPRNT, GROUTN, HALT,
SHAPE, SPACE2, TIMECK, (INPUT-OUTPUT)

Space required: 825
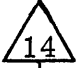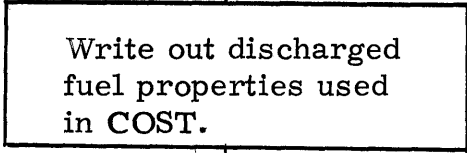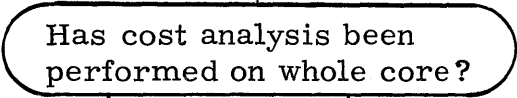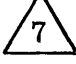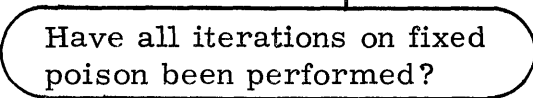
Discussion: This subroutine is reached from MAIN when ISSCNT $\neq$ 0.
It is the control program for the continuous steady-state fuel move-
ments, outin, graded, and bidirectional as discussed in Sections
IV C3. 3 and 3. 5.

Step	Flow Chart	Comments	Fortran Statement Number
1	15 CONSTS /38\	Start of run	
2	Read in and write out: Identification, flux time estimates and con-vergence criteria, also FCTR$_r$, the relative velocity or flux-time		5-35

433

			Fortran Statement
Step	Flow Chart	Comments	Number

Step 3 — Set up initial conditions, Set LPCNT = 0, Set $\theta_c = \theta_1$ — 36-40

Step 4 — (connector 24) — 40

Step 5 — LPCNT = LPCNT + 1, Compute $\theta_d(r)$ — $\theta_d(r)$ is used by subroutines GROUTN and BIDRCT — 40

Step 6 — 2 TIMECK(6) — Writes out the time

Step 7 — (connector 18, 21)

Step 8 — Set IMX = 0, Recompute $\theta_d(r)$ if IMUV = 3, bidirectional with velocity specified — INX is a control parameter — 55-70

Step 9 — (connector 27, 32) — Entry point when INX = 1

Step	Flow Chart	Comments	Fortran Statement Number

Step | Flow Chart | Comments | Fortran Statement Number

10 — IMUV = 1 ?

Y   N

11 — 16 GROUTN

18 BIDRCT

Computes the flux-time from flux plus $\theta_d(r)$, and obtains the 7 properties at each point.   100

12

13 — INX = 0 ?   460

14 — Y   N → 28   Exit point for cost calculation

15 — 2 TIMECK(7)   520

16 — 6 SPACE2

17 — Is this the first iteration?   530

Y   N

18 — 7   535

19 — Have iterations converged?   Uses input data, DELCNV as criterion of convergence   540

N   Y

435

Step	Flow Chart	Comments	Fortran Statement Number

20 — Have 11 Iterations been made? → N / Y

21 — N → 7

22 — Does C = 1 $\pm$ DELCRT? → N / Y

DELCRT is input data — 555

23 — Make new flux time estimates, θ_c

3
HALT(8)

Uses θ_2, input data, for first new estimate, linear extrapolation for the second, and least squares linear estimate for all subsequent θ_c's.

HALT is called if the input, $\theta_2 = \theta_1$

560-568

24 — 4

25 — Write out flux-times for outin and graded, or axial velocity in bidirectional

26 — Set INX = 1 — 599

27 — 9 — Exit for cost input data calculation

Step	Flow Chart	Comments	Fortran Statement Number

28 △14△ — Entry after cost input data calculation — 600

29 Write out discharged fuel properties used in COST. — 600

30 △ 12 COST △ — Performs cost analysis on discharged fuel

31 (Has cost analysis been performed on whole core?)

N   Y

32 △7△

33 (Have all iterations on fixed poison been performed?) — The number of Σ'_{wa} iterations is specified, as input data, LPMX — 680

N   Y

34 △ 19 SHAPE △ — SHAPE fixes new Σ_{wa} values and new values of θ_1 and θ_2.

35 △3△

Step	Flow Chart	Comments	Fortran Statement Number

36 NEXT = 0 ?   688

N   Y

37 Set IMUV = NEXT   690

38 △2   Entry to start a
                           new steady-state
                           continuous fuel
                           movement.

39 RETURN

16. GROUTN
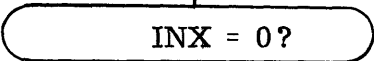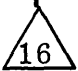
Purpose: to calculate the flux-time and the seven properties at each mesh point; and to calculate the properties of the discharged fuel for the cost analysis for the outin and graded fuel movements.

Input arguments: $\theta_d(r)$ = THETAR, the discharge flux-time parameter; θ_c, the current characteristic flux-time estimate; INX.

Output parameters: Flux-time at each mesh point: initial and discharge nuclide concentrations, center and average fuel burnup and fuel "on stream" time.

Subprograms called: AVPROP, PTPROP, NCGTHV, (INPUT-OUTPUT)

Space required: 633

Step	Flow Chart	Comments	Fortran Statement Number
1	16 GROUTN		
2	INX = 0? N Y	If INX = 0, the flux-times and seven properties are obtained. If INX ≠ 0, data is obtained for cost analysis.	
3	16		

439

Step	Flow Chart	Comments	Fortran Statement Number

4 — △12 — Entry point for new zone

5 — Does $\theta_d(r) = 0$ for this zone?   N   Y — $\theta_d(r)$ is zero if the zone is to be run OUTIN

6 — Compute the flux-times for Graded irradiation — 10-15

8 — △ 17 AVPROP — Computes the 7 average (graded) properties at each point in the zone.

9 — Compute the flux-times for Outin irradiation — 20-50

10 — △ 5 PTPROP — Computes the 7 properties at each point in the zone. — 55

11 — Have all zones been analyzed?

440

Step	Flow Chart	Comments	Fortran Statement Number

N   Y

12   △4

13   (Is IPSPPR = 0 ?)   Input data

N   Y

14   Write out the flux-times at each point   70–85

15   △21   Exit for return to CONSTS

16   △3   Entry point if INX = 1   100

17   (Does $\theta_d(r) = 0$ for this zone ?) $\theta_d(r) \neq 0$ for graded zone

N   Y

Step	Flow Chart	Comments	Fortran Statement Number

18

Compute initial and average discharge nuclide concentrations

△ 11 NCGTHV

(For graded)   110-130

19

Compute initial and average discharge nuclide concentrations

△ 11 NCGTHV

(For Outin)   150-165

20

Compute :burnups and time in reactor

21

△ 15

22

RETURN

17. AVPROP

Purpose: to compute the average with respect to flux-time of the seven point properties for graded irradiation, given the maximum flux-time

Input arguments: the data transferred from the FUEL Code plus the specified value of flux-time of the most-irradiated fuel.

Output parameters: the seven average properties

Subprograms called: HALT, (INPUT-OUTPUT)

Space required: 871

Discussion: See Section IV C3.5

Step	Flow Chart	Comments	Fortran Statement Number
1	17 AVPROP		
2	Is INIT = 0 ?		
3	8		
4	Compute the C coefficients of Eq. (4C70)		

Step	Flow Chart	Comments	Fortran Statement Number

5 — Have the C's for this set of properties been calculated?
  - Y
  - N

6 — Will this be the third set of C's?
  - Y
  - N

7 — 3 HALT(10)   Stop 10 for > 2 different sets of properties

3

8

9 — Compute the "Average Lagrangian Coefficients"

10 — Compute the seven average properties at each mesh point in the zone

11 — RETURN

18. BIDRCT

Purpose: to evaluate the flux-time and the seven flux-time properties at each mesh point; and to calculate the properties of the discharged fuel for the cost analysis, both of these for the bidirectional fuel movement.

Input arguments: } same as for GROUTN
Output parameters:

Subprograms called: NCGTHV, PTPROP, (INPUT-OUTPUT)

Space required: 938

Discussion: The mathematical model used is discussed in Appendix B. The actual description is found in Section IV C3. 3. This subroutine is called by CONSTS.

Step	Flow Chart	Comments	Fortran Statement Number
1	△ 18 BIDRCT		
2	Is INX = 0? (N) (Y)	INX = 0 for the flux-time and property calculation, INX = 1 for the discharge fuel calculation.	
3	△ 7		
4	Compute the flux-times in the two adjacent channels		5-15
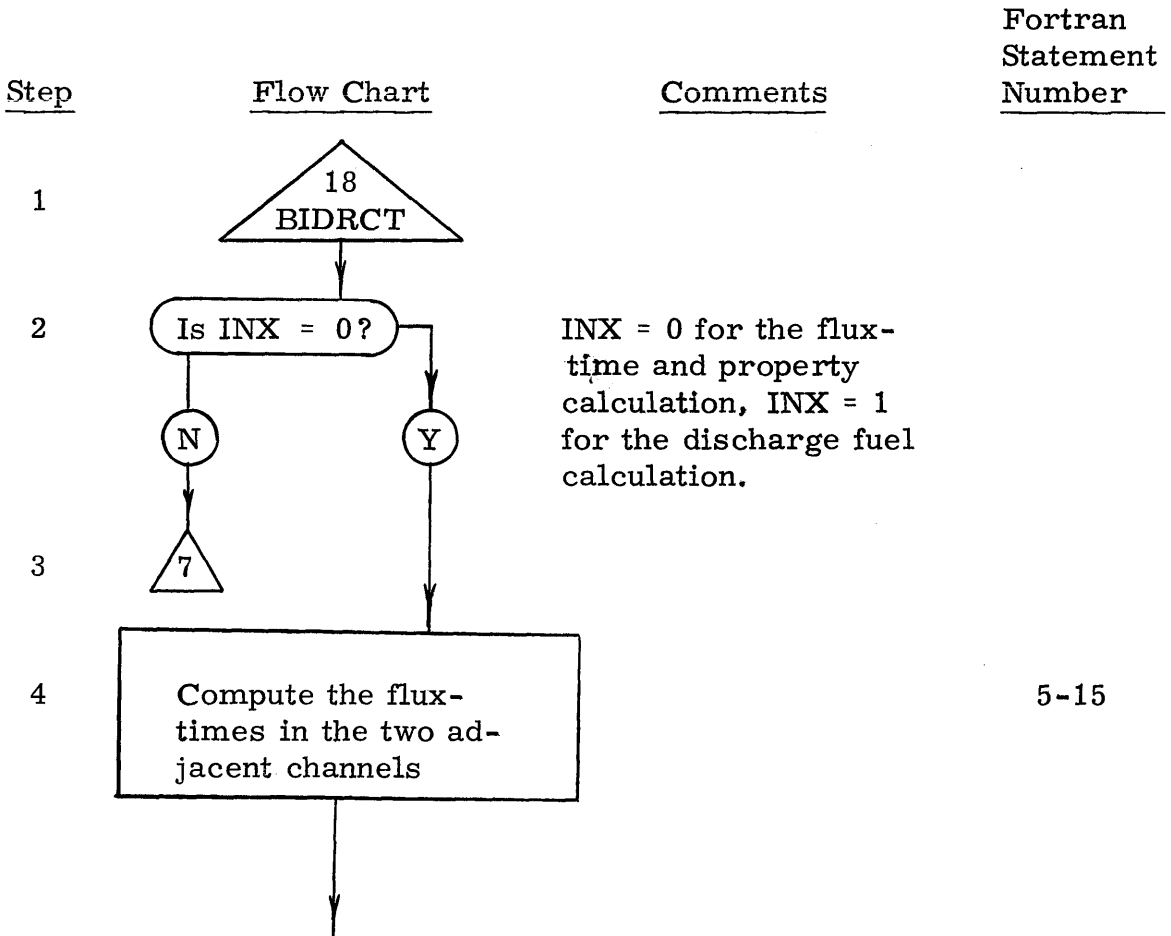
Step	Flow Chart	Comments	Fortran Statement Number
5	Compute the 7 flux-time properties averaged over both channels △ 5 PTPROP		20-35
6	△ 11	Return to CONSTS for flux evaluation	
7	△ 3	Entry for cost data calculation	80
8	Write out all flux times in both channels, also the discharge flux-times		80-100
9	Compute the initial and discharge nuclide concentration⌐ △ 11 NCGTHV		103-115
10	Compute the average and center burnup and time in reactor		115-200
11	△ 6	Entry for return to CONSTS	
12	△ RETURN		

446

19. SHAPE

Purpose: to adjust the fixed absolute poison for better power distribution and to make new flux-time estimates, θ_1 and θ_2.
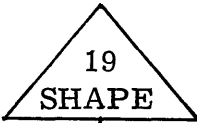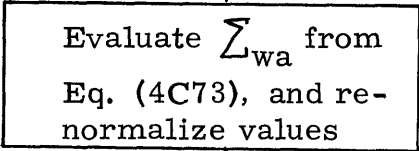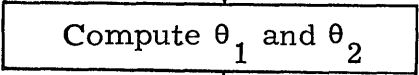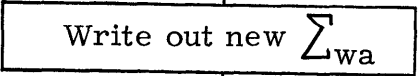
Input arguments: $\sum_{wa, r, z}$, $C_{28} = V_r \phi_{r, z}$, $POWD_{r, z}$, θ_c, θ_1, θ_2, IRL, JZL.

Output parameters: new values of $\sum_{wa, r, z}$, θ_1, and θ_2

Subprograms called: (INPUT-OUTPUT)

Space required: 274

Discussion: See Section IV C3. 6. This subroutine is called by CONSTS.

Step	Flow Chart	Comments	Fortran Statement Number
1	△ 19 SHAPE		
2	Evaluate $\sum_{wa}$ from Eq. (4C73), and re-normalize values		10-30
3	Compute θ_1 and θ_2		68
4	Write out new $\sum_{wa}$		70
5	△ RETURN		75

20. SHUFFL

Purpose: to perform the operations of discontinuous outin fuel movement and to evaluate the properties of discharged fuel.
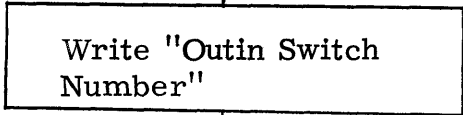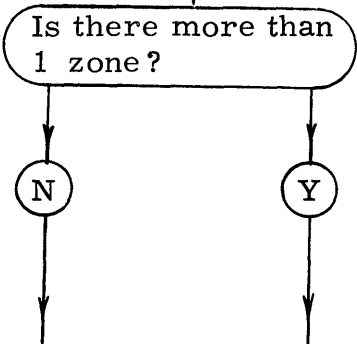
Input arguments: Flux-times, data required by COST, NCGTHV, and SPACON, and zone specifications.

Output parameters: New flux-times and zone specifications.

Subprograms called: COST, HALT, NCGTHV, SPACON, (INPUT-OUTPUT).

Space required: 1371

Discussion: See Section IV C3.2. This subroutine is reached from MAIN when IMUV = 2 or 3, and ISSCNT = 0.

Step	Flow Chart	Comments	Fortran Statement Number
1	△ 20 SHUFFL		
2	Write "Outin Switch Number"		2
3	Is there more than 1 zone? N Y		

Step	Flow Chart	Comments	Fortran Statement Number
4	3 / HALT(11)	Stop for insufficient no. of zones	3
5	INIT = 0? N Y	"Initial" control parameter	4
6	12		
7	Set INIT = 1		
8	14	Entry point for subsequent read-in.	8
9	Read in control data and write it out.		8-10
10	Flux-time gradient transfer? N Y		

449

Step	Flow Chart	Comments	Fortran Statement Number

11   Compute the Lagrangian fit coefficients for flux-time gradient transfer   500-550

12   △6

13   Is new control data required?   Under input data control.   15

     Y   N

14   △8

15   Is a cost analysis required?

     N   Y

16   △21

Step	Flow Chart	Comments	Fortran Statement Number

| Step | Flow Chart | Comments | Fortran Statement Number |

17 — Compute the initial and discharge average nuclide concentrations

△ 11 NCGTHV

Compute burnup and time in reactor — 36-65

18 — Write out the above results. — 100

19 — △ 12 COST

20 — Repeat cost analysis if this is the last fuel switch

21 — △16 — 165

22 — Compute and write out zone average burnups — 165-169

23 — △31 — Entry point for next zone — 170

24 — (Invert this zone ?) — Input control

451

Step	Flow Chart	Comments	Fortran Statement Number
25	Invert zone		171-173
26	Move the fuel?		174
27	Flux-time gradient transfer?		
28	Transfer the gradient		175-180
29	Transfer the average		182-186
30	All zones analyzed?		

Step	Flow Chart	Comments	Fortran Statement Number

N   Y

31   △23

32   Write out the new
     flux-times   188-192

33   Transfer the zone
     control parameters
     where necessary   210-215

34   4
         SPACON   SPACON is called
                             to re-evaluate the
                             "space constants"

35   RETURN   220

453

21. TRNSNT

Purpose: to perform the fuel management calculations for the continuous bidirectional fuel movement for the transient period following batch irradiation, during the approach to steady state.
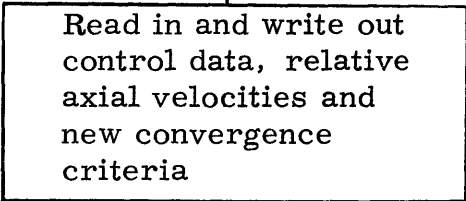
Input arguments: the end-of-batch fluxes and flux-times, plus all of the data required by **PTPROP** and **SPACE2.**

Output parameters: Spatial distributions of flux, flux-time and power, discharge burnup, and cost results.

Subprograms called: COST, FIPRNT, HALT, NCGTHV, PTPROP, SPACE2, TIMECK, (INPUT-OUTPUT)

Space required: 2250
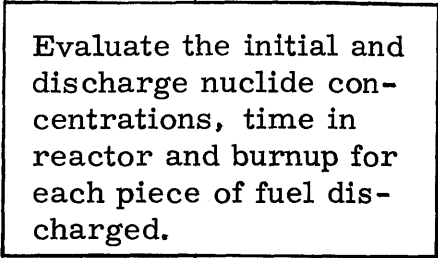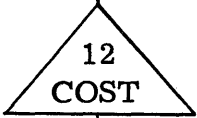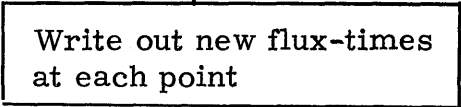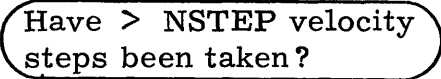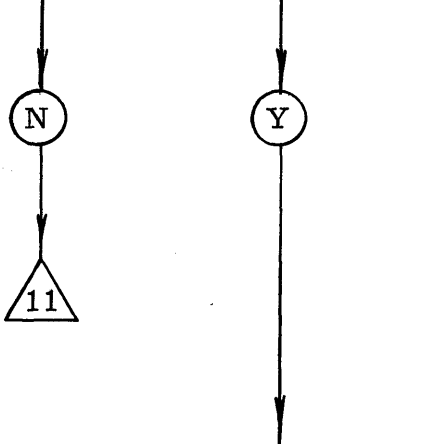
Discussion: This subroutine is reached from MAIN when IMUV = 4, and ISSCNT = 0. See Section IV C3. 3.

Step	Flow Chart	Comments	Fortran Statement Number
1	21 TRNSNT		
2	Read in and write out control data, relative axial velocities and new convergence criteria		2-10
3	9	Reentry point in loop for recomputation of end-of-batch conditions	30

Step	Flow Chart	Comments	Fortran Statement Number
4	**5** **PTPROP**	For given flux-times compute the seven properties at each point	35
5	**6** **SPACE2**	Evaluate fluxes and criticality	
6	Is C = 1 ± DELCRT?	Input convergence parameter	
	N Y		
7	Have NBAT loops been made?	Input control parameter	55
	N Y		
8	Make new flux-time estimates		60
9	3		
10	Set up initial conditions and make initial velocity estimate		65-105
11	32	Entry point for next velocity step.	110

Step	Flow Chart	Comments	Fortran Statement Number

12 — Is new control data required? — Under input data control. — 110

Y   N

13 — Read in and write out new data — 2-10

14 — Store current values of fluxes and flux-times — 125-130

15 — △24 — Reentry point in velocity iteration. — 135

16 — Have > 10 velocity iterations been made?

Y   N

17 — 3 HALT(11)

18 — Evaluate flux-times in adjacent channels — 139-175

19 — Evaluate the seven properties averaged over adjacent channels — 180-205

5 PTPROP

456

Step	Flow Chart	Comments	Fortran Statement Number

20 — △ 2 TIMECK(2)

21 — △ 6 SPACE2 — Computes new flux and criticality, etc.

22 — (Is C = 1 $\pm$ DELCRT?)

N   Y

23 — [Make new velocity estimate] — 215-240

24 — △ 15

25 — (Is the velocity negative?) — 26-52

Y   N

26 — △ 3 HALT(12) — 268

27 — [Evaluate the new time-in-reactor at each point] — 273-315

Step	Flow Chart	Comments	Fortran Statement Number

28 — Evaluate the initial and discharge nuclide concentrations, time in reactor and burnup for each piece of fuel discharged. — 315-520

29 — 12 COST

30 — Write out new flux-times at each point — 610-685

31 — Have > NSTEP velocity steps been taken?

N   Y

32 — 11

33 — RETURN — 131

458

22. DISCNT

Purpose: to perform the actual fuel movements and cost analysis for the discontinuous bidirectional fuel movement.
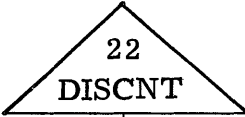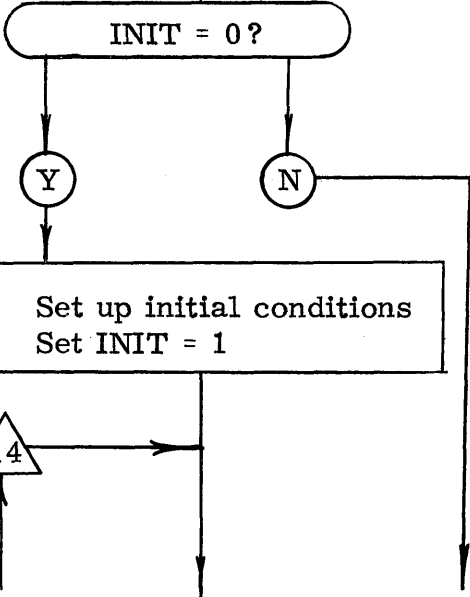
Input arguments: flux-times, plus the data required by NCGTHV.
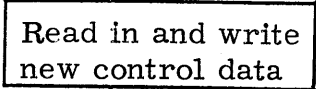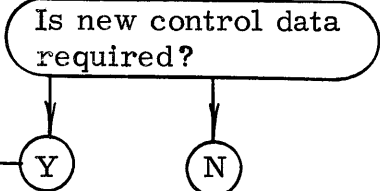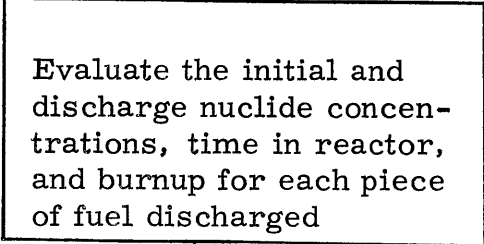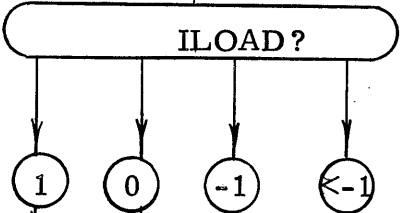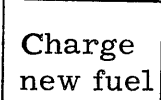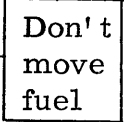
Output parameters: new flux-times, and cost results

Subprograms called: COST, NCGTHV, (INPUT-OUTPUT)

Space required: 1299

Discussion: This subroutine is reached from MAIN when IMUV = 5 and ISSCNT = 0. IDISC is set equal to two for the averaging of properties in adjacent channels in MAIN.

Step	Flow Chart	Comments	Fortran Statement Number
1	△ 22 DISCNT		
2	INIT = 0 ?	"Initial" control parameter in MAIN	
	Y N		
3	Set up initial conditions Set INIT = 1		
	△14		

Step	Flow Chart	Comments	Fortran Statement Number

4   Read in and write new control data   10-25

5   Is new control data required?   50-60

Y   N

6   Evaluate the initial and discharge nuclide concentrations, time in reactor, and burnup for each piece of fuel discharged   61-300

7   12 COST

8   ILOAD?   ILOAD is specified at each radial point.

1   0   -1   <-1

9   Charge new fuel   305-351

10   Don't move fuel

Step	Flow Chart	Comments	Fortran Statement Number
11	Recharge discharged fuel with end at end		
12	Recharge discharged fuel with end toward center		
13	Write out the new flux-times in adjacent channels at each point		355-385
14	Is more fuel to be moved before the next irradiation?		
	Y	N	
15	4		
16		RETURN	

461
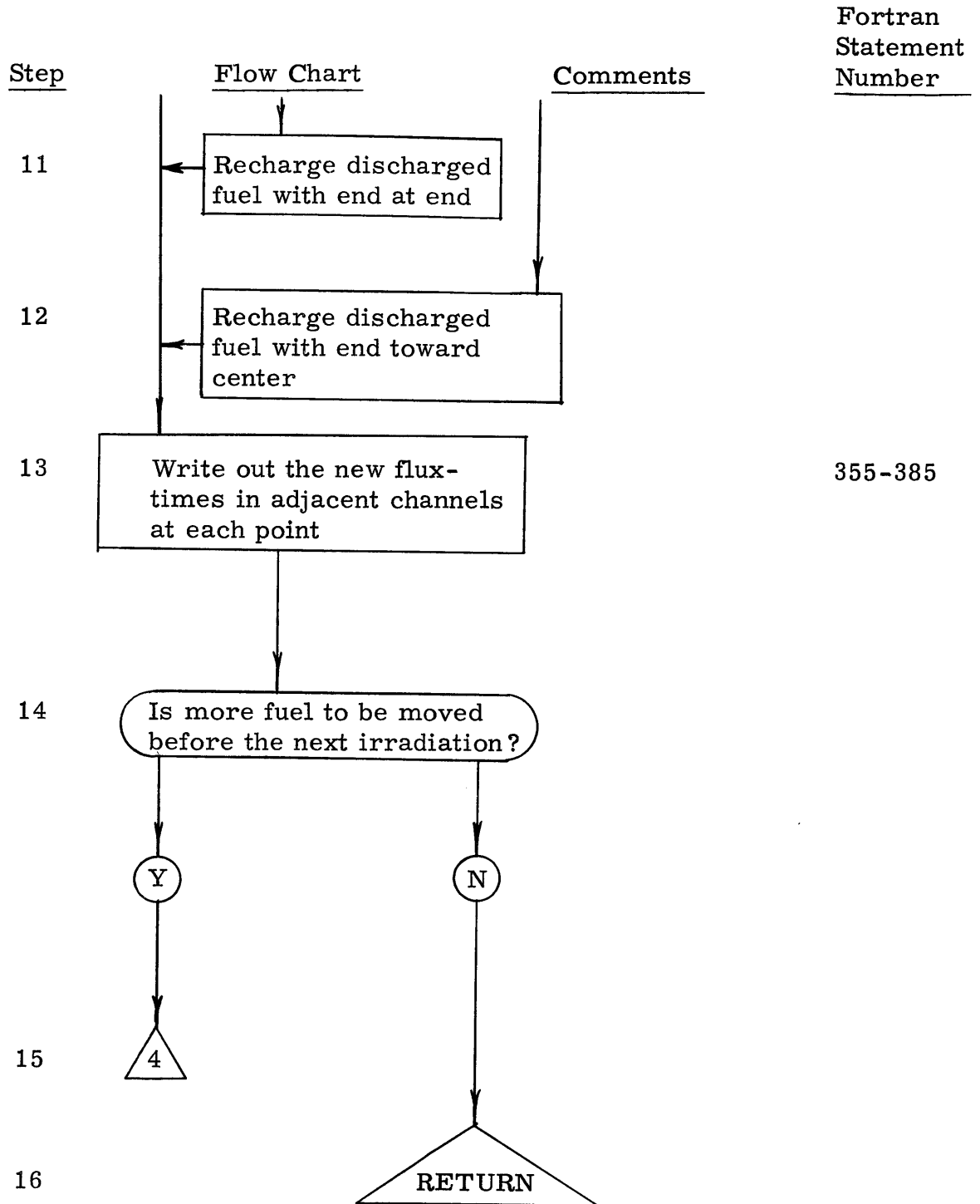
23. WTPE and GTTPE

Discussion: WTPE and GTTPE are MIT routines which greatly facilitate a large number of production runs on the MOVE Code. This feature is available in the MOVE Code only by use of a correction card. When it is used, however, the binary MAIN program and sub-routines are read into the computer, and the Fortran II loader or FMS loader performs its normal function. When execution is started, however, the first operation of the code is to read in 5 sets of cards with flux-time properties (FUEL Code output), and two sets of cost data. The instruction, CALL WTPE then causes the current contents of computer core memory including the above input data to be written on logical tape 9. On subsequent runs, the 2-card main program GTTPE (which effectively replaces the large binary deck) causes the contents of logical tape 9 to be read into core memory, and execution is started. Since there were five different types (or enrichments) of fuel, plus two cost sets originally in the core memory, it is not neces-sary to read in either fuel property data or cost data, provided the desired data was included in the original input. It is necessary only to remember the order in which the five sets of FUEL Code data were read in so that the proper enrichment or fuel type can be specified.

462

APPENDIX E

TABULATED FUEL CODE RESULTS

FOR THE CANDU REACTOR UNIT CELL

Tables E1 through E9 give the important unit cell properties of the CANDU reactor during irradiation. These properties are given for nine enrichments, ranging from natural to 2.5 a/o.

Table E1. Unit Cell Properties During Burnout: CANDU Reactor
Initial Enrichment 0.7206 a/o U^{235}

Thermal cross sections (barns)	Flux Time θ (n/kb)					
	0, Xe + Sm	1.0	2.0	3.0	4.0	5.0
$\sigma_{5,f}$	415.5	414.0	413.7	413.9	414.0	414.0
$\sigma_{9,f}$	690.1	692.9	694.0	694.2	694.2	694.3
$\sigma_{11,f}$	870.5	870.2	870.3	870.4	870.5	870.5
σ_5	489.5	487.8	487.5	487.7	487.8	487.8
σ_6	5.23	5.22	5.21	.5.21	5.22	5.22
$\sigma_7 = \sigma_{FP}$	35.8	33.7	32.6	32.0	31.5	31.1
σ_8	2.034	2.027	2.026	2.026	2.027	2.027
σ_9	1017.4	1022.9	1024.9	1025.1	1025.1	1025.3
σ_{10}	222.6	222.2	222.1	222.2	222.2	222.2
σ_{11}	1198.3	1197.8	1197.9	1198.1	1198.2	1198.3
σ_{12}	22.8	22.8	22.8	22.8	22.8	22.8
Atoms/bcm of fuel						
N_5	1.6395 E-4	9.872 E-5	5.942 E-5	3.576 E-5	2.152 E-5	1.296 E-5
N_6	0	1.004 E-5	1.592 E-5	1.928 E-5	2.112 E-5	2.207 E-5
$N_7 = N_{FP}$	0	1.434 E-5	1.470 E-4	2.155 E-4	2.802 E-4	3.421 E-4
N_8	2.2589 E-2	2.252 E-2	2.245 E-2	2.239 E-2	2.232 E-2	2.226 E-2

Table E1 (cont'd)

Atoms/b cm of fuel	Flux Time θ (n/kb)					
	0, Xe + Sm	1.0	2.0	3.0	4.0	5.0
N_9	0	4.069 E-5	5.490 E-5	5.937 E-5	6.040 E-5	6.032 E-5
N_{10}	0	6.441 E-6	1.640 E-5	2.508 E-5	3.183 E-5	3.687 E-5
N_{11}	0	1.161 E-6	4.420 E-6	7.619 E-6	1.003 E-5	1.172 E-5
N_{12}	0	1.134 E-7	1.001 E-6	2.920 E-6	5.622 E-6	8.805 E-6
Homogenized Properties						
$\Sigma'_{Xe\,Max}$	2.378 E-4	2.262 E-4	2.073 E-4	1.913 E-4	1.797 E-4	1.720 E-4
$\Sigma' - \Sigma'_{Xe}$	6.950 E-3	7.728 E-3	7.926 E-3	7.970 E-3	7.988 E-3	8.019 E-3
Σ'_f	3.478 E-3	3.578 E-3	3.397 E-3	3.198 E-3	3.042 E-3	2.933 E-3
$\nu\Sigma_f$	8.521 E-3	9.424 E-3	9.289 E-3	8.958 E-3	8.655 E-3	8.434 E-3
$(1-p)/(1+a)$	1.188 E-2	1.162 E-2	1.058 E-2	9.694 E-3	9.052 E-3	8.628 E-3
$\langle \eta(1-p) \rangle$	2.935 E-2	3.047 E-2	2.878 E-2	2.707 E-2	2.576 E-2	2.488 E-2
p	0.8772	0.8590	0.8411	0.8295	0.8218	0.8164
Σ'_{Mod}	4.436 E-4	4.483 E-4	4.470 E-4	4.449 E-4	4.429 E-4	4.414 E-4
Other Properties						
$\theta_o = nV_o t$	0	7.739 E-4	1.547 E-3	2.319 E-3	3.090 E-3	3.860 E-3
T_{neut}, °C.	139	142	142	142	142	142

Table E2. Unit Cell Properties During Burnout: CANDU Reactor
Initial Enrichment 0.85 a/o U^{235}

Thermal cross sections (barns)	Flux Time θ (n/kb)					
	0, Xe + Sm	1.5	3.0	4.5	6.0	7.5
$\sigma_{5,f}$	412.2	411.6	412.6	413.3	413.4	413.3
$\sigma_{9,f}$	693.7	696.1	695.7	695.1	695.0	695.3
$\sigma_{11,f}$	869.4	869.4	869.9	870.2	870.3	870.3
σ_5	485.8	485.0	486.2	487.0	487.2	487.0
σ_6	5.20	5.19	5.20	5.21	5.21	5.21
$\sigma_7 = \sigma_{FP}$	35.5	33.0	31.8	31.0	30.4	29.8
σ_8	2.019	2.016	2.020	2.023	2.024	2.023
σ_9	1025.1	1029.6	1028.3	1027.0	1026.8	1027.3
σ_{10}	221.6	221.4	221.8	222.0	222.1	222.0
σ_{11}	1196.7	1196.8	1197.5	1197.9	1198.0	1198.0
σ_{12}	22.7	22.7	22.7	22.7	22.7	22.7
Atoms/b cm of fuel						
N_5	1.934 E-4	9.050 E-5	4.229 E-5	1.977 E-5	9.244 E-6	4.327 E-6
N_6	0	1.580 E-5	2.274 E-5	2.558 E-5	2.652 E-5	2.660 E-5
$N_7 = N_{FP}$	0	1.261 E-4	2.388 E-4	3.390 E-4	4.318 E-4	5.207 E-4
N_8	2.256 E-2	2.245 E-2	2.235 E-2	2.225 E-2	2.215 E-2	2.206 E-2

466

Table E2 (cont'd)

	Flux Time θ (n/kb)					
	0, Xe + Sm	1. 5	3. 0	4. 5	6. 0	7. 5
N_9	0	5. 099 E-5	6. 022 E-5	6. 085 E-5	6. 008 E-5	5. 931 E-5
N_{10}	0	1. 171 E-5	2. 532 E-5	3. 468 E-5	4. 064 E-5	4. 434 E-5
N_{11}	0	2. 945 E-6	7. 996 E-6	1. 122 E-5	1. 304 E-5	1. 410 E-5
N_{12}	0	4. 729 E-7	3. 127 E-6	7. 504 E-6	1. 263 E-5	1. 795 E-5
Homogenized Properties						
$\Sigma_{Xe\ Max}$	2. 801 E-4	2. 398 E-4	2. 035 E-4	1. 815 E-4	1. 701 E-4	1. 645 E-4
$\Sigma - \Sigma_{Xe}$	7. 647 E-3	8. 317 E-3	8. 242 E-3	8. 158 E-3	8. 159 E-3	8. 220 E-3
Σ_f	4. 071 E-3	3. 845 E-3	3. 385 E-3	3. 075 E-3	2. 907 E-3	2. 823 E-3
$\nu\Sigma_f$	9. 973 E-3	1. 029 E-2	9. 441 E-3	8. 778 E-3	8. 402 E-3	8. 215 E-3
$(1-p)/(1+a)$	1. 365 E-2	1. 224 E-2	1. 033 E-2	9. 140 E-3	8. 515 E-3	8. 215 E-3
$\langle \eta(1-p)\rangle$	3. 370 E-2	3. 258 E-2	2. 871 E-2	2. 611 E-2	2. 472 E-2	2. 405 E-2
p	0. 8750	0. 8466	0. 8274	0. 8173	0. 8112	0. 8072
Σ_{Mod}	4. 506 E-4	4. 520 E-4	4. 470 E-4	4. 431 E-4	4. 407 E-4	4. 393 E-4
Other Properties						
$\theta_o = nV_o t$	0	1. 159 E-3	2. 315 E-3	3. 471 E-3	4. 626 E-3	5. 779 E-3
T_{neut}, °C.	145	146	144	143	143	143

Table E3. Unit Cell Properties During Burnout: CANDU Reactor
Initial Enrichment 1.00 a/o U^{235}

Thermal cross sections (barns)	Flux Time θ (n/kb)					
	0, Xe + Sm	1.5	3.0	4.5	6.0	7.5
$\sigma_{5,f}$	408.5	409.1	411.1	412.4	412.9	413.0
$\sigma_{9,f}$	697.9	699.1	697.4	696.1	695.6	695.6
$\sigma_{11,f}$	868.1	868.6	869.4	870.0	870.2	870.2
σ_5	481.5	482.1	484.5	486.0	486.6	486.6
σ_6	5.15	5.16	5.18	5.20	5.20	5.20
$\sigma_7 = \sigma_{FP}$	35.3	32.8	31.6	30.7	30.0	29.4
σ_8	2.003	2.005	2.014	2.020	2.021	2.022
σ_9	1033.9	1035.7	1031.9	1029.1	1028.0	1028.0
σ_{10}	220.4	220.6	221.3	221.7	221.9	221.9
σ_{11}	1194.9	1195.6	1196.8	1197.5	1197.8	1197.8
σ_{12}	22.5	22.5	22.6	22.7	22.7	22.7
Atoms/b cm of fuel						
N_5	2.275 E-4	1.067 E-4	4.991 E-5	2.334 E-5	1.092 E-5	5.114 E-6
N_6	0	1.860 E-5	2.677 E-5	3.009 E-5	3.120 E-5	3.129 E-5
$N_7 = N_{FP}$	0	1.432 E-4	2.656 E-4	3.709 E-4	4.661 E-4	5.561 E-4
N_8	2.253 E-2	2.241 E-2	2.231 E-2	2.221 E-2	2.211 E-2	2.202 E-2

Table E3 (cont'd)

Atoms/b cm of fuel	Flux Time θ (n/kb)					
	0, Xe + Sm	1.5	3.0	4.5	6.0	7.0
N_9	0	5.245 E-5	6.119 E-5	6.132 E-5	6.024 E-5	5.930 E-5
N_{10}	0	1.201 E-5	2.561 E-5	3.488 E-5	4.075 E-5	4.438 E-5
N_{11}	0	3.240 E-6	8.419 E-6	1.152 E-5	1.321 E-5	1.418 E-5
N_{12}	0	5.289 E-7	3.362 E-6	7.882 E-6	1.307 E-5	1.840 E-5
Homogenized Properties						
$\Sigma'_{\text{Xe Max}}$	3.289 E-4	2.666 E-4	2.177 E-4	1.886 E-4	1.734 E-4	1.659 E-4
$\Sigma'_i - \Sigma'_{\text{Xe}}$	8.443 E-3	8.841 E-3	8.554 E-3	8.338 E-3	8.265 E-3	8.284 E-3
Σ'_{f}	4.746 E-3	4.244 E-3	3.600 E-3	3.183 E-3	2.957 E-3	2.844 E-3
$\nu\Sigma'_{\text{f}}$	1.163 E-2	1.130 E-2	9.997 E-3	9.058 E-3	8.532 E-3	8.268 E-3
$(1-p)/(1+a)$	1.558 E-2	1.353 E-2	1.106 E-2	9.512 E-3	8.690 E-3	8.289 E-3
$\langle \eta(1-p)\rangle$	3.847 E-2	3.584 E-2	3.058 E-2	2.707 E-2	2.517 E-2	2.424 E-2
p	0.8727	0.8438	0.8252	0.8155	0.8099	0.8061
$\Sigma'_{\text{Mod.}}$	4.587 E-4	4.568 E-4	4.495 E-4	4.443 E-4	4.412 E-4	4.394 E-4
Other Properties						
$\theta_o = nV_o t_o$	0	1.157 E-3	2.313 E-3	3.468 E-3	4.621 E-3	5.774 E-3
T_{neut}, °C.	152	151	147	145	144	144

Table E4. Unit Cell Properties During Burnout: CANDU Reactor
Initial Enrichment 1.15 a/o U^{235}

Thermal cross sections (barns)	Flux Time θ (n/kb)					
	0, Xe + Sm	1.5	3.0	4.5	6.0	7.5
$\sigma_{5,f}$	405.0	406.6	409.6	411.6	412.4	412.7
$\sigma_{9,f}$	702.9	701.9	699.1	697.1	696.2	696.0
$\sigma_{11,f}$	866.9	867.7	868.9	869.7	870.0	870.1
σ_5	477.3	479.2	482.8	485.0	486.0	486.3
σ_6	5.11	5.13	5.17	5.19	5.20	5.20
$\sigma_7 = \sigma_{FP}$	35.0	32.7	31.4	30.4	29.7	29.0
σ_8	1.987	1.994	2.007	2.016	2.020	2.021
σ_9	1042.6	1041.7	1035.6	1031.2	1029.2	1028.8
σ_{10}	219.3	219.9	220.8	221.5	221.8	221.8
σ_{11}	1193.2	1194.4	1196.1	1197.1	1197.5	1197.7
σ_{12}	22.4	22.4	22.6	22.7	22.7	22.7
Atoms/b cm of fuel						
N_5	2.617 E-4	1.229 E-4	5.758 E-5	2.695 E-5	1.262 E-5	5.909 E-6
N_6	0	2.140 E-5	3.079 E-5	3.461 E-5	3.588 E-5	3.598 E-5
$N_7 = N_{FP}$	0	1.604 E-4	2.924 E-4	4.027 E-4	5.003 E-4	5.914 E-4
N_8	2.249 E-2	2.238 E-2	2.227 E-2	2.217 E-2	2.207 E-2	2.197 E-2

Table E4 (cont'd)

Atoms/b cm of fuel	Flux Time θ (n/kb)					
	0, Xe + Sm	1.5	3.0	4.5	6.0	7.5
N_9	0	5.388 E-5	6.214 E-5	6.178 E-5	6.040 E-5	5.929 E-5
N_{10}	0	1.230 E-5	2.588 E-5	3.515 E-5	4.084 E-5	4.442 E-5
N_{11}	0	3.540 E-6	8.839 E-6	1.182 E-5	1.337 E-5	1.425 E-5
N_{12}	0	5.866 E-7	3.599 E-6	8.257 E-6	1.351 E-5	1.884 E-5
Homogenized Properties						
$\Sigma_{Xe\ Max}$	3.775 E-4	2.933 E-4	2.319 E-4	1.957 E-4	1.766 E-4	1.673 E-4
$\Sigma - \Sigma_{Xe}$	9.225 E-3	9.362 E-3	8.866 E-3	8.518 E-3	8.370 E-3	8.349 E-3
Σ_f	5.410 E-3	4.640 E-3	3.815 E-3	3.290 E-3	3.007 E-3	2.865 E-3
$\nu\Sigma_f$	1.326 E-2	1.230 E-2	1.055 E-2	9.338 E-3	8.663 E-3	8.321 E-3
$(1-p)/(1+a)$	1.740 E-2	1.479 E-2	1.178 E-2	9.883 E-3	8.866 E-3	8.363 E-3
$\langle \eta(1-p) \rangle$	4.297 E-2	3.902 E-2	3.243 E-2	2.803 E-2	2.562 E-2	2.443 E-2
p	0.8705	0.8410	0.8229	0.8138	0.8085	0.8050
$\Sigma_{Mod.}$	4.668 E-4	4.615 E-4	4.520 E-4	4.455 E-4	4.4165 E-4	4.395 E-4
Other Properties						
$\theta_o = nV_o t_o$	0	1.156 E-3	2.310 E-3	3.464 E-3	4.617 E-3	5.769 E-3
T_{neut}, $^\circ$C.	159	156	150	146	145	144

Table E5. Unit Cell Properties During Burnout: CANDU Reactor
Initial Enrichment 1.30 a/o U^{235}

Thermal cross sections (barns)	Flux Time θ (n/kb)					
	0, Xe + Sm	1.5	3.0	4.5	6.0	7.5
$\sigma_{5,f}$	401.5	404.2	408.2	410.7	412.0	412.4
$\sigma_{9,f}$	706.0	704.8	700.9	698.1	696.7	696.3
$\sigma_{11,f}$	865.7	866.9	868.4	869.4	869.8	870.0
σ_5	473.3	476.4	481.1	484.0	485.5	485.9
σ_6	5.07	5.10	5.15	5.18	5.192	5.20
$\sigma_7 = \sigma_{FP}$	34.7	32.5	31.2	30.2	29.4	28.7
σ_8	1.971	1.983	2.001	2.012	2.018	2.019
σ_9	1051.0	1047.7	1039.2	1033.3	1030.4	1029.5
σ_{10}	218.1	219.1	220.4	221.2	221.6	221.7
σ_{11}	1191.6	1193.3	1195.4	1196.7	1197.3	1197.5
σ_{12}	22.2	22.3	22.5	22.6	22.7	22.7
Atoms/b cm of fuel						
N_5	2.958 E-4	1.393 E-4	6.530 E-5	3.058 E-5	1.432 E-5	6.712 E-6
N_6	0	2.419 E-5	3.480 E-5	3.912 E-5	4.055 E-5	4.067 E-5
$N_7 = N_{FP}$	0	1.774 E-4	3.191 E-4	4.344 E-4	5.344 E-4	6.266 E-4
N_8	2.246 E-2	2.234 E-2	2.223 E-2	2.213 E-2	2.203 E-2	2.193 E-2

Table E5 (cont'd)

Atoms/b cm of fuel	Flux Time θ (n/kb)					
	0, Xe + Sm	1.5	3.0	4.5	6.0	7.5
N_9	0	5.529 E-5	6.307 E-5	6.224 E-5	6.055 E-5	5.928 E-5
N_{10}	0	1.258 E-5	2.614 E-5	3.522 E-5	4.093 E-5	4.446 E-5
N_{11}	0	3.844 E-6	9.257 E-6	1.212 E-5	1.354 E-5	1.433 E-5
N_{12}	0	6.460 E-7	3.836 E-6	8.629 E-6	1.394 E-5	1.927 E-5
Homogenized Properties						
$\Sigma_{Xe\ Max}$	4.259 E-4	3.199 E-4	2.461 E-4	2.028 E-4	1.799 E-4	1.687 E-4
$\Sigma - \Sigma_{Xe}$	9.996 E-3	9.880 E-3	9.176 E-3	8.697 E-3	8.474 E-3	8.413 E-3
Σ_f	6.063 E-3	5.034 E-3	4.029 E-3	3.398 E-3	3.057 E-3	2.885 E-3
$\nu\Sigma_f$	1.486 E-2	1.330 E-2	1.110 E-2	9.618 E-3	8.793 E-3	8.374 E-3
$(1-p)/(1+\alpha)$	1.912 E-2	1.601 E-2	1.249 E-2	1.025 E-2	9.041 E-3	8.438 E-3
$\langle \eta (1-p) \rangle$	4.721 E-2	4.211 E-2	3.426 E-2	2.899 E-2	2.608 E-2	2.462 E-2
p	0.8685	0.8383	0.8207	0.8121	0.8072	0.8039
$\Sigma_{Mod.}$	4.749 E-4	4.664 E-4	4.546 E-4	4.466 E-4	4.421 E-4	4.396 E-4
Other Properties						
$\theta_0 = nV_0 t$	0	1.154 E-3	2.308 E-3	3.461 E-3	4.613 E-3	5.764 E-3
T_{neut}, $^\circ$C.	166	160	153	148	146	145

Table E6. Unit Cell Properties During Burnout: CANDU Reactor
Initial Enrichment 1.50 a/o U^{235}

Thermal cross sections (barns)	0, Xe + Sm	1.5	3.0	4.5	6.0	7.5
$\sigma_{5,f}$	397.0	401.0	406.3	409.6	411.3	412.0
$\sigma_{9,f}$	711.3	708.6	703.1	699.4	697.5	696.8
$\sigma_{11,f}$	864.2	865.8	867.8	869.0	869.6	869.8
σ_5	468.1	472.8	478.8	482.7	484.7	485.5
σ_6	5.02	5.07	5.13	5.17	5.18	5.19
$\sigma_7 = \sigma_{FP}$	34.4	32.3	31.0	29.9	29.0	28.3
σ_8	1.951	1.969	1.992	2.007	2.015	2.018
σ_9	1062.1	1055.6	1043.9	1036.0	1032.0	1030.5
σ_{10}	216.7	218.1	219.8	220.9	221.4	221.6
σ_{11}	1189.6	1191.8	1194.5	1196.2	1197.0	1197.3
σ_{12}	22.0	22.2	22.4	22.6	22.6	22.7
Atoms/b cm of fuel						
N_5	3.413 E-4	1.612 E-4	7.568 E-5	3.547 E-5	1.663 E-5	7.795 E-6
N_6	0.	2.792 E-5	4.015 E-5	4.512 E-5	4.677 E-5	4.690 E-5
$N_7 = N_{FP}$	0.	1.999 E-4	3.546 E-4	4.765 E-4	5.798 E-4	6.734 E-4
N_8	2.241 E-2	2.229 E-2	2.217 E-2	2.207 E-2	2.197 E-2	2.187 E-2

Table E6 (cont'd)

Atoms/b cm of fuel	Flux Time θ (n/kb)					
	0, Xe + Sm	1.5	3.0	4.5	6.0	7.5
N_9	0	5.712 E-5	6.428 E-5	6.283 E-5	6.075 E-5	5.926 E-5
N_{10}	0	1.293 E-5	2.646 E-5	3.542 E-5	4.103 E-5	4.449 E-5
N_{11}	0	4.256 E-6	9.810 E-6	1.251 E-5	1.375 E-5	1.442 E-5
N_{12}	0	7.274 E-7	4.154 E-6	9.122 E-6	1.450 E-5	1.984 E-5
Homogenized Properties						
$\Sigma_{Xe, Max}$	4.902 E-4	3.551 E-4	2.650 E-4	2.122 E-4	1.843 E-4	1.705 E-4
$\Sigma - \Sigma_{Xe}$	1.101 E-2	1.056 E-2	9.587 E-3	8.935 E-3	8.613 E-3	8.498 E-3
Σ_f	6.918 E-3	5.555 E-3	4.312 E-3	3.541 E-3	3.123 E-3	2.913 E-3
$\nu\Sigma_f$	1.695 E-2	1.462 E-2	1.183 E-2	9.989 E-3	8.966 E-3	8.444 E-3
$(1-p)/(1+a)$	2.126 E-2	1.759 E-2	1.343 E-2	1.074 E-2	9.274 E-3	8.537 E-3
$\langle \eta (1-p) \rangle$	5.251 E-2	4.612 E-2	3.667 E-2	3.025 E-2	2.668 E-2	2.487 E-2
p	0.8659	0.8348	0.8179	0.8099	0.8054	0.8025
$\Sigma_{Mod.}$	4.857 E-4	4.728 E-4	4.579 E-4	4.482 E-4	4.427 E-4	4.398 E-4
Other Properties						
$\theta_o = n_o t$	0	1.153 E-3	2.305 E-3	3.456 E-3	4.608 E-3	5.758 E-3
T_{neut}, °C.	175	167	156	150	147	146

Table E7. Unit Cell Properties During Burnout: CANDU Reactor
Initial Enrichment 1.75 a/o U^{235}

Thermal cross sections (barns)	Flux Time θ (n/kb)					
	0, Xe + Sm	1.5	3.0	4.5	6.0	7.5
$\sigma_{5,f}$	391.6	397.2	403.9	408.2	410.5	411.5
$\sigma_{9,f}$	717.8	713.2	706.0	701.1	698.5	697.4
$\sigma_{11,f}$	862.4	864.5	866.9	868.5	869.3	869.7
σ_5	461.8	468.3	476.1	481.4	483.8	484.9
σ_6	4.96	5.02	5.10	5.15	5.18	5.19
$\sigma_7 = \sigma_{FP}$	34.0	32.0	30.7	29.6	28.7	27.9
σ_8	1.927	1.951	1.982	2.001	2.011	2.015
σ_9	1075.5	1065.3	1049.8	1039.5	1034.0	1031.7
σ_{10}	215.0	216.9	219.0	220.4	221.1	221.4
σ_{11}	1187.1	1190.0	1193.3	1195.5	1196.6	1197.1
σ_{12}	21.7	22.0	22.3	22.5	22.6	22.7
Atoms/b cm of fuel						
N_5	3.982 E-4	1.887 E-4	8.879 E-5	4.167 E-5	1.954 E-5	9.169 E-6
N_6	0	3.256 E-5	4.682 E-5	5.260 E-5	5.452 E-5	5.468 E-5
$N_7 = N_{FP}$	0	2.279 E-4	3.987 E-4	5.290 E-4	6.363 E-4	7.317 E-4
N_8	2.236 E-2	2.222 E-2	2.211 E-2	2.200 E-2	2.190 E-2	2.181 E-2

Table E7 (cont'd)

Atoms/b cm of fuel	Flux Time θ (n/kb)					
	0, Xe + Sm	1.5	3.0	4.5	6.0	7.5
N_9	0	5.934 E-5	6.576 E-5	6.356 E-5	6.100 E-5	5.924 E-5
N_{10}	0	1.335 E-5	2.684 E-5	3.564 E-5	4.114 E-5	4.452 E-5
N_{11}	0	4.779 E-6	1.049 E-5	1.298 E-5	1.401 E-5	1.453 E-5
N_{12}	0	8.325 E-7	4.553 E-6	9.731 E-6	1.520 E-5	2.054 E-5
Homogenized Properties						
$\Sigma_{Xe, Max}$	5.702 E-4	3.990 E-4	2.886 E-4	2.240 E-4	1.898 E-4	1.728 E-4
$\Sigma - \Sigma_{Xe}$	1.224 E-2	1.141 E-2	1.010 E-2	9.231 E-3	8.787 E-3	8.604 E-3
Σ_f	7.961 E-3	6.199 E-3	4.666 E-3	3.719 E-3	3.207 E-3	2.947 E-3
$\nu\Sigma_f$	1.950 E-2	1.626 E-2	1.275 E-2	1.045 E-2	9.183 E-3	8.533 E-3
$(1-p)/(1+a)$	2.374 E-2	1.949 E-2	1.458 E-2	1.135 E-2	9.566 E-3	8.662 E-3
$\langle \eta (1-p) \rangle$	5.862 E-2	5.095 E-2	3.963 E-2	3.182 E-2	2.743 E-2	2.519 E-2
p	0.8629	0.8306	0.8144	0.8073	0.8033	0.8008
$\Sigma_{Mod.}$	4.991 E-4	4.810 E-4	4.622 E-4	4.502 E-4	4.435 E-4	4.399 E-4
Other Properties						
$\theta_o = n_o t_o$	0	1.151 E-3	2.301 E-3	3.452 E-3	4.602 E-3	5.752 E-3
T_{neut}, °C.	186	174	161	153	148	146

Table E8. Unit Cell Properties During Burnout: CANDU Reactor
Initial Enrichment 2.00 a/o U^{235}

Thermal cross sections (barns)	Flux Time θ (n/kb)					
	0, Xe + Sm	1.5	3.0	4.5	6.0	7.5
$\sigma_{5,f}$	386.4	393.4	401.6	406.9	409.7	411.0
$\sigma_{9,f}$	724.0	717.8	708.8	702.7	699.4	697.9
$\sigma_{11,f}$	860.8	863.2	866.2	868.0	869.0	869.5
σ_5	455.8	463.9	473.4	479.6	482.8	484.3
σ_6	4.90	4.98	5.07	5.13	5.17	5.18
$\sigma_7 = \sigma_{FP}$	33.6	31.7	30.5	29.4	28.4	27.5
σ_8	1.904	1.935	1.971	1.995	2.007	2.013
σ_9	1088.6	1074.8	1055.7	1042.9	1036.0	1032.9
σ_{10}	213.4	215.7	218.3	220.0	229.9	221.3
σ_{11}	1184.8	1188.2	1192.3	1194.8	1196.2	1196.9
σ_{12}	21.5	21.8	22.2	22.4	22.6	22.6
Atoms/b cm of fuel						
N_5	4.551 E-4	2.165 E-4	1.021 E-4	4.795 E-5	2.251 E-5	1.057 E-5
N_6	0	3.718 E-5	5.346 E-5	6.006 E-5	6.226 E-5	6.245 E-5
$N_7 = N_{FP}$	0	2.557 E-4	4.426 E-4	5.813 E-4	6.927 E-4	7.899 E-4
N_8	2.230 E-2	2.216 E-2	2.204 E-2	2.193 E-2	2.183 E-2	2.173 E-2

478

Table E8 (cont'd)

Atoms/b cm of fuel	Flux Time θ (n/kb)					
	0, Xe + Sm	1.5	3.0	4.5	6.0	7.5
N_9	0	6.150 E-5	6.718 E-5	6.426 E-5	6.124 E-5	5.922 E-5
N_{10}	0	1.375 E-5	2.718 E-5	3.584 E-5	4.123 E-5	4.453 E-5
N_{11}	0	5.308 E-6	1.117 E-5	1.344 E-5	1.426 E-5	1.464 E-5
N_{12}	0	9.409 E-7	4.950 E-6	1.033 E-5	1.587 E-5	2.122 E-5
Homogenized Properties						
$\Sigma_{Xe\ Max}$	6.497 E-4	4.425 E-4	3.121 E-4	2.357 E-4	1.954 E-4	1.751 E-4
$\Sigma - \Sigma_{Xe}$	1.344 E-2	1.225 E-2	1.061 E-2	9.525 E-3	8.959 E-3	8.710 E-3
Σ_f	8.979 E-3	6.837 E-3	5.018 E-3	3.898 E-3	3.291 E-3	2.982 E-3
$\nu\Sigma_f$	2.200 E-2	1.787 E-2	1.365 E-2	1.092 E-2	9.399 E-3	8.621 E-3
$(1-p)/(1+a)$	2.601 E-2	2.132 E-2	1.571 E-2	1.195 E-2	9.858 E-3	8.788 E-3
$\langle \eta (1-p) \rangle$	6.422 E-2	5.559 E-2	4.253 E-2	3.338 E-2	2.818 E-2	2.550 E-2
p	0.8603	0.8266	0.8111	0.8047	0.8013	0.7991
$\Sigma_{Mod.}$	5.123 E-4	4.892 E-4	4.665 E-4	4.521 E-4	4.443 E-4	4.401 E-4
Other Properties						
$\theta_o = n_o t_o$	0	1.149 E-3	2.298 E-3	3.447 E-3	4.597 E-3	5.745 E-3
T_{neut}, °C.	197	182	166	155	150	147

479

Table E9. Unit Cell Properties During Burnout: CANDU Reactor

Initial Enrichment 2.50 a/o U^{235}

Thermal cross sections (barns)	Flux Time θ (n/kb)					
	0, Xe + Sm	1.5	3.0	4.5	6.0	7.5
$\sigma_{5,f}$	376.8	386.2	379.1	404.2	408.1	410.0
$\sigma_{9,f}$	736.1	726.8	714.3	705.9	701.3	699.1
$\sigma_{11,f}$	857.7	860.9	864.6	867.1	868.5	869.2
σ_5	444.6	455.6	468.2	476.4	481.0	483.2
σ_6	4.79	4.90	5.02	5.10	5.15	5.17
$\sigma_7 = \sigma_{FP}$	32.9	31.2	30.0	28.9	27.9	26.9
σ_8	1.860	1.902	1.951	1.983	2.000	2.009
σ_9	1113.6	1093.3	1067.2	1049.6	1040.0	1035.3
σ_{10}	210.3	213.4	216.9	219.1	220.4	221.0
σ_{11}	1180.6	1185.0	1190.1	1193.6	1195.5	1196.4
σ_{12}	21.0	21.5	22.0	22.3	22.5	22.6
Atoms/b cm of fuel						
N_5	5.688 E-4	2.727 E-4	1.291 E-4	6.078 E-5	2.858 E-5	1.343 E-5
N_6	0	4.636 E-5	6.669 E-5	7.492 E-5	7.766 E-5	7.791 E-5
$N_7 = N_{FP}$	0	3.106 E-4	5.297 E-4	6.853 E-4	8.048 E-4	9.056 E-4
N_8	2.218 E-2	2.203 E-2	2.191 E-2	2.179 E-2	2.169 E-2	2.160 E-2

Table E9 (cont'd)

Atoms/b cm of fuel	Flux Time θ (n/kb)					
	0, Xe + Sm	1.5	3.0	4.5	6.0	7.5
N_9	0	6.560 E-5	6.991 E-5	6.561 E-5	6.170 E-5	5.917 E-5
N_{10}	0	1.447 E-5	2.777 E-5	3.616 E-5	4.134 E-5	4.452 E-5
N_{11}	0	6.380 E-6	1.249 E-5	1.434 E-5	1.474 E-5	1.485 E-5
N_{12}	0	1.166 E-6	5.741 E-6	1.150 E-5	1.719 E-5	2.253 E-5
Homogenized Properties						
$\Sigma_{Xe\ Max}$	8.071 E-4	5.289 E-4	3.590 E-4	2.594 E-4	2.065 E-4	1.798 E-4
$\Sigma - \Sigma'_{Xe}$	1.577 E-2	1.390 E-2	1.161 E-2	1.011 E-2	9.302 E-3	8.920 E-3
Σ_f	1.094 E-2	8.093 E-3	5.718 E-3	4.254 E-3	3.458 E-3	3.052 E-3
$\nu\Sigma_f$	2.681 E-2	2.106 E-2	1.545 E-2	1.184 E-2	9.833 E-3	8.799 E-3
$(1-p)/(1+\alpha)$	3.003 E-2	2.476 E-2	1.791 E-2	1.315 E-2	1.044 E-2	9.042 E-3
$\langle \eta(1-p)\rangle$	7.415 E-2	6.433 E-2	4.818 E-2	3.646 E-2	2.968 E-2	2.614 E-2
p	0.8556	0.8191	0.8049	0.8000	0.7975	0.7960
$\Sigma'_{Mod.}$	5.387 E-4	5.057 E-4	4.752 E-4	4.562 E-4	4.458 E-4	4.405 E-4
Other Properties						
$\theta_o = n_o t$	0	1.147 E-3	2.294 E-3	3.440 E-3	4.587 E-3	5.735 E-3
T_{neut}, °C.	220	198	175	160	153	149

APPENDIX F

CATALOGUE OF COMPUTER RUNS

Following is a list of the computer runs performed in connection with this work. In the numbering system used, the letter designates the fuel management technique, and the first number designates the purpose of the run as listed below. The second numbers from 1 to 9 refer to fuel enrichments: natural, 0.85, 1.0, 1.15, 1.30, 1.50, 1.75, 2.0, and 2.5 a/o, respectively.

A - Bidirectional, Continuous Steady-State

      A1.1, 3, 5, 6   -   Uniform Radial Burnup

      A2.1, 3, 5, 6   -   Uniform Axial Velocity

      A3.1   -   Reference Design Variations

      A4.1, 3   -   Mixed Enrichment, Natural + 1.0 a/o

      A5.1   -   Reference Design

      A6.1, 2, 3, 5, 6 -   Minimum Power Density

      A7.1, 3, 5 ,   -   Fixed Poison Use

      A8.1, 3, 5   -   Minimum Volume

B - Bidirectional, Continuous Startup

      B1.1   -   Reference Design Startup

C - Bidirectional, Discontinuous

      C1.1, 2, 3, 5, 16 - Startup, Natural U; 2, 3, 5, and 16 zones

D - Batch

      D1.1, 5, 7, 9   -   Enrichment Survey

      D2.5, 7   -   Use of Burnable Poison

      D3.1, 5, 6, 7   -   Radial Variation of Control Poison

      D4.6, 7   -   Use of Mixed Enrichments + Rad. Var. of Σ_w

      D5.5, 6, 7   -   Effect of Volume Changes

E - Discontinuous Outin

      E1.1, 2, 3   -   Use of Axial Inversion and Effect of No. of Zones

      E2.3, 5, 6, 7   -   Startup with Natural Center and Steady-State Operation

      E3.5   -   Optimum Batch Startup and Steady-State

F - Continuous Graded

      F1.1, 3, 5   -   Enrichment Study

      F2.1, 3, 5   -   Radial Variation of Burnup

G - Continuous Outin

      G1.1, 2, 3   -   Enrichment Study

APPENDIX G

NOMENCLATURE

This section summarizes the nomenclature used in this work, giving the first text reference for each symbol used. For convenience, the section is divided to treat 1) English letters, 2) Greek letters, 3) Subscripts, and 4) Superscripts.

1. English Letters.

Text Symbol	FORTRAN Symbol	Description	Text Reference
$A(x)$	A(I)	Hardening parameter in Wilkins equation	(4B1)
ALAG	ALAG	Lagrangian fit coefficient	(4C25)
A_ψ	APSI	Fractional change in disadvantage factor per flux-time step	(4B37)
B	BURNUP	Average Burnup	(4C36)
C	C	Core criticality	(4C35)
C_i	C(I,J)	Unit cost of component "i" in cost set, "j"	Table 4.2
C_E	CE	Unit cost of separative work	Table 4.2
C_p	CPF	Unit cost of UF_6	(4C75)
$\overline{C}_{mt}$	CONED(1)	Material partial fuel cost	(4C97)
$\overline{C}_{fb}$	CONED(2)	Fabrication " " "	(4C98)
$\overline{C}_{rp}$	CONED(3)	Reprocessing " " "	(4C99)
$\overline{C}_1$	CONED(4)	UF_6 " " "	(4C100)
$\overline{C}_{wc}$	CONED(5)	Working capital " " "	(4C101)

484

Text Symbol	FORTRAN Symbol	Description	Text Reference
$\overline{C}_{cap}$	CONED(6)	Capital Investment Cost	(4C102)
$\overline{C}_{op}$	CONED(7)	Operating Cost	(4C103)
C_1	C1	Constant term in resonance escape probability	(4B18)
C_3	—	Constant No. 3	(4C19-22)
C_4	—	Constant No. 4	(4C18)
C_5	C5	Ratio of average to maximum Xe poisoning	(4C27)
C_7	—	Constant No. 7	(4C23)
C_8	—	Constant No. 8	(4C24)
D	D	Diffusion Coefficient	Table 4.1
D_6	D6	Per diem rental charge on reprocessing plant	(4C80)
D_7	D7	Unit cost of converting $UO_2 (NO_3)_2$ to UF_6	(4C81)
$d_{i,j,u}$	D(I,J,K)	Leakage terms in spatial equations	(4C15)
E	—	Neutron energy	(4B2)
E_c	EVCUT	Cutoff energy of the thermal region	(4B4)
E_o	—	0.0253 ev	(4B9)
$e_{i,j}$	E(I,J)	Non-leakage terms in spatial equations	(4C15)
FNAT	FNAT	Fraction of blended fuel which comes from natural uranium	(4C79)
f	—	Fraction of mesh point moved in bidirectional	(4C46)

Text Symbol	FORTRAN Symbol	Description	Text Reference
$f(r)$	FCTR(I)	Relative discharge flux-times or axial velocities	(4C55)
f_d	FDAMP	Damping factor	(4C52)
f_i	F(I)	Material adjustment factor in cost analysis	Table 4.1
g_i	—	Radial mesh spacing	Figure 4.2
H	H	Height of Reactor Core	—
h	HL	Axial mesh spacing	Figure 4.2
$I(\theta)$	—	Integral term	(4C69)
IRL	IRL	Number of radial mesh points	—
JZL	JZL	Number of axial mesh points	—
k_∞	CAINF	Infinite multiplication factor	(4B50)
L_o	FLOAD	Plant load factor	Table 4.2
L	—	Over-all load factor	(4C96)
L'	—	Fueling load factor	(4C96)
N_m	AN(M)	Concentration of nuclide "m"	(4B17)
n	—	Total neutron density	(4B8)
n_{th}	—	Thermal neutron density	(4B8)
n_{epi}	—	Epithermal neutron density	(4B8)
$P(\theta)$	—	Generalized flux-time property	(4C25)
PDENAV	PDENAV	Average power density	(4C38)
$POWD_{i,j}$	POWD(I,J)	Power density	(4C73)
p_m	P(M)	Resonance escape probability for nuclide "m"	(4B17)

Text Symbol	FORTRAN Symbol	Description	Text Reference
P_{mod}	—	Resonance escape probability of non-fuel material	(4B28)
q	—	Slowing down density	Figure 4.1
R_i	R(I)	Outer radius of the "i"th radial mesh region	Figure 4.2
R	RPR	Reprocessing rate	(4C80)
RI_m^{∞}	RI(M)	Resonance integral	Table 4.1
SPPDAV	SPPDAV	Specific power of the fuel	Table 4.2
T_o	—	Specific power of the fuel 293.7° K	(4B6)
T_{mod}	TMOD	Moderator temperature	(4B2)
t_{neut}	TNEUT	Neutron temperature	(4B7)
t_R	TR	Full power time of fuel in reactor	(4C37-8)
V_i	C13(I)	Volume of radial mesh region i	(4C31)
V_{fl}	VFL	Volume fraction of fuel in unit cell	(4B18)
V_z	—	Axial fuel velocity in bidirectional	(4C57)
v	—	Neutron velocity	—
v_o	—	2200 m/s	(4B5)
W_i	W(I,J)	Weight of material i for cost set j	(4C74)
$W(\theta)$	—	Importance weighting function	(4C65)
WFL	WFL	Mass of fuel in core	Table 4.2
x	—	Normalized neutron velocity	(4B2)

Text Symbol	FORTRAN Symbol	Description	Text Reference
x	—	Weight fraction of U^{235} in fuel	(4C75)
x_0	XO	Optimum waste composition	(4C75)
x_{opt}	XOPT	Optimum blending composition	(4C76)
$Y(x)$	Y(I)	Flux per unit velocity	(4B1)
$Y_{Xe,m}$	YXE(m)	Xenon fission product yield of nuclide m	Table 4.1
ZSYM	ZSYM	Axial symmetry control parameter	(4C24)

2. Greek Letters

Text Symbol	FORTRAN Symbol	Description	Text Reference
α_m	ALPHA(M)	Ratio of capture of fission in resonance	Table 4.1
γ	GAMMA	Net thermal efficiency	Table 4.2
δH	DELH	Axial reflector savings	(4C24)
δR	DELR	Radial reflector savings	(4C23)
ϵ	EPSI	Fast fission factor	Figure 4.1
η_m	ETA(m)	Fission neutrons per resonance absorption	Figure 4.1
θ	TH	Thermal flux-time	—
θ_0	THETAO	2200 m/s flux-time	IVB 3.5
$\theta_{d(r)}$	THETAR(I)	Discharge flux-time	(4C63)
$\theta_{(r,z)}$	THETA(I,J)	Spatial flux-time	—
λ_{xe}	XELAM	Xenon decay constant	(4C27)
λ_{11}	ALAM11	Pu^{241} decay constant	(4B44)

Text Symbol	FORTRAN Symbol	Description	Text Reference
ν_m	ANU(M)	Neutrons per fission in nuclide m	Figure 4.1
$\nu\Sigma_f$	C10	Thermal Production Cross-Section	(4B31)
$\xi\Sigma_s$	SDP	Slowing down power of the fuel	IVB 3.1
Σ	—	Thermal neutron absorption cross-section	IVB 3.1
Σ_1	—	Macroscopic fast removal cross-section	Figure 4.1
Σ_f	C53	Macroscopic thermal fission cross-section	(4B30)
Σ_w	SIGMW	Control poison absorption cross-section	Figure 4.1
Σ_{wn}	SIGMWN	Relative control poison cross-section	(4C31)
Σ_{w1}	SIGMW1	Control poison normalizing constant	(4C31)
$\Sigma_{xe,max}$	SGXEMX	Maximum Xe cross-section	(4B35)
Σ_{TOT}	—	Total non-control poison absorption cross-section	(4B36)
$\Sigma_{s,fl}$	SGMSFL	Scattering cross-section of the fuel	(4B19)
$\overline{\sigma}_m$	SIG(M)	Spectrum average microscopic cross-section for nuclide m	(4B4)
σ_{FP}	SIG(7)	Cross-section per fission product pair	IVB 3.6
σ_o	—	2200 m/s microscopic absorption cross-section	(4B5)
τ	TAU	Fermi age	(4C7)
ϕ	PHIS	Thermal flux	IVB 3.5

Text Symbol	FORTRAN Symbol	Description	Text Reference
ϕ_o	—	2200 m/s flux	IVB 3.5
ϕ_1	—	Fast flux	Figure 4.1
ψ	PSI	Thermal disadvantage factor	(4B37)
$\psi_{1,m}$	PSI1(M)	Resonance disadvantage factor of nuclide m	(4B19)

3. Subscripts

c	—	See E_c	(4B4)
d	—	See f_d	(4C52)
epi	—	Epithermal	—
f	—	Fission	—
FP	—	Fission product	—
fl	—	Fuel	—
i	—	Radial index or cost component index	—
j	—	Axial index or cost set index	—
m	—	Nuclide index	—
mod	—	See T_{mod} - moderator	—
neut	—	See t_{neut}	(4B7)
o	—	See T_o, v_o, L_o	—
r	(I)	Radial index	—
R	—	See t_R	(4C37)
s	—	Scattering	—

Text Symbol	FORTRAN Symbol	Description	Text Reference
Sm	—	Samarium group of fission products	—
th	—	Thermal	—
w	—	Control poison	—
Xe	—	Xe fission products	—
z	—	Axial index	—

4. Superscripts

Text Symbol	FORTRAN Symbol	Description	Text Reference
o	—	Initial	—
∞	—	See (RI)	Table 4.1
$\wedge$	—	Effective cross-section for 2200 m/s flux	—
—	—	Spectrum-averaged or in cost analysis, infers mills/kwh basis	—

APPENDIX H

BIBLIOGRAPHY

A21.   Archibald, J. A., CUREBO, A Generalized Two-Space
        Dimension Code with Cross-Section and Depletion
        Calculation for IBM 704. KAPL-1885, April, 1959.

A22.   Archibald, J. A., the KARE System for Computing Life
        Studies Automatically. Trans. A:N:S: 3, No. 1,
        Paper 5-1.

A23.   Amberg, S. L., A Study of Fuel Cycles in Organic Moderated
        Nuclear Reactors, M.S. Thesis, Dept. of Nucl. Eng.,
        MIT, February, 1960.

A41.   Guide to Abstracts and Manuals for Computer Program Inter-
        change, Amer. Inst. Ch. E., 1959.

A61.   The Canadian Study for a Full-Scale Nuclear Power Plant,
        AECL 557, January, 1958.

A62.   Arnold, W. H. Jr., A Study of the Use of Fuel Management
        to Lower Power Costs in the Yankee Atomic Electric
        Plant, Nuclear Utility Services Report 104, May, 1961.

B21.   Benedict, M., R. T. Shanstrom, S. L. Amberg, N. B. McLeod
        and P. Steranka, FUELCYC. A New Computer Code for
        Fuel Cycle Analysis — Part II, Nuclear Sci. and Eng.
        (in press).

B41.   Benedict, M. and T. H. Pigford, "Nuclear Chemical Engi-
        neering", McGraw-Hill Book Co., Inc., New York, 1957.

B42.   Buckner, John K.: Effective Fission Product Absorption
        Cross-Sections, M.S. Thesis, Dept. of Nuclear Eng.,
        MIT, September, 1960.

C21.   Callaghan, J. B. et al., TURBO- A Two Dimensional, Few
        Group Depletion Code for the IBM 704, WAPD-TM-95,
        November, 1957.

C22. Caldwell, W. R., TNT-1, A Program for the Solution of the
     Reactor Depletion Problem in Three Dimensions on
     the Philco-2000, WAPD-TM-231.

C41. Craig, D. S. et al: Long Irradiation of Natural Uranium,
     AECL 615, September, 1958. (P/205).

C42. Crowther, R. L., and J. W. Weil: The Effective Cross-
     Section of Pu^{240} in Long Term Reactivity
     Calculations, GEAP-2058.

C51. Cooper, W. A., H. Rose, J. J. Syrett: Long Term Reactivity
     Changes in Windscale and NRX Irradiated Uranium
     Bars, AERE R/R 2311.

E41. Survey of Initial Fuel Costs of Large U.S. Nuclear Power
     Stations, A Report of the Technical Appraisal Task
     Force on Nuclear Power to the Board of Directors
     of the Edison Electrical Institute, 1958.

G41. Gray, J. L.: Presentation to the House of Commons Special
     Committee on Research, AECL-1000.

G42. Gill, S.: A Process for Step by Step Integration of Differ-
     ential Equations in an Automatic Digital Computing
     Machine, Proc. Cambridge Phil. Soc. 47, 96, (1951).

G51. Gunst, S. B., E. D. McGarry, J. J. Scoville: The Reactivity
     of Natural UO_2 Irradiated to 6 n/kb, Nucl. Sci. and Eng.,
     7, 407-418 (May, 1960).

H41. Hunton, F. W. and D. Johnson: Costing of Reactor Fuels,
     Paper at Atomic Industrial Forum, December, 1960,
     Kaiser Engineers.

H42. Henderson, W. J. and D. G. Hurst: The Effect of Flux
     Flattening on the Economics of Heavy Water Moderated
     Reactors, AECL 949, December, 1959.

H43. Hurst, D. G.: Calculated Cross-Sections of Irradiated
     Fission Product, CRRP-659.

H44.   Hildebrand, F. B.: "Introduction to Numerical Analysis",
           McGraw-Hill Book Co., Inc., New York, 1956.

H51.   Hart, R. G. et al: Chemical and Isotopic Analysis of
           Irradiated Uranium Slugs, AECL 813.

K51.   Kushneriuk, S. A.: Effective Cross-Sections and Neutron
           Flux Distributions in a Natural Uranium Rod, AECL 497.

L41.   Lambertus, H.: Private communication of June 13, 1961.

L51.   Littler, D. J.: Measurements of the Change in Cross-Section
           of Irradiated Uranium Made by Modulating the Power of
           a Nuclear Reactor, AERE RS/R 2092.

L52.   Lewis, W. B.: Reactivity Changes Expected and Observed in
           the Long Irradiation of Natural Uranium in the NRX
           Reactor, AECL 187.

L61.   Lewis, W. B.: Basic Considerations in the Design of a Full
           Scale Heavy Water and Natural Uranium Power Reactor,
           AECL 785, March, 1959.

M21.   McDaniel, C. T., Fuel Cycle Analysis of Stepwise Fuel
           Movement in a Pressurized Water Reactor, M.S. Thesis,
           Dept. of Nucl. Eng., MIT, June, 1960.

N21.   Neill, J. M., Reactivity Lifetime and Cost Characteristics of
           a Thorium-Fueled Reactor, M.S. Thesis, Dept. of
           Nucl. Eng., MIT, February, 1961.

R41.   Rickert, Royce J.: Economic Consequences of Design Vari-
           ations in Water Reactor Fuel Elements, Paper at
           International Atomic Energy Agency Symposium on
           Fuel Element Fabrication, May 10-13, 1960.

S21.   Steranka, P., Fuel Cycle Analyses for a Pressurized Water
           Reactor, M.S. Thesis, Dept. of Nucl. Eng., MIT,
           January, 1960.

S22.   Shanstrom, R.T., and M. Benedict, FUELCYC. A New
         Computer Code for Fuel Cycle Analysis — Part I,
         Nuclear Sci. and Eng. (in press).

S41.   Shanstrom, R. T., M. Benedict and C. T. McDaniel: Fuel
         Cycles in Nuclear Reactors, NYO-2131.

S42.   SL-1674: Power Cost Normalization Studies, Civilian Power
         Reactor Program, 1959, Sargent and Lundy.

S43.   Smith, H. A. et al: A Study of a Full-Scale Uranium and
         Heavy Water Nuclear Power Plant, A/CONF.15/P/208,
         1958.

U21.   Uematsu, K., Fuel Cycle Analysis of Plutonium Recycle in a
         Gas-Cooled, Graphite-Moderated, Natural Uranium
         Reactor, M.S. Thesis, Dept. of Nucl. Eng., MIT,
         January, 1961.

U41.   U.S. Federal Register, Vol. 26, p. 4765, May 30, 1961.

U42.   U.S. Federal Register (Notice on Spent Fuel Reprocessing),
         Vol. 23, 1707, March 12, 1958.

U43.   U.S. Federal Register (Losses in Conversion), Vol. 26,
         4435, May 23, 1961.

U44.   USAEC Press Release, D-138 on revision of charges for
         enriched and depleted UF_6.

W21.   Waucquez, M., Study of Fuel Cycles in Organic Moderated
         Reactors, M.S. Thesis, Dept. of Nucl. Eng., June, 1960.

W41.   Westcott, C. H.: Effective Cross-Section Values for Well
         Moderated Thermal Reactor Spectra, 3rd Ed., AECL 1101.

W51.   Ward, A.G. and D. S. Craig, Measurements of the Reactivity
         Change with Irradiation for Natural Uranium Samples
         Irradiated in NRX, AECL 812.

W52.   Ward, A. G., and D. S. Craig, Analysis of Measurements of
         the Reactivity Change with Irradiation for Natural
         Uranium Samples, AECL 814.

W61.	Wolberg, John R., Homogeneous Addition of a Burnable Poison to a Slightly Enriched System.	GEAP 3234, August, 1959.